NOTICES

When Government drawings, specifications, or other data are used for any purpose other than in connection with a definitely related Government procurement operation, the United States Government thereby incurs no responsibility nor any obligation whatsoever; and the fact that the Government may have formulated, furnished, or in any way supplied the said drawings, specifications, or other data, is not to be regarded by implication or otherwise as in any manner licensing the holder or any other person or corporation, or conveying any rights or permission to manufacture, use, or sell any patented invention that may in any way be related thereto.

Items and materials used in the study, or called out in the report by trade name or specifically identified with a manufacturer, were not originated for use in this specific study or for applications necessary to this study. Therefore, the failure of any item or material to meet requirements of the study is no reflection on the quality of a manufacturer's product or on the manufacturer. No criticism of any item or material is implied or intended, nor is any indorsement of any item or material by the USAF implied or intended.

Copies of this report should not be returned to the Aeronautical Systems Division unless return is required by security considerations, contractual obligations, or notice on a specific document.

Qualified requesters may obtain copies of this report from the Defense Documentation Center (DDC), (formerly ASTIA), Arlington Hall Station, Arlington 12, Virginia.

FOREWORD

This report was prepared by the Vought Aeronautics Division of Ling-Temco-Vought, Inc., Dallas, Texas, under contract number AF 33(657)-12517, BPSN number 6299-655A. The contract effort was administered under the cognizance of the Directorate of New Programs and Research Projects (ASZX), Aeronautical Systems Division, Air Force Systems Command, Wright-Patterson Air Force Base, Ohio. The effort described by this report began 1 October 1963 and was concluded 31 December 1964.

Numerous subcontractors and consultants made significant contributions to this report.

This report consists of two parts: PART I - SUMMARY and PART II - TECHNICAL INFORMATION. Part I is a single document summary of the program. Part II is a detailed statement of all the significant technical information gained through the contracted work. A list of the volumes in Part II appears on the following page.

PART II

VOLUME 1	DESIGN AND FABRICATION STUDIES – FLYAWAY
VOLUME 2	AERODYNAMIC ANALYSIS AND TESTS – AIRFRAME
VOLUME 3	STRUCTURES AND MATERIALS – AIRFRAME
VOLUME 4	DYNAMIC ANALYSIS AND TESTS – AIRFRAME
VOLUME 5	NUCLEAR SHIELDING AND RADIATION – AIRFRAME
VOLUME 6	SECONDARY POWER AND AIR CONDITIONING – FLYAWAY
VOLUME 7	RELIABILITY, MAINTAINABILITY AND VALUE ENGINEERING – FLYAWAY
VOLUME 8	NUCLEAR RADIATION EFFECTS TEST NO. 9 – FLYAWAY
VOLUME 9	NUCLEAR RADIATION EFFECTS TEST NO. 10 – FLYAWAY
VOLUME 10	NUCLEAR RADIATION EFFECTS TEST NO. 18 – FLYAWAY
VOLUME 11	GUIDANCE AND MISSION CONTROL – FLYAWAY
VOLUME 12	CONTROLS – FLYAWAY
VOLUME 13	FLIGHT TEST SUBSYSTEMS – FLYAWAY
VOLUME 14	BOOSTER – FLYAWAY
VOLUME 15	PAYLOAD – FLYAWAY
VOLUME 16	SYSTEM SIMULATION
VOLUME 17	BASING, SUPPORT SUBSYSTEMS AND FLIGHT SAFETY STUDIES
VOLUME 18	AIRFRAME, PROPULSION INTEGRATION
VOLUME 1	UNINSTALLED PROPULSION SYSTEM PERFORMANCE
VOLUME 20	AIR INDUCTION SYSTEM CONTROLS ANALYSIS AND TESTS
VOLUME 21	INLET ANALYSIS AND TESTS
VOLUME 22	ONE-THIRD SCALE PROPULSION SYSTEM TEST
VOLUME 23	INLET, BYPASS, AND NOZZLE MECHANICAL DESIGN
VOLUME 24	SYSTEMS ANALYSIS
VOLUME 25	PROGRAM PLANNING

(This abstract is unclassified)

ABSTRACT

Presented in this document are the test results of Nuclear Radiation Effects Test No. 18 which was a dynamic credibility demonstration conducted in the Air Force Ground Test Reactor during the time period of 29 July through 5 August 1964. This work was performed in support of Air Force Contract AF33(657)-12517. Planning and execution of the irradiation provided specific test data on subsystems, components, and materials representative of those which would be used in a nuclear powered ramjet missile. The test articles evaluated were the product of an extensive development program to provide nuclear radiation tolerant subsystems which would meet the LASV-N performance characteristics.

The test articles representing the major subsystem areas (digital computer simulator, A to D shaft position encoder, magnetic core controlled multiplexer, two axis inertial platform subsystem, rate gyros and accelerometers, and electromechanical filter system) were dynamically irradiated during a total exposure of 187 Mw-hrs. Nuclear radiation exposure levels ranged from 9×10^{15} n/cm^2 ($E > 0.3$ Mev) to 1×10^{17} n/cm^2 ($E > 0.3$ Mev), and 1×10^{10} ergs/gm-(C) to 4×10^{11} ergs/gm-(C); with the maximum flux being 5×10^{11} n/cm^2-sec ($E > 0.3$ Mev) and 6×10^{9} ergs/gm-(C)-hr. Detailed results of the irradiation are presented in this report.

This technical report has been reviewed and is approved.

JOHN S. McCOLLOM, Director,
Directorate of New Programs
and Research Projects

TABLE OF CONTENTS

TABLE OF CONTENTS (Continued)

LIST OF FIGURES

LIST OF FIGURES (CONTINUED)

LIST OF FIGURES (CONTINUED)

LIST OF FIGURES (CONTINUED)

LIST OF FIGURES (CONTINUED)

LIST OF FIGURES (CONTINUED)

LIST OF TABLES

LIST OF TABLES (CONTINUED)

1.0 INTRODUCTION

Nuclear Radiation Effects Test No. 18 (RET #18) was conducted in the Air Force Ground Test Reactor during the period from 29 July to 6 August 1964. This was the last major subsystem irradiation scheduled under the LASV-N2 contract. The primary objective was to demonstrate the credibility of developing complex subsystems which could operate reliably in the Low Altitude Supersonic Vehicle nuclear radiation environment.

The test articles listed in Table 1 were dynamically evaluated during the 187 megawatt-hour irradiation. These test articles were specifically developed as part of the LASV-N2 subsystem development program and incorporated state-of-the-art nuclear radiation hardening concepts. A view of the three test pallets located on the north ramp of the Ground Test Reactor complex is shown in Figure 1. Closer detail and test article identification are shown in Figures 2, 3, and 4.

Unless otherwise specified the integrated neutron fluxes expressed in this report are for energies greater than 0.3 Mev.

Manuscript released December 1964 for publication as an ASD Technical Report.

TABLE 1
TEST ARTICLES DYNAMICALLY IRRADIATED IN RADIATION EFFECTS TEST NO. 18

SUBSYSTEM	PALLET POSITION IN THE G.T.R	NO. OF TEST ARTICLES Irr.	DESCRIPTION OF TEST ARTICLE
Computer	North		Digital Computer Simulator
		1	(a) Basic Timing Circuit (BT)
		1	(b) Microprogram Module (MPM)
		1	(c) Input/Output Module (ICM)
		1	(d) Data Memory Module (DMM)
		1	(e) Combined Matrix Register (CMR)
		1	(f) Combined Control Register (CCR)
		1	(g) Combined Address Register (CAR)
		1	(h) Combined Data Register (CDR)
	North	1	V-Scan A to D Shaft Position Encoder
Telemetry	North	2	Four Stage Magnetic Core Controlled Multiplexer
Inertial	West		Two-Axis Platform Subsystem
		1	(a) G9 Gyro*
		2	(b) Electromagnetic Accelerometer (EMA)*
		3	(c) Resolvers*
		2	(d) Torque Motors*
		4	(e) Preamplifiers
		4	(f) Midamplifiers (2 ea for Acc & Gyros)
		1	(g) Platform Control Amplifier
		1	(h) Electromagnetic Accelerometer Control Amplifier
		1	(i) Three Phase Transformer
		4	DC Amplifiers, Chopper Stabilizer
		4	Voltage Reference Devices
		1	Multivibrators
		1	Magnetic Core Reference
		1	Sola Transformer
		2	Quartz Resonators
Controls	East	2	Rate Gyros
		1	Rate Integrator Gyro
			Electro-Mechanical Filter System (Pitch Breadboard)
		2	(a) Vacuum Tube Servo Amplifiers
			(b) Mechanical Package
		2	(1) AC Servo Motors
		2	(2) AC Generators
			(3) Misc Bearings and Gears
		3	(4) Induction Pots.
Rad. Eff.	North	1	Thin-Film Field-Effect Transistors

* Platform Mounted

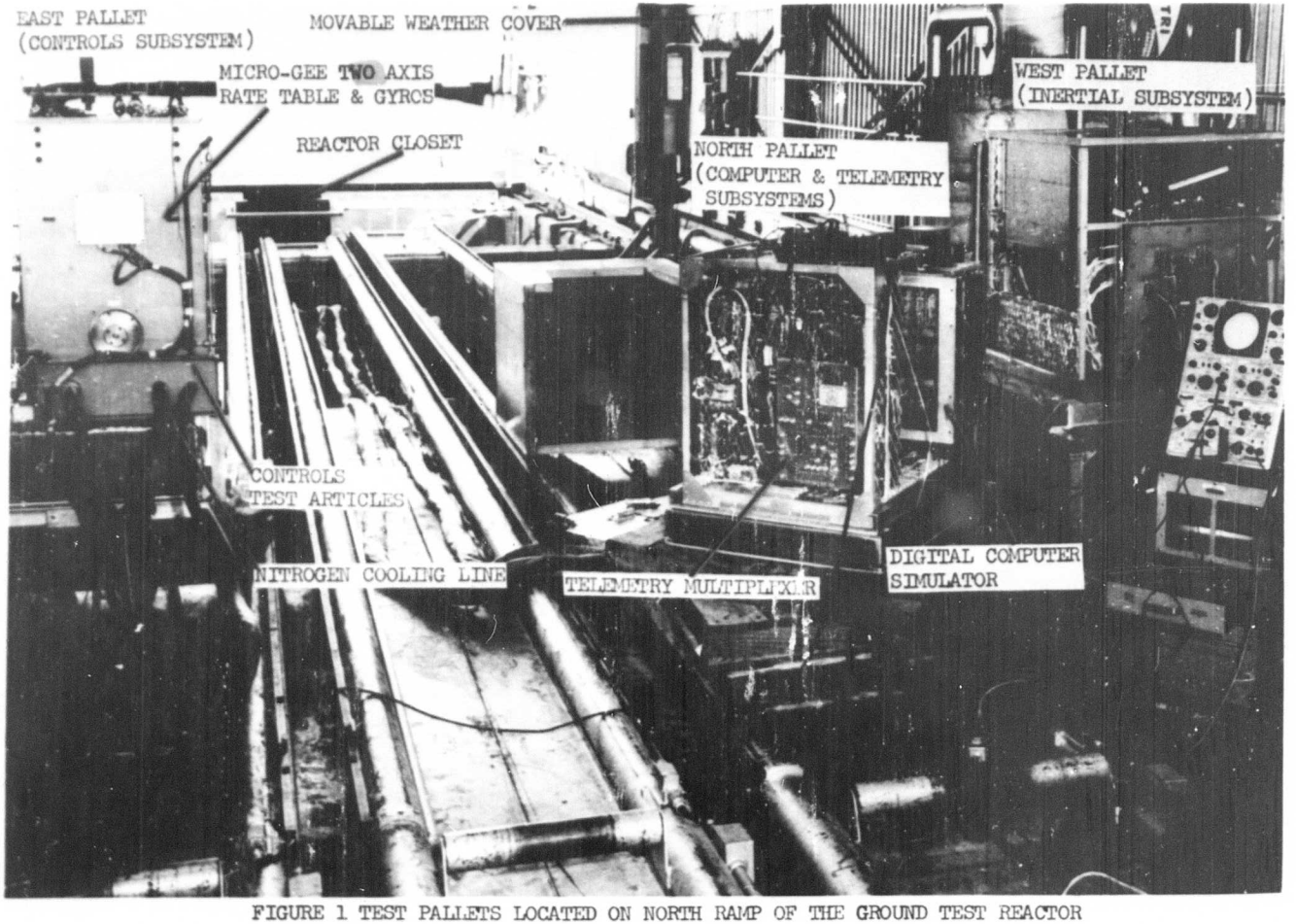

FIGURE 1 TEST PALLETS LOCATED ON NORTH RAMP OF THE GROUND TEST REACTOR

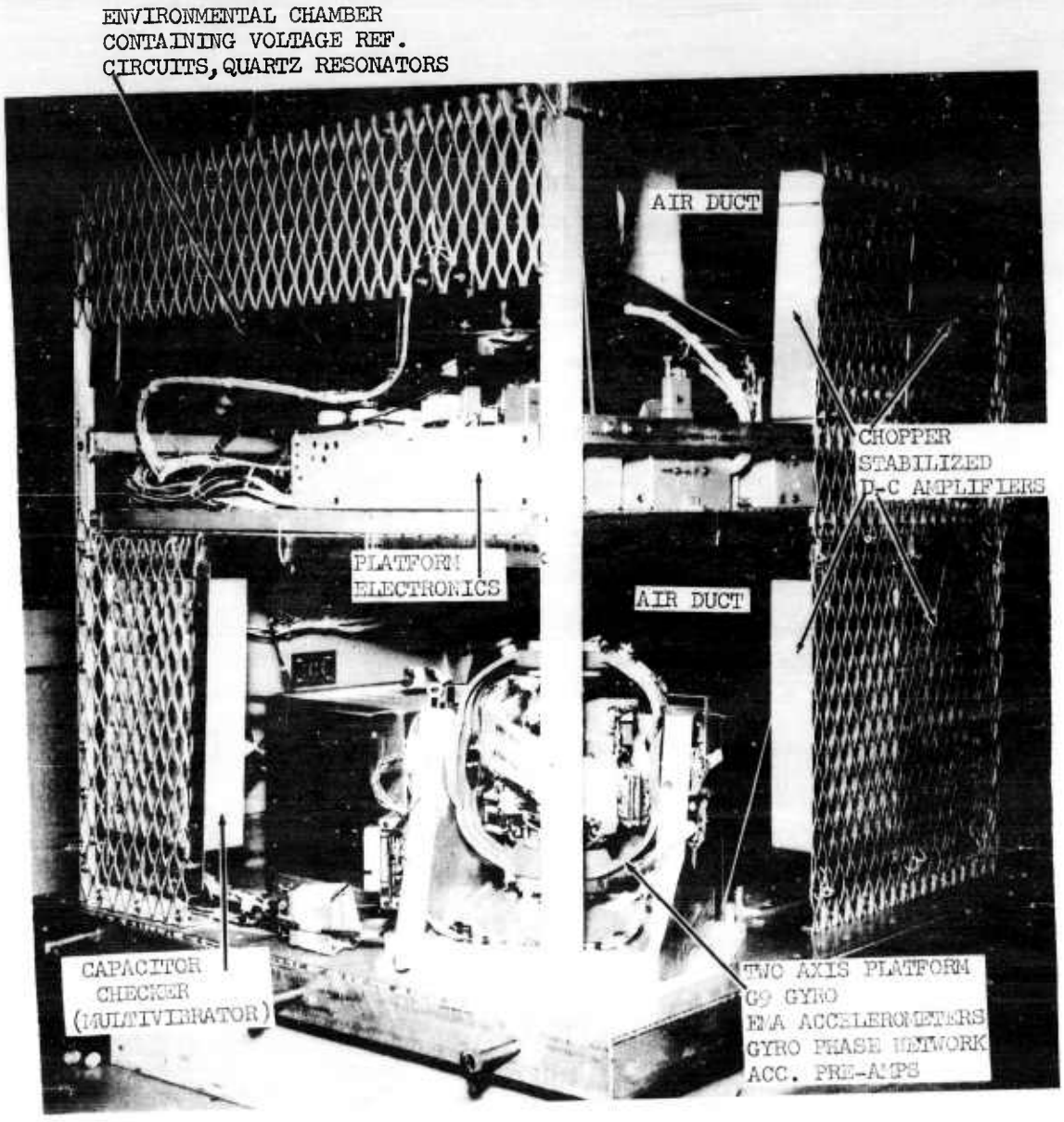

FIGURE 2 WEST PALLET CONTAINING THE INERTIAL SUBSYSTEM TEST ARTICLES

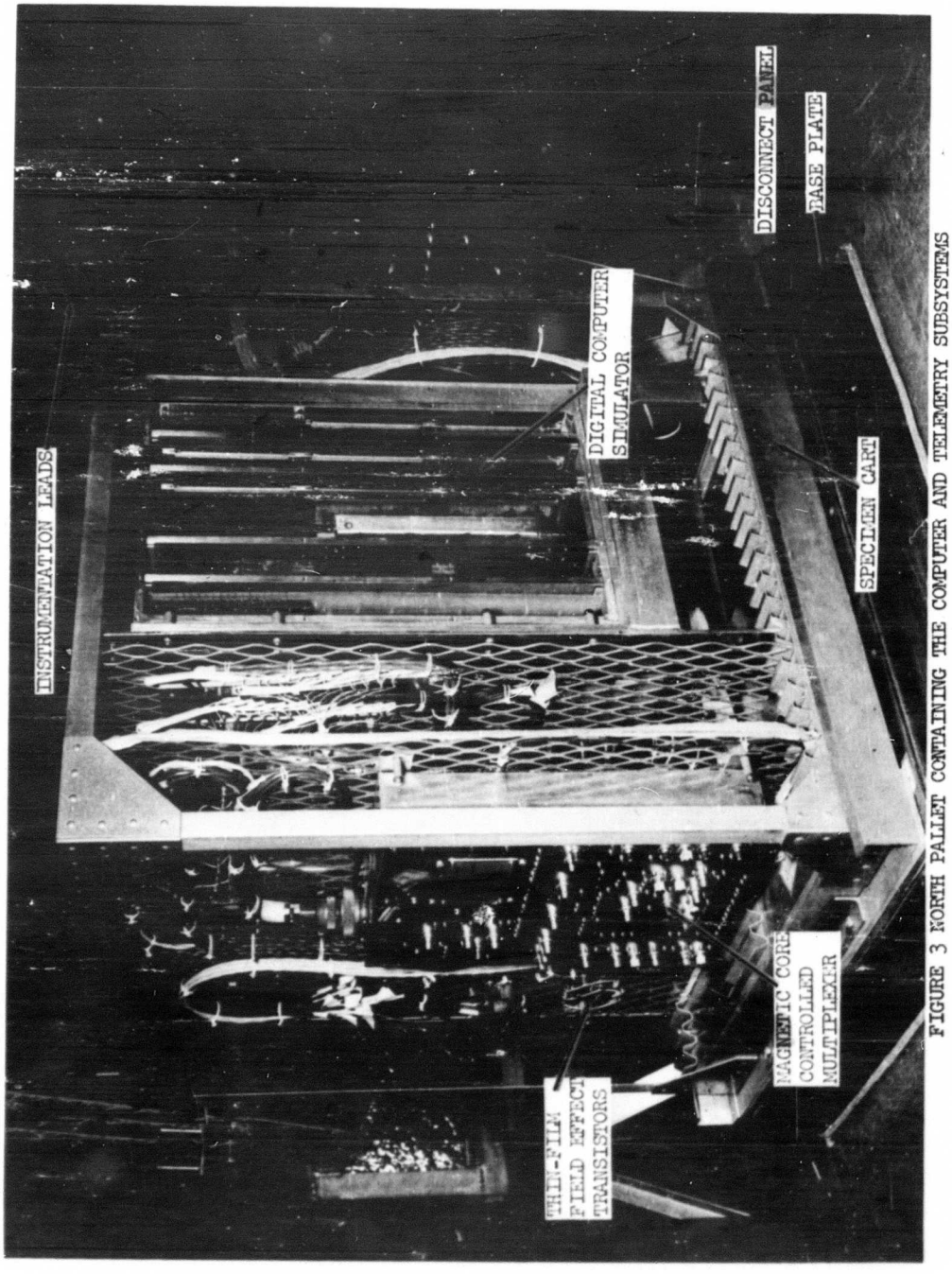

FIGURE 3 MONTH PALLET CONTAINING THE COMPUTER AND TELEMETRY SUBSYSTEMS

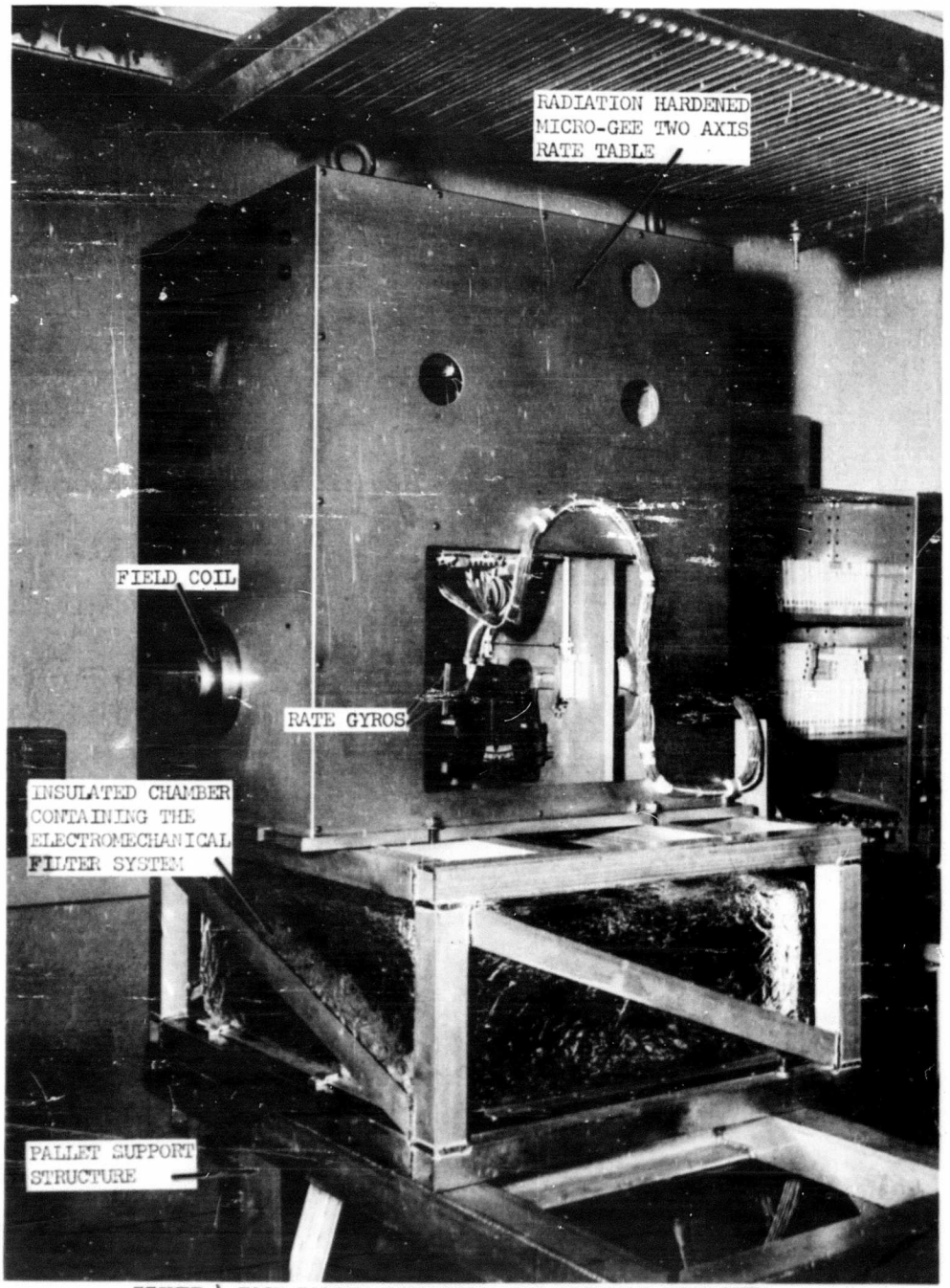

FIGURE 4 EAST PALLET CONTAINING THE CONTROLS SUBSYSTEM

2.0 COMPUTER

2.1 V-SCAN SHAFT ANGLE ENCODER

2.1.1 INTRODUCTION AND TEST ARTICLE DESCRIPTION

Two V-scan shaft angle encoders were procured from Encoder Division, Litton Precision Products, Van Nuys, California. These encoders are electrically identical with the commercially available Model AD11-13M Miniature V-scan Shaft Angle Encoder. This encoder has a range of 8,192 binary counts for 32 revolutions of the input shaft. Readout is 13 bits, serial or parallel, obtained from 8-bit and 5-bit commutating discs connected by a 32 to 1 reduction gear train.

This test was performed to qualify an analog-to-digital device capable of expressing a shaft angle in digital terms compatible with the LASV-N2 central computer input requirements. The V-scan configuration was selected because of its ability to read out a binary number possessing ambiguity only in the least significant digit (LSD) using a minimum number of brushes and no diodes. A detailed discussion of the principles of operation of the V-scan encoder may be found in Reference (1).

2.1.2 NUCLEAR ANALYSIS

Investigation of the materials used in the commercially available Model AD11-13M shaft encoder showed several materials known to be marginal or unsatisfactory at the required nuclear radiation levels. These materials were replaced by more satisfactory materials. A listing of the materials in the encoders as tested is presented in Table 2. The only questionable item not replaced was the commutator disc. Time and expense prohibited replacing this item with one of more radiation-resistant materials. Metallic-clad epoxy resins have been qualified for printed circuits, but have not been previously tested in this application. Since the unit was hermetically sealed, a buildup of hydrogen, oxygen, and chlorine due to outgassing of the potting compound was expected. Since materials in the commutating discs and the percentages of the metals in the brushes were proprietary with the manufacturers, it was not possible to predict the amount of damage to be expected in these components. Formation of $NiCl_2$ and $ZnCl_2$ might result in some slight pitting of the brushes and the formation of some $AlCl_2$ was expected. However, formation of appreciable amount of these chlorides during the irradiation was not anticipated.

TABLE 2

NUCLEAR RADIATION EFFECTS ANALYSIS OF THE V-SCAN ENCODER

NUCLEAR DESIGN REQUIREMENT: GAMMAS: 9(9) ERGS/GM—(C)
NEUTRONS: 5(15) N_v/CM^2

MANUFACTURER: LITTON PRECISION PRODUCTS MODEL: AD 11—13B

CODE NO.	GENERAL DESCRIPTION OF CIRCUIT, PART OR ELEMENT	VALUE	ORIGINAL ELEMENT			LIMITING NUCLEAR EXPOSURE		REMARKS
			PART OR DRAWING NUMBER	MFR	ELEMENT MATERIAL DESCRIPTION	ERGS/GM (C)	N_v/CM^2	
	Lubricant*		335	Standard Oil of Calif.	Nuclear Resistant Grease	1(11)		*Modifications for radiation-hardened unit
	Insulation Tape*				Silicon Rubber	1(10)		
	Flex Circuitry*			DuPont	Mylar	9(9)		
	Potting Compound*		2641 A/B	Emerson & Cummings	Epichlorhydrin of Bisphenol	9(9)		
	Filler				Silica			
	Catalyst				Aliphatic Amine			
	Brush Blocks*				Fiberglass Epoxy	1(11)		
	External Wire*				Irradiated Polyethylene	6(10)		
	Brush Block Adhesive*		Hysol 1C		Epichlorhydrin of Bisphenol	9(9)		
	Filler				Silica			
	Catalyst				Thizatropic Amine			
	Metals		2024-T4 & 6061-T6		Aluminum		>1(18)	
					Brass		>1(18)	
			4130		Steel		>1(18)	
					Copper		>1(18)	
			320, 303, 416 440C		CRS		>1(18)	Corrosive stainless steel
	Solder				63% Pb, 37% Tin		>1(18)	
	Brushes		Paliney #7		Au, Pb, Ag, Cu, Ni, Zn		>1(18)	% proprietary with mfr
	Commutative Disc.					1(11)		Composition proprietary with manufacturer
	Disc				Fiberglass Epoxy	"		
	Cladding				Gold Alloy	"		

NOTES: (X) INDICATES POWERS OF TEN

2.1.3 TEST PROCEDURE

Development of the necessary interfacing circuitry and program permitted using the SDS 920 computer to both control and monitor these test articles. Backup capabilities were also provided to monitor each brush individually in both the forward and reverse direction using a Tektronix 545 oscilloscope. Figure 5 is an instrumentation block diagram of the test as it was performed.

Figure 6 is a flow chart of the test program developed. As shown on the timing chart of Figure 6, a delayed ready signal was generated each time the LSD bit changed state. The variable ready signal delay permitted delaying initiation of the ready signal beyond an intermittent pulse which was observed immediately behind the trailing edge of the LSD high state. Upon initiation of the test program, a forward direction search for an "all one's" condition on the lag brushes was performed. During coincidence of the "ready" signal and "PIN" signal following each subsequent transition of the LSD bit, all lead and lag brush states were read and their states stored in memory. During the work comparison routine, the word formed by the brushes was compared to the current word stored in the counter. If the two words were not in agreement, an error routine was run which logically compared the lead brush word to the counter word and the lag brush word to the complement of the counter word to determine the bit states in error. Errors were totaled in memory by bit position and retrieved at the end of the test cycle. A similar test cycle was then run in the reverse direction. Table 3 is a sample routine for determining whether errors were obtained during a "read" period and, if so, which brushes were in error.

Since both the servo motor and the gear box were mounted on the pallet and subjected to the same radiation environment as the encoder, care was taken to ensure that they would operate satisfactorily to the end of the test. All nuclear radiation sensitive materials were replaced with materials which had been previously qualified to the anticipated test radiation levels.

2.1.4 TEST RESULTS AND CONCLUSIONS

The shaft encoder test article received a gamma exposure of 2.9×10^{11} ergs/gm-(C) and an integrated neutron flux of 8.3×10^{16} n/cm^2 during 69 hours of reactor operation as shown in Figure 7. Test article ambient temperature was monitored continuously throughout the test and was found to remain within a 105° ($\pm 10^{\circ}$)F envelope. A test cycle was run using the Data Management System (DMS) every one to two hours and the various bits were periodically monitored visually to check for noise and waveform degradation.

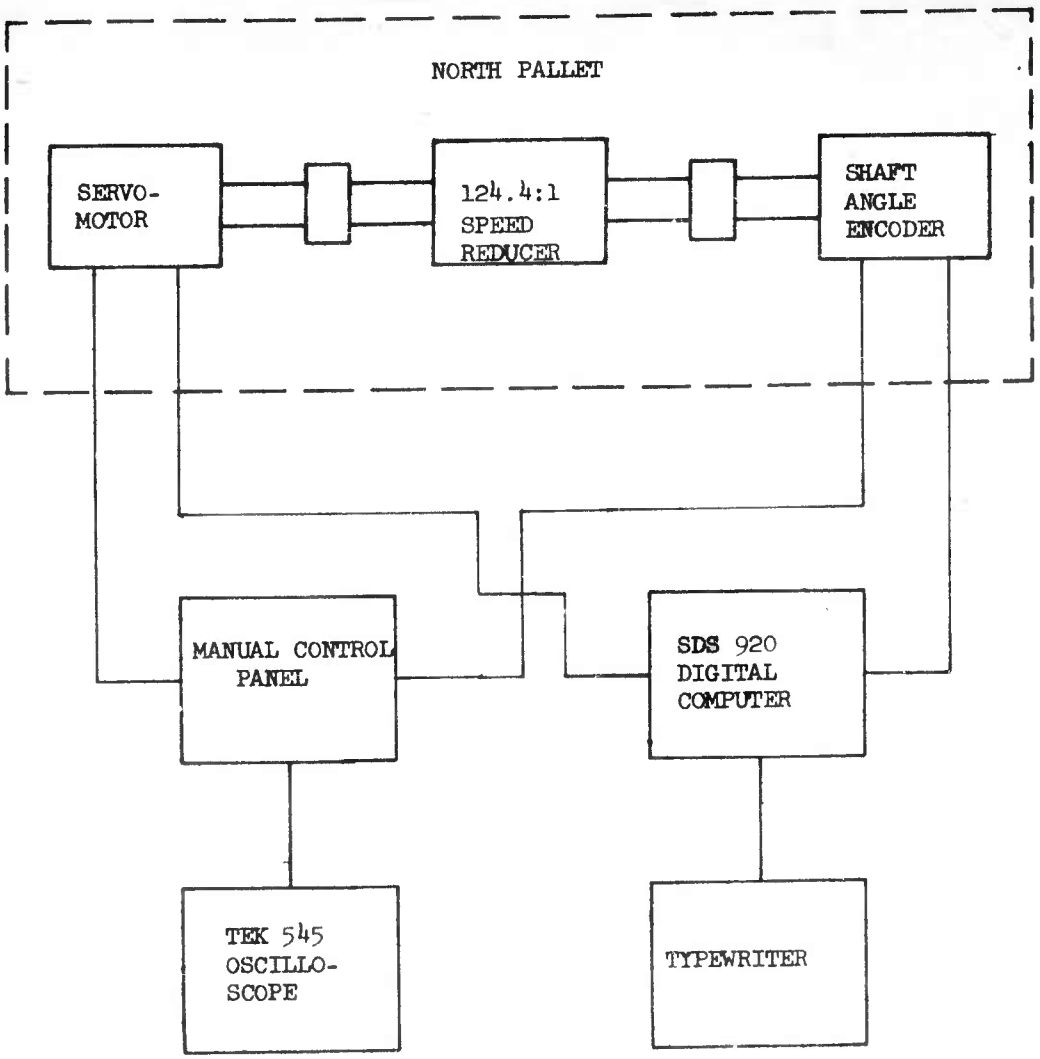

FIGURE 5 SHAFT ANGLE ENCODER TEST INSTRUMENTATION BLOCK DIAGRAM

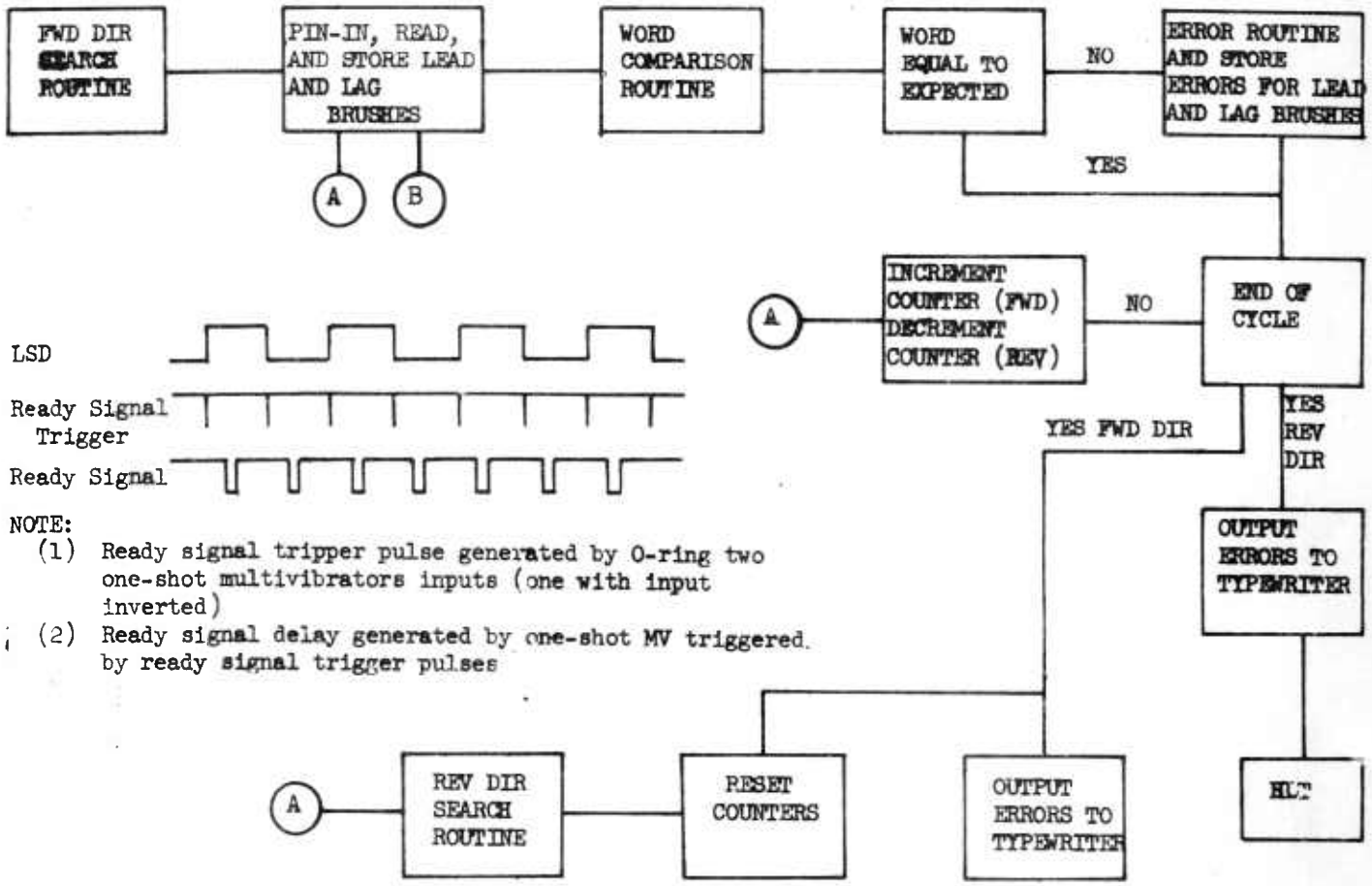

FIGURE 6 SHAFT ANGLE ENCODER TEST PROGRAM FLOW CHART AND TIMING CHART

TABLE 3 (SHEET 1) SHAFT ANGLE ENCODER TEST SAMPLE ROUTINE

Bit	2^{12}	2^{11}	2^{10}	2^{9}	2^{8}	2^{7}	2^{6}	2^{5}	2^{4}	2^{3}	2^{2}	2^{1}	LSD	Remarks
Lead brush	0	0	0	1	0	1	0	1	1	1	0	1	1	Correct word -
Lag brush	0	0	0	1	0	1	0	1	0	1	0	1	1	01253
Lead brush	0	1	0	1	0	1	0	0	1	1	0	1	1	Error word stored -
Lag brush	0	0	0	1	1	1	0	1	0	1	0	0	1	05611
														Word comparison routine -
LDA	0	0	0	1	1	1	0	1	0	1	0	0	1	Lag brush word
RSH 1	0	0	0	0	1	1	1	0	1	0	1	0	0	Shifted out LSD bit stored
ETR	0	0	0	1	0	1	0	1	0	1	0	1	1	Computer word (01253)
RA (1)	0	0	0	0	0	1	0	0	0	0	0	0	0	Stored
LDA	0	1	0	1	0	1	0	0	1	1	0	1	1	Lead brush word
RSH 1	0	0	1	0	1	0	1	0	0	1	1	0	1	Shifted out LSD bit stored
ETR	1	1	1	0	1	0	1	0	1	0	1	0	0	Complement of counter word
RA (2)	0	0	1	0	1	0	1	0	0	0	1	0	0	Stored
MRG RA (1) & RA (2)	0	0	1	0	1	1	1	0	0	0	1	0	0	Stored words merged
LSH 1	0	1	0	1	1	1	0	0	0	1	0	0	1	Stored LSD bits merged
														Error word (05611) displayed
														Error routine -
LDA	0	1	0	1	1	1	0	0	0	1	0	0	1	Error word (05611)
EOR	0	0	0	1	0	1	0	1	0	1	0	1	1	Counter word (01253)
RA (3)	0	1	0	0	1	0	0	1	0	0	0	1	0	"1's" indicate bit errors
RSH 1	0	0	1	0	0	1	0	0	1	0	0	0	1	Store
ETR	0	0	0	1	0	1	0	1	0	1	0	1	1	Counter word (05611)
LDA	0	0	1	0	0	1	0	0	1	0	0	0	1	Stored RSH 1
ETR	1	1	1	0	1	0	1	0	1	0	1	0	0	Complement of counter word
RA	0	0	1	0	0	0	0	0	1	0	0	0	0	Lead brush errors bits right of "1's"

TABLE 3 (SHEET 2) SHAFT ANGLE ENCODER TEST SAMPLE ROUTINE

ETR	EOR	MRG	
A · M = A	A ⊕ M = A	A + M = A	LDA - load A Register
0 0 0	0 0 0	0 0 0	RSH 1 - right shift 1 bit
0 1 0	0 1 1	0 1 1	ETR - extract (AND)
1 0 0	1 0 1	1 0 1	RA - register A
1 1 1	1 1 0	1 1 1	MRG - merge (OR)
			EOR - Exclusive OR
			LSH 1 - left shift 1 bit

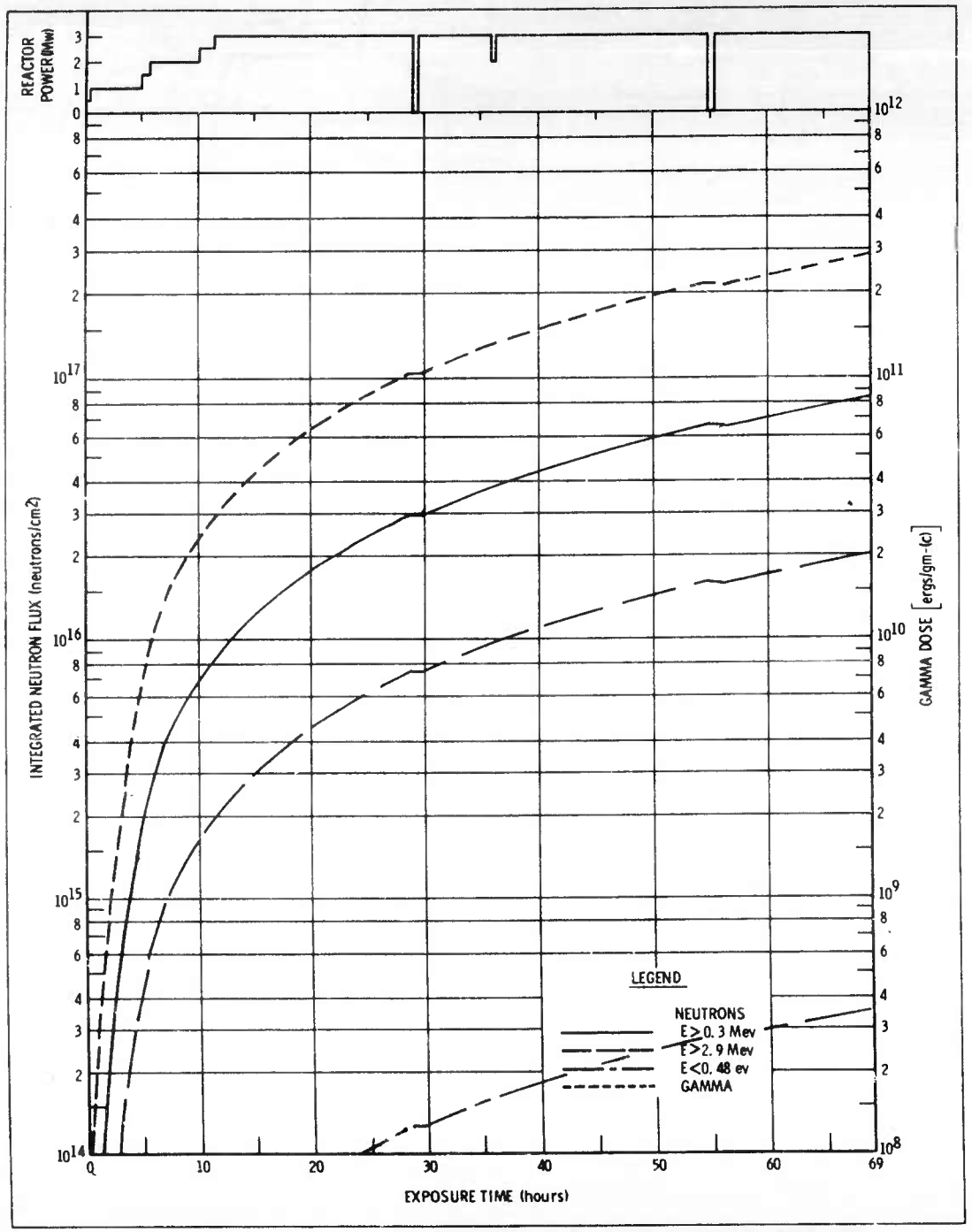

FIGURE 7 NUCLEAR RADIATION EXPOSURE OF THE LITTON ENCODER

The first error counts occurred after about 10 hours of exposure (1.6×10^{10} ergs/gm-(C) and 5×10^{15} n/cm^2). These errors were normally single counts and were on the lag brushes of bit positions 4 and 5. At that time most data runs were still error-free. By the time an integrated flux of 8×10^{15} n/cm^2 was reached, random errors were appearing in nearly every reverse direction print-out. These errors were usually 1 or 2 counts, on bit positions 2 through 6, and normally on the lag brush. The first error count in the forward direction appeared at about this time. Other than random single counts, error counts did not appear in the forward direction until the unit had received an integrated neutron exposure of 1.5×10^{16} n/cm^2. Large error counts on the zero bit position indicated damage to LSD bit segments. This damage was such as not to affect operation in the reverse direction and eventually cleared. At 4×10^{16} n/cm^2 only a few random error counts were being obtained in both directions. However, at 4.5×10^{16} n/cm^2 appreciable error counts were appearing in both directions on both brushes. These error counts gradually increased in number and appeared on more bit positions until by the time a total exposure of 6×10^{16} n/cm^2 was reached, all bit positions were recording errors in both directions on both brushes.

Visual monitoring of the bit positions during the test showed a gradual increase in noise with the lag brushes normally exhibiting the greater amounts. This noise varied with rotation direction, brush and bit, with the worst spikes of milliseconds duration and amplitude comparable to bit "1" state amplitude. Initially this noise was observed for the first few shaft rotations after a period of exposure during which the disc was not rotated. This would indicate formation of an insulated coating, such as an oxide, on the bit segments. This noise later became permanent, indicating damage to the segments themselves.

During post-irradiation analysis, the second encoder was operated for about 500,000 revolutions and then both units were disassembled and examined. The mylar flex circuitry and the brush blocks of the irradiated unit were found to have become rather brittle, although not enough to have affected operation of the unit under vehicle environmental conditions. When examined under a magnification of 10, the brushes of both units showed no evidence of wear or pitting. The commutating discs of both units were worn under the brush tracks. Under magnification, both the epoxy and the gold cladding of the unirradiated disc showed some grooving with the cladding worn away at the edges of some of the bit segments, and gold flaking distributed on the insulation areas. The disc of the irradiated unit, with possibly one-fourth the wear, showed extensive damage. The epoxy was badly grooved and the segment cladding was wiped out onto the epoxy as though the cladding had softened during exposure. In one instance, the cladding extended almost completely across the insulated area to the next segment. Although the cladding did not separate from the epoxy disc during the test, it was much easier to remove than was the cladding of the unirradiated unit.

Test results and post-irradiation analysis indicate that, while a metallic-clad epoxy is satisfactory for applications where sliding contact is not made with the cladding, its use in this instance is marginal. Damage appears to be a function of the nuclear radiation exposure level and use rate. Although the encoder was tested only at comparatively low speed (approximately 90 shaft revolutions per minute), it is probable that high-speed operation, such as slewing, would increase the damage rate. Before additional testing of the encoder is undertaken, it is recommended that either the commutating disc be hardened or a contactless principle such as that used in the Litton Model MAD11-13A Non-Contact Magnetic Encoder be used. If the latter principle is employed, the materials used in the commutating disc of the unit tested are probably satisfactory.

2.2 GUIDANCE COMPUTER

2.2.1 INTRODUCTION AND TEST ARTICLE DESCRIPTION

This test was performed to evaluate the operation of a breadboard digital computer in a nuclear environment. The computer test vehicle, developed by Burroughs Corporation, Paoli, Pennsylvania, and designed to the general specifications listed in Table 4, contains all of the major functional elements of a guidance computer. All components and types of circuits used have been satisfactorily tested in earlier LASV-N radiation effects tests.

TABLE 4

COMPUTER TEST VEHICLE GENERAL SPECIFICATIONS

Characteristic	Description
Computer Type	Parallel, digital, single address, general purpose
Number Representation	Binary, two's complement, fixed point, fractional
Data Word	16 bits, including sign
Data Memory	64 words, 16 bits, coincident-current ferrite core, destructive read-out
Program Word	13 bits (operation code - 7; operation address - 6)
Program Memory	Externally programmed, with transmission of single instructions to Test Vehicle
Microprogram Memory	43 words, 22 bits, core rope, fixed storage
Clock Rate	100 kilocycles
ADD time	30 microseconds
Output	Parallel transmission of accumulator contents
Input	Parallel transmission of instruction word

2.2.1.1 Test Vehicle Description

The test vehicle was 20 5/8 inches wide, 14 11/16 inches deep, and 18 11/16 inches high, weighed 80 pounds, and consumed approximately 500 watts of power. It contained the five major logic units discussed below and shown in Figure 8 and was designed to perform the thirteen instructions listed in Table 5. A detailed description of its operation and construction is contained in Reference (2). Table 6 lists the components used in the test vehicle.

TABLE 5

COMPUTER TEST VEHICLE INSTRUCTIONS

Order Code	Code Name	Execution Time (μs)	Microprogram Address
CLA	Clear Load Accumulator	30	01
STA	Store Accumulator	30	02
CLC	Clear Load Constant	30	03
SLC	Shift Load Constant	20	04
ADD	ADD	40	05
XOR	Exclusive-OR	30	06
IOR	Inclusive-OR	40	07
LAN	Logical-AND	40	10
MXR	Matrix Exclusive-OR	20	11
SAR	Shift Accumulator Right	20	12
LIN	Logical Inverse	20	13
INA	Increment Accumulator	30	14
TAR	Telemetry Accumulator	160	15

2.2.1.2 Test Vehicle Functional Description

The five assemblies performing the logic functions of the test vehicle are shown in Figure 8. This logic was designed to simulate as closely as possible the logic requirements of the anticipated final computer configuration. Table 7 is a glossary of abbreviations used to describe the various circuits and units of the test vehicle.

2.2.1.2.1 Basic Timing Unit

The basic timing unit of the test vehicle receives from external pulse generators an A-phase timing pulse and a B-phase timing pulse. From these two pulses, the basic timing unit generates the timing pulses used throughout the test vehicle. A complete cycle, consisting of two A-phase clocks and three B-phase clocks, is 10 microseconds. This allows the 100 kc operation of the test vehicle. A block diagram of this unit is shown in Figure 9.

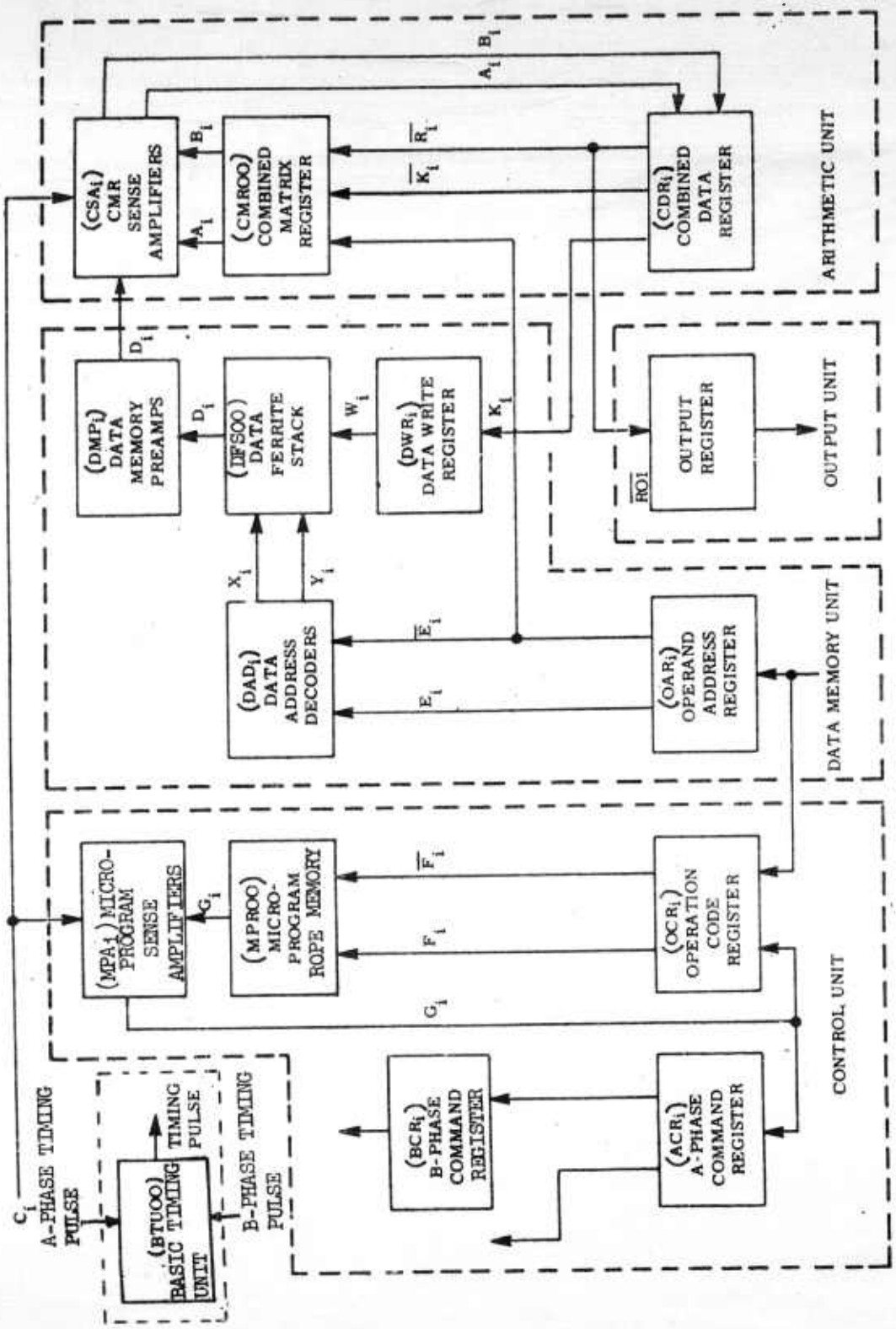

FIGURE 8 COMPUTER TEST VEHICLE LOGIC FUNCTIONAL ASSEMBLIES

TABLE 6 LISTING OF PARTS AND MATERIALS USED IN COMPUTER TEST VEHICLE

Item No.	CBR	CDR	CRA	MPR	OAR	OCR	DWR	AC1	AC2	AC3	SC1	AC4	AC5	BC1	BOR	DL	DAD	OPS	DMP	SPA	DLD	STTO	DG	TRO	BRORO	TCD	SP-	D--T	CB-T	Backplane & Trays	Terminal Board	Cabinet
1	X	X	X	X	X	X	X	X	X	X	X	X	X	X	X	X	X	X	X	X	X	X	X	X	X	X	X	X	X	X	X	
2	X	X	X	X	X	X	X	X	X	X	X	X	X	X	X		X	X	X	X	X	X	X	X	X	X	X	X	X			
3		X	X		X	X		X	X	X	X	X	X	X	X		X		X	X	X	X	X	X	X	X	X					
4	X			X	X	X	X	X	X	X	X	X	X	X	X		X	X		X	X	X	X	X	X		X	X	X		X	
5		X	X		X	X	X	X	X	X	X	X	X	X	X		X	X	X	X	X	X	X	X	X	X	X	X	X		X	
6	X	X		X	X	X	X	X	X	X	X	X	X	X	X		X			X	X	X										
7																		X										X	X			
8																											X				X	
9		X	X		X	X	X	X	X	X	X	X	X	X	X		X		X									X	X			
10																				X	X	X	X	X	X	X	X					
11			X			X		X	X	X		X	X		X				X									X	X			
12			X			X		X	X	X		X	X		X				X									X	X			
13			X																X	X	X	X	X	X	X	X	X					
14			X																X	X	X	X	X	X	X	X	X					
15			X																X	X	X	X	X	X	X	X						
16																				X			X				X	X	X			
17			X																X	X	X	X	X	X	X	X	X	X	X			
18			X																X	X	X	X	X	X	X	X		X				
19			X																													
20																								X	X	X	X	X	X			
21			X																	X					X	X	X	X	X			
22			X																X								X					
23			X																X	X			X				X					
24		X	X																X							X						
25			X																X													
26																				X	X	X	X	X	X	X						
27			X																X													
28			X																X							X						
29																				X	X	X	X	X	X							
30			X																X	X	X	X	X	X	X	X						
31			X																X	X	X	X	X	X	X	X	X	X	X			
32			X																X	X	X	X	X	X	X	X						
33																		X									X	X	X			
34																														X		
35																														X		
36																X																
37																														X		X
38	X			X																										X		
39			X			X		X	X	X		X	X		X				X	X	X	X	X	X	X	X	X	X	X	X		X
40	X	X	X	X	X	X	X	X	X	X	X	X	X	X	X	X	X	X	X	X	X	X	X	X	X	X	X	X	X	X	X	

Item No.	ITEM	PART OR TYPE NO.	MANUFACTURER	MATERIALS
1	Hook-up wire		Raychem	Irradiated polyethylene over copper.
2	Magnet wire			Formvar over copper. / Polyurethane over copper.
3	Logic diode	hpa 1004	Hewlett Packard	Silicon epitaxial in miniature glass case.
4	Glass/epoxy board	G10		Epoxy impregnated glass cloth.
5	Lugs		Cambridge Thermionic	Silver plated brass.
6	Bimag core	2301 __ series	Burroughs EID	4-79 Molypermalloy tape, 303 stainless bobbin, MgO insulation, high density polyethylene cover.
7	Toroid	333-M1	RCA	Wide temperature square loop ferrite.
8	Toroid	CF101	Indiana General	T1 type non-square ferrite.
9	Header (core holder)		Fabricated	Gold plated pins in "Marlex" (irrad. polyethylene).
10	Header (core holder)	12903088	Burroughs	Gold plated pins in glass filled diallyl-phthalate. (Special approval See text)
11	Cup core	333 P 133 B4-3C	Ferroxcube	3C type non-square ferrite.
12	Bobbin	333 F 170	Ferroxcube	Nylon.
13	Cup core	CE 300	Indiana General	T1 type non-square ferrite.
14	Bobbin	070 F280	Ferroxcube	Nylon . (Special approval. See text.)
15	Shield bead	K300-100-3B	Ferroxcube	3B type non-square ferrite.
16	Resistor	RS-2C series	Dale	Wire-wound, silicon encapsulated.
17	Resistor	Types A and C	Corning Glass	Tin oxide on glass.
18	Capacitor	03F series	General Electric	Aluminum on Mylar.
19	Capacitor	CY series	Corning Glass	Glass ribbon, aluminum foil.
20	Capacitor		Centralab	Disc ceramic.
21	Capacitor	SC11	Sprague	Monolithic ceramic.
22	Choke	4435-13	Jeffers	Copper on phenolic coil form.
23	Choke	1313, 1315, 4485 series	Jeffers	Copper on iron coil form.
24	Printed circuit board	Photoceram	Corning Glass	Copper on ceramic boards.
25	Tunnel diode	1N3718	General Electric	Germanium, metal case.
26	Nuvistor triode	A15330	RCA	Metal-ceramic case.
27	Nuvistor Tetrode	7587	RCA	Metal-ceramic case.
28	Tube socket	13305 10 000	Cinch	Mica-filled epoxy.
29	Tube socket	13365 10 002	Cinch	Mica-filled epoxy.
30	Heat convectors	NF300 series TR 101 TR 102	Wakefield Engineering ICE Inland Co. ICE Inland Co.	Beryllium copper. Beryllium copper. Beryllium copper
31	Mylar tape	#56	Scotch	Mylar.
32	Mylar washers	0.002" Mylar	Transil Wrap Co.	Sheet Mylar.
33	Cement (corona dope)	GC-50	GC Electronic	Polyester-modified phenolic, red enamel, silicon.
34	Circuit board clamps			Beryllium copper.
35	Shock absorbers	#3146/33	Scotch	Polyethylene.
36	Delay line		ESC Corporation	Corning Glass capacitors, glass coil form inductors, steel enclosure with glass-to-metal compression sealed terminals, potted with beach cend.
37	Aluminum			Aluminum.
38	Connector		ELCO	Gold plated beryllium copper contacts in machined G10 glass epoxy.
39	Screws, nuts, washers, spacers and lockwashers			Stainless steel or cadmium plated steel
40	Solder	60/40	Kester	60% Sn, 40% Pb

TABLE 7 (SHEET 1) GLOSSARY OF ABBREVIATIONS

ABBREVIATION	MEANING
ABC	Steered "B" Time Current - Sets A and B command register and operation code register
AC	"A" Command Register
BC	"B" Command Register
BTUOO	Basic Timing Unit
CDR	Combined Data Register-Composed of DR and DK registers
CMROO	Combined Matrix Register
CSA	Combined Sense Amplifier
DAD	Data Address Decoder
DFSOO	Date Ferrite Stack
DG	Driver Gate - Supplies current source to control drivers output
DK	One of two registers of combined data register in which the logical AND function is performed
DL	Delay Line
DMP	Data Memory Preamplifier
DR	One of two registers of combined data register in which the logical Exclusive-OR function is performed
DWR	Data Write Register
DX	Distribution Transformers
EOI	End of Instruction - Signal to interface indicating the end of instruction
IU	Interface Unit
MPA	Microprogram Sense Amplifiers
MPROO	Microprogram Rope
MRP	Data Memory Read Pulse
MWP	Data Memory Write Pulse

TABLE 7 (SHEET 2) GLOSSARY OF ABBREVIATIONS

ABBREVIATION	MEANING
OAR	Operand Address Register
OCROO	Operation Code Register
RMO	Reset Matrix and Output Cores - Resets matrix register, serial output cores, and microprogram memory
ROA	Read Operand Address Register
SOROO	Serial Output Register
SPA	Sense Preamplifier
SPA1	Strobe Preamplifier of Matrix Register and Microprogram Register
SPA2	Strobe Preamplifier of Data Memory
SSGBO	Sense Screen Grid Blocking Oscillator
SSG1, SSG2	Sense Screen Grid of Sense Amplifiers
STBO	Self-Timed Blocking Oscillator - Triggered ON, timed by square core
TBO	Triggered Blocking Oscillator
TCD	Triggered Current Driver

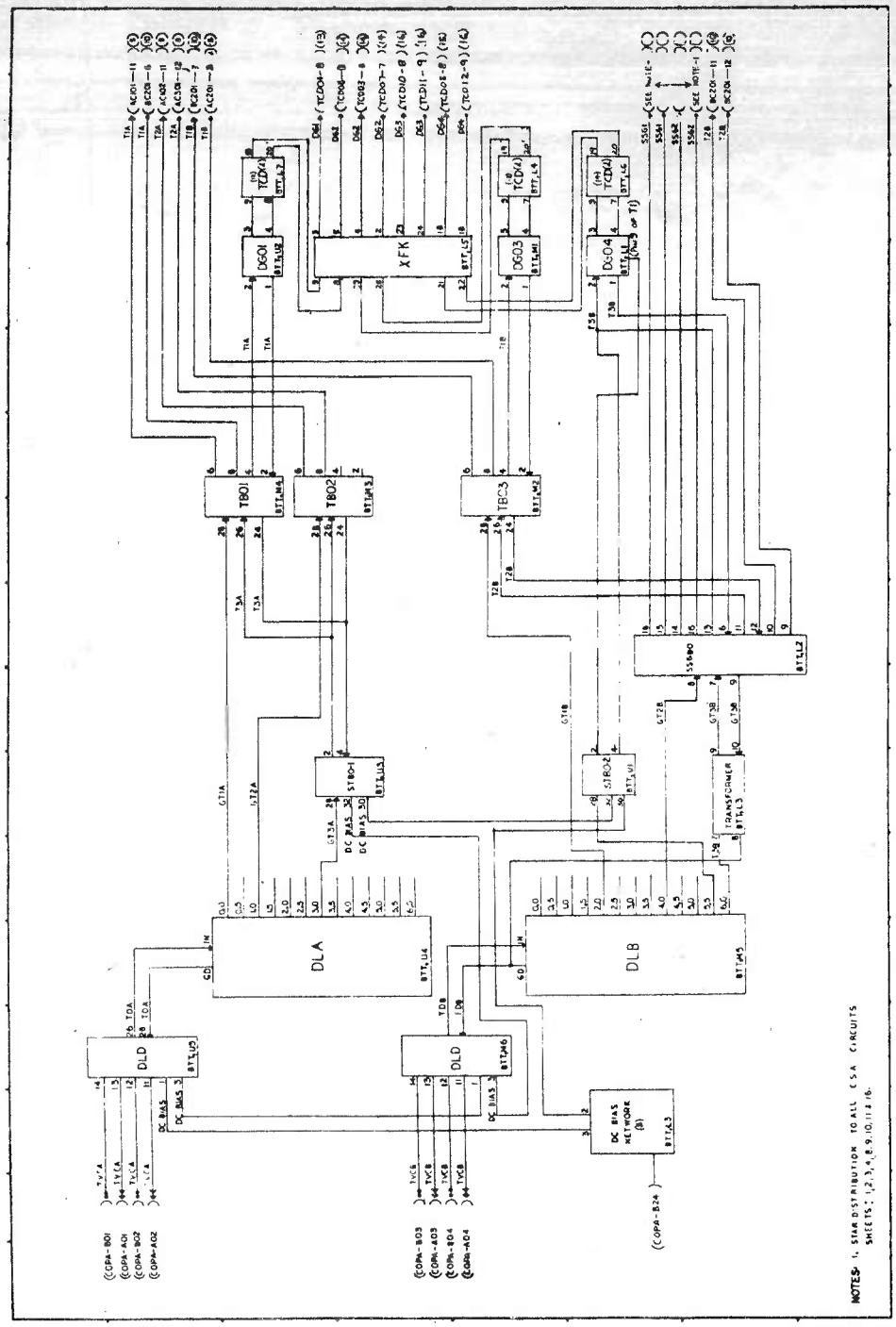

FIGURE 9 BLOCK DIAGRAM OF COMPUTER TEST VEHICLE BASIC TIMING UNIT

2.2.1.2.2 Control Unit

The control unit is composed of the microprogram memory, the memory sense amplifiers, the command registers, and the operation code register.

The microprogram memory (Figure 10) is a magnetic-core rope memory consisting of 43 cores, each of which contains a 22-bit command word composed of a 15-bit subcommand field and a 7-bit address field. To execute an instruction, three or more command words must be removed from memory. The location of the first command word is specified by the operation code of the instruction word, and the location of each subsequent command word is specified by the address field of the previous command word.

Each of the 43 cores of the microprogram memory stores one command word, which contains all of the necessary subcommands to execute one instruction cycle, as well as the address of the next instruction cycle. Each microprogram memory sense line represents a subcommand. If a particular subcommand is to be performed during a given instruction cycle, then its associated line will thread the core containing the subcommands for that instruction cycle. When that core is addressed, an output will be produced on that sense line.

The command register is divided into two registers: the A-command register (Figure 11) commands during A-phase of the cycle, and the B-command register (Figure 12) commands during B-phase of the cycle. The A-command register is an 18-bit, 36-core register, and the B-command register is a 13-bit, 26-core register. The registers have two types of core circuits; a trigger type and a current steering type. The trigger type circuit is used to trigger a triggered current driver (TCD) when that core has been set by microprogram. The current steering type circuit steers the current of a triggered TCD when that core has been set by microprogram. Employment of the current steering circuit allows the use of one TCD for several subcommands.

During the B-phase of the first cycle, the subcommands are removed from the microprogram memory and set into the A-command register. In the A-phase of the following cycle, those A-phase subcommands which were read out of the microprogram in the previous cycle are generated and the B-command register is set by the A-command register. In B-phase of the cycle, those subcommands which were set in the B-command register by the A-command register in A-phase are now generated. Also, the A-command register is again set by the microprogram with subcommands of the next cycle.

The operation code register (Figure 13) is a 7-bit, 14-core register which is also the address register for the microprogram memory. The address is received either from the interface

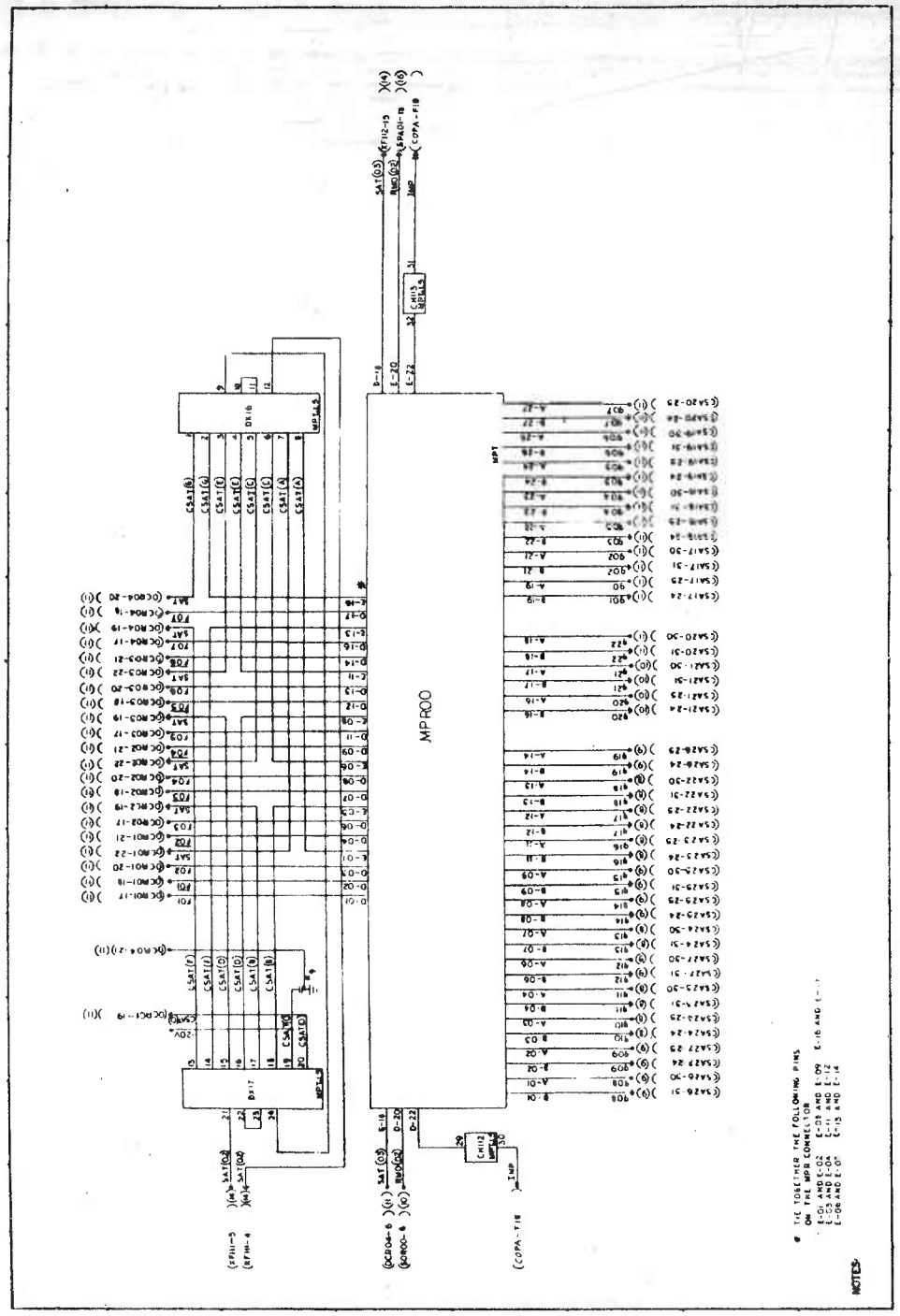

FIGURE 10 BLOCK DIAGRAM OF COMPUTER TEST VEHICLE MICROPROGRAM ROPE MEMORY

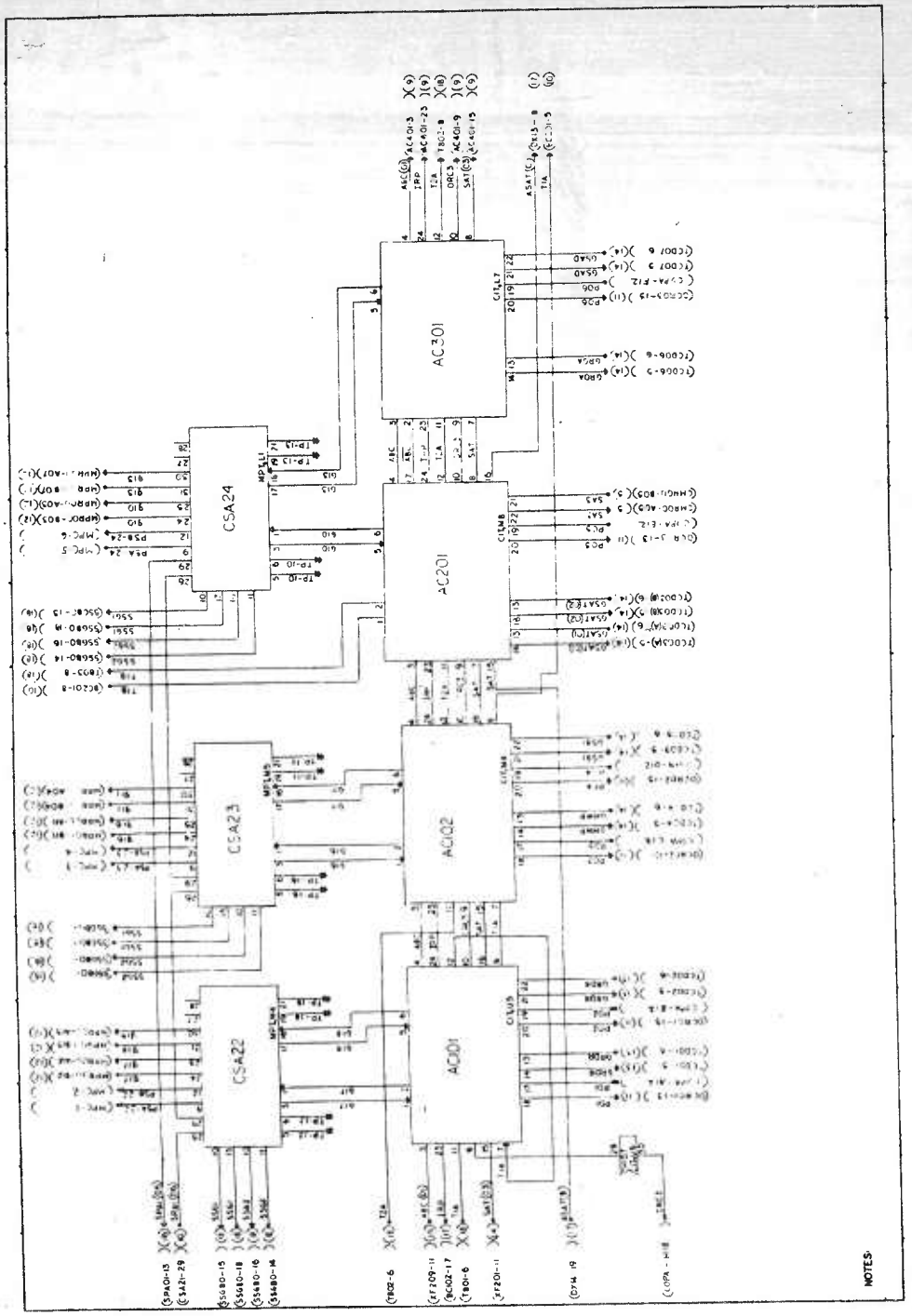

FIGURE 11 (SHEET 1) BLOCK DIAGRAM OF COMPUTER TEST VEHICLE A COMMAND REGISTER

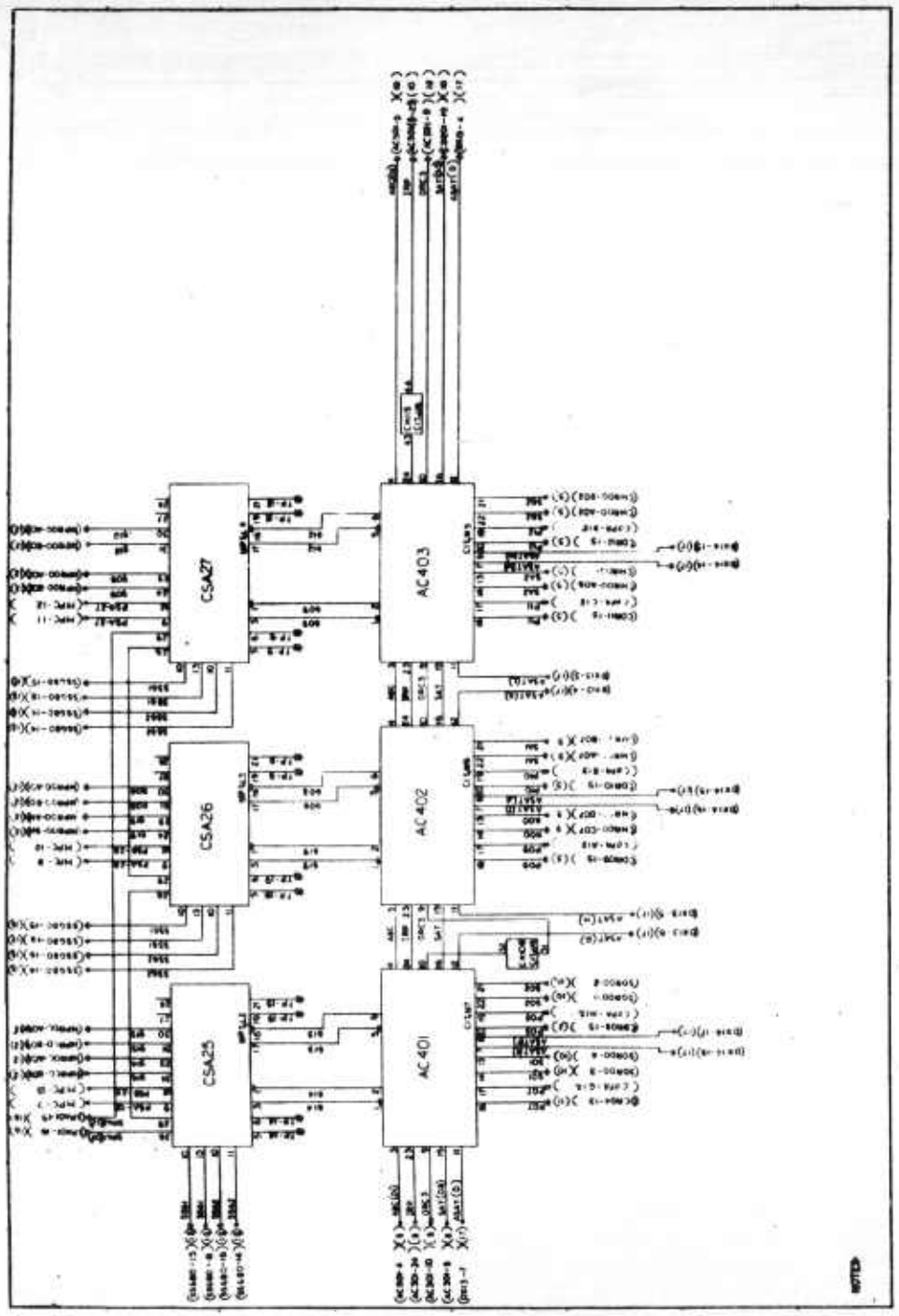

FIGURE 11 (SHEET 2) BLOCK DIAGRAM OF COMPUTER TEST VEHICLE A COMMAND REGISTER

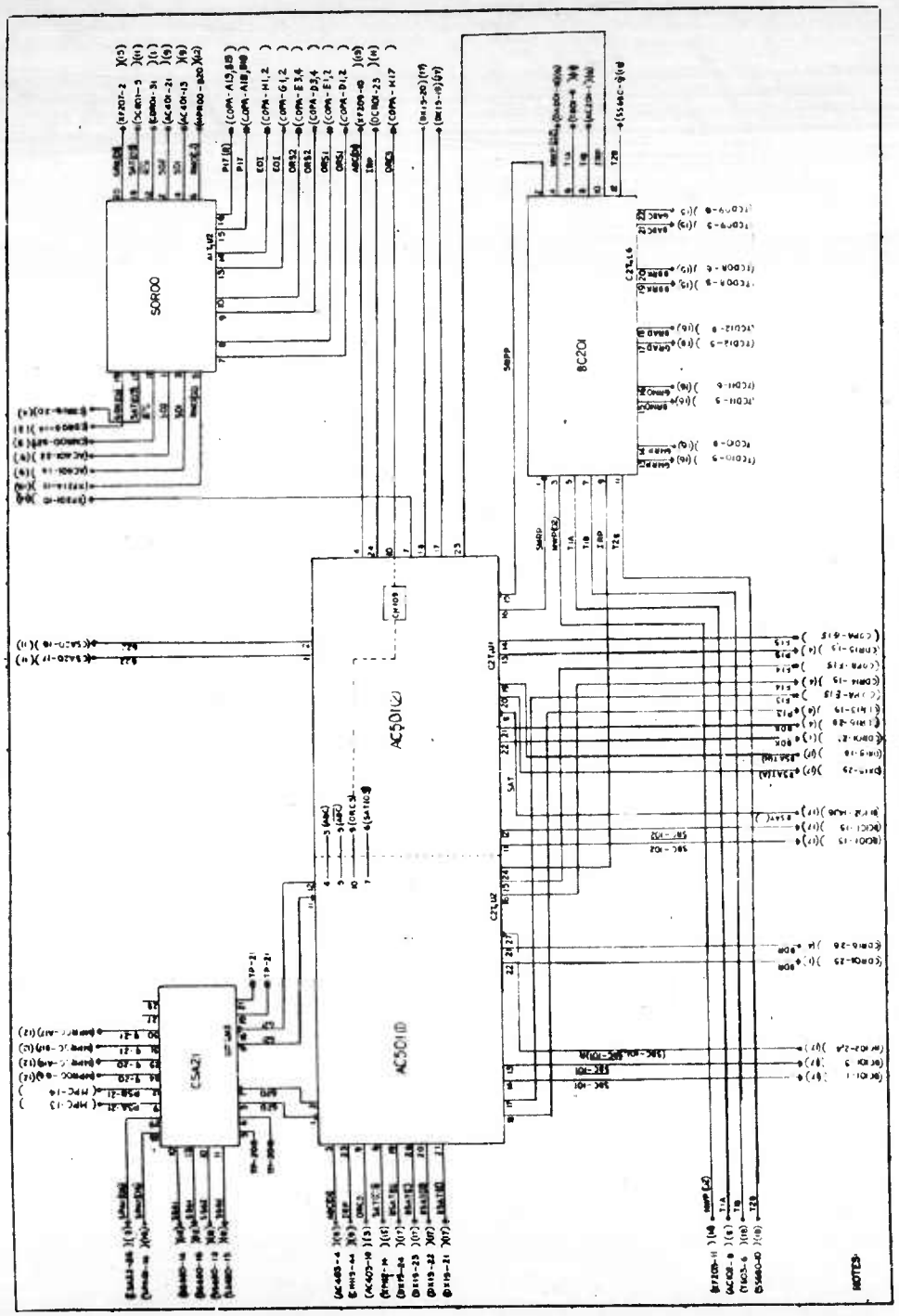

FIGURE 12 BLOCK DIAGRAM OF COMPUTER TEST VEHICLE B COMMAND REGISTER

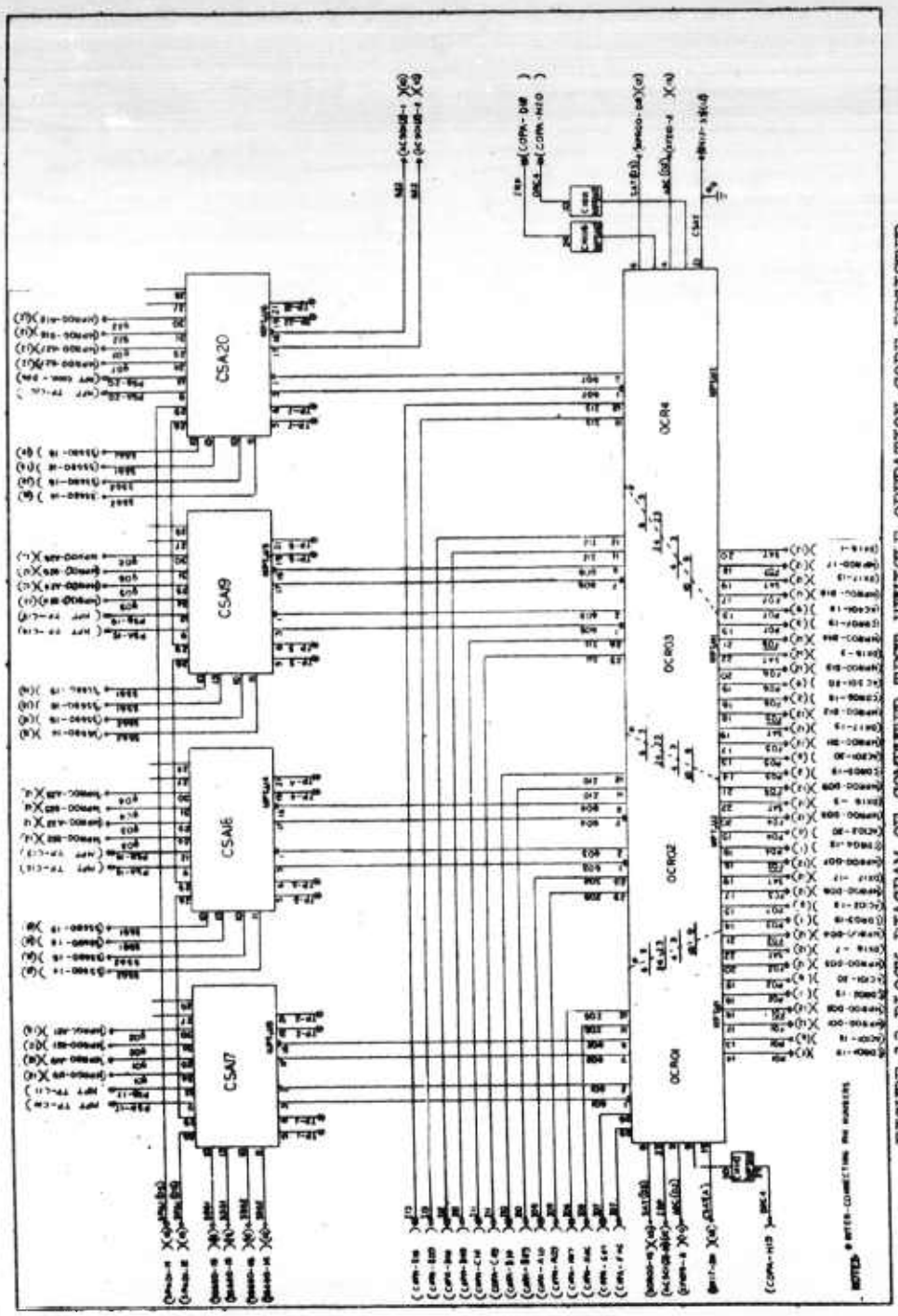

FIGURE 13 BLOCK DIAGRAM OF COMPUTER TEST VEHICLE OPERATION CODE REGISTER

unit or from the microprogram memory. Its contents specify the location of the core which contains the next command word.

2.2.1.2.3 Arithmetic Unit

The arithmetic unit is composed of the combined matrix register, shown in Figure 14 with its sense amplifiers, and the combined data register, shown in Figure 15. The combined matrix register is composed of five magnetic core ropes (MA1, MA2, MA3, MB1, and MB2) as follows:

(a) The MA1 matrix register is a 16-core rope which temporarily stores the unaltered contents of the DR register.

(b) The MA2 matrix register is a 16-core rope which temporarily stores and performs an "end-around, one-bit shift-right" of the contents of the DR data register.

(c) The MA3 register is a 16-core rope which temporarily stores and performs a "four bit-positions shift-left" of the twelve least significant bits of the DR and stores the contents of the four least significant bits of the operand address register in its four least significant bit-positions.

(d) The MB1 register is a 137-core rope which temporarily stores and performs the simultaneous carry function, permitting unprecedented speed of operation for a magnetic computer system.

(e) The MB2 rope is a 16-core register which temporarily stores the contents of the DK data register when transfer to the MB2 register is made.

The combined data register is composed of two 16-bit core registers, DR and DK, and their associated logic cores. The DR and DK registers can receive simultaneously an A-data word (from either MA1, MA2, or MA3) or a B-data word (from either MB1, MB2, or data memory). When the A and B words are set into the DR register an Exclusive-OR is performed on each bit of the words. When the A and B words are set into the DK register the AND function is performed on each bit of the words.

The contents of the DR register may be transferred to the MA1, MA2, MA3, and MB1 ropes, and the contents of the DK register may be transferred to the MB1 and MB2 ropes.

During phase A of the first cycle of the instruction, the contents of the operand address register are decoded by the address decoders in the Data Memory Unit (see 2.2.1.2.4). Also,

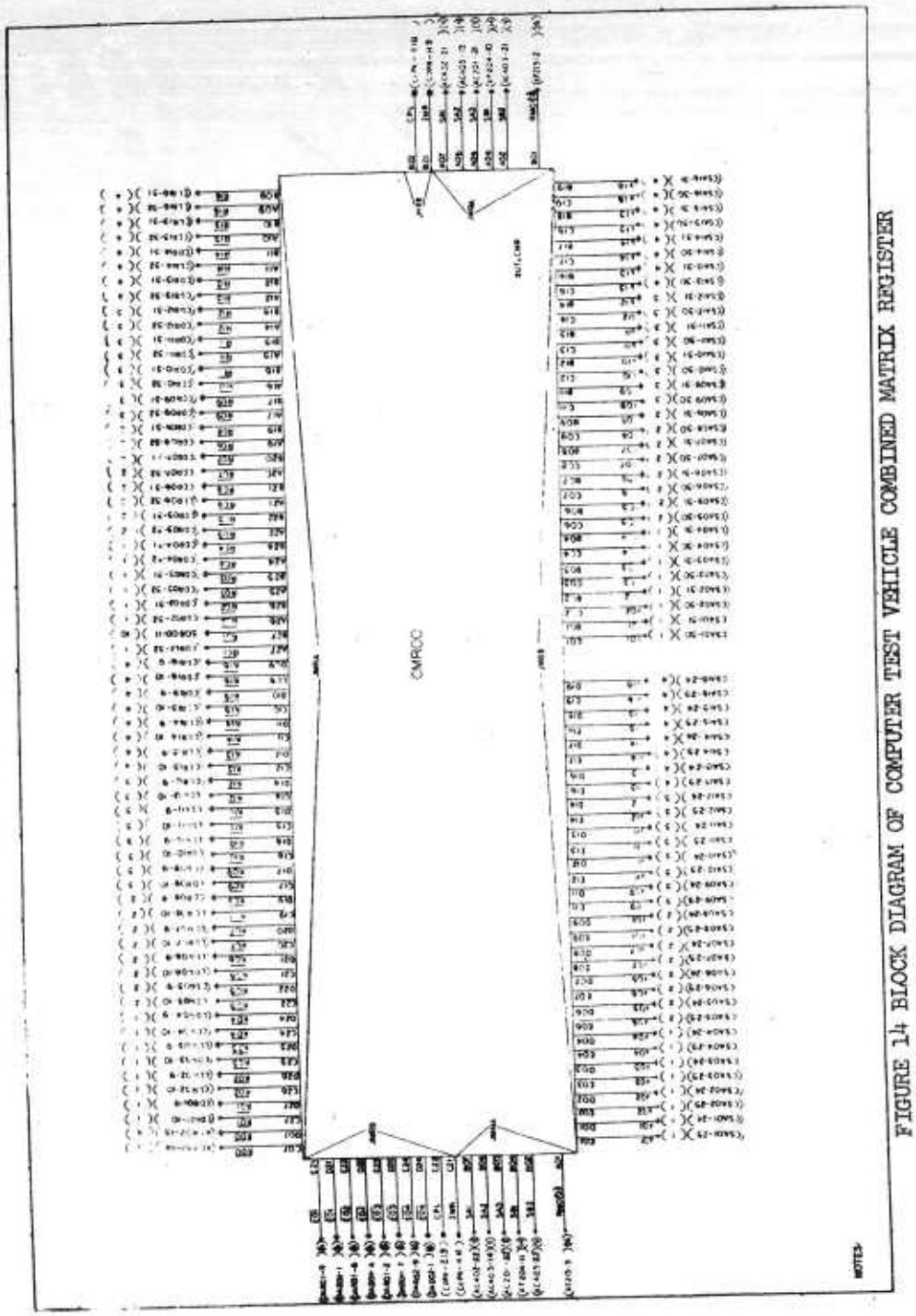

FIGURE 14 BLOCK DIAGRAM OF COMPUTER TEST VEHICLE COMBINED MATRIX REGISTER

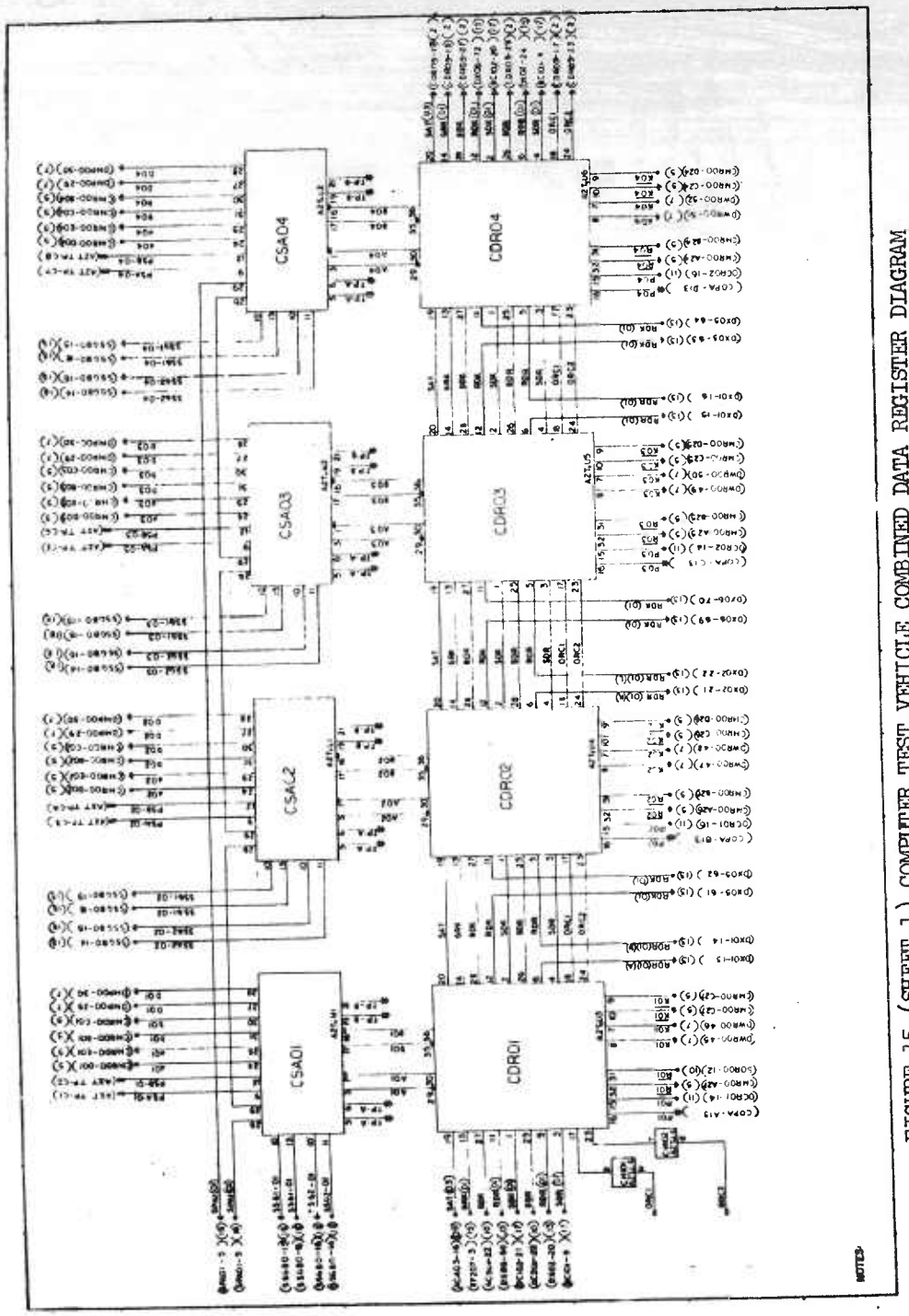

FIGURE 15 (SHEET 1) COMPUTER TEST VEHICLE COMBINED DATA REGISTER DIAGRAM

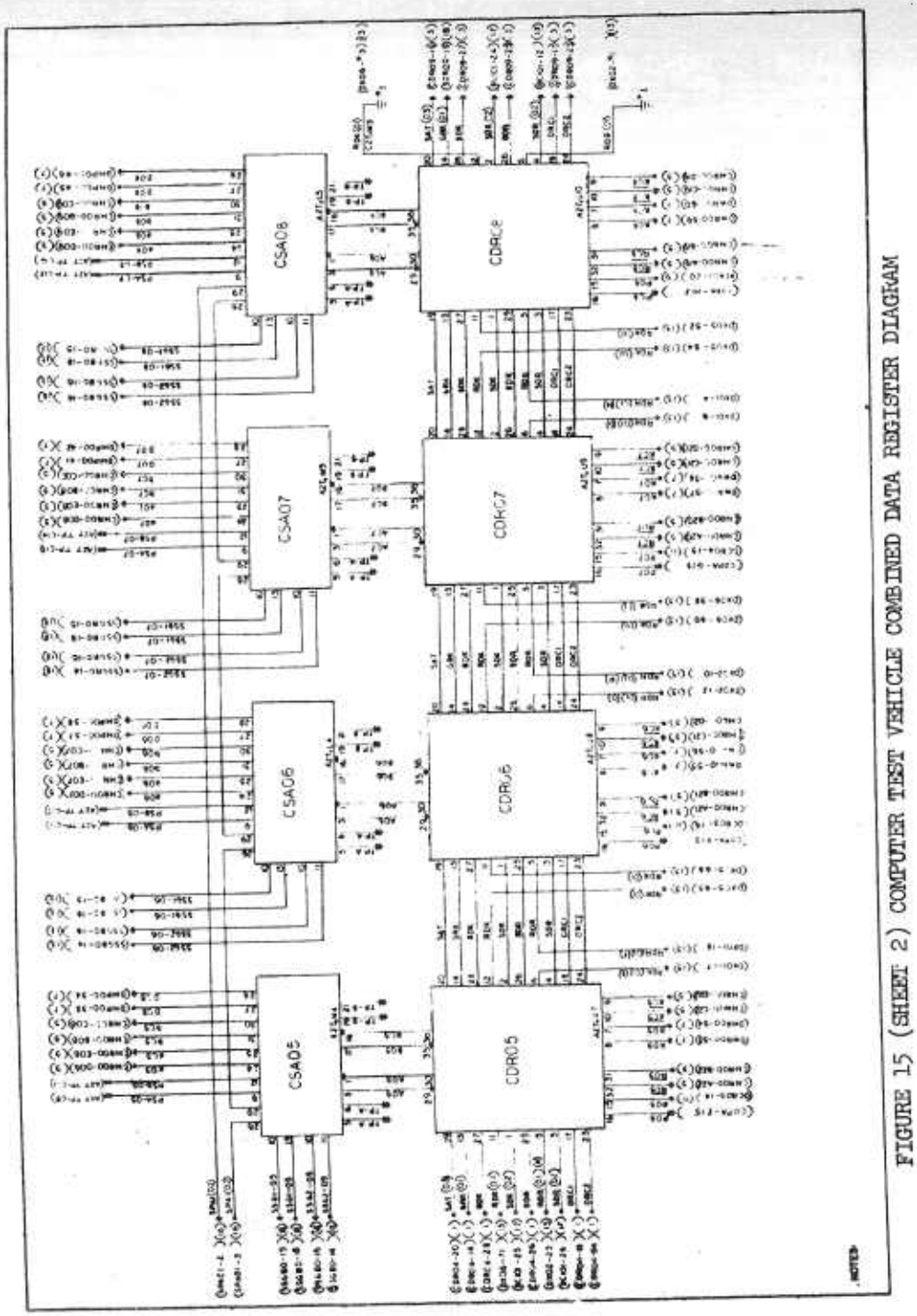

FIGURE 15 (SHEET 2) COMPUTER TEST VEHICLE COMBINED DATA REGISTER DIAGRAM

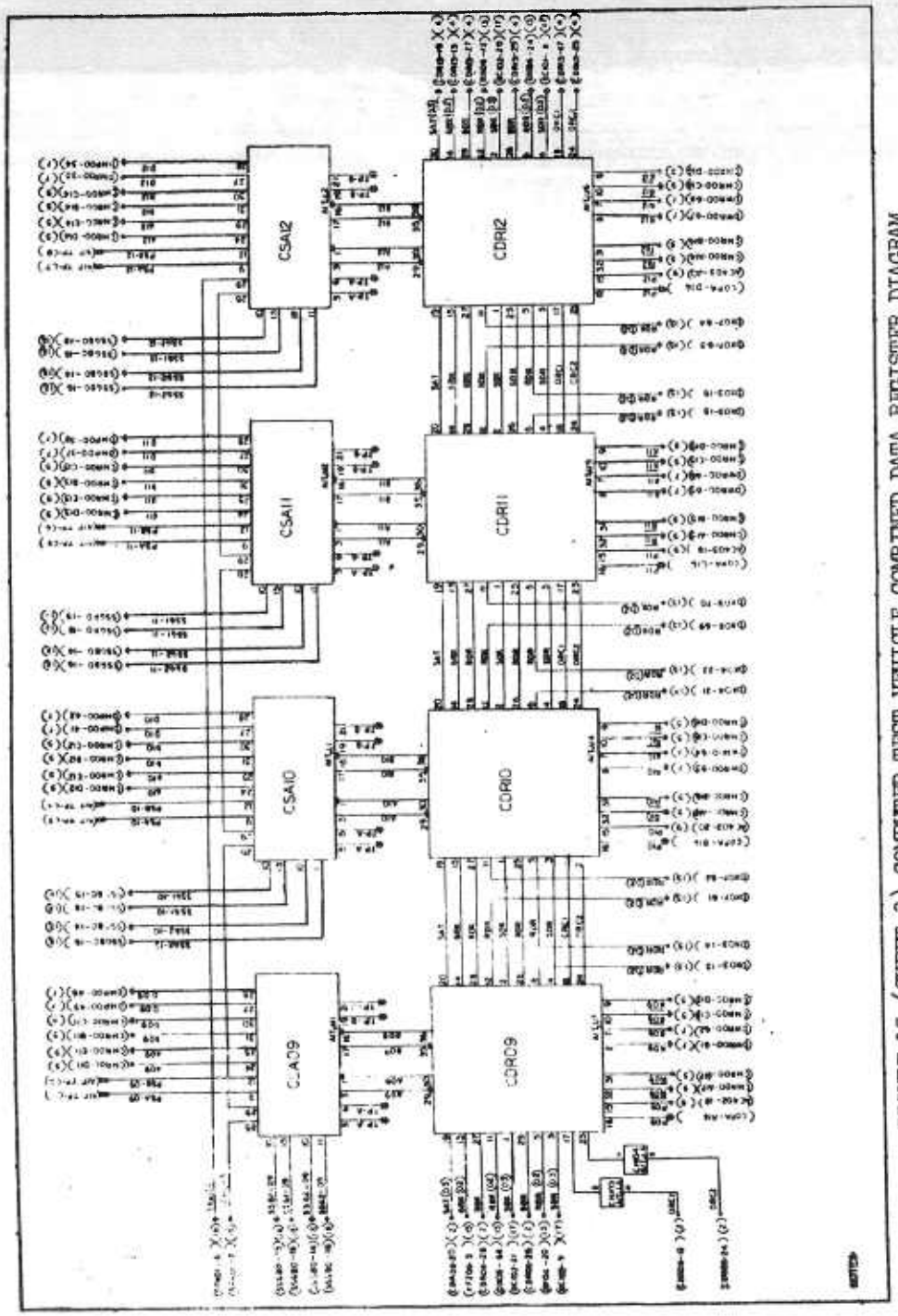

FIGURE 15 (SHEET 3) COMPUTER TEST VEHICLE COMBINED DATA REGISTER DIAGRAM

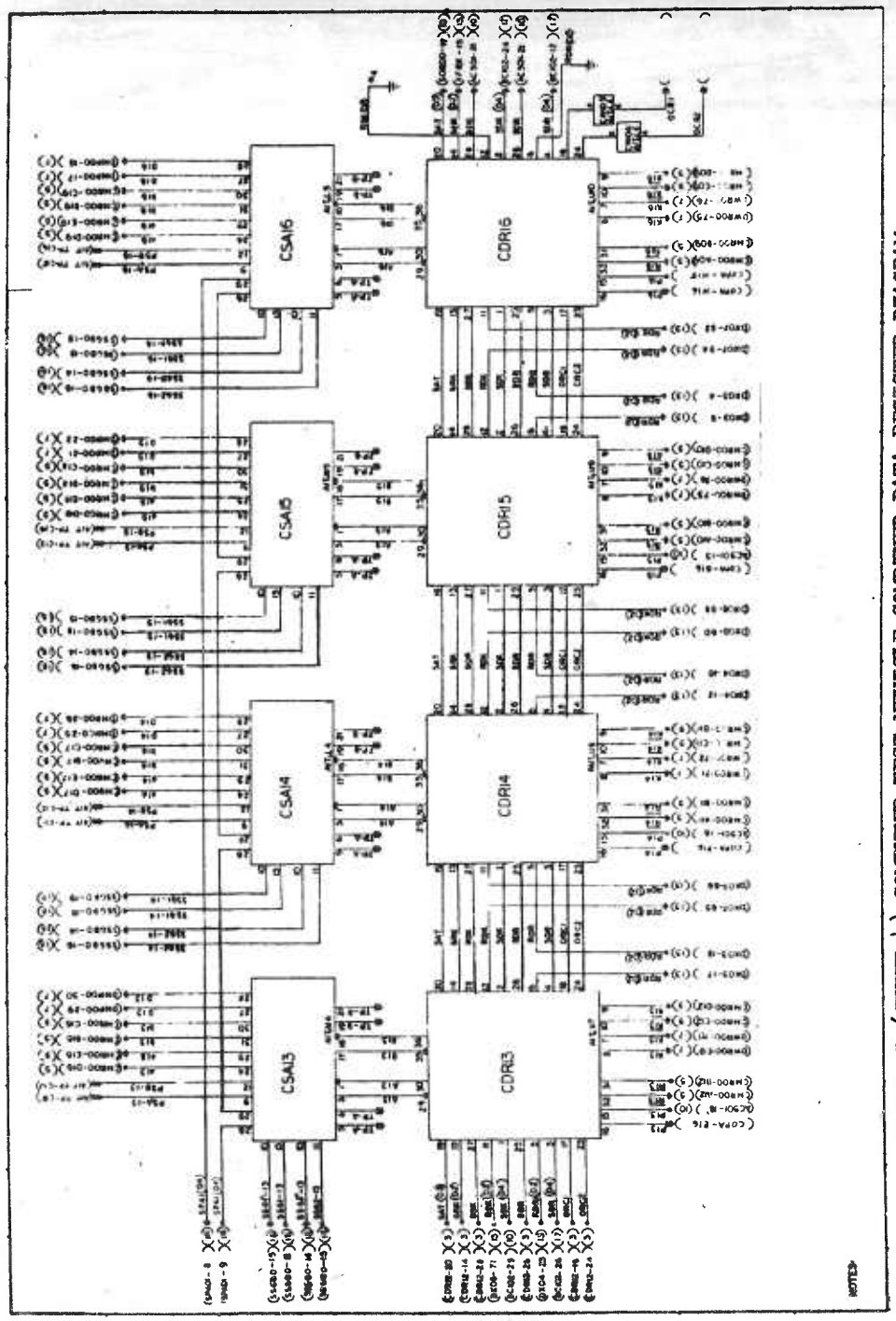

FIGURE 15 (SHEET 4) COMPUTER TEST VEHICLE COMBINED DATA REGISTER DIAGRAM

each bit of the MA1 core rope is set to the ONE state. In phase B of the first cycle, the B word in the data memory location specified by the address decoders and the A word located in the MA1 rope are removed. The two words, A and B, are transferred to the DK data register, where the B word is stored unaltered. (A was in the ONE state, thus the AND function of A and B produces the B word.)

In phase A of the second cycle, the B word in the DK register is transferred to its buffer register, MB2, while the A word in DK is transferred to its buffer register, MA1. The A and B words are unaltered in the transfer. Also, the B word is transferred to the data memory write register and restored in memory.

In phase B of the second cycle, the contents of the MB2 and MA1 registers are transferred to the DR and DK registers, respectively. This results in the Exclusive-OR (half-add sum) of the A and B words being stored in the DR register and the AND of the A and B words being stored in the DK register.

In phase A of the third cycle, the contents of the DK and DR registers are transferred to the MB1 rope, where the "half-add carry" is formed. The DR is also transferred to its buffer, MA1, thus retaining the "half-add sum."

In phase B of the third cycle, the contents of the MB1 and MA1 registers are transferred to the DR register, where the Exclusive-OR of the "half-add sum" and "half-add carry" results in the completed addition.

2.2.1.2.4 Data Memory Unit

The data memory unit is composed of the data memory and its sense preamplifiers, the data address decoders, the data memory write register and the operand address register, as shown in Figure 16. The data memory is a 64-word (16 bits per word), coincident-current, ferrite core, destructive-read memory. The memory cycle consists of decode, read, write, and reset. The duration of the memory cycle is 20 microseconds, which is compatible with the clock rate and the requirements of the arithmetic unit.

The data address decoder consists of a read address decoder and a write address decoder, which select the X-line (one of eight) and the Y-line (one of eight) on which read or write current will flow.

The sense preamplifiers receive the outputs from the 16 sense lines of data memory during the read cycle and transfer these outputs to the B-channel sense amplifiers of the arithmetic unit, where the outputs are ORed with the outputs of the B-channel of the combined matrix register of the arithmetic unit.

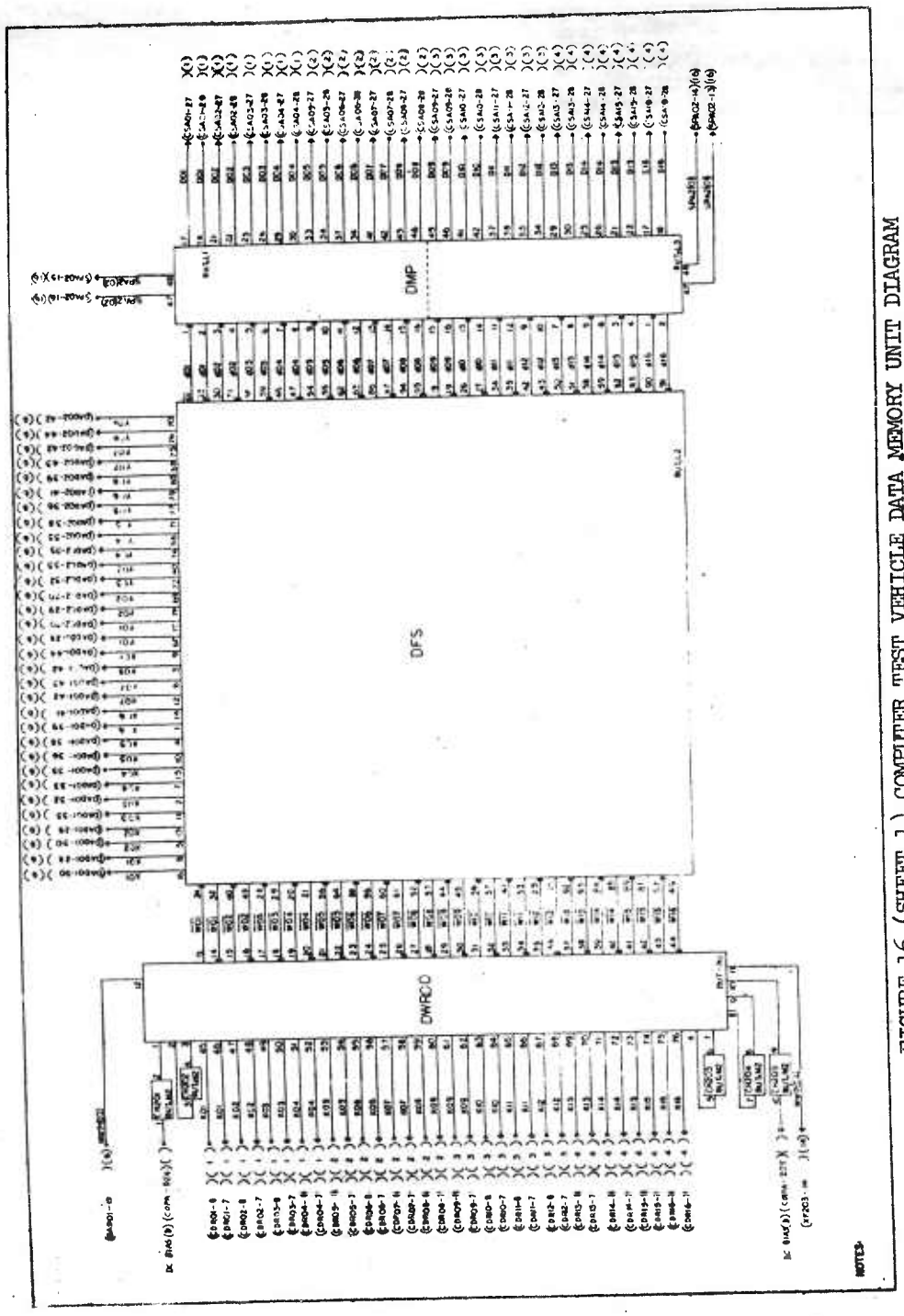

FIGURE 16 (SHEET 1) COMPUTER TEST VEHICLE DATA MEMORY UNIT DIAGRAM

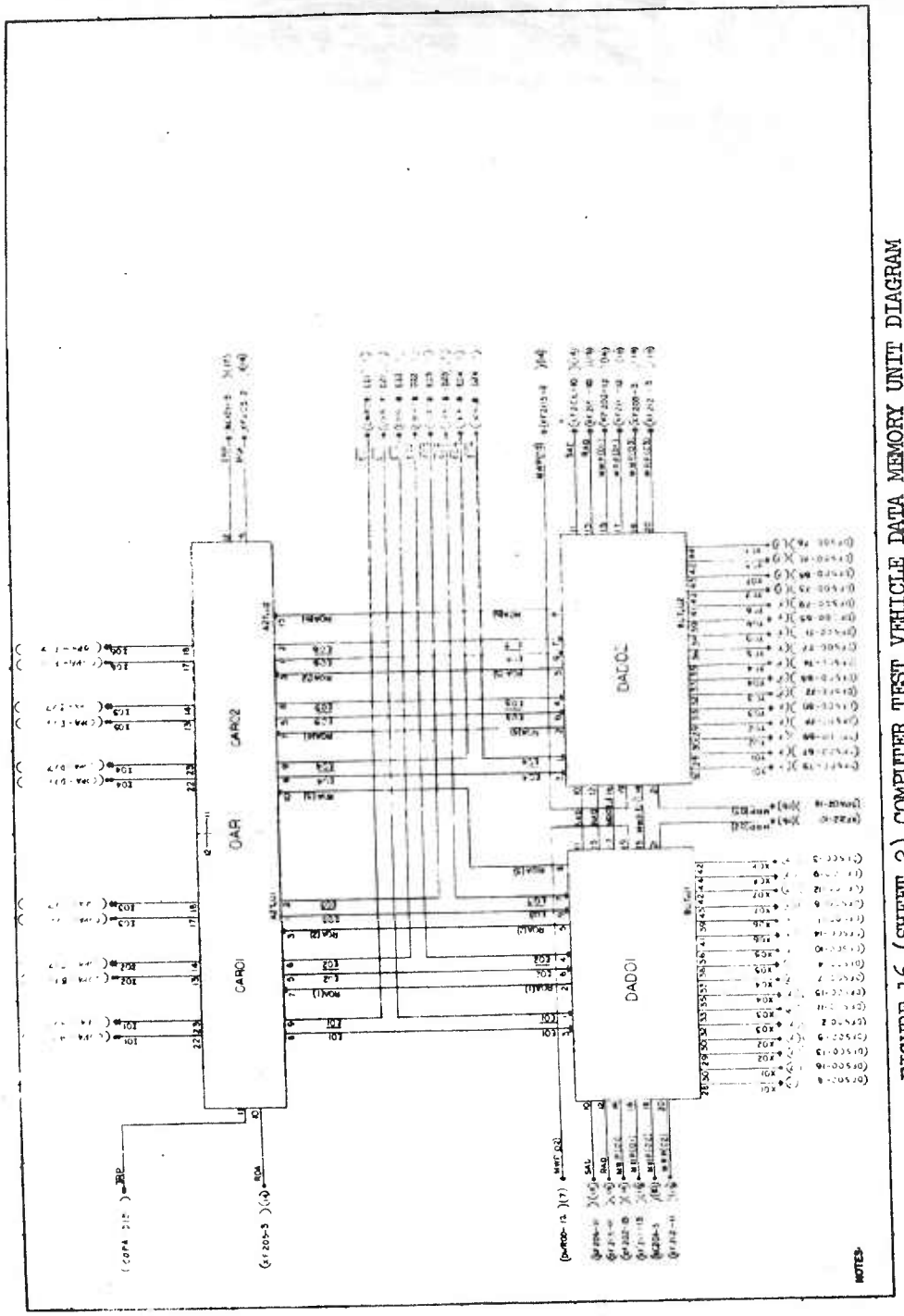

FIGURE 16 (SHEET 2) COMPUTER TEST VEHICLE DATA MEMORY UNIT DIAGRAM

The data memory write register, consisting of 16 cores, receives the 16-bit word to be written into data memory from the combined data register of the arithmetic unit. The word is transferred to data memory and written into the memory location specified by the operand address register and then decoded by the write address decoder.

The operand address register is a 6-bit, 12-core register which receives from the interface unit the six bits of the instruction word which specify the operand address. The contents of the operand address register are transferred to the read address decoder and the write address decoder. Also, the four least significant bits can be transferred to the MA3 matrix register of the arithmetic unit. Therefore, the data word can be inserted into the test vehicle through the operand address register and then to the MA3 matrix register of the arithmetic unit.

2.2.1.2.5 Output Unit

There are two output registers in the test vehicle, the serial output register and the parallel output register. The serial output register is a 3-bit, 6-core register used to serially transfer the 16-bit contents of the DR data register to the interface unit, one data bit and one clock bit at a time. It also sends an end-of-instruction signal to the interface unit at the end of each test vehicle instruction.

The parallel output register is composed of four registers (I, II, III, and IV) which are logically ORed at their outputs. Control lines from the interface unit select the desired register:

(a) Parallel Output Register I is a 16-bit core register which stores the A data word of the arithmetic unit. This is the normal parallel output to the interface unit.

(b) Parallel Output Register II is a 16-bit core register which stores the B data word of the arithmetic unit.

(c) Parallel Output Register III is a 15-bit core register which stores the subcommand field from the microprogram.

(d) Parallel Output Register IV is a 7-bit core register which stores the address field of the microprogram.

2.2.1.3 Test Vehicle Circuits Description

Both active and passive circuits are used in the test vehicle. Active circuits consist of several types of vacuum tube circuits and one type of tunnel diode amplifier which is used as a sense preamplifier. Each vacuum tube circuit uses either two or four tubes in parallel and is designed to operate satisfactorily with one tube open. The passive circuits are the rope cores, core and diode registers, current steering circuits, and data memory.

2.2.1.3.1 Blocking Oscillators

Blocking oscillators are used to generate voltage pulses, and through a series resistor, current pulses, for various control purposes. Types of blocking oscillators are:

(a) The delay line driver (DLD), as shown in Figure 17, is a type of self-timed blocking oscillator designed to drive the 500 ohm tapped delay line, shown in Figure 9, with a +40 volt pulse (referred to -15 volts), and with a special input circuit to permit triggering by the clock pulse supplied on a coaxial cable from the interface unit.

(b) The self-timed blocking oscillator (STBO), as shown in Figure 18, is a blocking oscillator using cathode-to-grid feedback through a square-core transformer which is reset by direct current. The core of this transformer is a toroid of ultra-thin molypermalloy tape. STBO's are used when it is not convenient or necessary to supply a turn-off pulse to time the trailing edge but to supply turn-off pulses to TBO's and to one of the DG circuits.

(c) The triggered blocking oscillator (TBO), shown in Figure 19, is similar to the STBO, except that the cathode-to-grid feedback is through a cup-core pulse transformer. The trigger of the TBO and the turn-off pulse leading edge are both timed by delay line taps. The TBO output voltage pulses are used to time all other pulses in the machine.

(d) The sense screen gate blocking oscillator (SSGBO), shown in Figure 20, is a special TBO designed for high power output. It generates positive and negative voltage pulses to control the screens of all vacuum tube sense amplifiers in the machine (54 circuits, 108 tubes).

All blocking oscillators are designed as current demand circuits. The cathode-to-grid feedback supplied a fraction of total cathode current (about 1/3) as grid current, and as plate

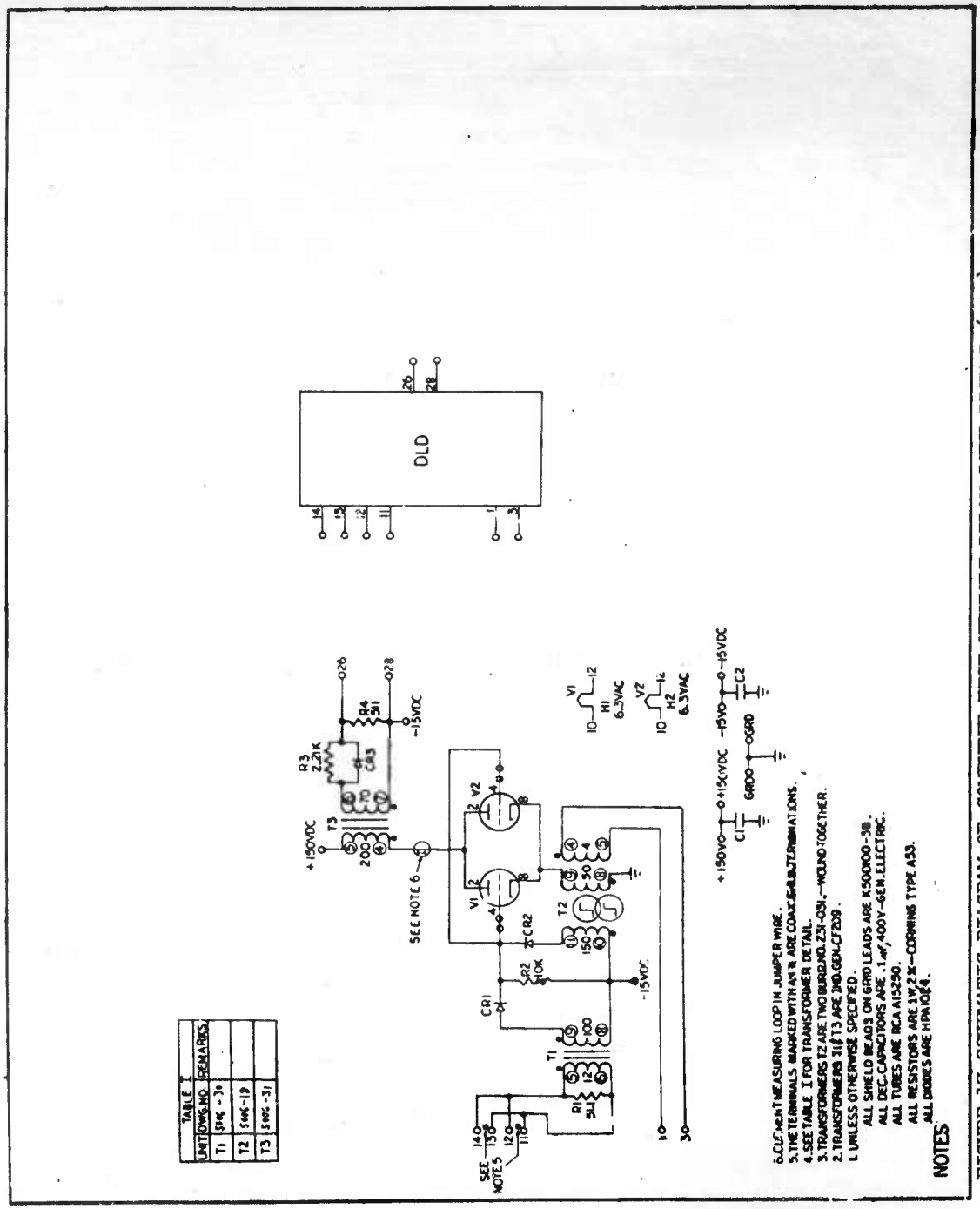

FIGURE 17 SCHEMATIC DIAGRAM OF COMPUTER TEST VEHICLE DELAY LINE DRIVER (DLD) BLOCKING OSCILLATOR

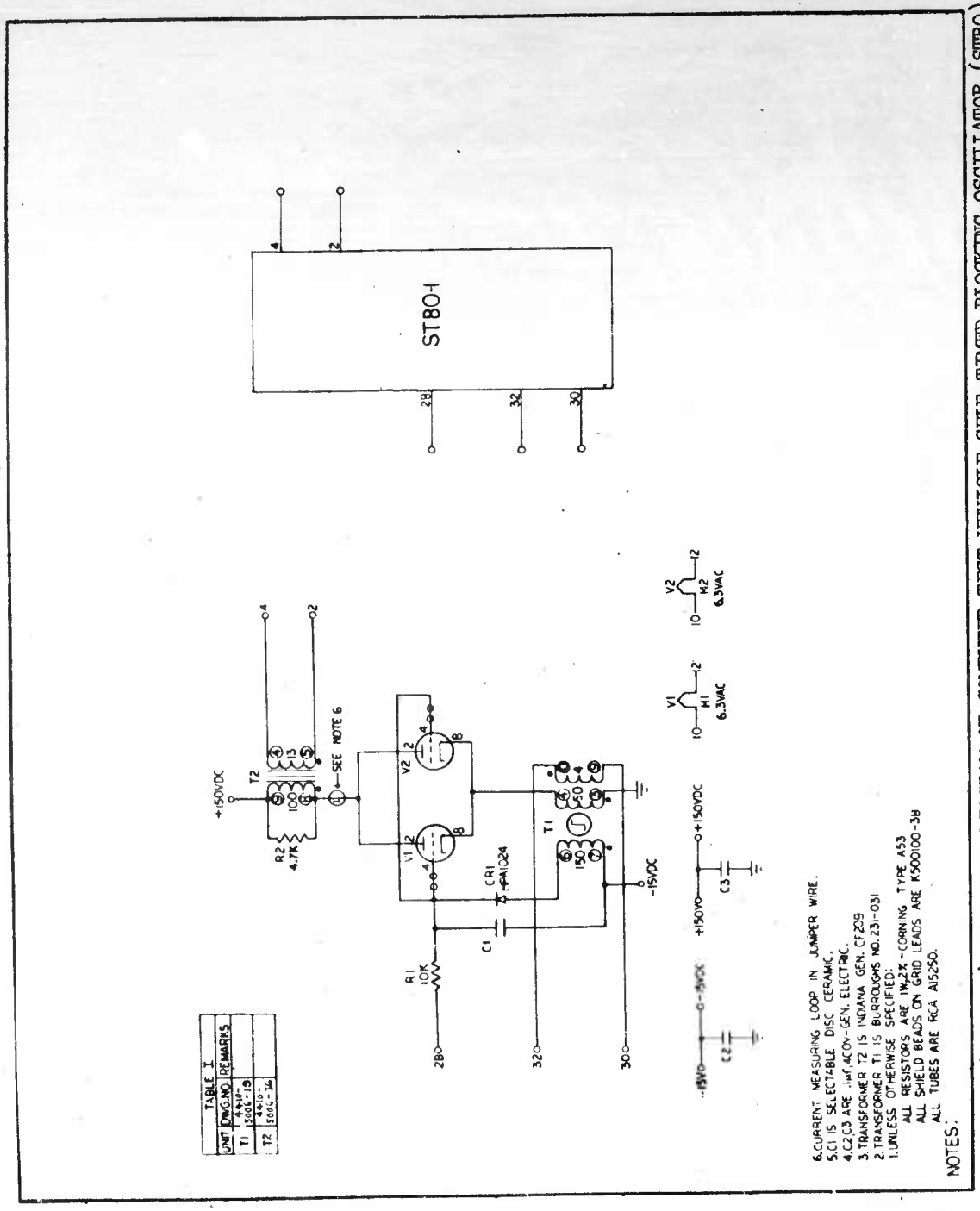

FIGURE 18 (SHEET 1) SCHEMATIC DIAGRAM OF COMPUTER TEST VEHICLE SELF-TIMED BLOCKING OSCILLATOR (STBO)

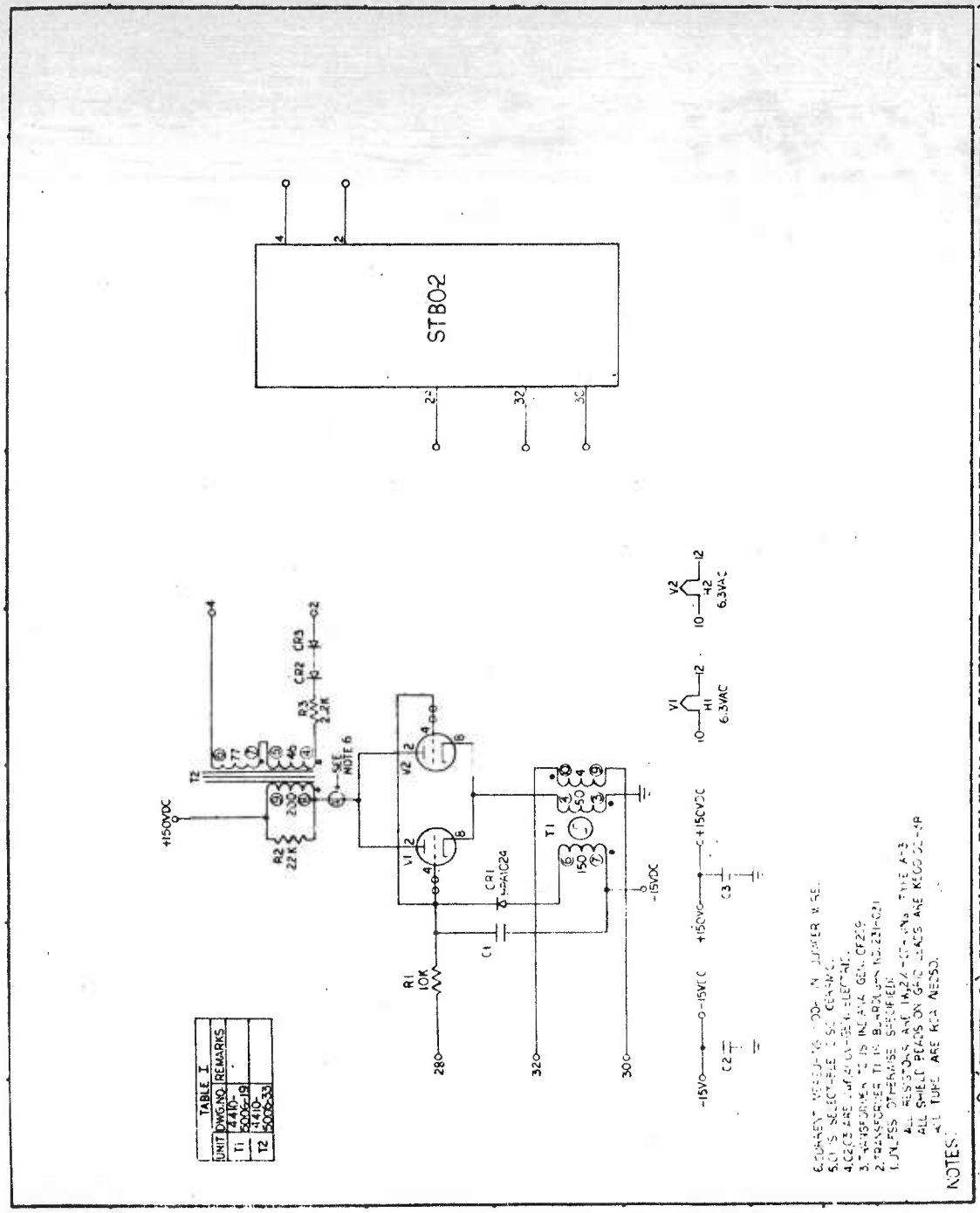

FIGURE 18 (SHEET 2) SCHEMATIC DIAGRAM OF COMPUTER TEST VEHICLE SELF-TIMED BLOCKING OSCILLATOR (STBO)

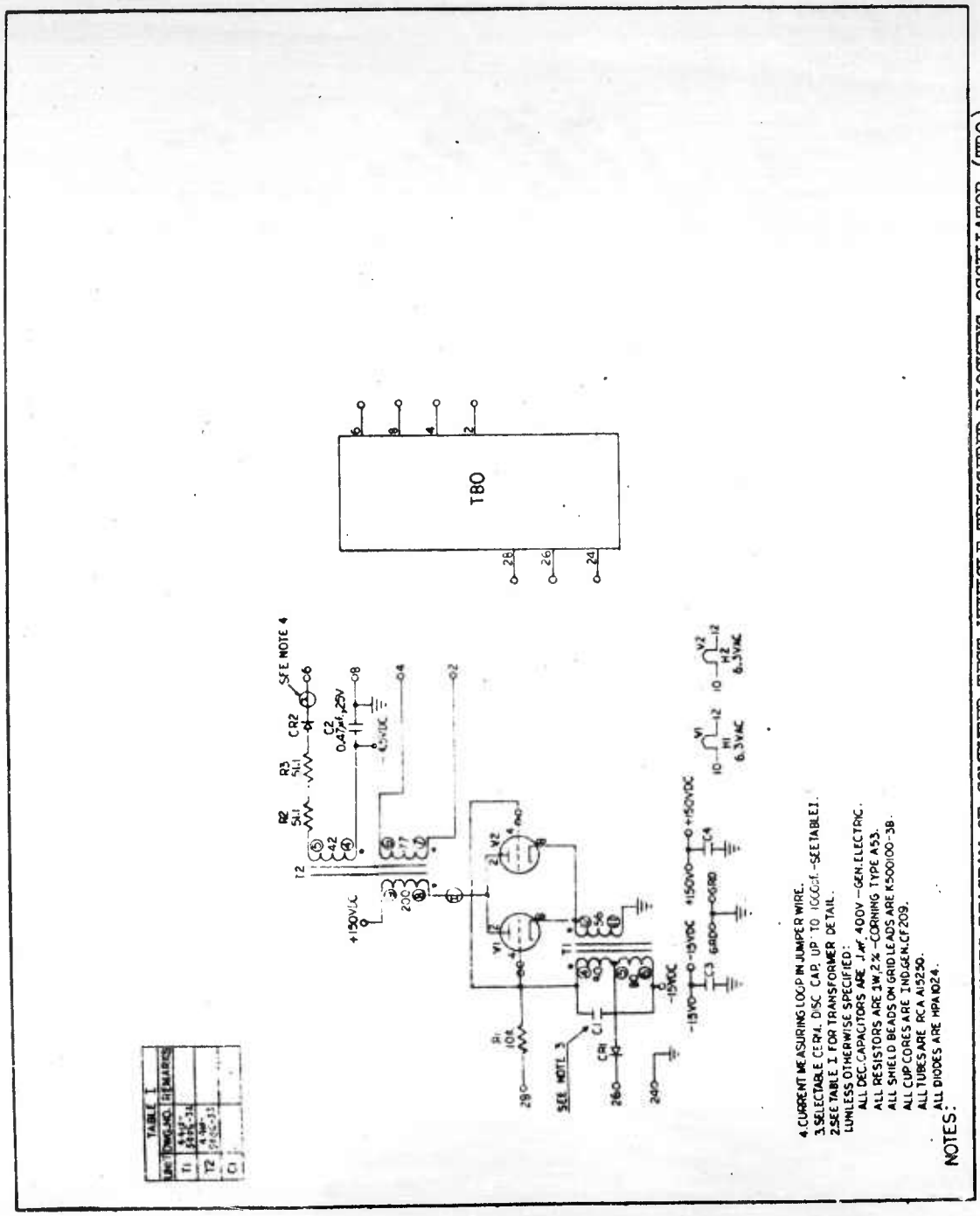

FIGURE 19 SCHEMATIC DIAGRAM OF COMPUTER TEST VEHICLE TRIGGERED BLOCKING OSCILLATOR (TBO)

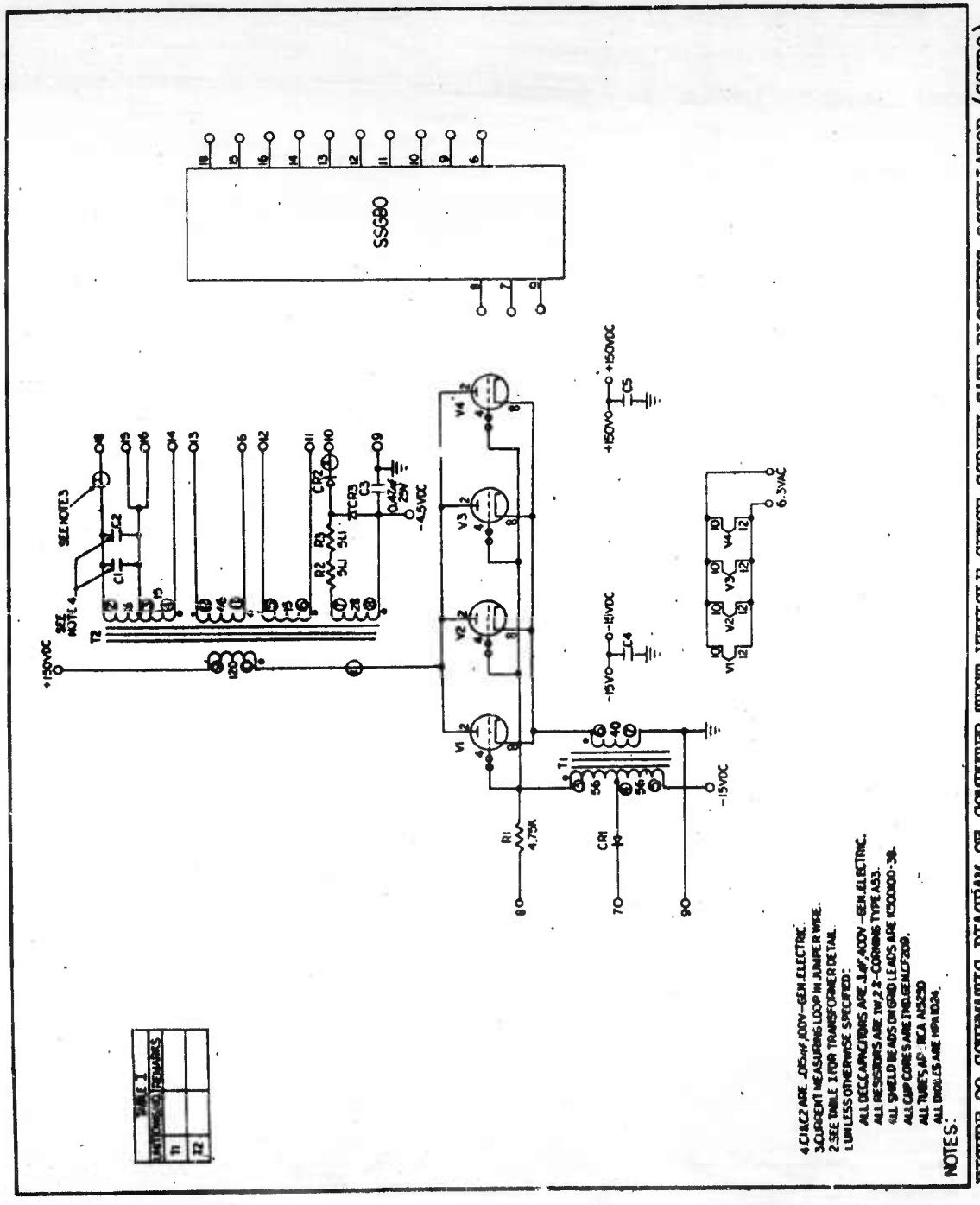

FIGURE 20 SCHEMATIC DIAGRAM OF COMPUTER TEST VEHICLE SENSE SCREEN GATE BLOCKING OSCILLATOR (SSGBO)

load increases the grid current does also.

2.2.1.3.2 Current Drivers

Two types of current drivers were used in the test vehicle. The first type, represented by the preamplifier strobe (SPA) shown in Figure 21, and the driver gate (DG), shown in Figure 22, supplied an output current pulse of constant amplitude. A DC current is supplied to the cathode, and when the tubes are held off by grid bias, this current flows through a diode to ground. The tube is turned on by a positive-going voltage pulse applied to the grid. While it is on, the cathode is positive so all the DC current flows from the cathode to the plate. The current magnitude and load are such that there is no grid current, thus the plate current pulse amplitude is exactly the same as the cathode current pulse. To maintain the current constant in spite of the cathode voltage swing, a series inductance is used in the cathode circuit. The duration of the current output pulse is determined by the duration of the voltage pulse driving the circuit. The DG circuit uses a transformer in series with the plate load to supply negative feedback which is arranged to control the fall time of the current pulse at 0.5 seconds.

Since this type of circuit may not draw grid current, output pulse power is limited. Output power of the SPA current driver is sufficient to drive up to 32 tunnel dicde preamplifiers. Each SPA circuit includes a TBO for control as shown by V_1-V_2 in Figure 21. This TBO is triggered by the current pulse driving the signal source to the preamplifier being strobed. The DC current driver was designed to control the triggered current drivers; however, the output pulse power was found to be sufficient to control only one or two TCDs reliably. Therefore, each DG controls one TCD and this TCD controls other TCDs.

The second type of current driver used, the triggered current driver (TCD) as shown in Figure 23, supplied the controlled current pulses used to drive most of the magnetic circuits in the test vehicle.

The TCD circuit resembles a TBO with cathode-to-grid feedback through a pulse transformer. However, the total cathode current is limited by the secondary of a control transformer in series with the cathode, with DG control current supplied to the primary. Negative feedback is also connected through the control transformer to reduce the effect of variations in grid current with variations in load voltage, since this circuit does not saturate. The grid current effect is not completely eliminated; there is a small variation ($\pm 5\%$) of plate current with load voltage. The control transformer primary is tapped so that the TCD output is 100, 150 or 250 ma, depending on the connection of the DG. The 150 and 250 ma TCD's use four tubes.

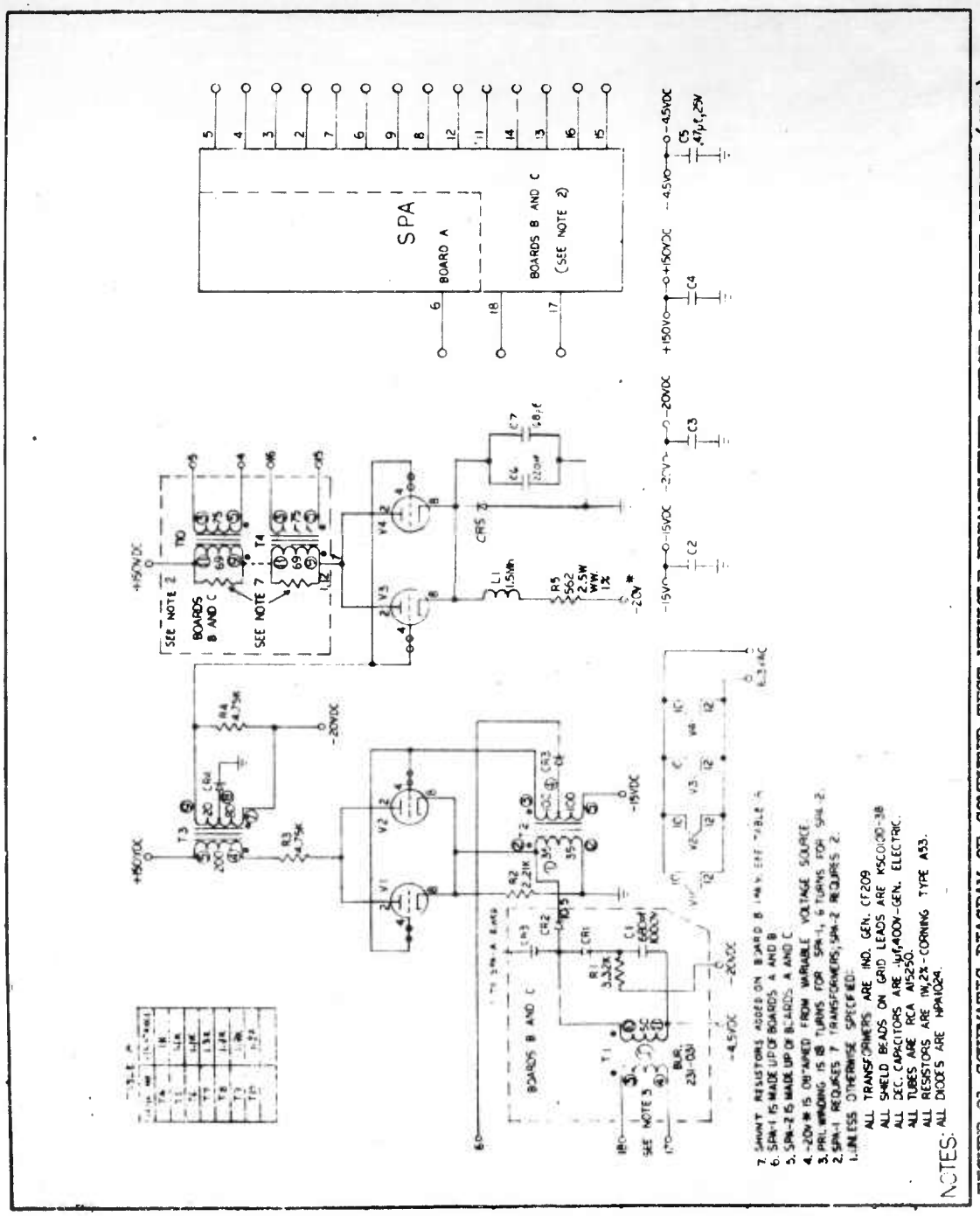

FIGURE 21 SCHEMATIC DIAGRAM OF COMPUTER TEST VEHICLE PREAMPLIFIER STROBE CURRENT DRIVER (SPA)

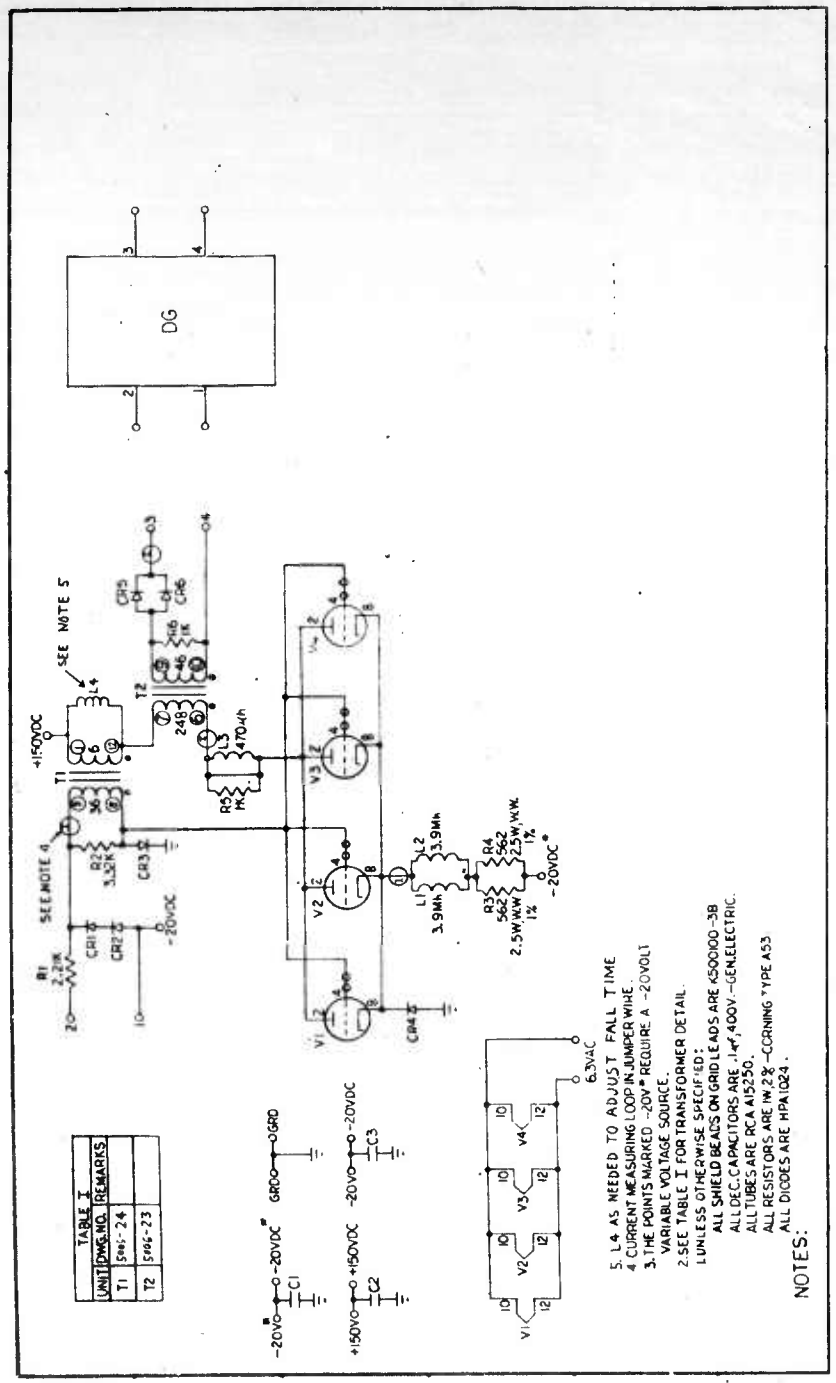

FIGURE 22 SCHEMATIC DIAGRAM OF COMPUTER TEST VEHICLE DRIVER GATE CURRENT DRIVER (DG)

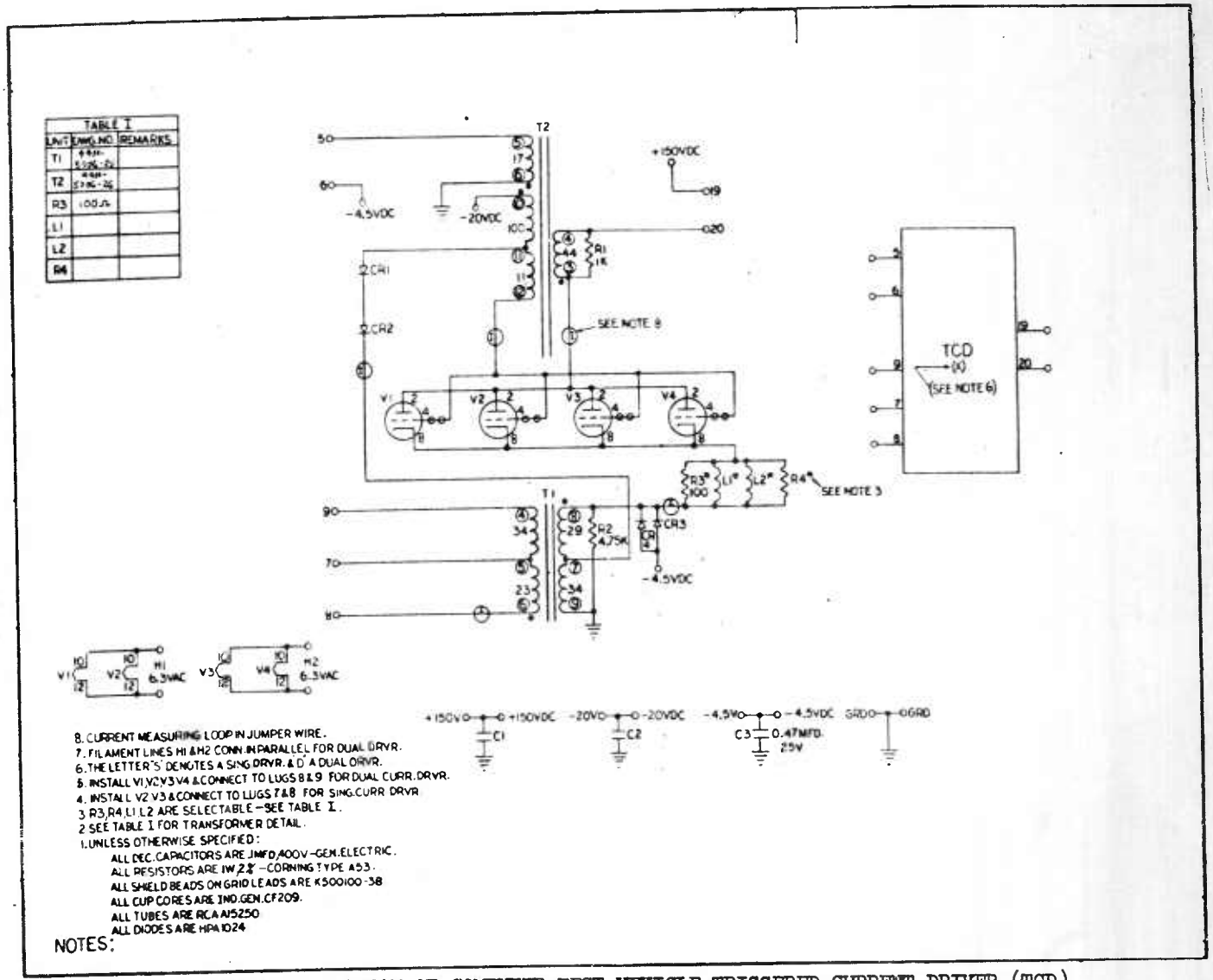

FIGURE 23 SCHEMATIC DIAGRAM OF COMPUTER TEST VEHICLE TRIGGERED CURRENT DRIVER (TCD)

The TCD is triggered under the microprogram or basic timing control while the DG is on, and is turned off by the turnoff of DG current. The rise of the current is therefore controlled by the load impedance and the fall is controlled by the DG trailing edge waveform. Also the leading edge is timed by the trigger while the trailing edge is timed by DG. If no trigger is supplied to the TCD, no output is produced. The DG current is then bypassed to the -4.5 volt supply through a diode.

2.2.1.3.3 Sense Amplifier

Each of the combined sense amplifier (CSA) cards, as shown in Figure 24, contain two tunnel diode preamplifiers and two vacuum tube sense amplifiers, with a second input to one of the latter to accept the output of a third preamplifier from the data memory.

The vacuum tube sense amplifiers (VSA-1 and VSA-2) use two type-7587 tetrodes in parallel. The circuit is a blocking oscillator using plate-to-cathode feedback through a pulse transformer. The circuit is triggered by application of screen voltage, provided that the grid voltage is near ground when the screen pulse is applied.

In the normal condition, the screen and grid are both at -4.5V. If the preamplifier triggers because a sense signal was received, its output is coupled to the grid and causes it to rise to or near ground. However, the grid rise is slow, and if it were allowed to trigger the circuit, the time of triggering would be ill defined. Therefore, the screen is held negative until the desired time, i.e., when a positive pulse (SSG1) raises the screen to +10V and triggers the circuit. An equal but opposite negative pulse (SSG2) is connected to the grid through a 4.7 pf capacitance to neutralize the screen-to-grid capacitance in the tube and circuit. The circuit is turned off by the end of SSG pulse, when the screen returns to -4.5V.

The tunnel diode sense preamplifiers (SPA-1 and SPA-2) and the data memory preamplifiers (DMP), as shown in Figure 25, differ only in the number of turns on T1 and the value of L1.

A core switching signal is received on the sense line at the input terminals. The signal produces a circulating current which flows through the secondary of transformer T1 and through the tunnel diodes. This produces a forward current in one of the tunnel diodes and a reverse current in the other. The magnitude of this current is controlled by the input signal, the inductance L, and the turns ratio of transformer T1. The circulating current is controlled by the above parameters to be approximately 40 percent of the value required to switch the tunnel diode to its high-voltage state.

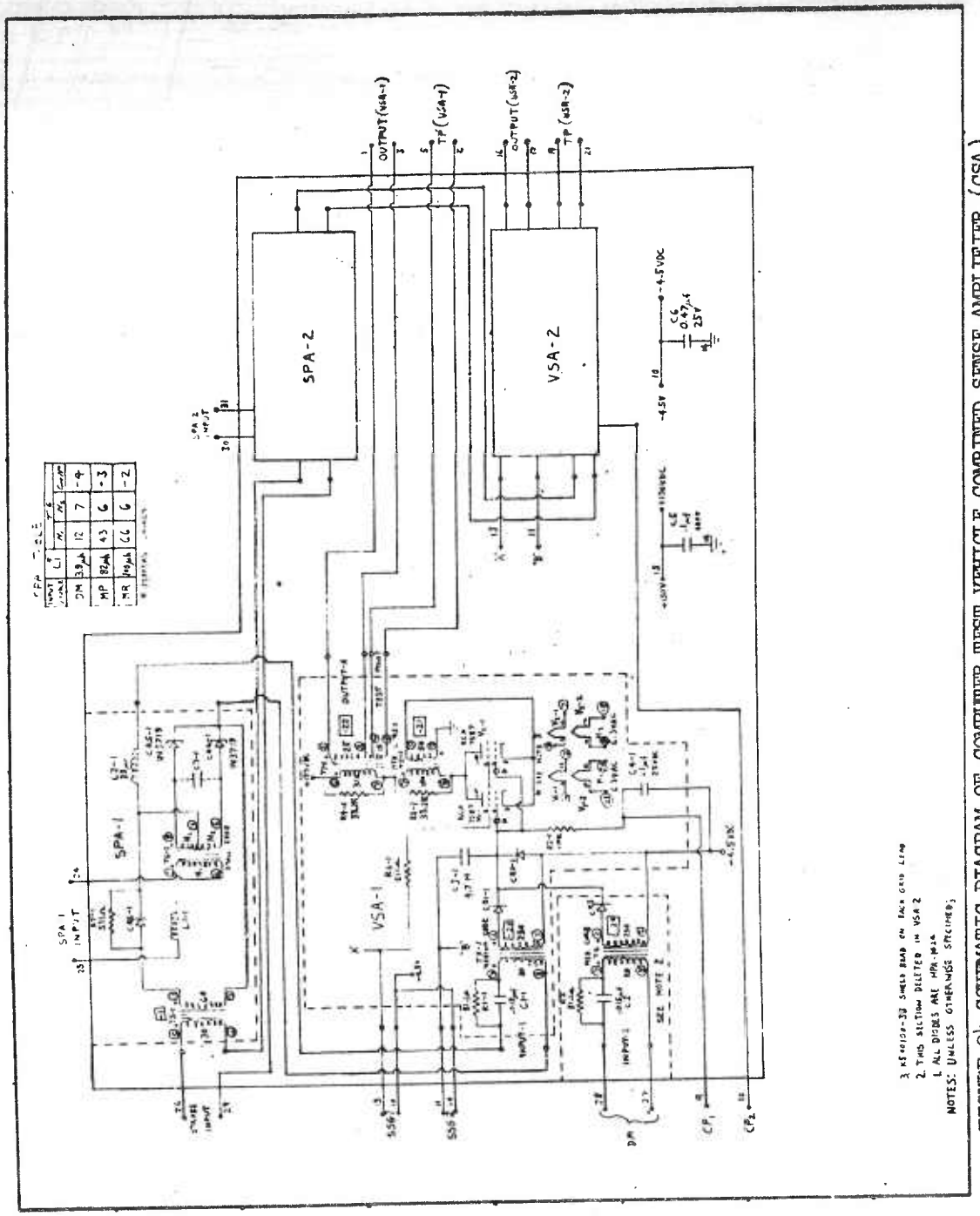

FIGURE 24 SCHEMATIC DIAGRAM OF COMPUTER TEST VEHICLE COMBINED SENSE AMPLIFIER (CSA)

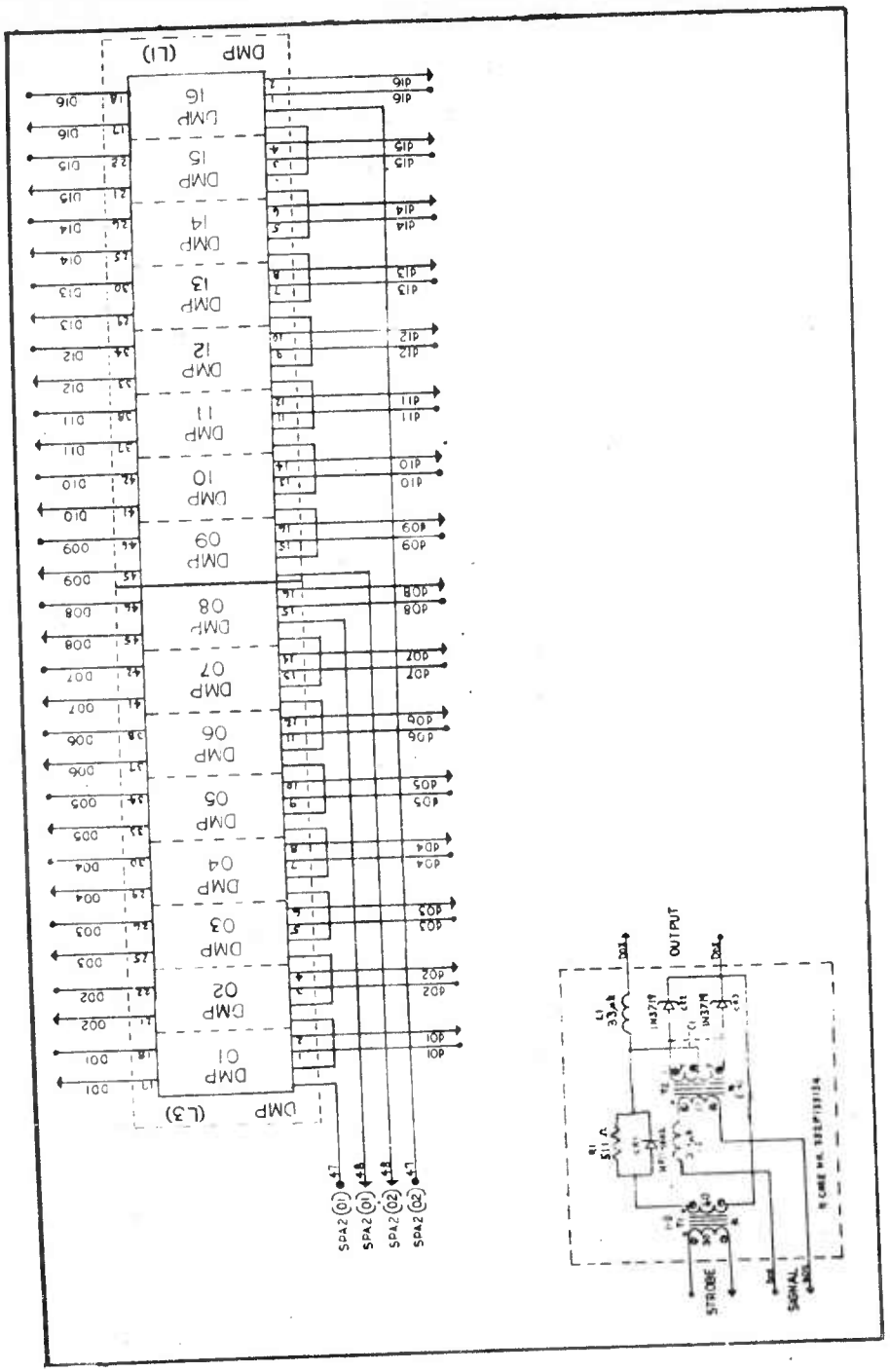

FIGURE 25 DIAGRAM OF COMPUTER TEST VEHICLE DATA MEMORY PREAMPLIFIERS (DMP)

At a time near the peak of the circulating current, a strobe signal is applied to the strobe input terminals. The strobe signal is a pulse of constant current which is coupled through transformer T2 and is then connected to flow into the center tap of transformer T1. Since the secondary of this transformer is bifilar wound, the current splits evenly, half flowing to each of the tunnel diodes. The magnitude of the strobe current is selected to cause the tunnel diode which was forwarded biased by the circulating current to switch to its high-voltage state under the combined influence of the circulating current plus the strobe current. When the first tunnel diode switches state, in a direction opposite to the original circulating current, this new current causes the second tunnel diode to switch to its high-voltage state. Since the voltage which produces the circulating current (the original input signal) is of short duration, the circulating current decays according to a time constant which is controlled by the value of the input inductor L1 and the dynamic resistance of the tunnel diodes reflected through transformer T1. This time constant is controlled to be approximately 0.8 microsecond. After the tunnel diodes have switched to their high-voltage state and the circulating current has decayed, the strobe current maintains the diodes in the high voltage state. The load current which is drawn from the preamplifier has a controlled rise time and peak amplitude and is sufficiently low that the current in the diodes never falls below the valley current. At the end of the strobe current, the diodes are deenergized, thus completing the operation.

2.2.1.3.4 Core Ropes

Core ropes are memory circuits consisting of square-loop cores strung on "ropes" of wires. The microprogram rope (MPR) and the combined matrix register (CMR) are the core rope circuits used in the test vehicle. The logical functions of each rope are determined by the linking or bypassing of the cores by the various wires. The functions are:

(a) Set

(b) Reset

(c) Inhibit

(d) Sense

A set line links every core of the rope. The Set current sets every core which is not inhibited. Set may be either unconditional or conditional, depending on the rope function. The Inhibit current pulse coincides with, or overlaps in time, the Set pulse and has the same amplitude. The input to the rope is represented by the pattern in which inhibit lines are driven. Every core linked by Inhibit current is prevented from setting.

After the selected core or cores are set, they are reset to read out the desired function. Reset lines link every core in the rope, and in this machine are unconditional. A single triggered current driver (RMO) resets all ropes in the test vehicle.

Sense lines link cores of the rope in a pattern determined by the desired logic. When the rope is reset, a signal is generated on every sense line linking the core that has been set. In MPR, the rope is used to decode the operation code and read out the next operation code. Thus each core represents a micro instruction, and the sense lines linking it are those which control the single operations which occur in that clock cycle, together with the 7-bit operation code for the next clock cycle of the instruction.

2.2.1.3.5 Core and Diode Registers

Core and diode register circuits are set according to sense amplifier outputs. A register control pulse (ABC or GRK) current is steered through one or the other of two paths in the circuit by the voltage signal from the sense amplifier. This voltage signal is pulse transformer coupled to back-bias one or the other of two diodes, so that the set current flows through the other one.

In the control registers (Figures 26 through 29) one or more cores are directly set or reset by the steered control current (ABC), one path for which is through a set winding on the register core and the other through a reset winding on the same core. After passing through all required windings, the two paths rejoin and go on to the next bit. The combined data register (CDR), shown in Figure 30, is set according to logic combinations of the two groups of sense amplifier outputs, A and B, where $R = A \oplus B$ and $K = A \cdot B$.

All control and data registers have two cores per bit. In some control register bit positions the TRUE output is a voltage pulse which triggers a current driver. In this case, only one core is ever set, the second core having a winding connected to balance out the ZERO noise when the bit is in the ZERO state. In all other cases the two cores are used for current steering, and the meaningful states (ONE and ZERO) are with one core Set and the other Reset.

2.2.1.3.6 Data Memory

The data memory consists of 16 "planes," each plane being an array of 64 ferrite cores in an 8 by 8 square. Each column of 8 cores is threaded by an X drive line, which threads the corresponding column in all 16 planes and so links 128 cores. Similarly, each row is linked by a Y drive line, also through all 16 planes. In each plane, every core is threaded by a sense line, so that there are 16 sense lines, one for each plane. Also in each plane, every

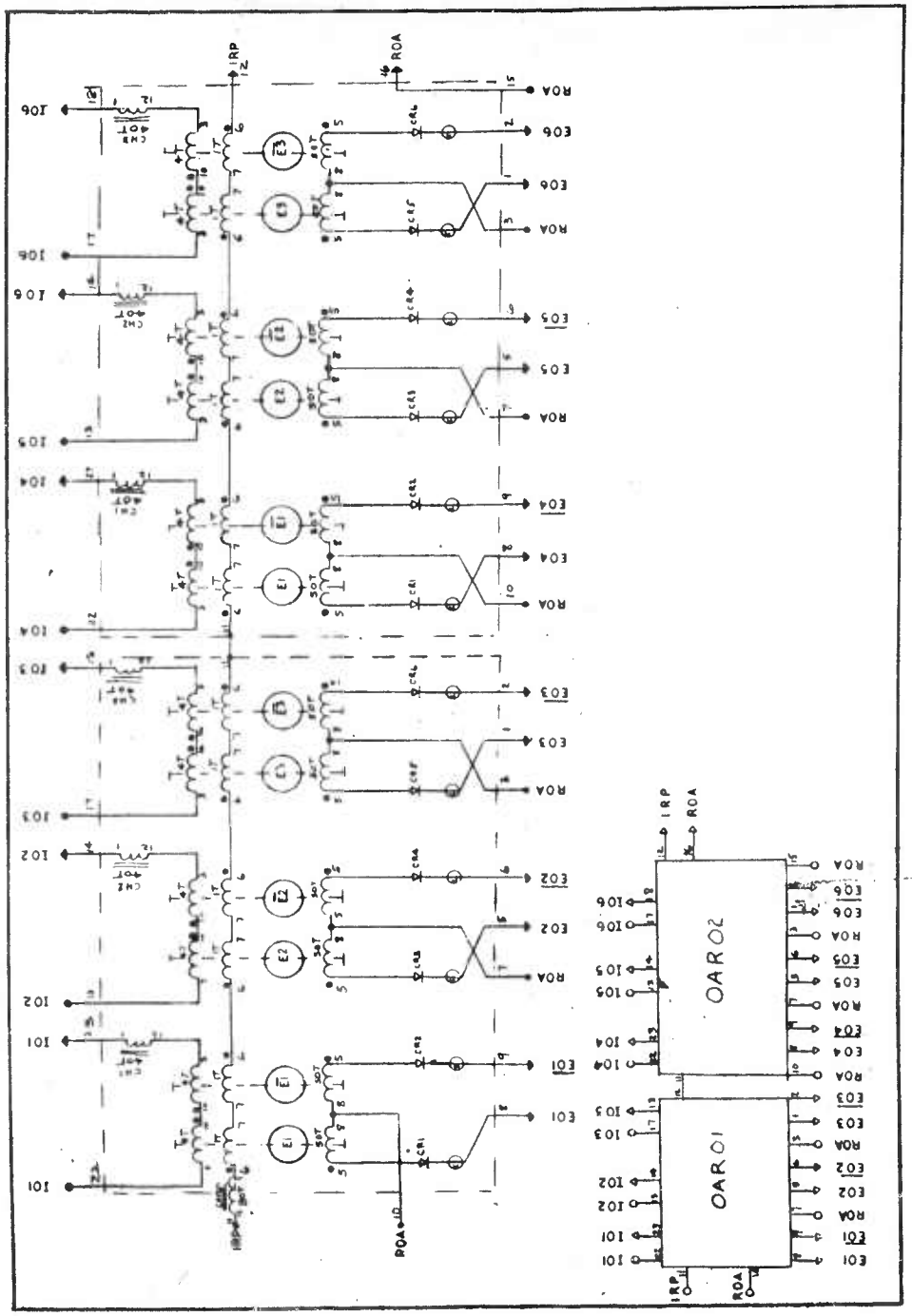

FIGURE 26 SCHEMATIC DIAGRAM OF COMPUTER TEST VEHICLE OPERAND ADDRESS REGISTER (OAR1 and OAR2)

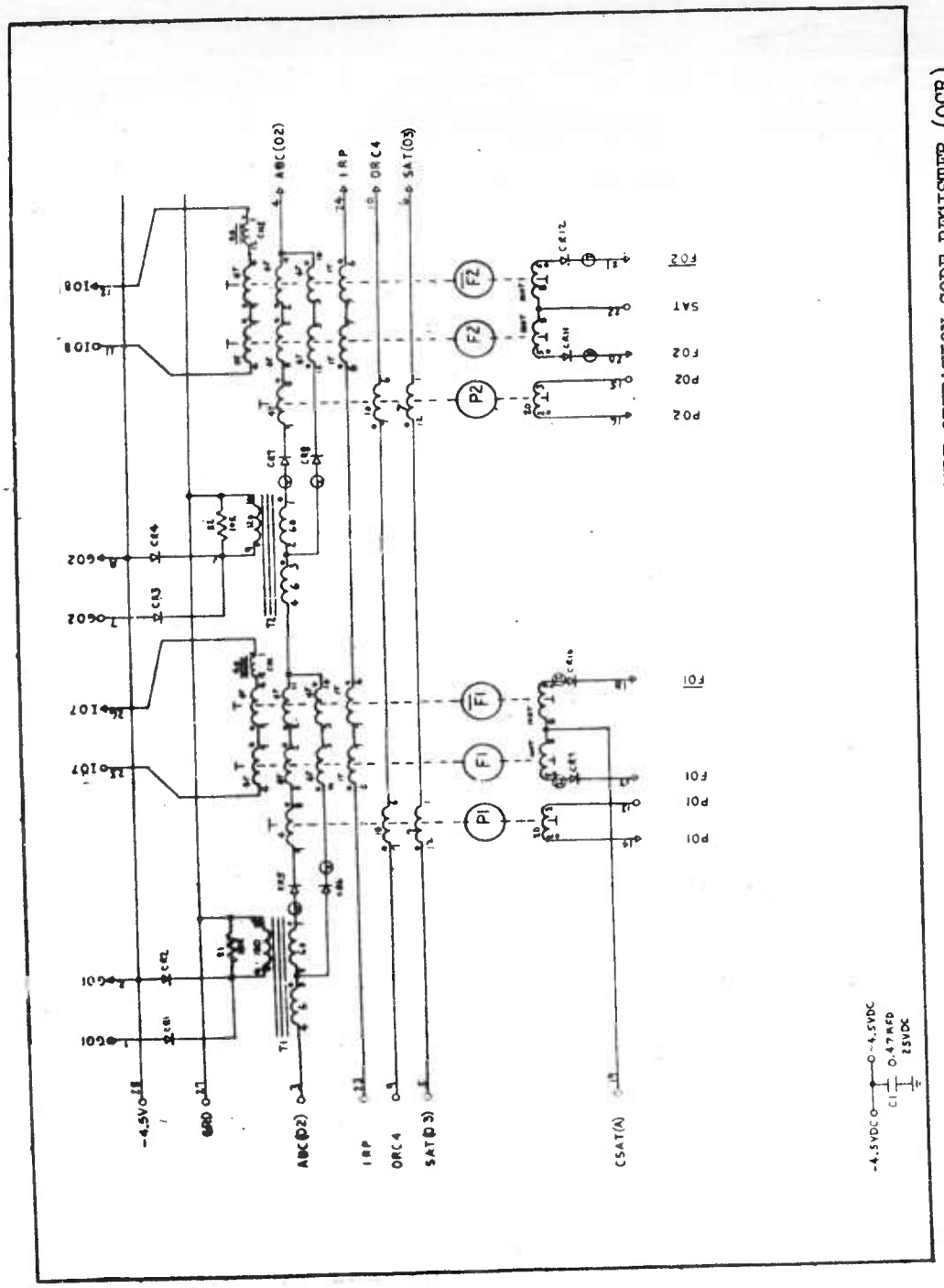

FIGURE 27 (SHEET 1) SCHEMATIC DIAGRAM OF COMPUTER TEST VEHICLE OPERATION CODE REGISTER (OCR)

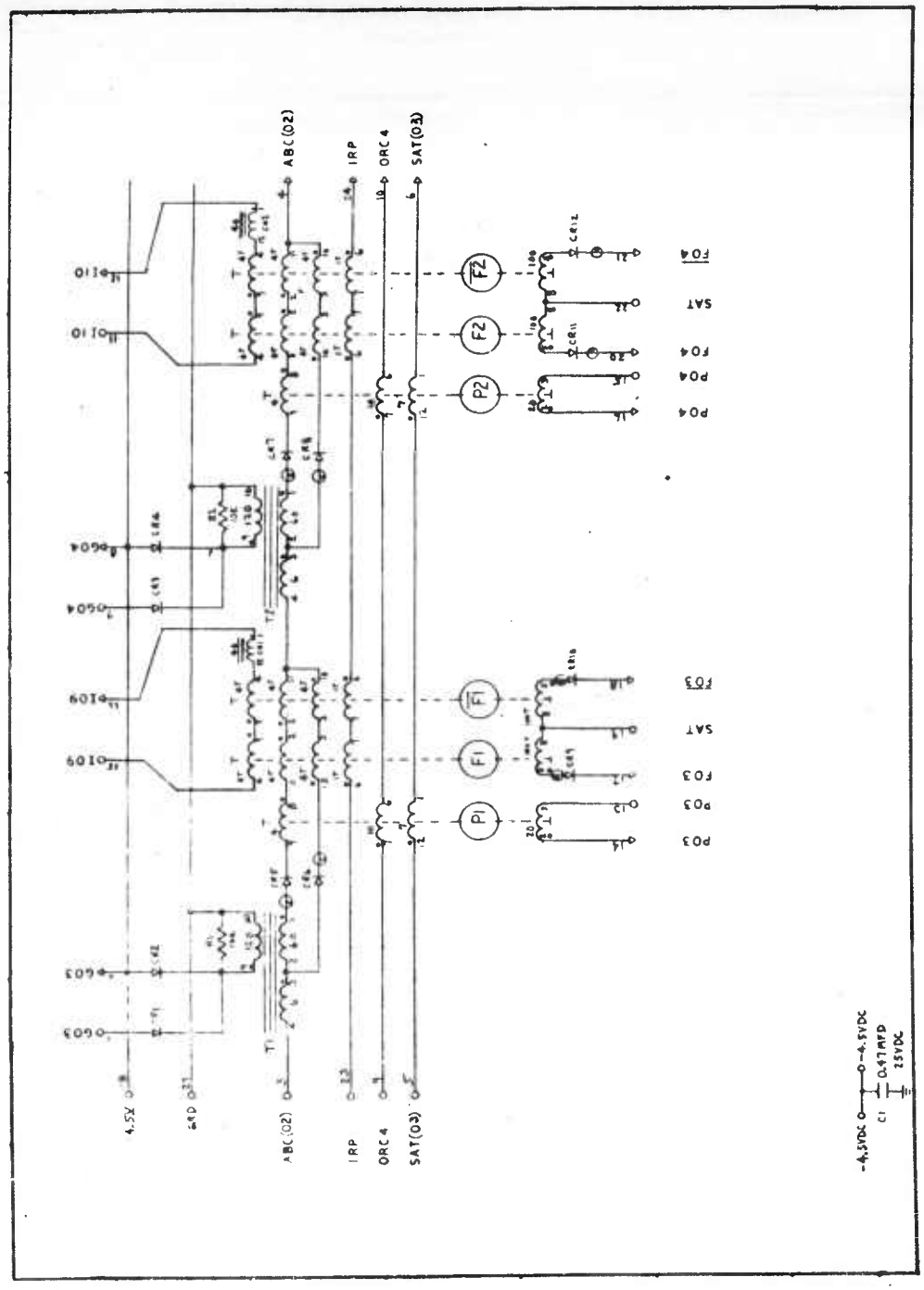

FIGURE 27 (SHEET 2) SCHEMATIC DIAGRAM OF COMPUTER TEST VEHICLE OPERATION CODE REGISTER (OCR)

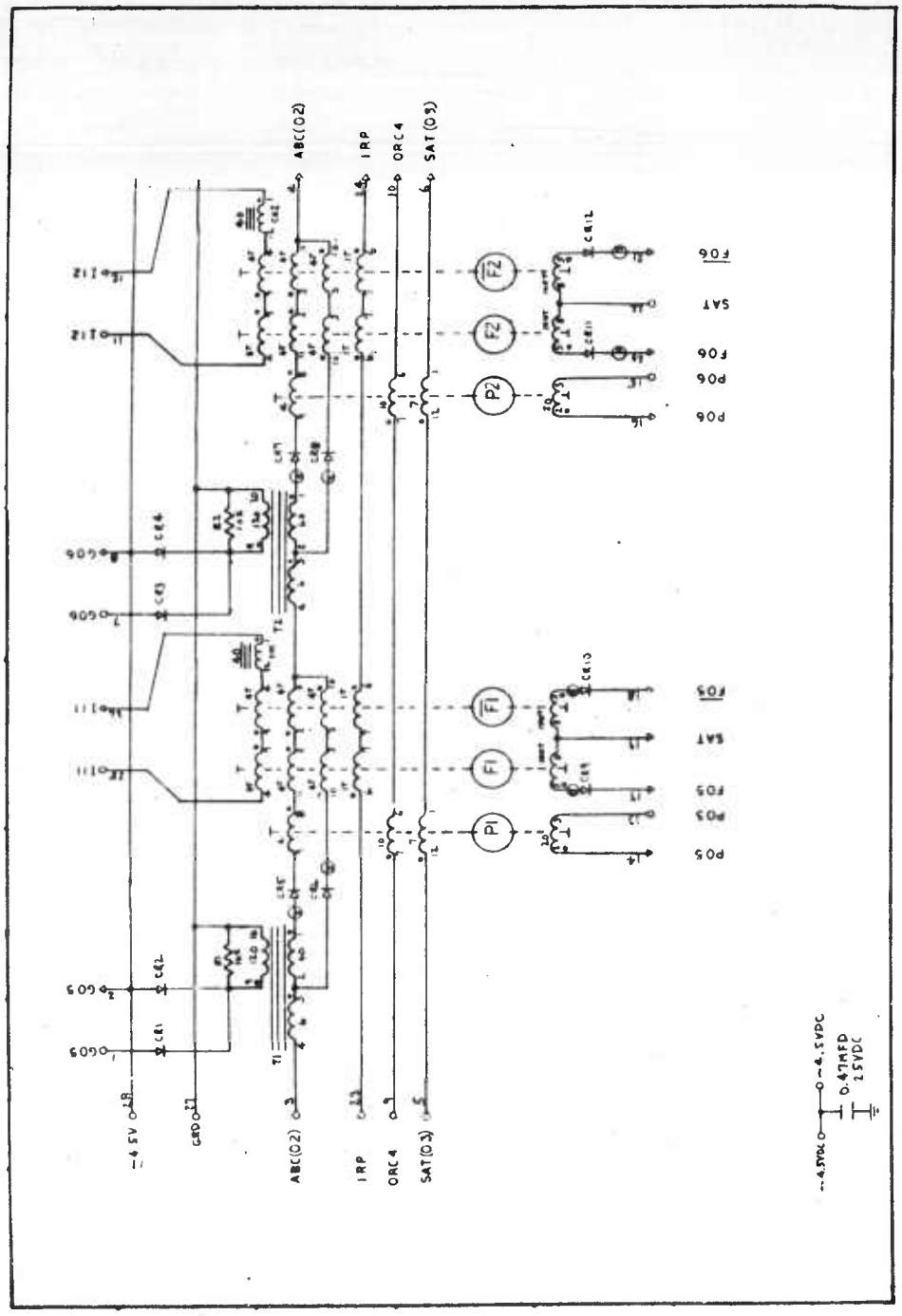

FIGURE 27 (SHEET 3) SCHEMATIC DIAGRAM OF COMPUTER TEST VEHICLE OPERATION CODE REGISTER (OCR)

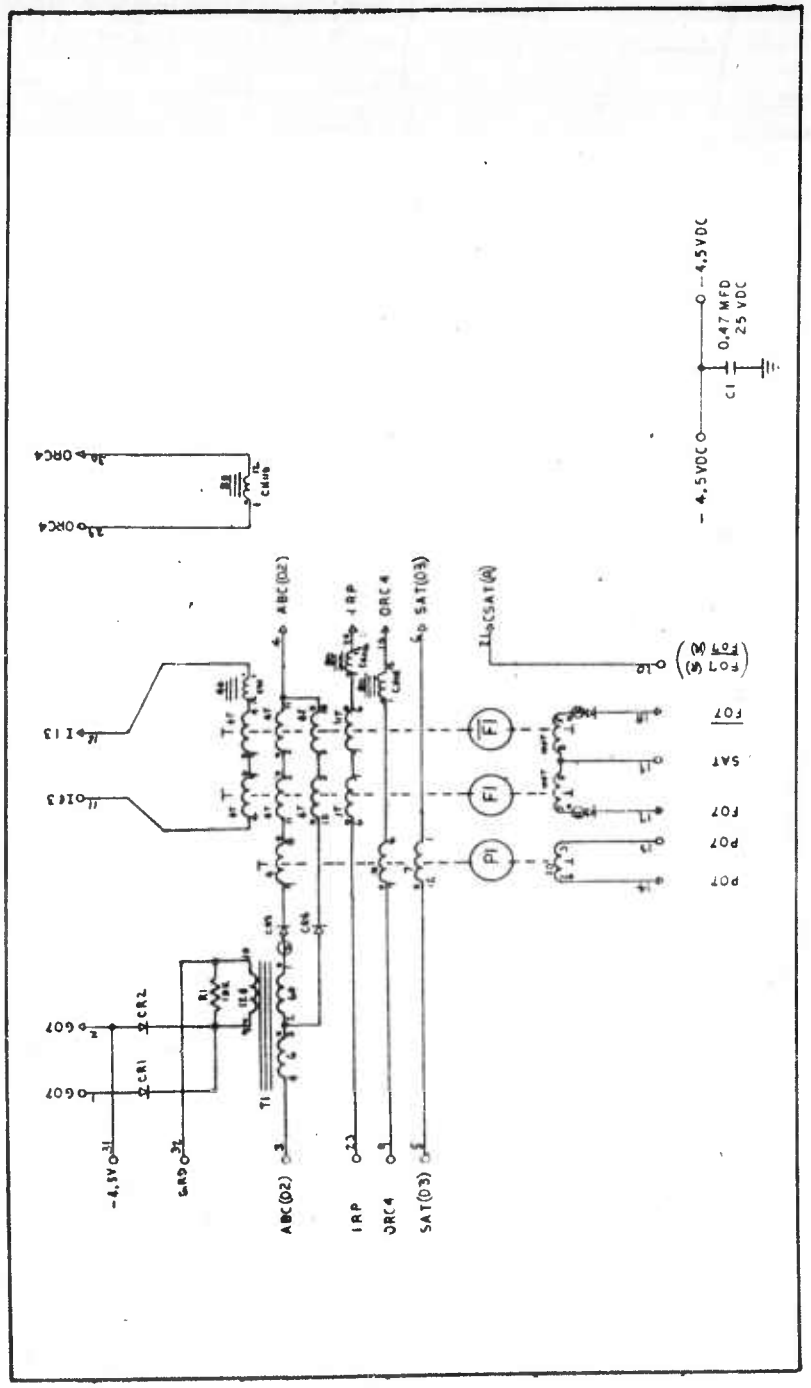

FIGURE 27 (SHEET 4) SCHEMATIC DIAGRAM OF COMPUTER TEST VEHICLE OPERATION CODE REGISTER (OCR)

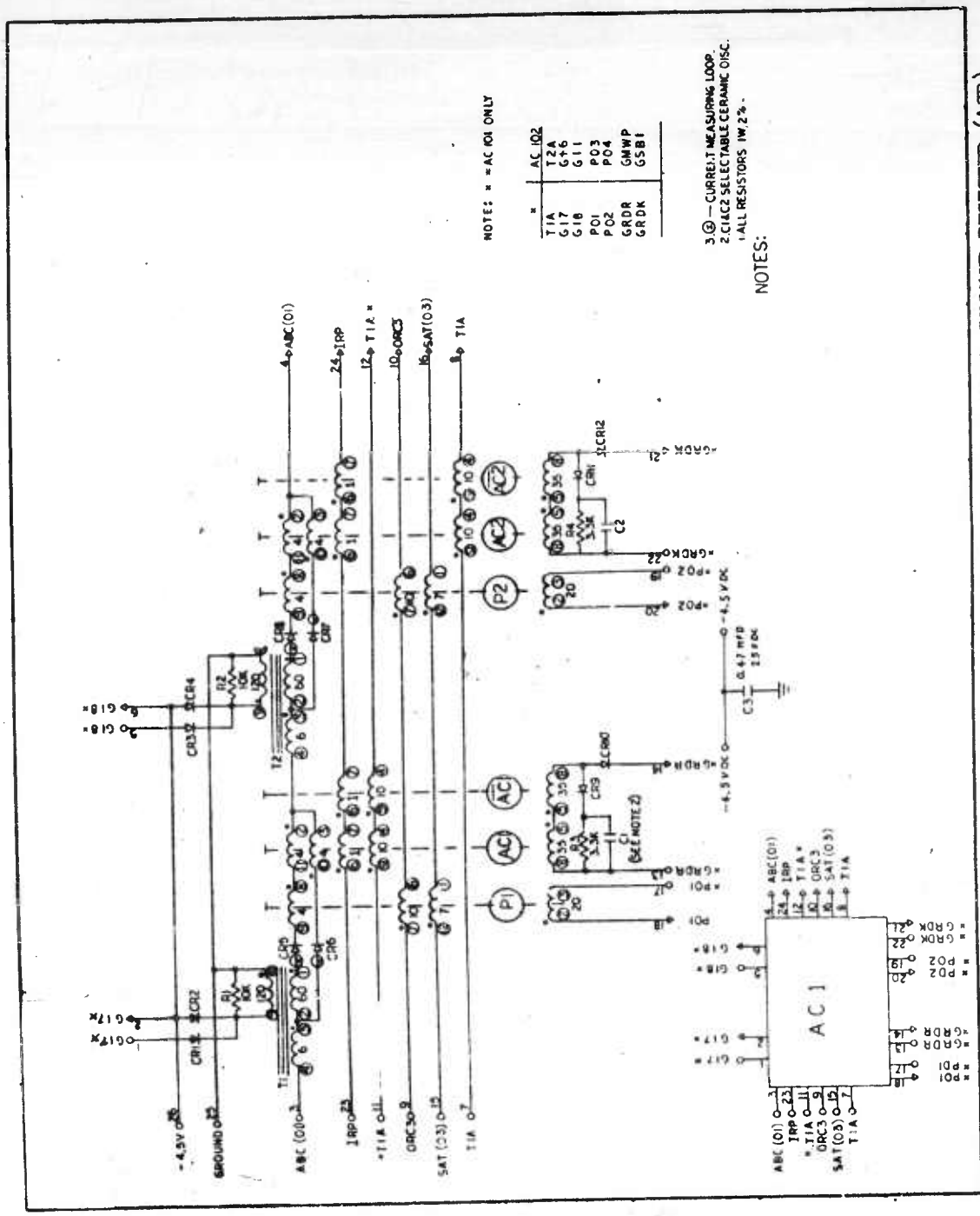

FIGURE 28 (SHEET 1) SCHEMATIC DIAGRAM OF COMPUTER TEST VEHICLE A-PHASE COMMAND REGISTER (ACR)

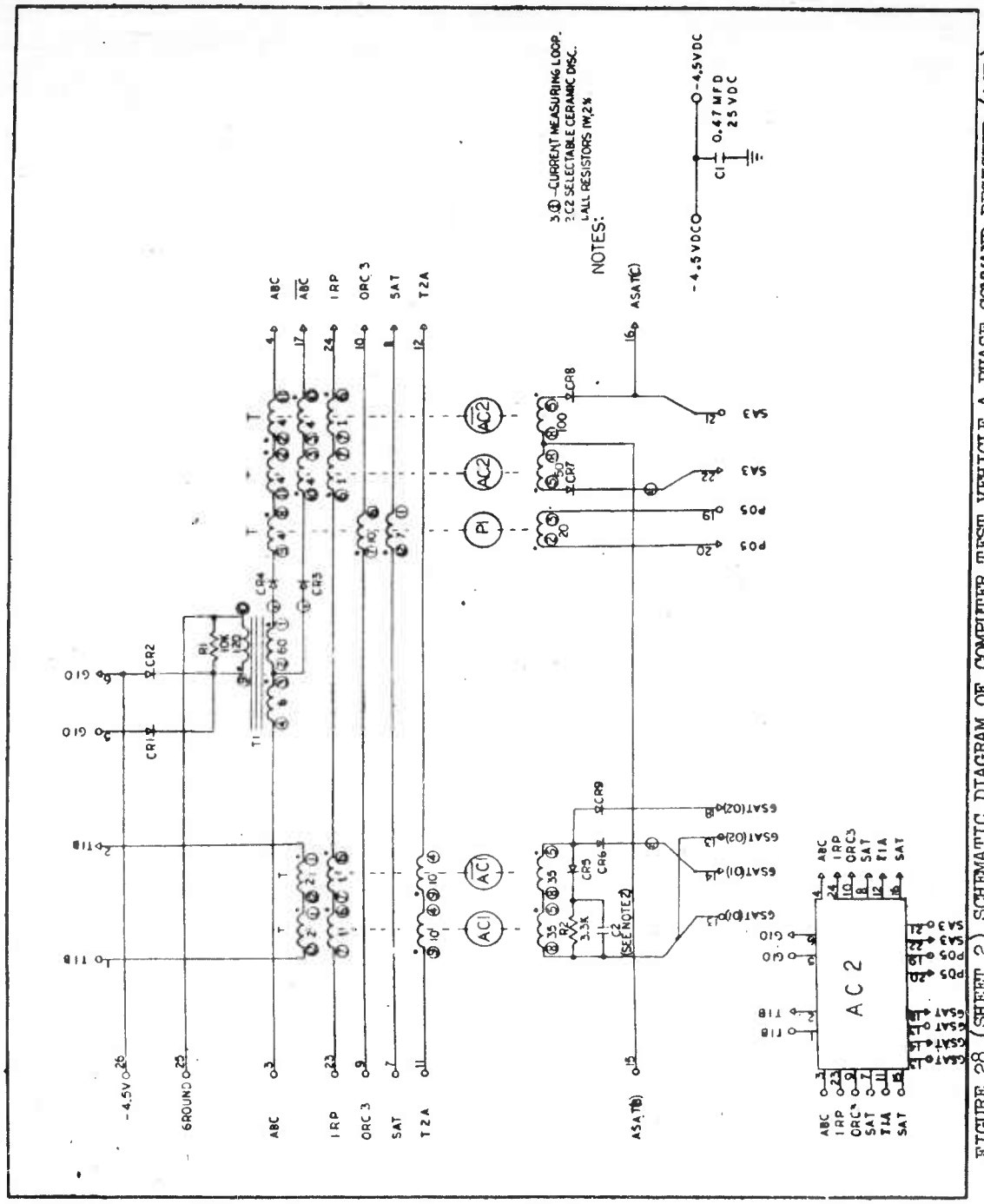

FIGURE 28 (SHEET 2) SCHEMATIC DIAGRAM OF COMPUTER TEST VEHICLE A-PHASE COMMAND REGISTER (ACR)

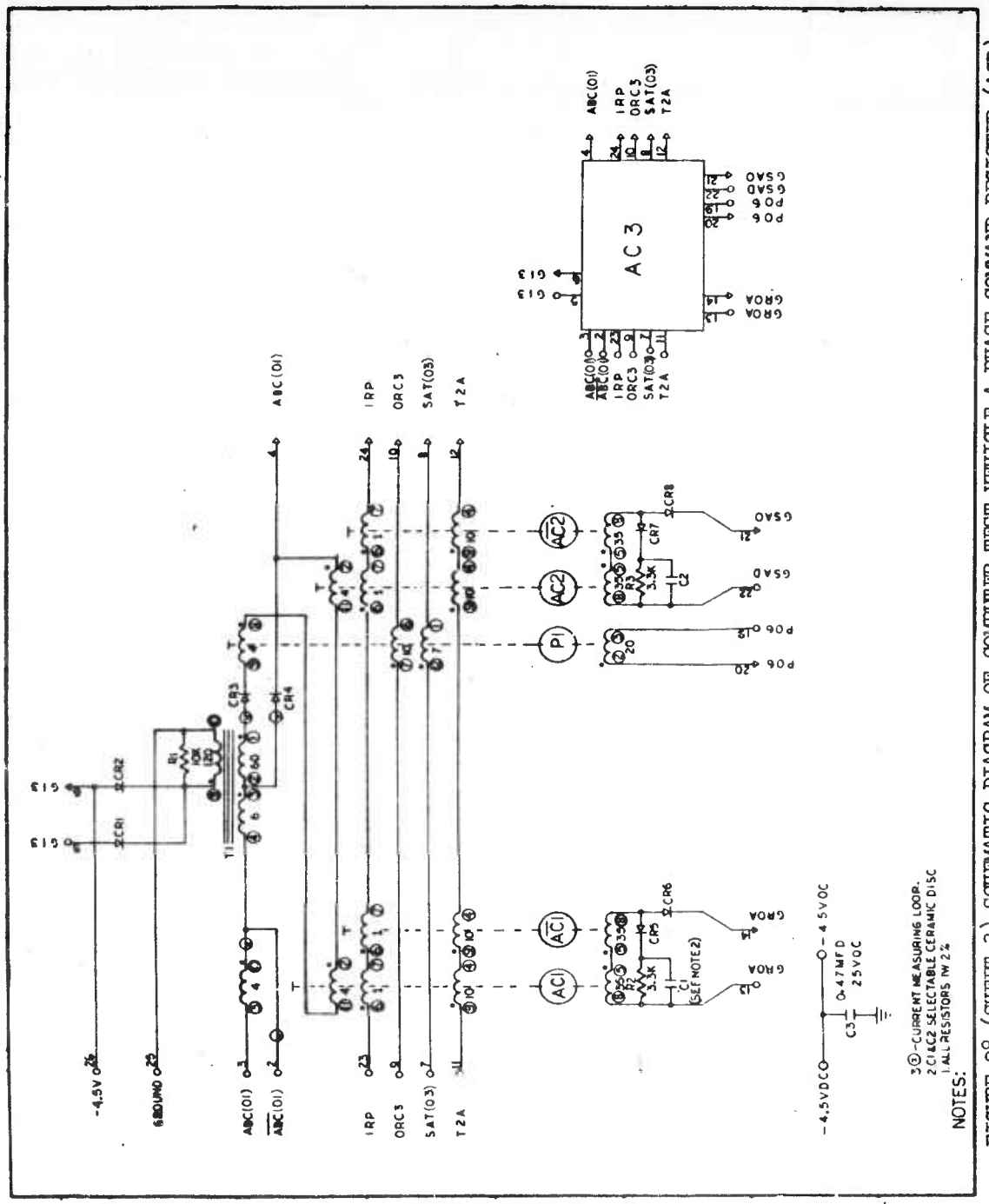

FIGURE 28 (SHEET 3) SCHEMATIC DIAGRAM OF COMPUTER TEST VEHICLE A-PHASE COMMAND REGISTER (ACR)

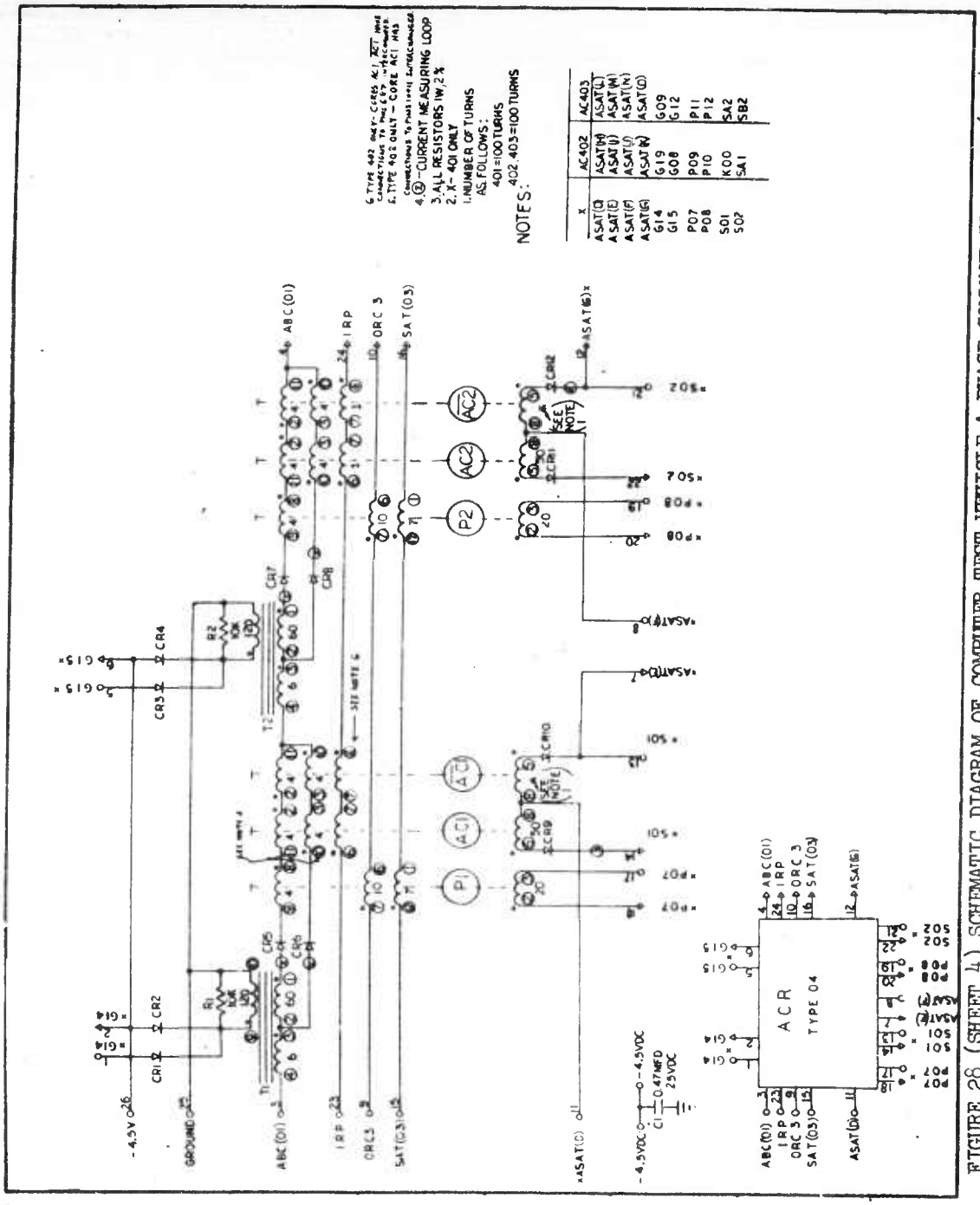

FIGURE 28 (SHEET 4) SCHEMATIC DIAGRAM OF COMPUTER TEST VEHICLE A-PHASE COMMAND REGISTER (ACR)

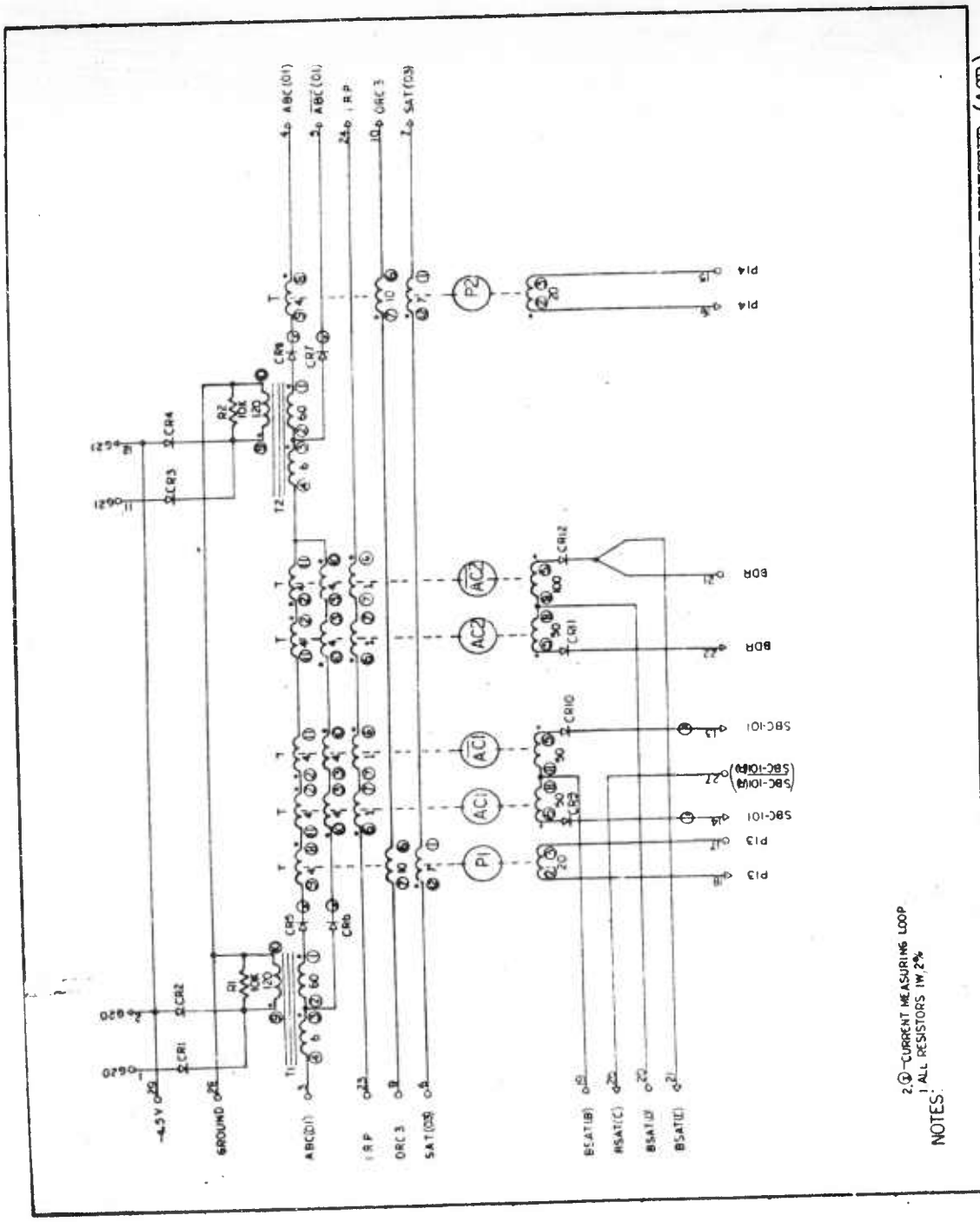

FIGURE 28 (SHEET 5) SCHEMATIC DIAGRAM OF COMPUTER TEST VEHICLE A-PHASE COMMAND REGISTER (ACR)

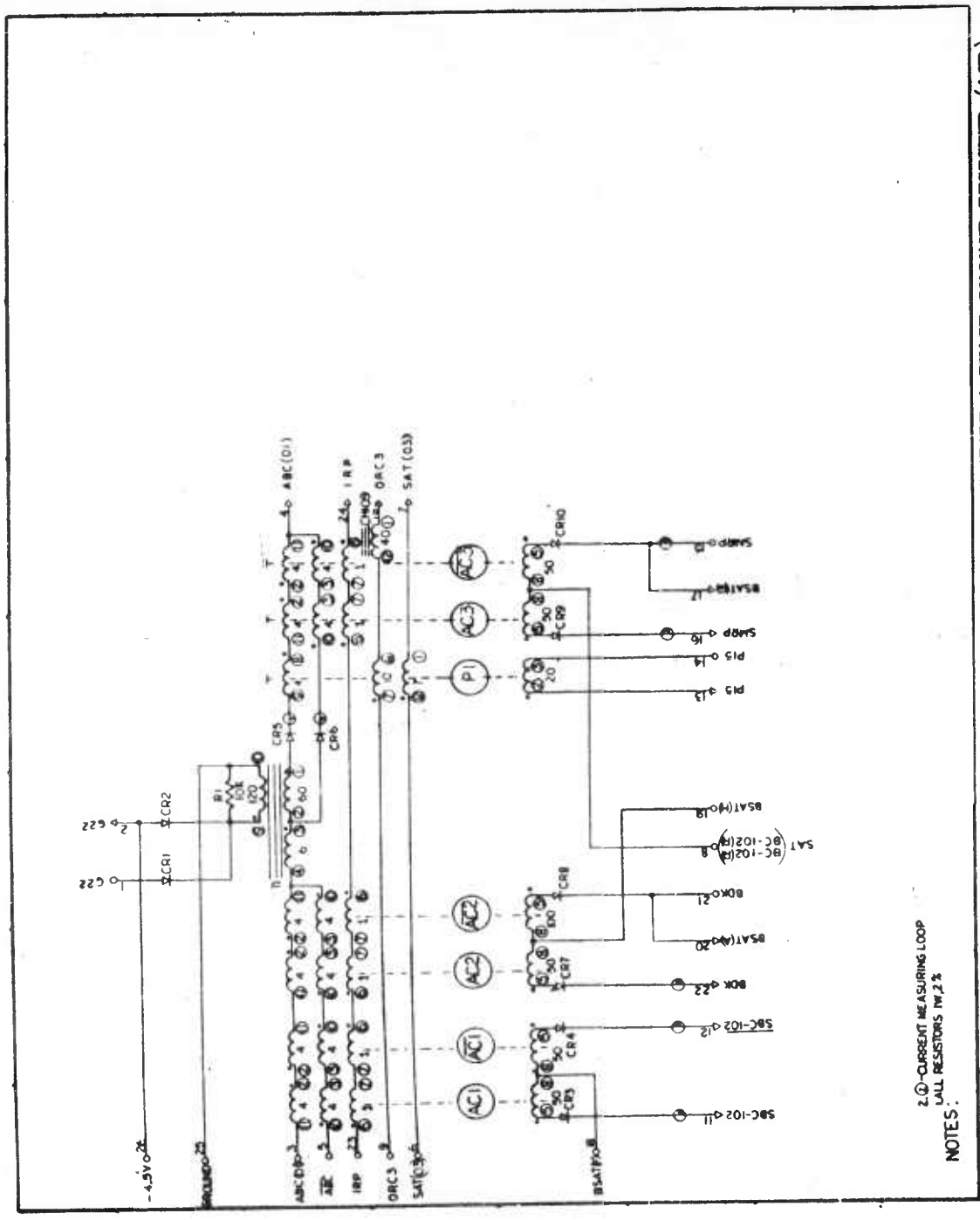

FIGURE 28 (SHEET 6) SCHEMATIC DIAGRAM OF COMPUTER TEST VEHICLE A-PHASE COMMAND REGISTER (ACR)

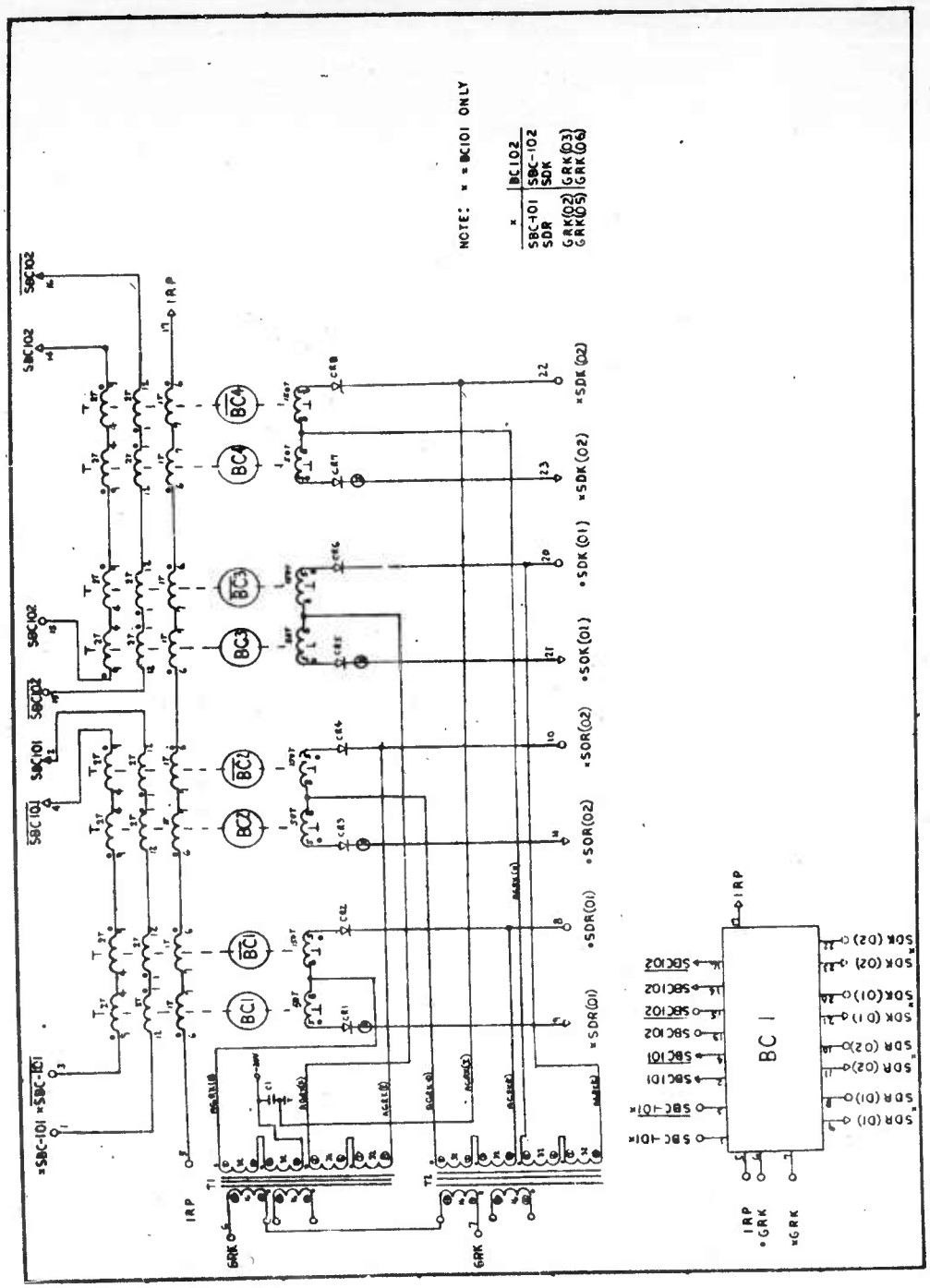

FIGURE 29 (SHEET 1) SCHEMATIC DIAGRAM OF COMPUTER TEST VEHICLE B-PHASE COMMAND REGISTER (BCR)

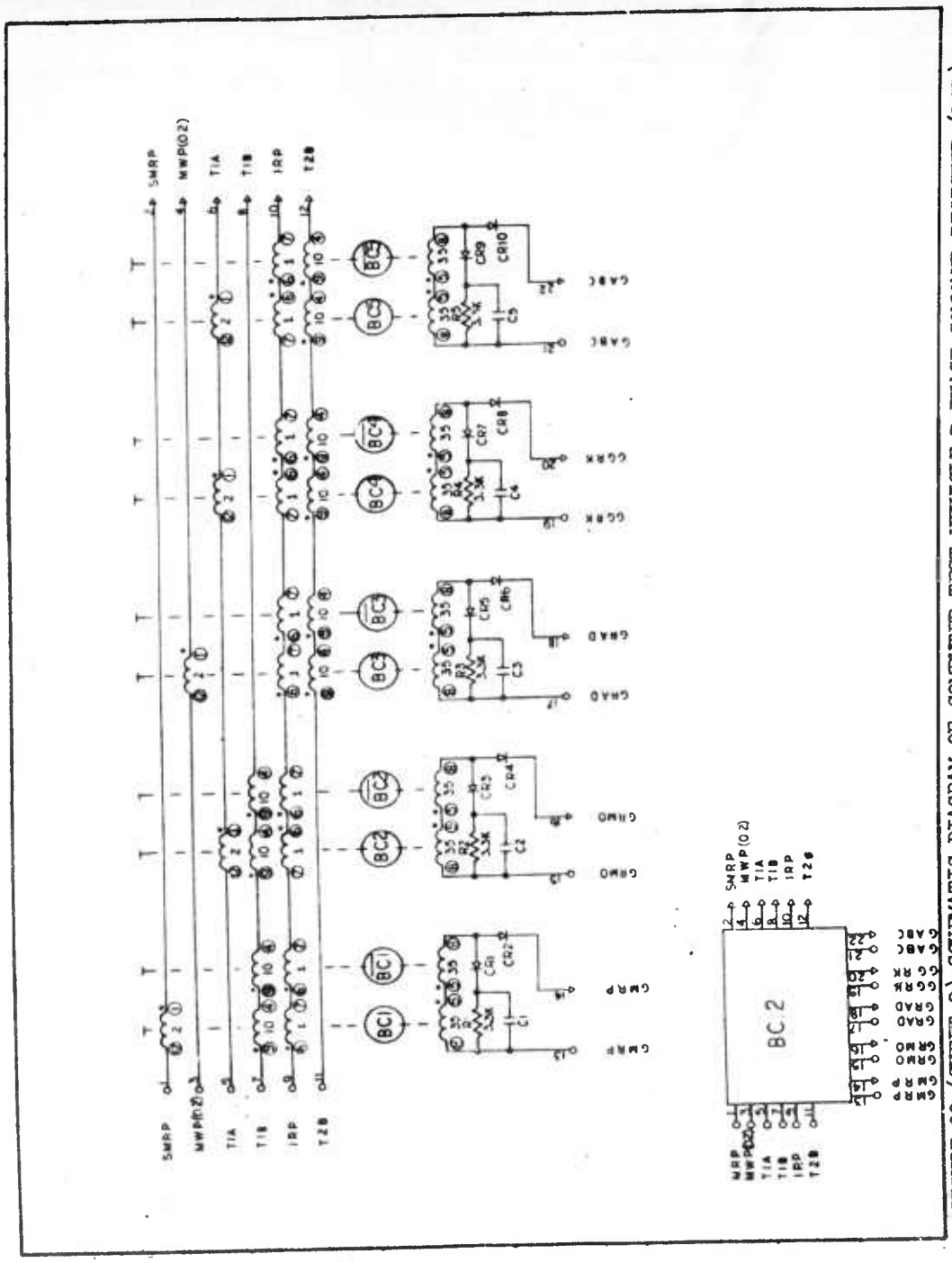

FIGURE 29 (SHEET 2) SCHEMATIC DIAGRAM OF COMPUTER TEST VEHICLE B-PHASE COMMAND REGISTER (BCR)

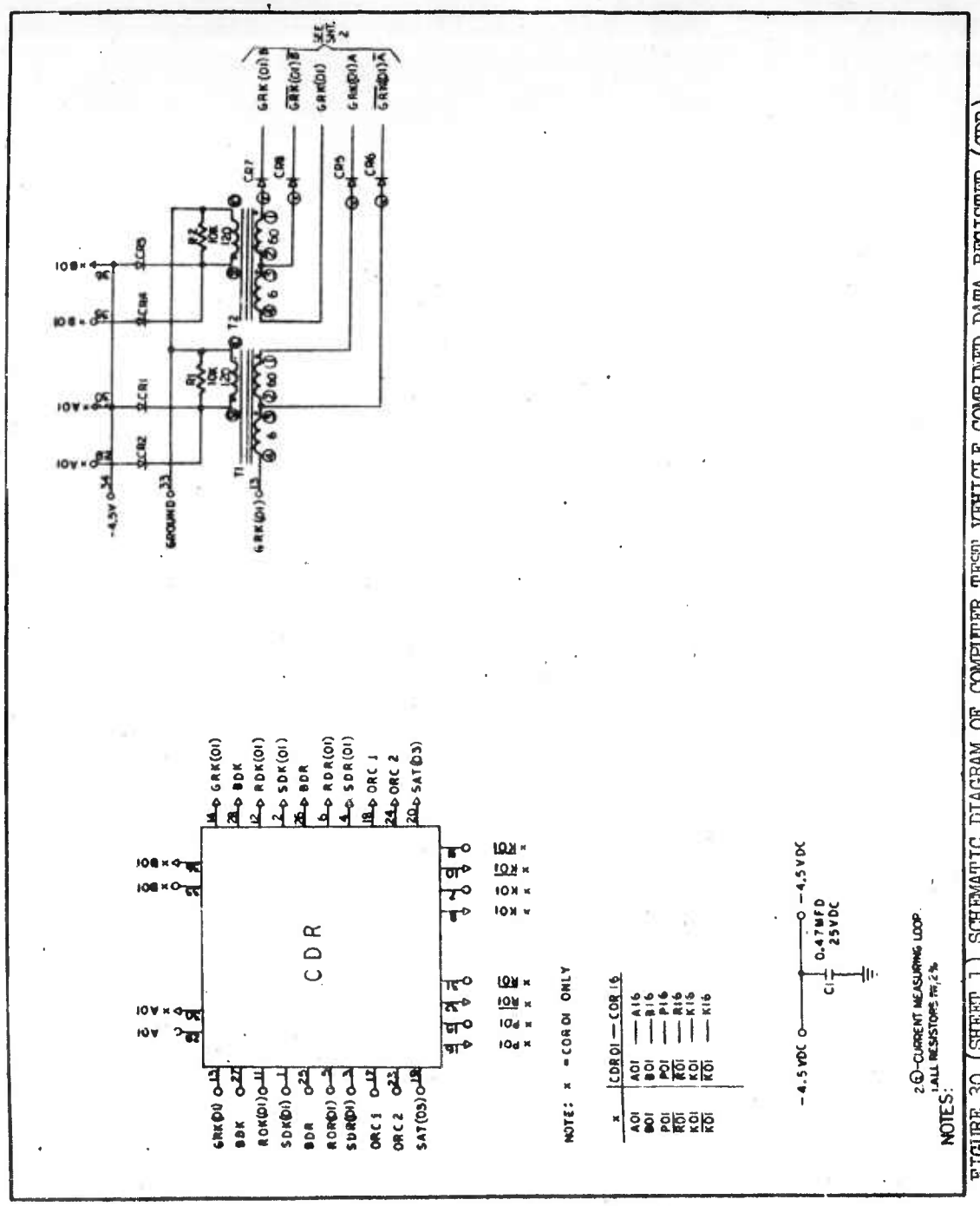

FIGURE 30 (SHEET 1) SCHEMATIC DIAGRAM OF COMPUTER TEST VEHICLE COMBINED DATA REGISTER (CDR)

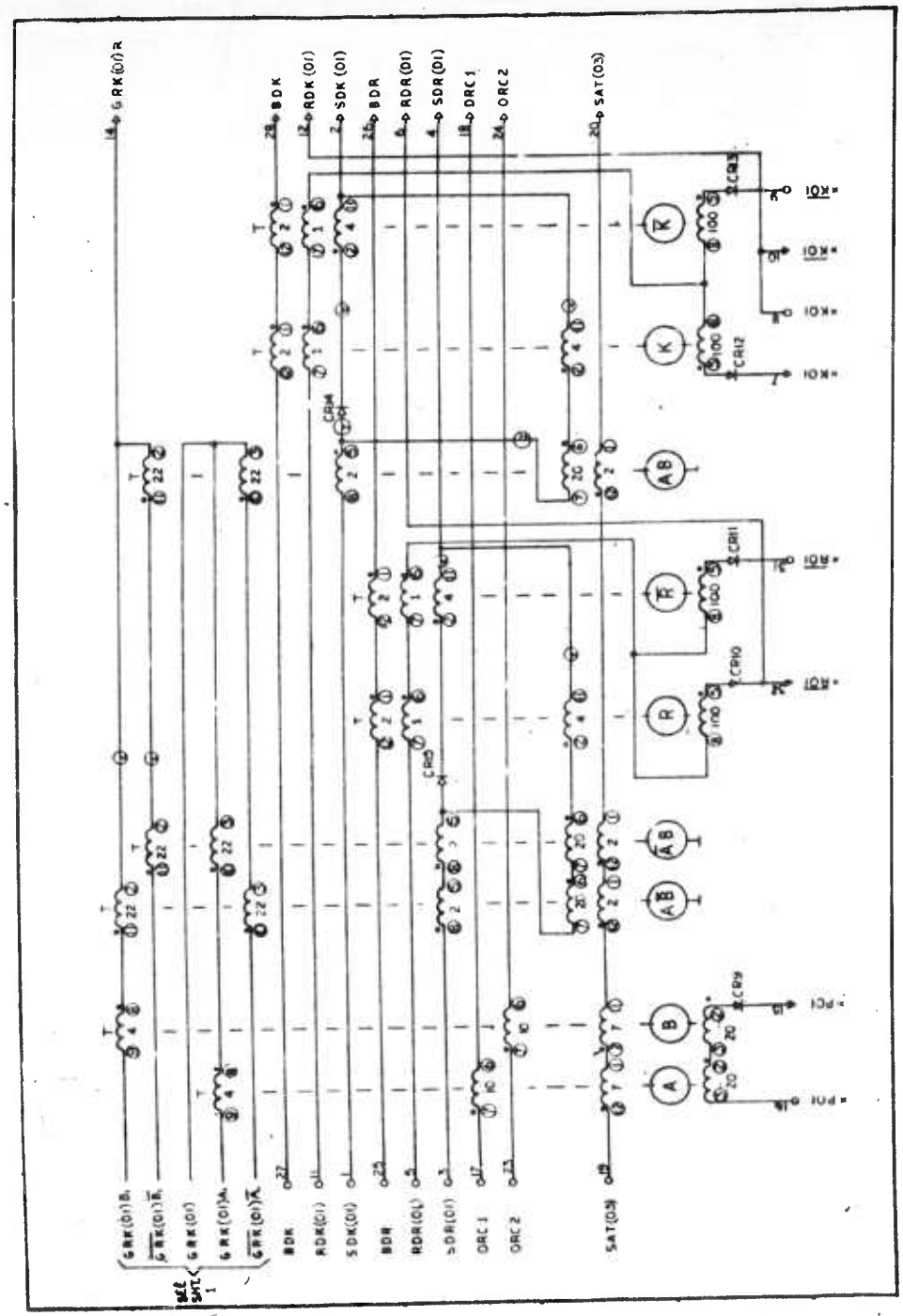

FIGURE 30 (SHEET 2) SCHEMATIC DIAGRAM OF COMPUTER TEST VEHICLE COMBINED DATA REGISTER (CDR)

core is threaded by an inhibit (or "information") line, so that there are 16 inhibit lines. Thus, each core is threaded by four circuits (five wires): X drive, Y drive, inhibit, and sense. The geometry is such that every core is linked by the X and Y wires in the same polarity, and by the inhibit wires in the opposite polarity. The sense wire links alternate cores in opposite directions for noise cancellation. Individual cores are addressed by simultaneously energizing a particular X and Y line.

The following circuits are required to operate the memory:

(a) Data address decoders (DAD), shown in Figure 31, to decode the 6-bit data address stored in the operand address register (OAR) and to select one of eight X and one of eight Y lines to be driven

(b) Memory drivers to drive the memory read pulse current (MRP driver) and memory write pulse current (MWP driver) into the selected X and Y lines

(c) A memory data register to receive the data word read out (DK register is used for this purpose)

(d) A means for selecting inhibit lines to be driven. This function is performed in the data memory write register (DWR), shown in Figure 32, in which inhibit current is derived from the MWP current and is controlled, bit by bit, by the information read from the DK register

(e) Sense preamplifiers and sense amplifiers.

2.2.1.3.7 Miscellaneous Circuits

Radiation hardened delay lines are used to derive detailed timing pulses from the A-and B-phase clock pulses. One tapped, lumped-constant (LC) delay line is used for each phase. The specifications are:

(a)	Impedance	500 ohms
(b)	Delay	6.0 μsec.
(c)	Rise Time	0.3 μsec.
(d)	Attenuation	$<$3 db
(e)	Taps	Every 0.5 μsec.

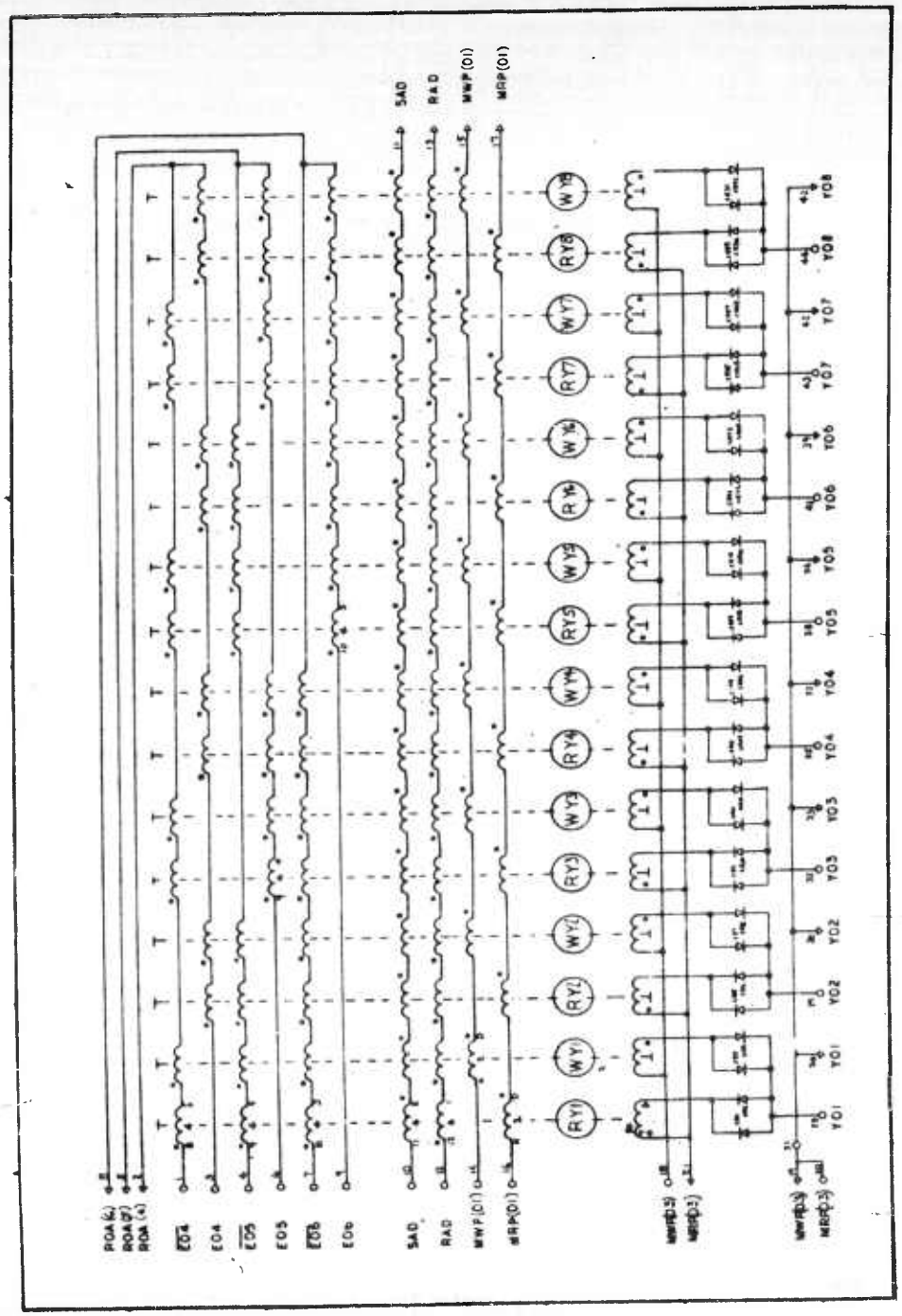

FIGURE 31 (SHEET 1) SCHEMATIC DIAGRAM OF COMPUTER TEST VEHICLE DATA ADDRESS DECODER (DAD)

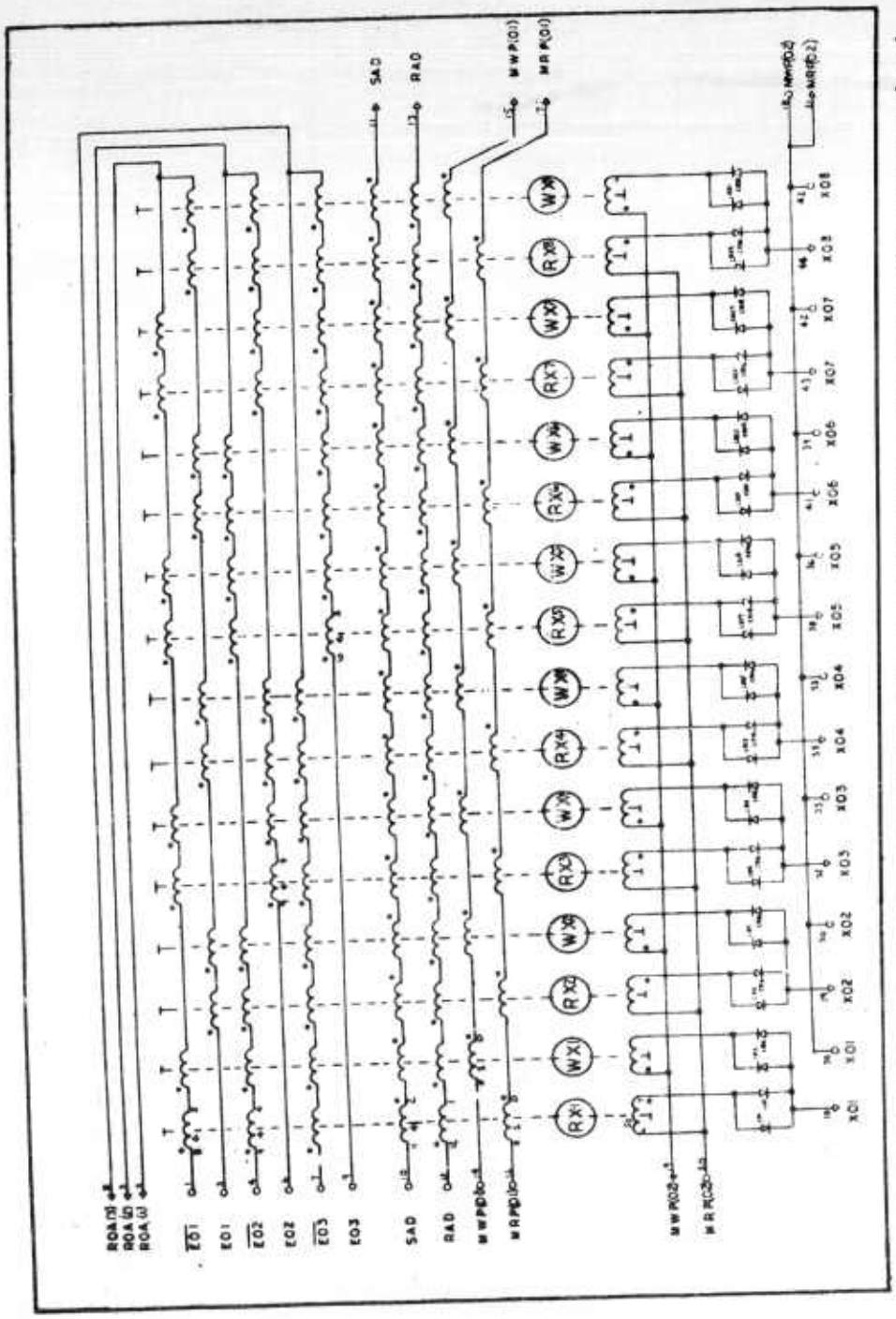

FIGURE 31 (SHEET 2) SCHEMATIC DIAGRAM OF COMPUTER TEST VEHICLE DATA ADDRESS DECODER (DAD)

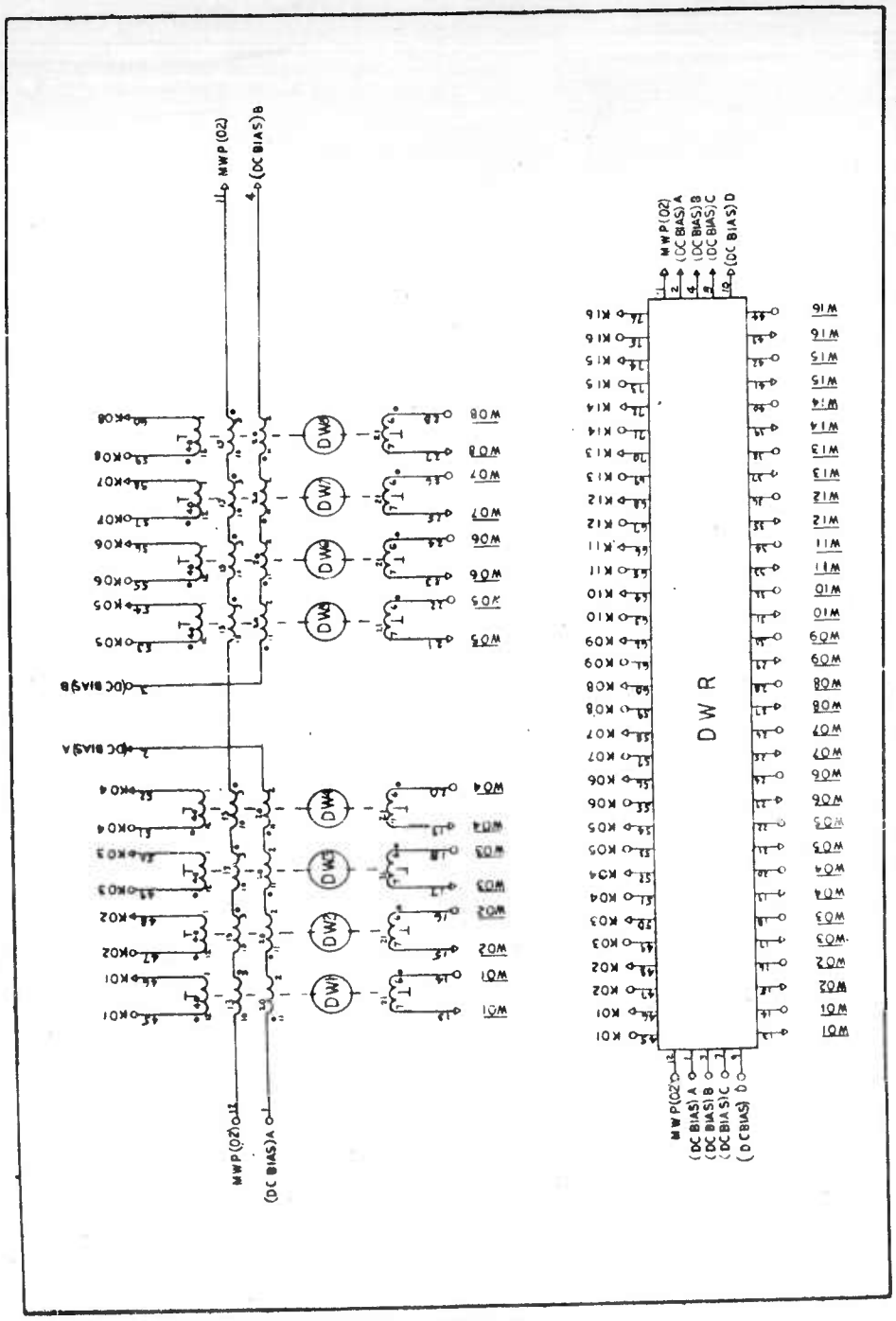

FIGURE 32 (SHEET 1) SCHEMATIC DIAGRAM OF COMPUTER TEST VEHICLE DATA MEMORY WRITE REGISTER (DWR)

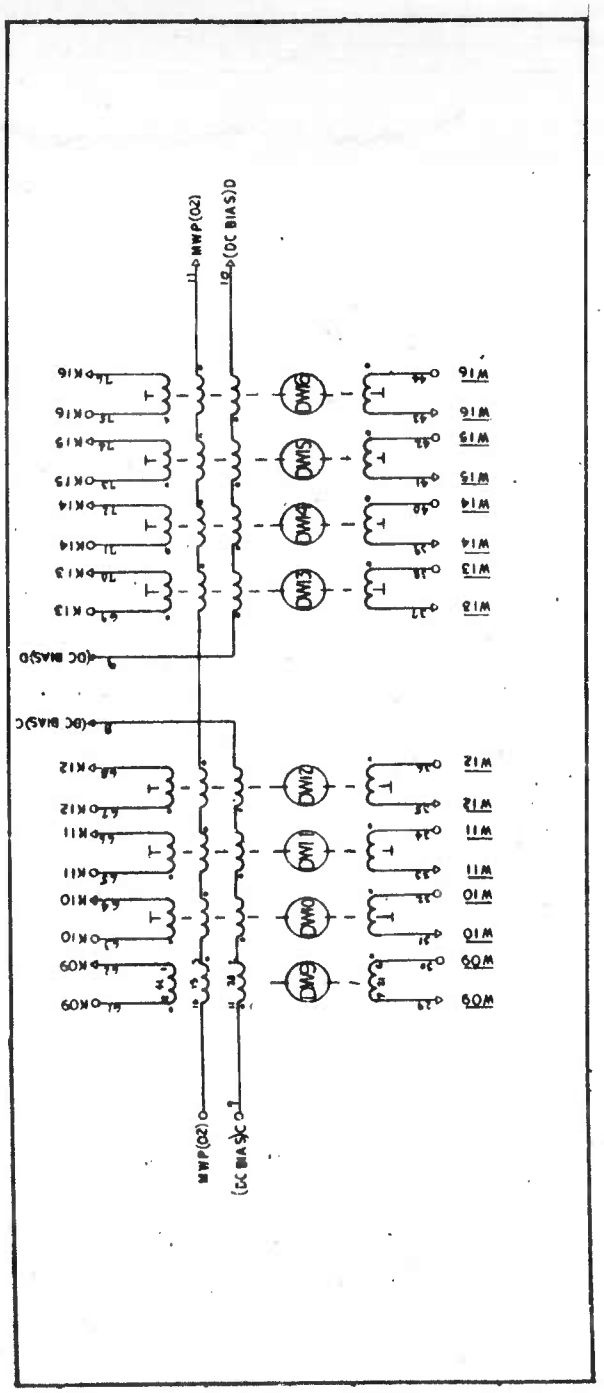

FIGURE 32 (SHEET 2) SCHEMATIC DIAGRAM OF COMPUTER TEST VEHICLE DATA MEMORY WRITE REGISTER (DWR)

The delay line is constructed of inductors and glass capacitors and is hermetically sealed in a can filled with loose, clean sand for shock resistance. Each delay line is driven by a 2 μsec. pulse of 40 volts (referred to -15 volts), and energy is available at each tap to trigger a TBP or STBO directly (through a 10k decoupling resistor) without appreciable loss of signal on the line. In the phase B line, part of the energy dissipated in the 500 ohm termination is used to turn off SSGBO.

Pulse transformer circuits are used in several applications. Pulse transformers are used in all vacuum tube plate output circuits to isolate plate voltage (+150 vdc) from the following circuits. When two or more loads require isolation because of different current pulse amplitude or DC voltage level requirements, the primary windings of two or more pulse transformers are connected in series in the plate circuit. This was frequently done in triggered current driver circuits. Pulse transformers are also used as distribution transformers in driven current steering circuits. Additional uses of pulse transformers are in the control of register setting from sense amplifiers, in which the pulse transformer acts as an impedance match between the sense amplifier and the register, and to enable SPA current drivers to supply strobe current pulses to multiple tunnel diode preamplifiers. The primary windings of two to four pulse transformers are connected in series in the plate circuit of the SPA tube and the secondary of each transformer is used to drive the primary windings of pulse transformers at the inputs of eight preamplifiers.

2.2.1.3.8 Current Steering

Current steering was used extensively in the test vehicle logic design since it reduces appreciably the number of TCDs required. It can be used to direct a current through or bypass a light load, just as if the load were driven by a conditionally triggered TCD. About 60- current steering circuits are used, representing a savings of as many drivers and twice as many tubes.

Current steering utilizes the fact that the driven winding on a core being set presents a much higher impedance than the same winding on a core that has already been set; so in a parallel connected circuit containing a reset core in one branch and a set core in series with a load in the other, current driven through the circuit will flow mostly in the load. It is practical to make the impedance ratio large enough that 99% or more of the current flows through the load, while the impedance of the whole circuit is only 50% greater than the load alone. If the initial states of the cores are reversed, then very little current flows in the load and almost all bypasses it. Several such current steering-load combinations are driven in series by an unconditional driver, and current to the various loads is controlled by the states of the appropriate cores. A diode in

series with each steering winding is necessary to isolate the cores during setting.

2.2.2 NUCLEAR ANALYSIS

All components and circuits incorporated into the guidance computer test vehicle had been successfully evaluated in earlier radiation tests to levels which exceed the design requirements. Although both the logic and the tunnel diodes exhibited definite degradation, their operating parameters remained within the computer design requirements. No other components were appreciably affected. All circuits tested operated satisfactorily to well above 1×10^{10} ergs/gm - (C) and 1×10^{16} n/cm^2.

It was very probable that of the large numbers of logic and tunnel diodes used, some would degrade enough to affect the operating thresholds of their circuits. It was not expected, however, that circuit failures due to nuclear exposure would be experienced below design requirements. Since these circuits would be located nearest the reactor face, radiation-induced failures would probably occur first in the core-diode combined data register or in its associated tunnel diode preamplifiers. Results of previous tests indicate that these failures should be expected at an integrated neutron flux of about 1×10^{16} n/cm^2.

2.2.3 TEST PROCEDURE

2.2.3.1 Test Instrumentation

A test instrumentation block diagram is shown in Figure 33. The test vehicle interface unit serves as a buffer translator between the SDS 920 computer of the Data Management System and the test vehicle. It also permitted exercising the test vehicle manually or with punched cards. Figure 34 is a block diagram showing interconnections between the interface unit and other equipment in the final system reactor test configuration. This configuration is the prime test configuration wherein the SDS 920 computer would transmit 14 bits of information (7 bits of operation code, 6 bits of operand address or data, and a 1-bit strobe) to the test vehicle via the interface unit. The test vehicle will in turn generate an answer to be transmitted via the interface unit to the SDS 920. The answer data to the SDS 920 is 17 bits (16 bits of data and the EOI level).

2.2.3.2 Test Operation Modes

The three modes of operation mentioned in paragraph 2.2.3.1 were available to the operator as shown in Figure 35. The mode intended for use during the test uses the SDS 920 computer to

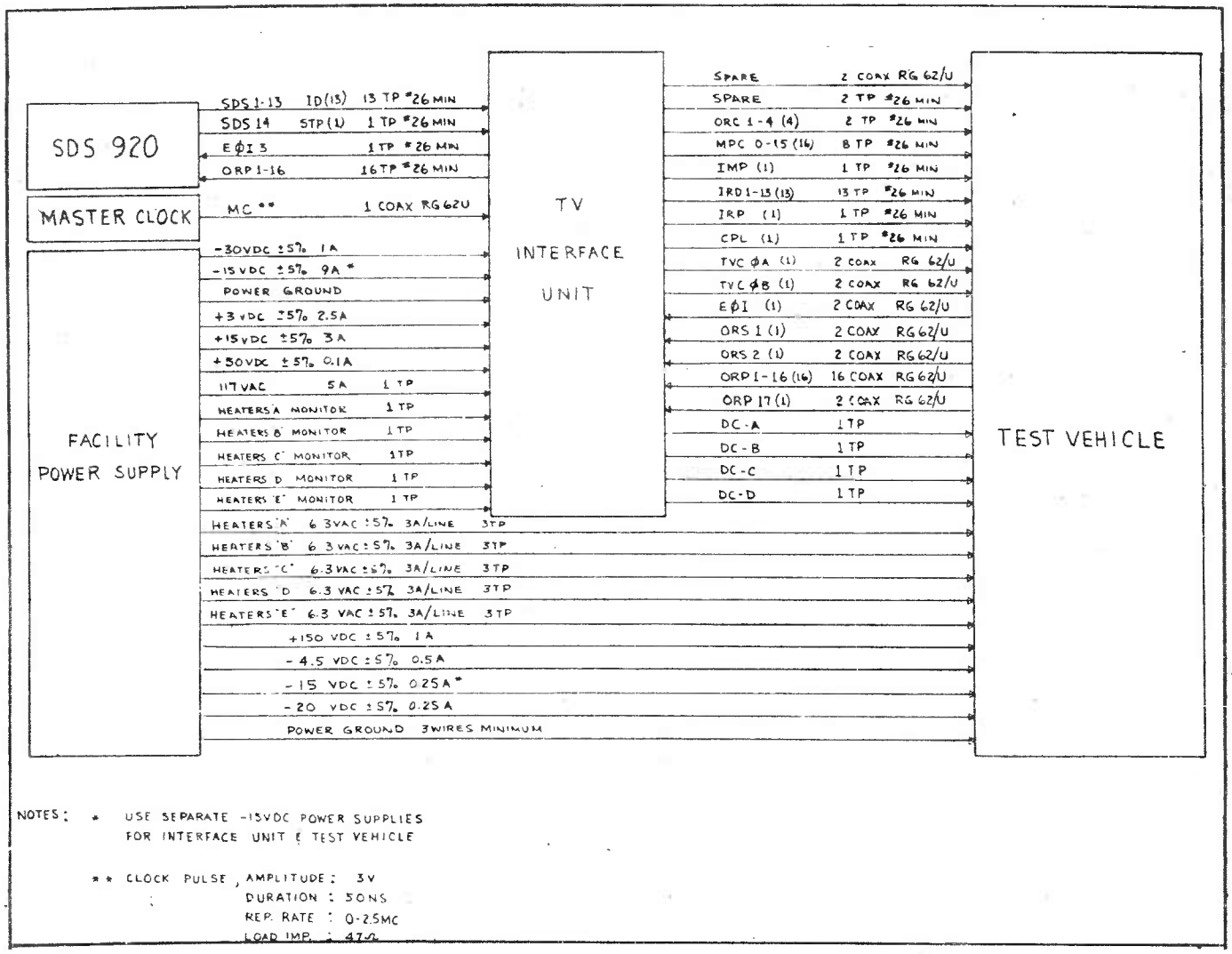

NOTES: * USE SEPARATE -15VDC POWER SUPPLIES FOR INTERFACE UNIT & TEST VEHICLE

** CLOCK PULSE, AMPLITUDE: 3V
DURATION: 50NS
REP. RATE: 0-2.5MC
LOAD IMP.: 47Ω

FIGURE 33 BLOCK DIAGRAM OF COMPUTER TEST INSTRUMENTATION

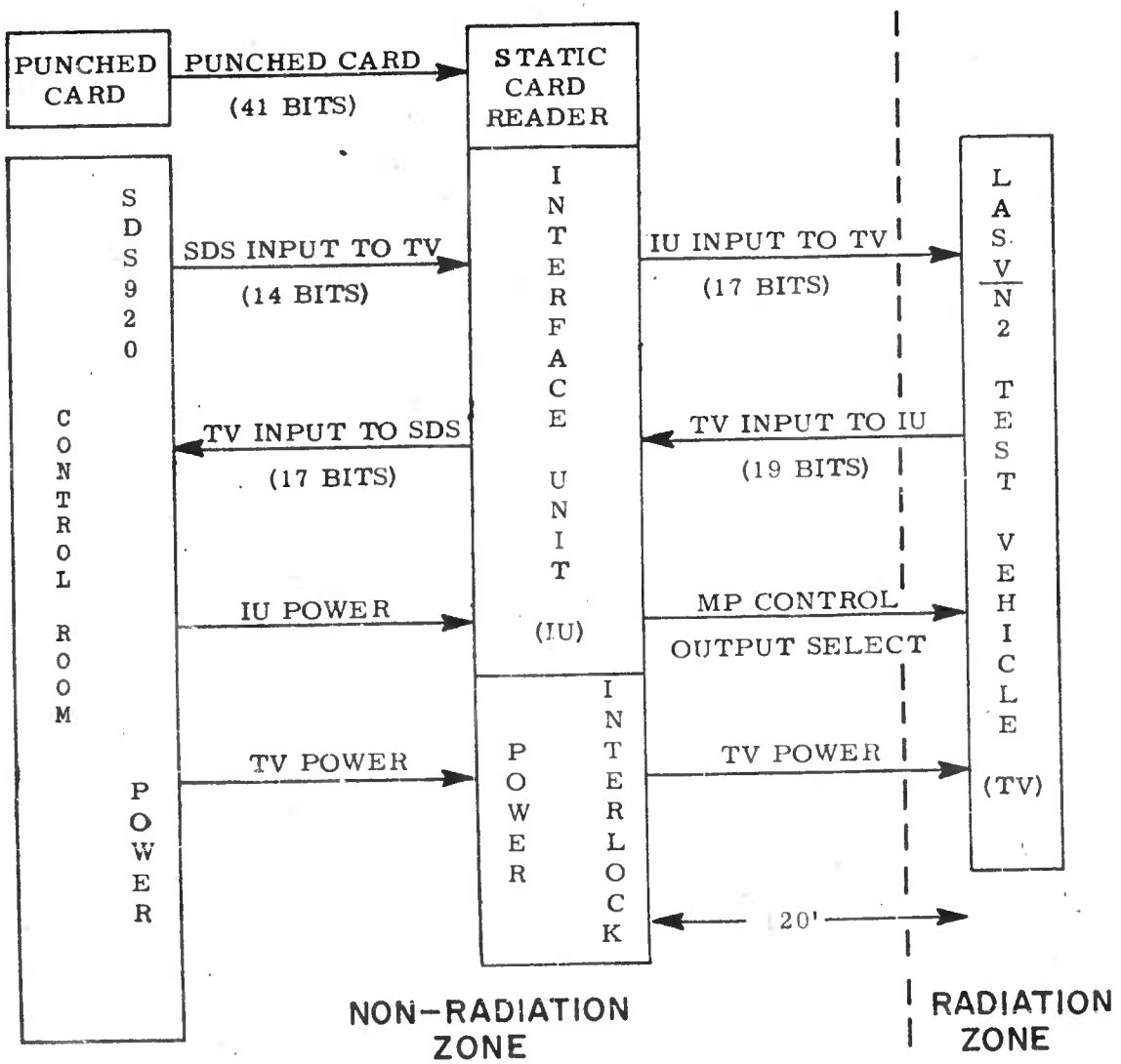

FIGURE 34 COMPUTER TEST SIGNAL INTERCONNECTIONS

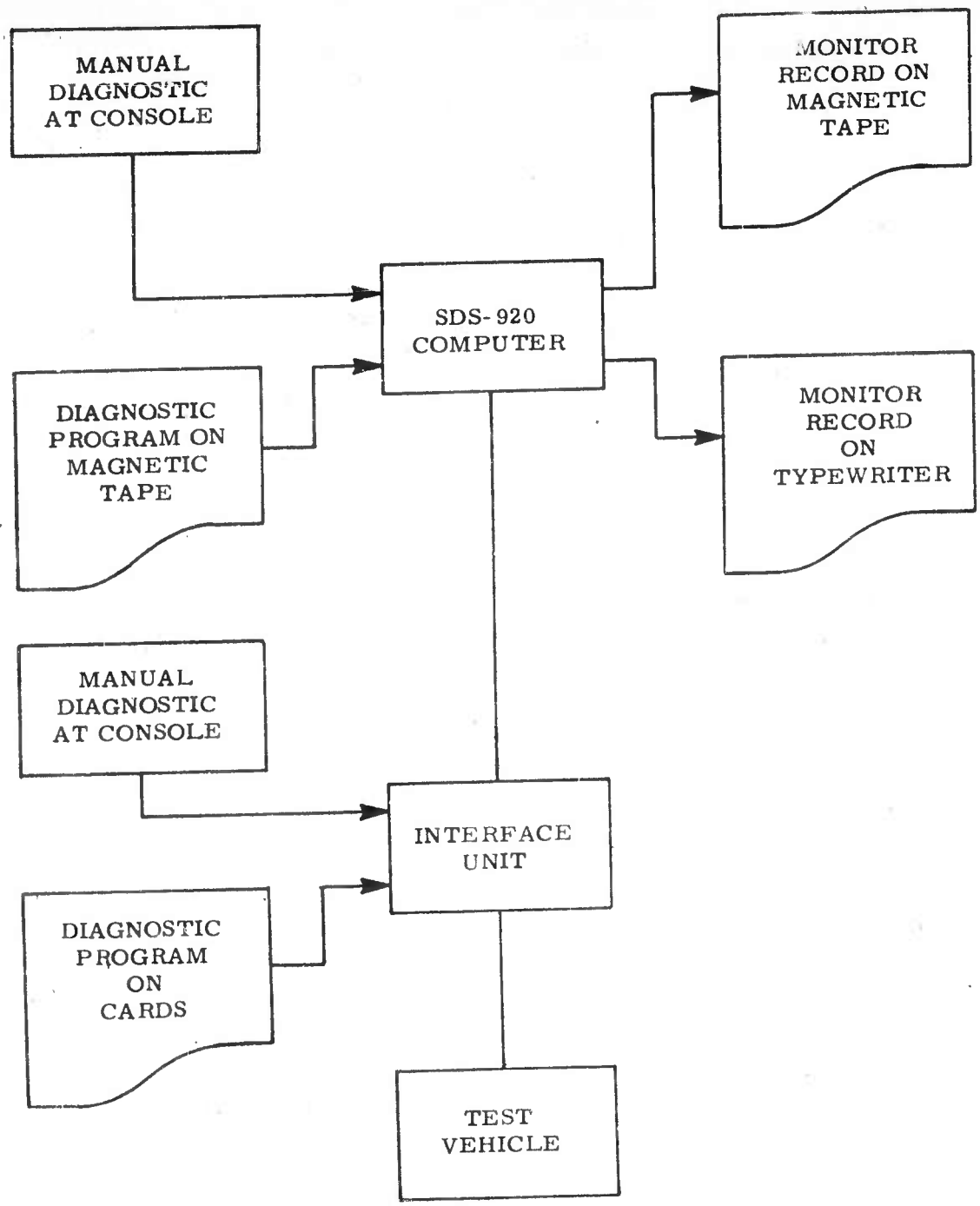

FIGURE 35 BLOCK DIAGRAM OF COMPUTER TEST VEHICLE OPERATION MODES DATA FLOW

both control and monitor the test vehicle through the interface unit. A diagnostic routine was written onto magnetic tape which exercised all logic circuits and elements in the test vehicle. During each test cycle, errors were printed out by an IBM electric typewriter and also stored on magnetic tape.

As a backup mode, a program was punched into cards and a static card reader incorporated into the interface unit. Both card contents and test vehicle output were displayed on the interface unit registers.

A manual operation mode was also available. In that mode, the test vehicle was exercised by instructions entered into a register on the interface unit front panel. The test vehicle output for each instruction was displayed on an interface unit register. This mode was used to troubleshoot the test vehicle or to exercise portions of it after radiation-induced damage had degraded operation of the test vehicle to the point that operation in the SDS 920 computer mode was no longer possible.

The test format, as developed, was intended to perform two functions. A diagnostic routine, run with all bias settings at optimum, exercises all test vehicle logic circuits as a confidence check. The marginal checks were performed by running a diagnostic routine while varying, individually, control currents A, B, C, and D, and the -4.5 volt supply. An operating margin was defined as that value at which errors first appear in the routine. Those checks were run to determine changes in the various operating margins under irradiation. Currents A and C controlled the tunnel diode preamplifier strobe pulse amplitude, with A controlling the microprogram and combined data register preamplifiers and C controlling the data memory preamplifiers. Current B controlled the amplitude of all control driver current pulses. Current D controlled, slightly, the amplitude of the inhibit current in the data memory. The -4.5 volt bias was the bias supply for all vacuum tube sense amplifiers and had a critical effect on their sensitivity.

2.2.4 TEST RESULTS AND CONCLUSIONS

Maximum and minimum gamma exposures and total integrated neutron fluxes for the test were obtained by mounting dosimetry on the center lines of the test vehicle nearest to and farthest from the reactor face. Figure 36 is a plot of the maximum nuclear radiation exposure as a function of reactor operating time, while Figure 37 is a plot of the minimum nuclear radiation exposure. The approximate nuclear radiation exposure at any location in the test vehicle may be obtained by interpolating values obtained from these two sets of curves.

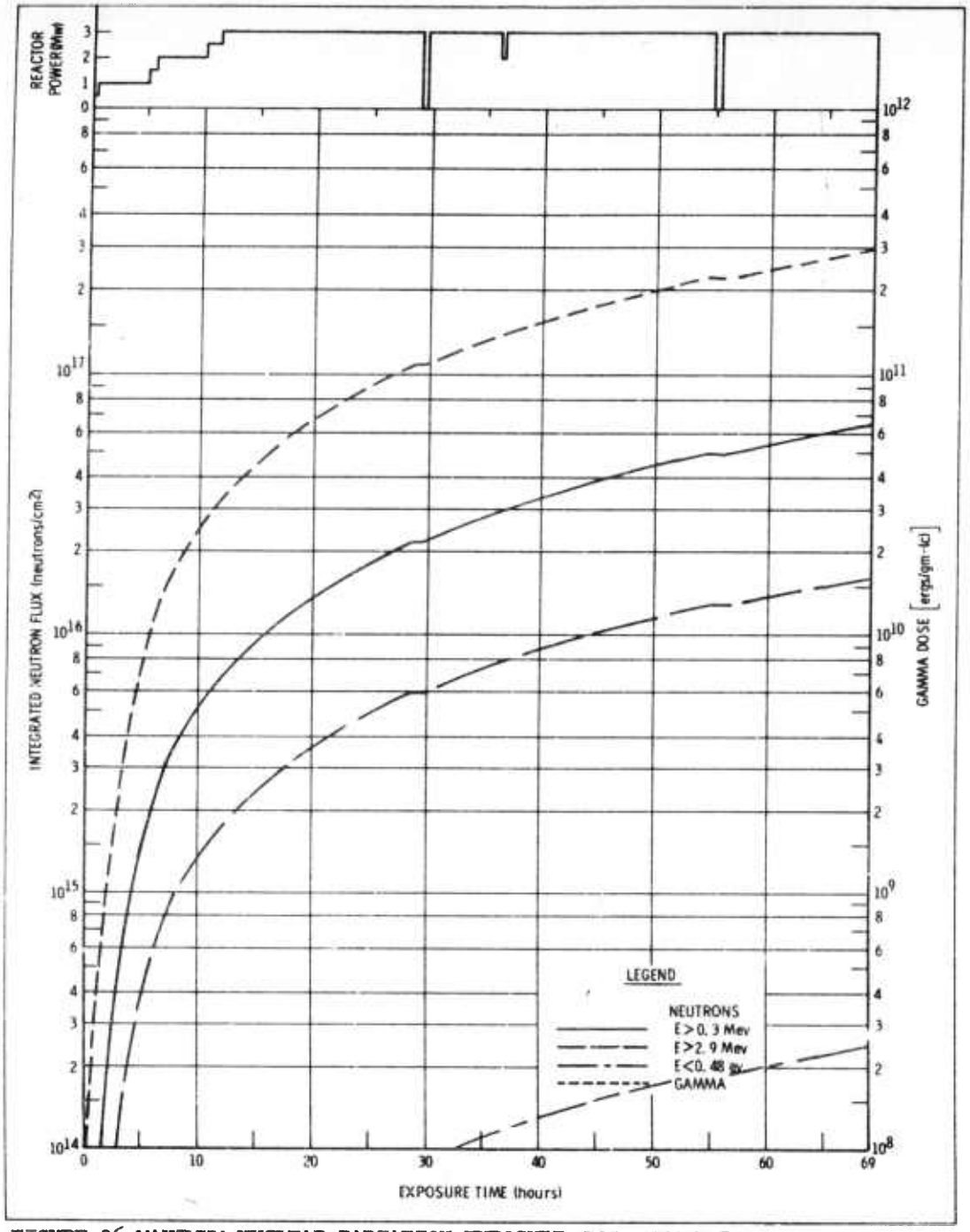

FIGURE 36 MAXIMUM NUCLEAR RADIATION EXPOSURE FOR THE BURROUGHS COMPUTER TEST VEHICLE

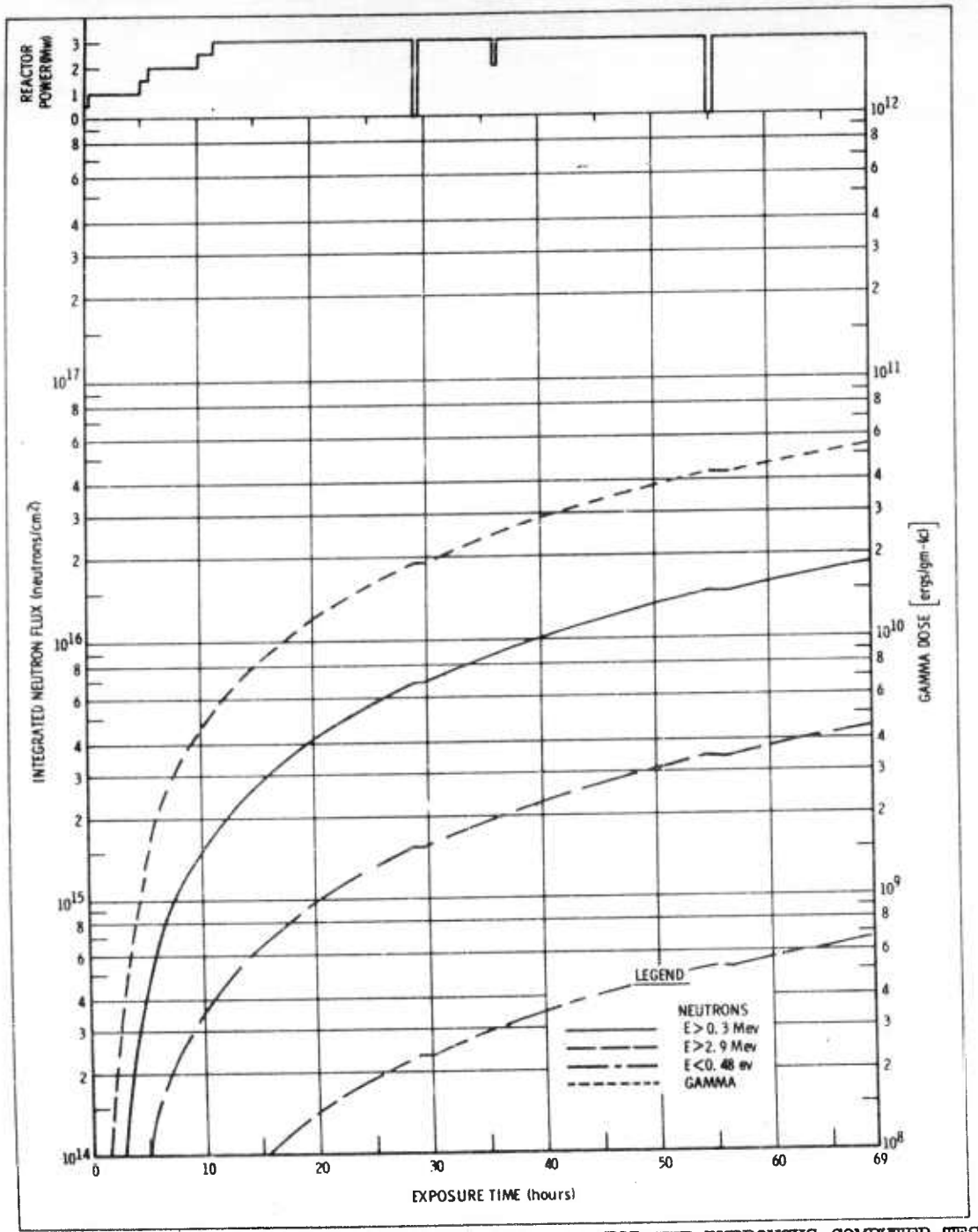

FIGURE 37 MINIMUM NUCLEAR RADIATION EXPOSURE FOR THE BURROUGHS COMPUTER TEST VEHICLE

During the pre-irradiation testing at the reactor site, failure of a logic diode removed the bias from the vacuum tubes in a pulse-generating circuit. Normal operation was regained by replacing the diode and tubes.

Two areas of difficulties were experienced during the test. The first, intermittent circuit continuity due to differences in thermal coefficient of expansion of mating materials, was corrected by ambient pallet temperature control. The second area of difficulty was in the design of a strobe circuit which had inadequate provision for system interaction effects. This effect was reflected in the rapid narrowing of the operating margins of bias A under irradiation and in the narrowing down on other test parameters. Both of these problems are discussed in detail in Reference (3).

Marginal check performed during the test showed that during the first 16 hours of exposure, bias A operating end limits (discussed above) narrowed to about 20 percent of its pre-irradiation value and were very sensitive to other bias settings, while bias B, C and D, and -4.5 vdc end limits remained virtually constant for the duration of the test.

With all biases set at their optimum values, operation with only one bad bit in the readout was obtained after 32 hours of exposure. At that time the maximum exposure (on reactor side) was slightly over 10^{11} ergs/gm-(C) and 2×10^{16} n/cm^2 and the minimum exposure was 2×10^{10} ergs/gm-(C) and 7×10^{15} n/cm^2. After 37 hours (1.5×10^{11} ergs/gm-(C) and 3×10^{16} n/cm^2), four of the first eight bits of the combined data register (located nearest the reactor) had failed completely, indicating failure of the most heavily exposed tunnel diode preamplifiers. Although it was no longer possible to run the diagnostic routine, circuits were exercised manually for the remainder of the test. Except for the first eight bits of the combined data register, normal operation of all component circuits was obtained after 44 hours. After 67 hours, the first indications of failure in the microprogram were observed when part of the preamplifiers failed to trigger with certain data patterns. The operand address register, located on the face nearest the reactor, was still operating at that time however.

Due to the high activity level of the test vehicle, post-irradiation testing of the complete unit was not scheduled. However, tunnel and logic diodes of both failed and operative circuits were removed and returned to Burroughs for evaluation.

Results of this test indicate that, with proper design and packaging, a digital computer meeting guidance computer requirements and capable of operating in a nuclear environment of 10^{11} ergs/gm-(C) gammas and 10^{16} n/cm^2 is feasible with components, circuitry, and techniques presently available.

3.0 TELEMETRY

3.1 MAGNETIC CORE CONTROLLED MULTIPLEXER

3.1.1 INTRODUCTION

In any time multiplexing system, analog inputs must be sampled in a repetitive sequential manner. For most pulse code modulation (PCM) telemetry applications, high sampling rates preclude the use of mechanical commutators, therefore electronic gates are used, one for each analog signal.

Two four-channel nuclear radiation - tolerant multiplexers were designed and manufactured by Molecular Research Inc. for evaluation in a nuclear radiation environment. These circuits use a magnetic core-controlled electronic gate known as a diode bridge-type gate, as shown in Figure 38. This circuit is to be used in a nuclear radiation hardened PCM telemetry system.

3.1.2 TEST ARTICLE DESCRIPTION

3.1.2.1 Basic Multiplexer Circuitry

The multiplexer consists of four diode bridge gates, a magnetic register which functions as a time sequential analog gate driver, and three core driver stages.

The core, in switching from the "1" to "0" flux state, acts as a current source providing current to both legs of the diode bridge and charges capacitor C_1, as shown in Figure 38. Superimposed on the currents in the diode bridge are analog signal currents. During "gate off" time the capacitor C_1 provides back bias to the diode gate. R_5 provides a discharge path for C_1, thereby necessitating a charge current during "gate on" time. This charge current is used to forward bias the diode gate.

Time sequential pulses are produced by the magnetic core register through the ability of the cores to store binary information. The operation of the register can best be explained by assuming that all cores are initially in the "0" state. The set driver is activated, setting the first core to the "1" state. Upon command from the shift driver, the first core is switched to the "0" state and a charge is stored in the transfer capacitor, C_5. As soon as the shift pulse has passed, the transfer driver discharges capacitor C_5 through the input winding of the succeeding core in such a direction as to switch the core to the "1" state. Upon command of the next shift pulse, the cycle is repeated, i.e., binary information is transferred from one core via the transfer

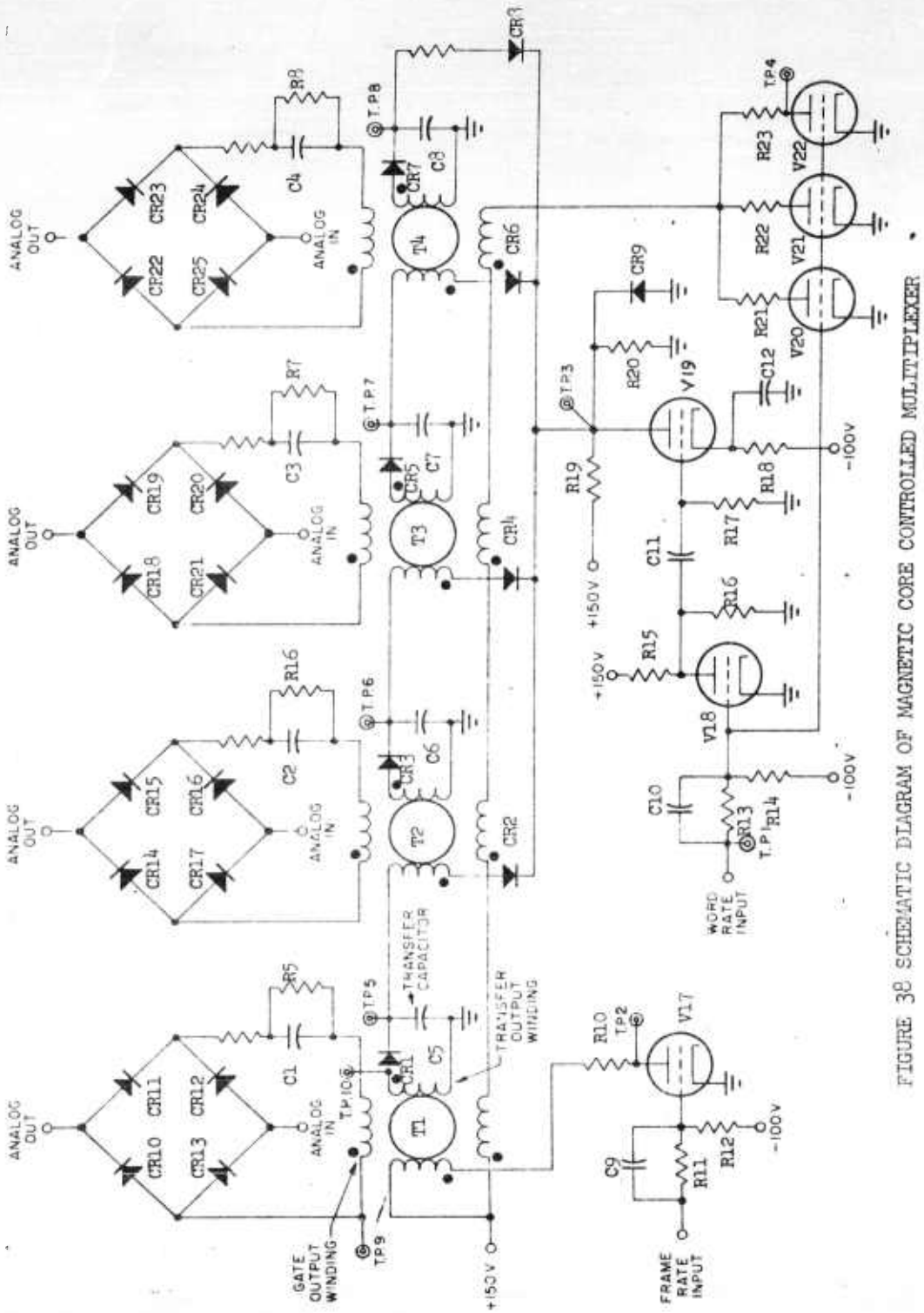

FIGURE 38 SCHEMATIC DIAGRAM OF MAGNETIC CORE CONTROLLED MULTIPLEXER

capacitor to the next core.

The purpose of the three-core driver stages, i.e., set driver, shift driver, and transfer driver, is to convert an input voltage signal into an output current pulse of sufficient amplitude to switch one magnetic core. The set driver operates at frame rate and receives its input from the output of the frame counter. The set driver provides current drive to the first core in the register. The shift driver operates at word rate providing current drive to all cores in series. Since only one core in the series string can contain a "1", the shift current will switch the core to the "0" state and place a charge on the transfer capacitor. The transfer driver operates at word rate and serves to discharge the transfer capacitor through the input winding of the following core, thus switching that core to the "1" state.

3.1.2.2 Synchronization Circuitry

The function of the synchronization circuitry is to generate command pulses to step the multiplexer through a complete cycle. The synchronizer test article consists of a clock pulse shaper, a four-to-one counter, a delay monostable multivibrator, and two monostable multivibrator pulse shapers. The synchronizer is controlled by a word rate command pulse from an external clock generator as shown in Figure 39. The detail synchronizer circuit diagrams are not presented in this report; however, they are conventional circuits utilizing 7586 Nuvistors as active elements. A list of all the components used in these circuits are presented in Table 8.

3.1.3 NUCLEAR RADIATION EFFECTS ANALYSIS

All the components which were utilized in the multiplexer were chosen for their proven nuclear radiation tolerance. The components and materials used had been evaluated in previous nuclear radiation effects tests. After a detail analysis (Table 8), it was concluded that, with the exception of the HPA 1002 silicon epitaxial planar semiconductor diodes, no change in the performance of the circuit should be expected until an integrated exposure of 4×10^{10} ergs/gm-(C) and 3×10^{16} n/cm^2 had been exceeded. The design goal for telemetry circuitry is 1.8×10^{10} ergs/gm-(C) and 1×10^{16} n/cm^2.

Of primary concern was the operation of the diode gates. A number of the HPA 1002 diodes had been evaluated in a static radiation effects test as well as a few in a dynamic radiation effects test. One diode quad was also evaluated in a static irradiation. The results of these tests indicated that an offset in gate voltage of approximately 40 mv could be expected at an integrated exposure of 2×10^{16} n/cm^2. The diodes which were used in the gates of the multiplexer were matched such that only 1 mv of error was induced

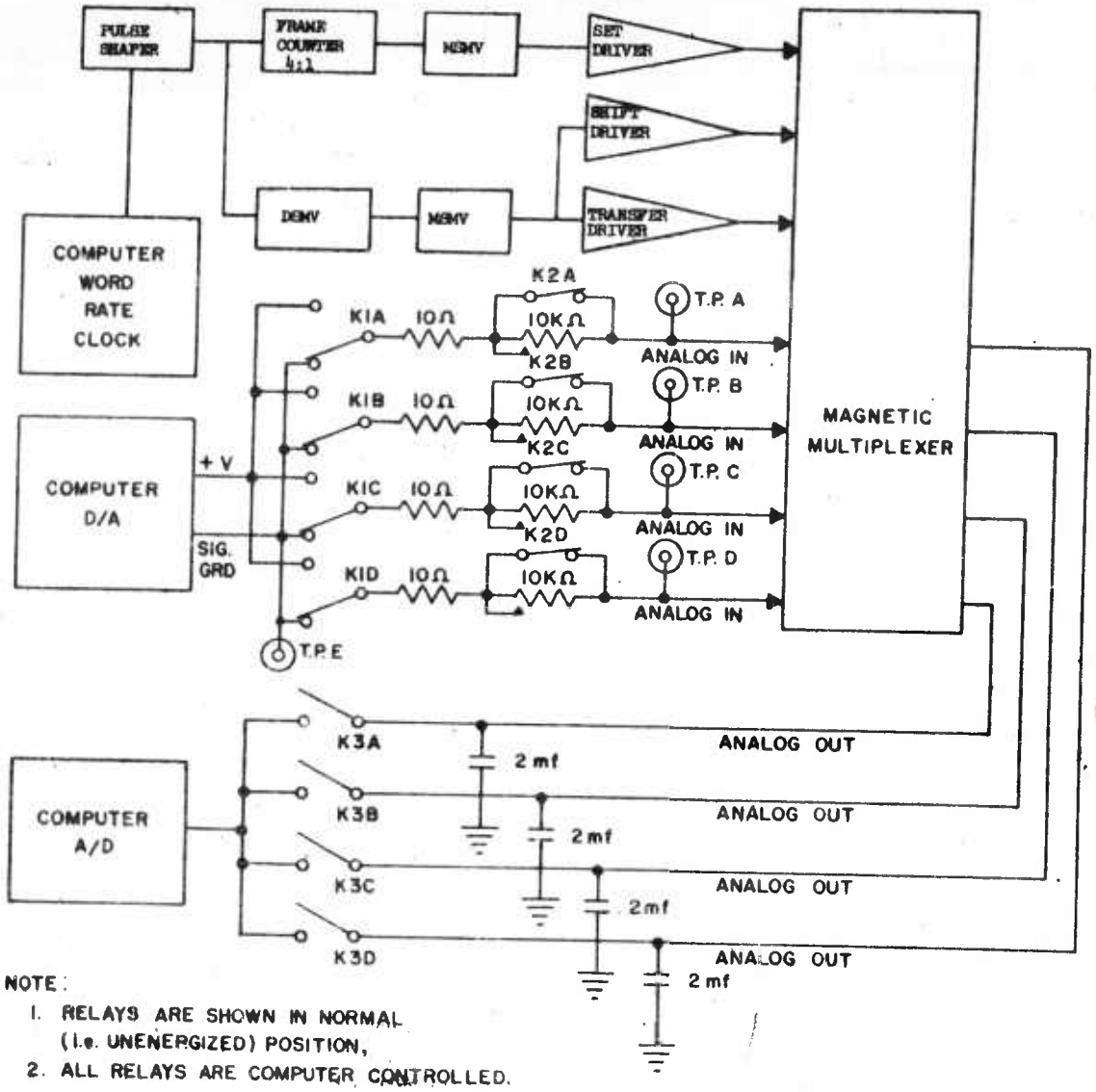

NOTE:

1. RELAYS ARE SHOWN IN NORMAL (i.e. UNENERGIZED) POSITION,
2. ALL RELAYS ARE COMPUTER CONTROLLED.

FIGURE 39 MULTIPLEXER INSTRUMENTATION DIAGRAM

TABLE 8

NUCLEAR RADIATION EFFECTS ANALYSIS OF THE MULTIPLEXER

NUCLEAR DESIGN REQUIREMENT: GAMMAS: 1.8(10) ERGS/GM-(C)
NEUTRONS: 1(16) N_v/CM^2

MANUFACTURER: MOLECULAR RESEARCH, INC.

CODE NO.	GENERAL DESCRIPTION OF CIRCUIT, PART OR ELEMENT	VALUE	ORIGINAL ELEMENT			LIMITING NUCLEAR EXPOSURE		REMARKS
			PART OR DRAWING NUMBER	MFR	ELEMENT MATERIAL DESCRIPTION	ERGS/GM (C)	N_v/CM^2	
	Multiplexer							
C1-4, C11	Capacitor, 5%, 300 wv	.01 MFD	CYFM-30	Corning	Glass and Al.	6(10)	2.6(17)	+3% cap. ch.
C5 - C8	" " "	.0068 MFD	CYFM-30	"	"	"	"	"
C9-C10	" " 500 wv	56 PF	CYFM-10	"	"	"	"	"
C12	" " 200 wv	.15 MFD	CDM 154 YCJ	G.E.	Mylar	8.5(10)		10% cap. ch.
R1-R4	Resistor, 1W, 2%	6.81K	S20	Corning	Tin oxide & glass	7(10)	5(16)	1% res. ch.
R5-R8	" " "	100K	"	"	"	"	"	"
R9	" " "	2.21K	"	"	"	"	"	"
R10	" 2W "	10K	S25	"	"	"	"	"
R11, R13	" " "	150K	S20	"	"	"	"	"
R12, R14	" " "	274	"	"	"	"	"	"
R15, R16	" 2W "	18K	S25	"	"	"	"	"
R17	" 1W "	47K	S20	"	"	"	"	"
R18	" 2W "	12.1K	S25	"	"	"	"	"
R19	" " "	68.1K	"	"	"	"	"	"
R20	" " "	33.2K	"	"	"	"	"	"
R21-R23	" " "	8.25K	"	"	"	"	"	"
CR1-CR9	Diodes, Semiconductor		HPA 1015	Hewlett Packard	Silicon		1(16)	Same as HPA 1002 except selected for breakdown greater than 50V.
CR10-CR25	" "		HPA 1002	"	"		1(16)	
V17-22	Triode		7586	RCA	Ceramic and metal	4(10)	3(16)	N. D.
T1-T4	Magnetic Cores		80581-1/8-A 590	Magnetic Inc.	Orthonal		3(16)	N. D.
---------	Clock Pulse----------							
C1	Capacitor, 5%, 300VDC	.01 MFD	CYFM 30	Corning	Glass and alum.	6(10)	2.6(17)	+3% cap. ch.
R1	Resistor, 1W, 2%	15K	S20	"	Tin oxide & glass	7(10)	5(16)	1% res. Ch.
R2	" " "	3.32K	"	"	"	"	"	"
R3	" 2W "	10K	S25	"	"	"	"	"

NOTES: (X) INDICATES POWERS OF TEN

TABLE 8

NUCLEAR RADIATION EFFECTS ANALYSIS OF THE MULTIPLEXER

NUCLEAR DESIGN REQUIREMENT: GAMMAS: 1.8(10) ERGS/GM-(C)
NEUTRONS: 1(16) N_v/CM^2

MANUFACTURER: MOLECULAR RESEARCH, INC.

CODE NO.	GENERAL DESCRIPTION OF CIRCUIT, PART OR ELEMENT	VALUE	ORIGINAL ELEMENT			LIMITING NUCLEAR EXPOSURE		REMARKS
			PART OR DRAWING NUMBER	MFR	ELEMENT MATERIAL DESCRIPTION	ERGS/GM (C)	N_v/CM^2	
V1	Triode, Nuvistor		7586	RCA	Ceramic & Metal	4(10)	3(16)	N. D.
--------	Monostable Multivibrator							
C1, C2	Capacitor, 5%, 500V	56 pf	CYFM-10	Corning	Glass and Al.	6(10)	2.6(17)	
C3-1*	" " " 300V	390 pf	CYFM-15	Corning	Glass and Al.	6(10)	2.6(17)	*Indicates no. of multivibrator in which component is used
C3-2*	" " " 300V	560 pf	CYFM-15	Corning	Glass and Al.	6(10)	2.6(17)	
C3-3*	" " 300V	900 pf	CYFM-15	Corning	Glass and Al.	6(10)	2.6(17)	
R1	Resistor, 1W, 2%	681 K	S20	Corning	Tin oxide & glass	7(10)	5(16)	1% res. ch.
R2	Resistor, 1W, 2%	10 K	S20	Corning	Tin oxide & Glass	7(10)	5(16)	1% res. ch.
R3	Resistor, 2W, 2%	10 K	S25	Corning	Tin oxide & glass	7(10)	5(16)	1% res. ch.
R4	Resistor, 1W, 2%	150 K	S20	Corning	Tin oxide & Glass	7(10)	5(16)	1% res. ch.
R5	Resistor, 1W, 2%	182 K	S20	Corning	Tin oxide & Glass	7(10)	5(16)	1% res. Ch.
R6-1*,2*	Resistor, 1W, 2%	150 K	S20	Corning	Tin oxide & Glass	7(10)	5(16)	1% res. ch.
R6-3*	Resistor, 1W, 2%	100 K	S20	Corning	Tin oxide & Glass	7(10)	5(16)	1% res. ch.
R7	Resistor, 4W 2%	10 K	S30	Corning	Tin oxide & Glass	7(10)	5(16)	1% res. ch.
V1	Diode, Nuvistor		R60165	RCA	Ceramic & Metal	4(10)	3(16)	N. D.
V2, V3	Triode, Nuvistor		7586	RCA	Ceramic & Metal	4(10)	3(16)	N. D.
--------	4:1 Counter							
C1-C6	Capacitor, 5%, 500V	56 pf	CYFM-10	Corning	Glass and Al.	6(10)	2.6(17)	+3% cap. ch.
R1, R4	Resistor 1W, 2%	10K	S20	Corning	Tin oxide and Glass	7(10)	5(16)	1% res. ch.
R2,3,5,6	Resistor 2W, 2%	10K	S25	Corning	Tin oxide and Glass	7(10)	5(16)	1% res. ch.
R7,10,11, 12,15,16	Resistor 1W, 2%	180 K	S20	Corning	Tin oxide and Glass	7(10)	5(16)	1% res. ch.
R8,9,13,14	" 1W, 2%	150 K	S20	Corning	Tin oxide and Glass	7(10)	5(16)	1% res. ch.
V1,2,5,6	Diode, Nuvistor		R60165	RCA	Ceramic & Metal	4(10)	3(16)	N. D.
V3,4,7,8	Triode, Nuvistor		7586	RCA	Ceramic & Metal	4(10)	3(16)	N. D.
--------	Test Point Amplifiers							
V1	Triode Nuvistor		7586	RCA	Ceramic & Metal	4(10)	3(16)	N. D.

NOTES: (X) INDICATES POWERS OF TEN

TABLE 8

NUCLEAR RADIATION EFFECTS ANALYSIS OF THE MULTIPLEXER

NUCLEAR DESIGN REQUIREMENTS: GAMMAS: 1.8(10) ERGS/GM-(C)
NEUTRONS: 1(16) N_r/CM^2

MANUFACTURER: MOLECULAR RESEARCH, INC.

CODE NO.	GENERAL DESCRIPTION OF CIRCUIT, PART OR ELEMENT	VALUE	ORIGINAL ELEMENT			LIMITING NUCLEAR EXPOSURE		REMARKS
			PART OR DRAWING NUMBER	MFR	ELEMENT MATERIAL DESCRIPTION	ERGS/GM (C)	N_r/CM^2	
C1	Capacitor, 5%, 500V	220 pf	CTFM-15	Corning	Glass and Al.	6(10)	2.6(17)	+3% cap. ch.
R1	Resistor, 1W, 1%	475 K	S20	Corning	Tin oxide and Glass	7(10)	5(16)	
R2-1*2*4*	Resistor, 1W, 1%	100 K	S20	Corning	Tin oxide and Glass	7(10)	5(16)	* Indicates no. of amplifier in which component is used
R2-3*5*6* 7*,8*	Resistor, 1W, 1%	475K	S20	Corning	Tin oxide and Glass	7(10)	5(16)	
R3, 4	Resistor, 1W, 1%	18.2 K	S20	Corning	Tin oxide and Glass	7(10)	5(16)	
--------	Miscellaneous Hardware----------							
	Chassis	10"x14"x3"	AC 414	Bud	Aluminum		>1(17)	N. D.
	Terminals		2045-4	Cambion	Ceramic & Metal		>1(17)	N. D.
	Connector ENC		GRMI-604	Gremar	Metal & Rexolite #1422	2(10)	3(16)	25% damage
	Connector Socket	MS3102	A-28-21SXC32	Cannon	Metal & Dyallyl Phthalate	3(10)	3(16)	25% damage
	Connector Plug	M3106A	A-28-21PXC32	Cannon	"	3(10)	3(16)	25% damage
	Cable clamp adapters		AN3057-1C	Cannon	Metal		>1(17)	N. D.
	Tube Sockets		5NS	Cinch	Metal & mica filled phenolic	3.9(11)		25% damage
	Magnet Wire		AWG 38	G.E.	Formvar ins.	4(10)		25% damage
	Corona Dope		450	U. C. Electronics		2(10)		25% damage
	Wire			Raychem	Irradiated Polyethylene	6(10)		25% damage
	Dicie Circuit Board		D-10		Fiberglass epoxy	1(10)		25% damage

NOTES: (X) INDICATES POWERS OF TEN

when a 5v analog was passed through the gate with 3 ma of "gate on" current flowing. Changes (up to 10%) in the forward characteristics of these units will not seriously affect the performance of the gate if all characteristics are changed at the same rate; however, if one diode changes faster than the others the voltage drop across this unit will change for the same "gate on" current and this voltage will be superimposed on the analog output signal, thus causing an error to exist.

3.1.4 TEST PROCEDURE

The multiplexers were mounted on the front of the test chamber in the north position of the Ground Test Reactor. System 2 was exposed to the highest flux of 4.0×10^9 ergs/gm-(C)-hr and 4.9×10^{11} n/cm^2-sec. No dose rate effects were noted at these levels. The integrated exposures for the components were 2.1×10^{11} ergs/gm-(C) and 9.1×10^{16} n/cm^2 for System 1 and 2.5×10^{11} ergs/gm-(C) and 1.1×10^{17} n/cm^2 for System 2. Integrated exposures for any time during the test may be found in Figures 40 and 41.

Figure 39 depicts the instrumentation used for each multiplexer. SDS Data Management System (DMS) printouts recorded multiplexer gate input and output for all four gates of each system. Gate analog inputs were stepped from 0 to 5 to 0 volts in 1-volt steps for analog signal source impedances of 10 ohms and 10,000 ohms. In addition to the printouts, eight test points were monitored using a Tektronix 555 oscilloscope. These test points yielded representations of:

(a) shaped word rate inputs

(b) set driver output

(c) transfer driver output

(d) shift driver output

(e,f,g,h) core transfer capacitor waveforms

3.1.5 TEST RESULTS

Extensive review of the "raw date" (i.e., computer printouts and test point waveform photographs) indicates a very favorable performance was obtained. In analyzing the data, the computer printouts were reduced to curves of multiplexed analog signals, as converted by the DMS A/D converter, versus integrated neutron exposure for each gate and source impedance. It was observed, within the accuracy of the DMS (10 mv), that no offsets occurred for any of the gates up to the design goal of 1.8×10^{10} ergs/gm-(C) and 1×10^{16} n/cm^2. The first gate degradation trend

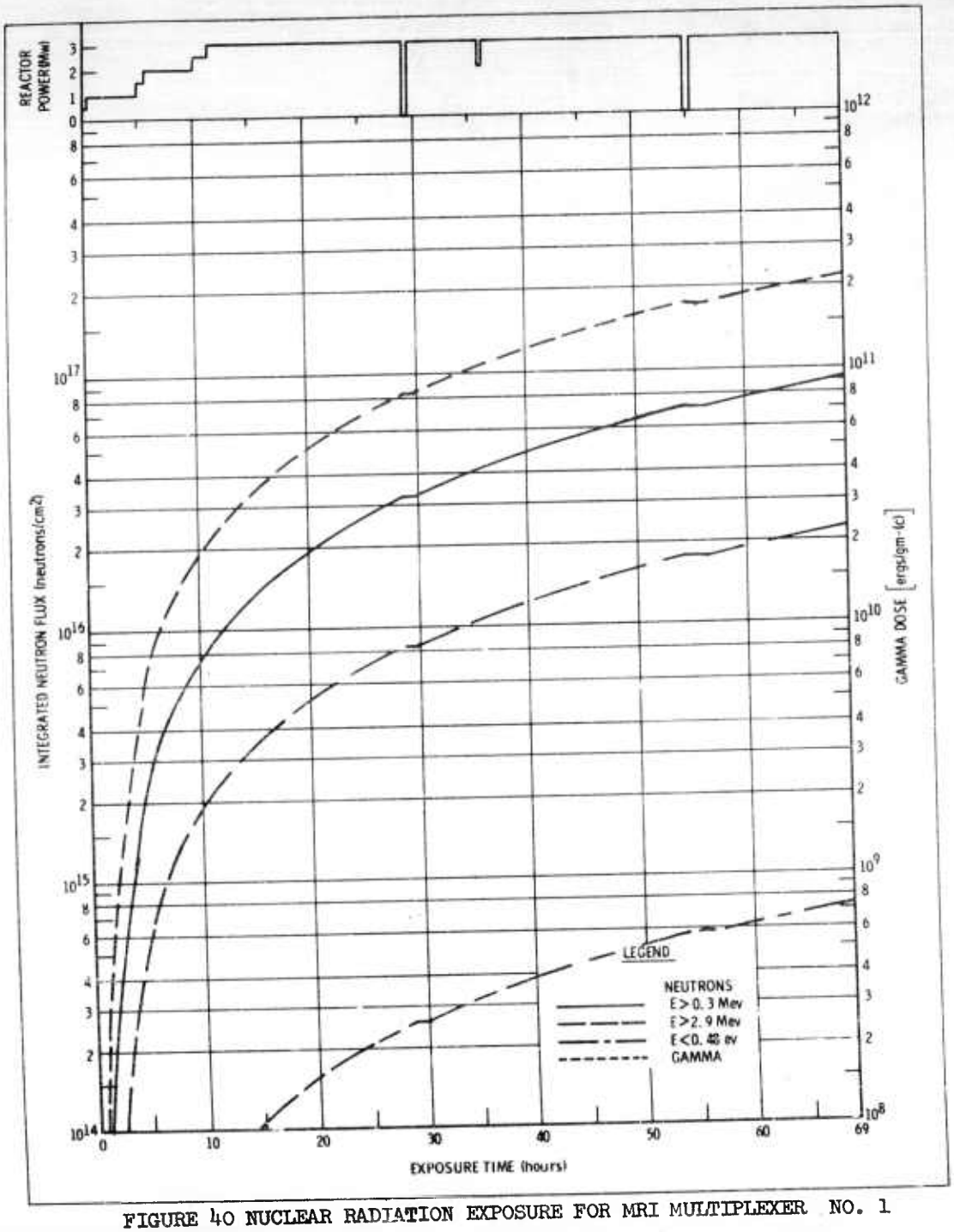

FIGURE 40 NUCLEAR RADIATION EXPOSURE FOR MRI MULTIPLEXER NO. 1

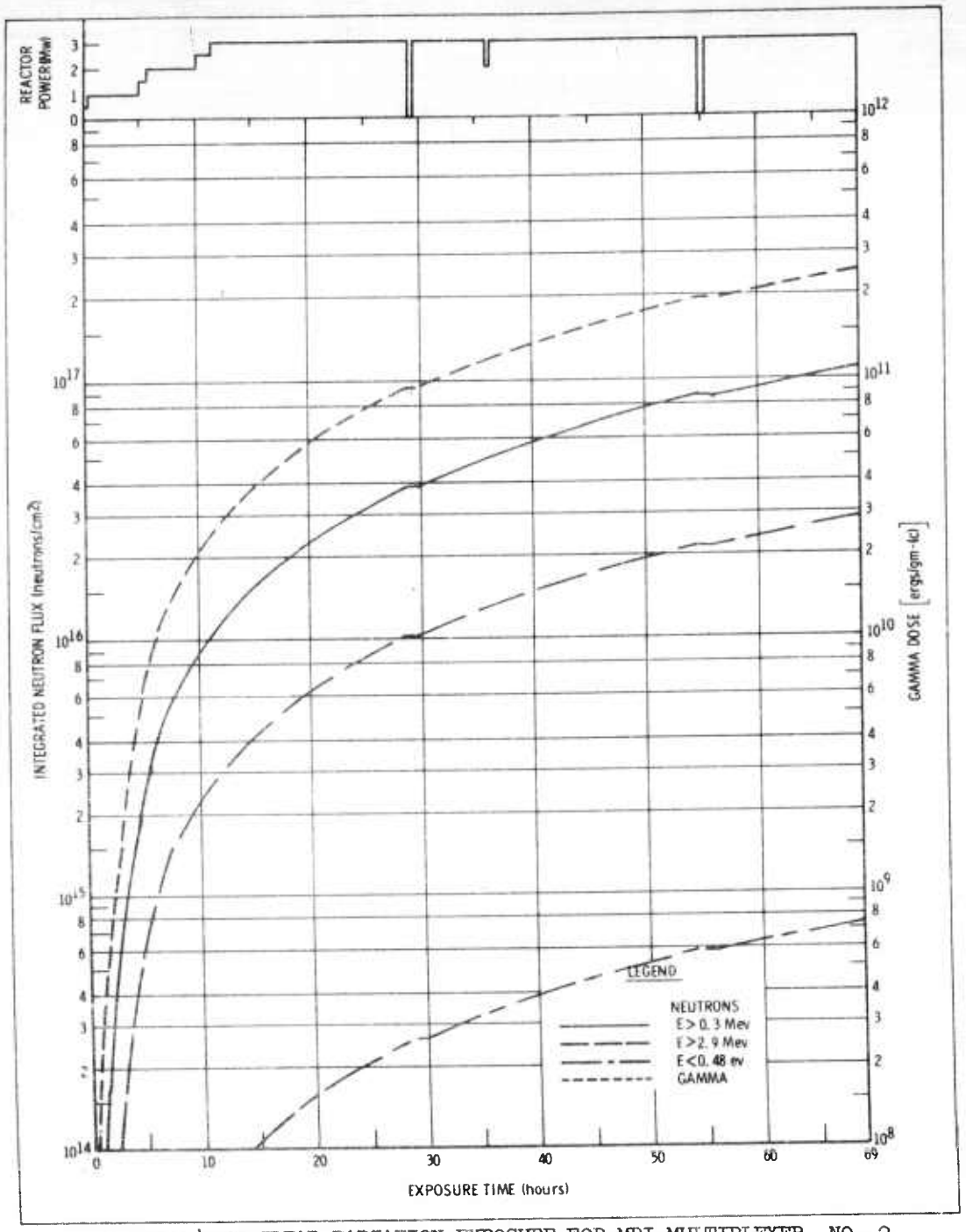

FIGURE 41 NUCLEAR RADIATION EXPOSURE FOR MRI MULTIPLEXER NO. 2

was noted for the worst case gates at an integrated exposure of 1.7×10^{16} n/cm^2. Gate No. 4 in each system exhibited the largest degradation (See Figures 42 and 43).

The best gate performance for either system is shown for gate 3, system 1 in Figure 44. All plotted data of deviation from base line versus integrated neutron exposure showed that gate offset for the 10K source degraded slightly before the gate offset for the 10 ohm source impedance case. It is expected that this apparent difference was due to leakage paths caused by degradation of the dielectric characteristic of the G-10 fiber glass epoxy used to mount the diode gates.

Photos showing "gate on" time during irradiation were compared with similar pre-test photos and revealed a reduction in "gate on" time as tabulated in Table 9. As a result of this comparison no evidence was found to connect "gate on" time changes to "gate offset" changes. It is believed that the above mentioned reduction in "gate on" time is due to degradation in forward characteristics of the transfer diodes, in particular diodes CR2, CR4, CR6, and CR8 of systems 1 and 2. The degradation is demonstrated in part by the change in lower charging voltage levels for the respective transfer capacitors.

Post-irradiation static tests were performed on all the irradiated diode gates and on some of the individual diodes. The static measurements of "gate offset" correlate directly, in all cases, with the diode gates' dynamic operation in the nuclear environment, as shown in Tables 10 and 11 and Figure 45. The diodes behaved as expected with respect to forward and reverse characteristics. For a 1 ma diode operating point in the forward direction, V_f was observed to change by factors in the range of 2 to 3. For a 1 ma diode operating point in the reverse direction, V_r was observed to change by factors in the range of 1.3 to 1.6. Due to the fact that diode V_f did change and "gate offset" is a direct function of diode match in the forward direction, it is expected, and was observed, that diode tracking changed for each gate.

The result of this test demonstrated that all channels of each magnetic multiplexer operated very successfully up to and through the nuclear design goal of 1.8×10^{10} ergs/gm-(C) and 1×10^{16} n/cm^2; therefore, no design changes are recommended.

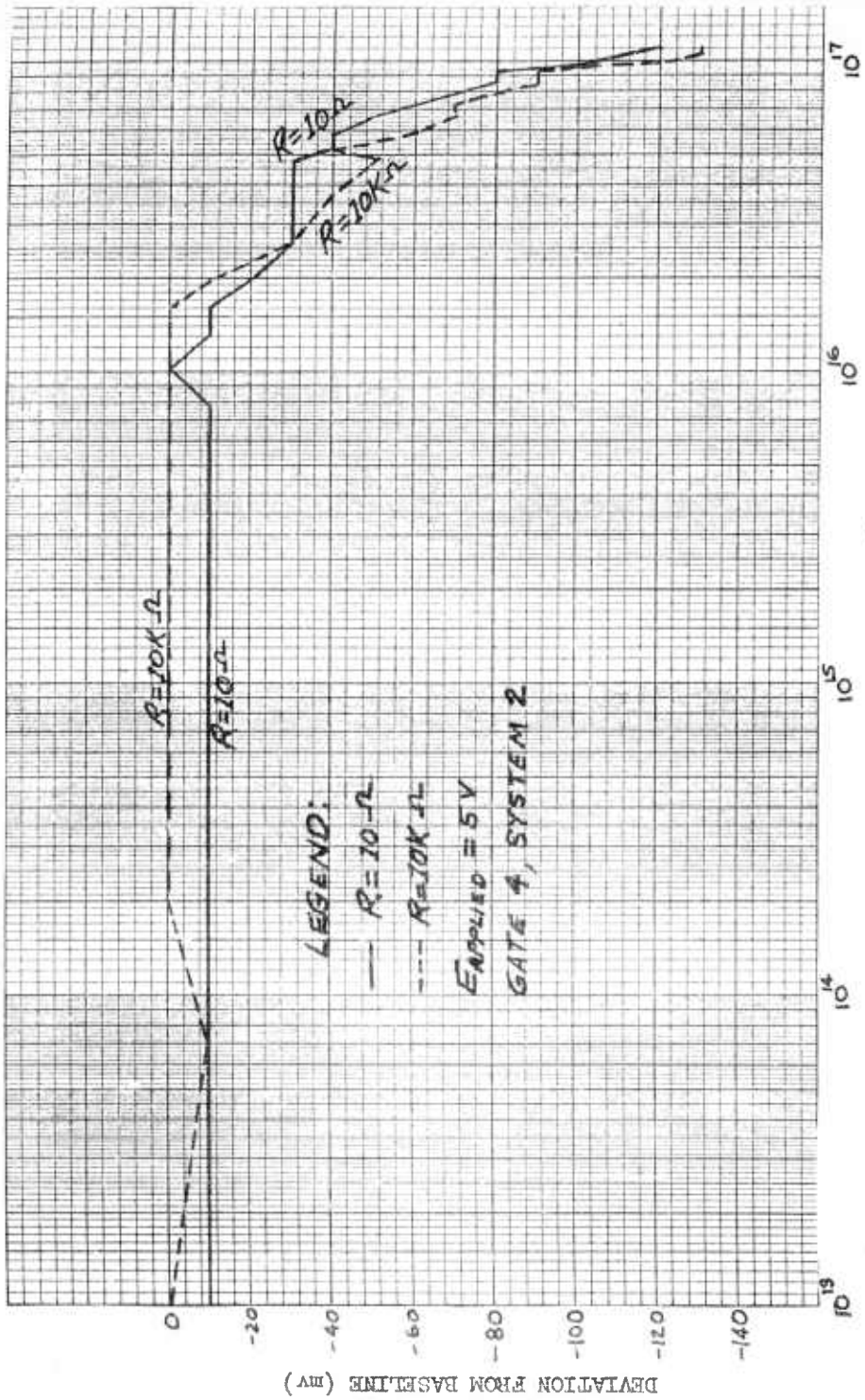

FIGURE 42 DIODE GATE 4, SYSTEM 2, OFFSET AS A FUNCTION OF INTEGRATED NEUTRON FLUX

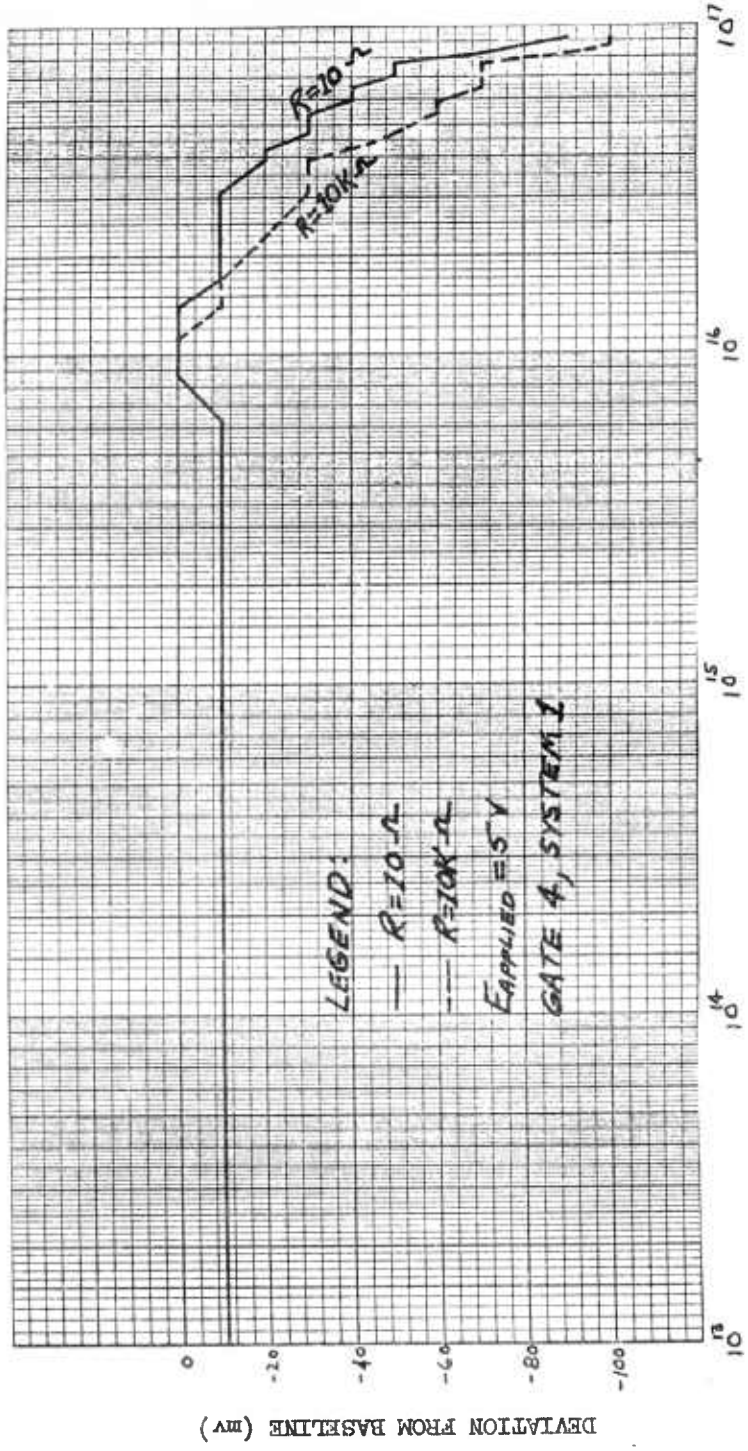

FIGURE 43 DIODE GATE 4, SYSTEM 1 OFFSET AS A FUNCTION OF INTEGRATED NEUTRON FLUX

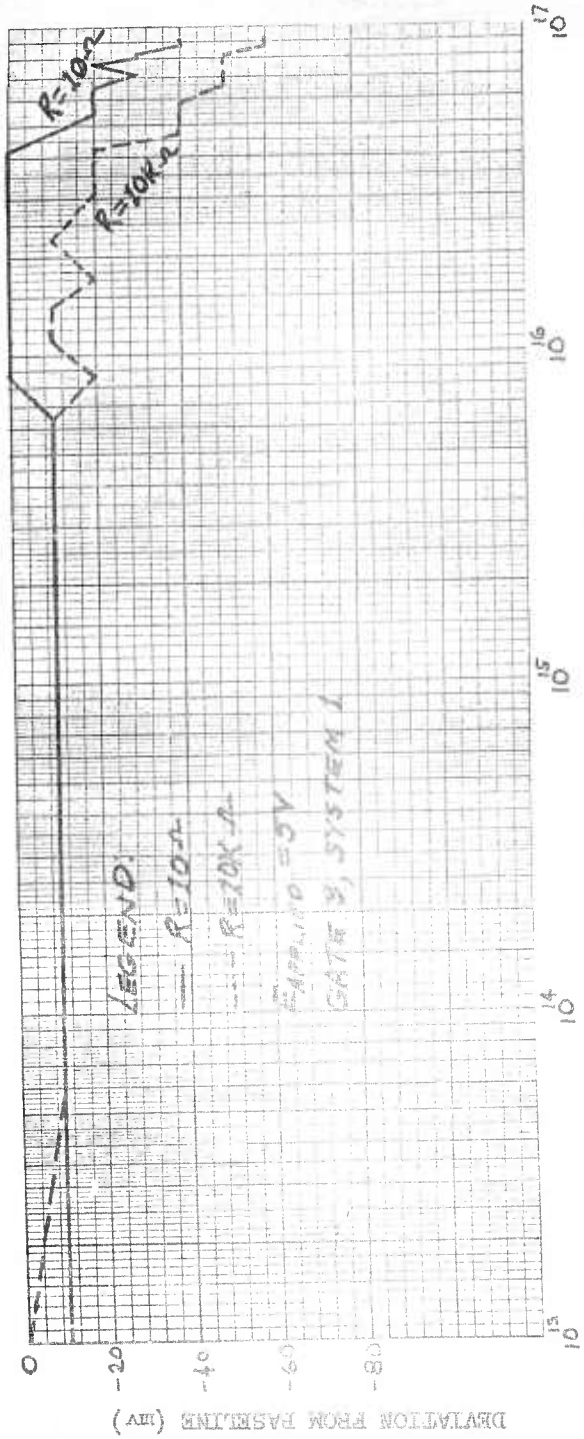

FIGURE 44 DIODE GATE 3, SYSTEM 1 OFFSET AS A FUNCTION OF INTEGRATED NEUTRON FLUX

TABLE 9 DEGRADATION OF "GATE ON" TIME

The following changes in "gate on" time were found from the photographs of test points 5, 6, 7, and 8.

after 40 hours elapsed time

at $4.8 \times 10^{16} n/cm^2$, system 1 showed no degradation in "gate on" time

at $5.8 \times 10^{16} n/cm^2$, system 2 showed the following changes

Gate 1	no degradation
Gate 2	decrease of approximately 10%
Gate 3	" " 10%
Gate 4	" " 20%

after 61 hours elapsed time

at $7.8 \times 10^{16} n/cm^2$, system 1 shows the following changes in "gate on" time

Gate 1	no degradation
Gate 2	decrease of approximately 15%
Gate 3	" " 20%
Gate 4	" " 20%

at $9.2 \times 10^{16} n/cm^2$, system 2 shows the following changes in "gate on" time

Gate 1	no degradation
Gate 2	decrease of approximately 20%
Gate 3	" " 20%
Gate 4	" " 30%

TABLE 10 POST-TEST EVALUATION OF SYSTEM 1 DIODE GATES

System No.	Gate No.	Diode** No.'s	Control Current	Analog Input		Analog Output		Offset (mv)	
				Before	After	Before	After	Before	After*
		CR1-CR4	0.5 ma	.00113	.0016	.00070	.0065	0.43	-4.9
				2.4993	2.5108	2.4989	2.5159	0.44	-5.1
				4.9998	4.9950	4.9993	5.0005	0.49	-5.5
1	1		1.0	.00174	.0021	.00134	.0074	0.30	-5.3
				2.4996	2.5065	2.4993	2.5116	0.30	-5.1
				4.9997	4.9983	4.9993	5.0040	0.40	-5.7
			3.0	.00105	.0016	.00067	.0091	0.38	-7.5
				2.4998	2.4912	2.4995	2.4986	0.30	-7.4
		CR5-CR8	0.5 ma	.00091	.0020	.00148	.0161	-0.51	-14.1
				2.5003	2.5060	2.5003	2.5196	-0.50	-13.6
				5.0007	5.0146	5.0013	5.0290	-0.57	-14.4
1	2		1.0	.00006	.0016	.00059	.0190	-0.53	-17.4
				2.5004	2.4957	2.5009	2.5127	-0.50	-17.0
				5.0005	5.0134	5.0011	5.0309	-0.60	-17.5
			3.0	.00058	.0020	.00104	.0256	-0.46	-23.6
				2.5008	2.4945	2.5012	2.5182	-0.40	-23.7
		CR9-CR12	0.5 ma	.00007	.0017	.00051	-.0010	-0.44	+2.7
				2.5006	2.5005	2.50093	2.4968	-0.33	+3.7
				5.0000	5.0234	2.5004	5.0196	-0.40	+3.8
1	3		1.0	.00073	.0020	.00126	-.0007	-0.53	+2.7
				2.5007	2.5020	2.5012	2.4990	-0.50	+3.0
				5.00025	5.0063	5.0008	5.0034	-0.55	+2.9
			3.0	.00091	.0015	.00150	.0002	-0.59	+1.3
				2.4996	2.4999	2.50003	2.4989	-0.43	+1.2
				5.0002	5.0048	5.0010	5.0036	-0.80	+1.2
		CR13-CR16	0.5 ma	.00040	.0019	.00097	.0480	-0.57	-46
				2.5003	2.5042	2.5008	2.5509	-0.50	-47
				5.0004	5.0290	5.0009	5.0775	-0.50	-49
1	4		1.0	.00005	.0017	.00055	.0568	-0.50	-55
				2.5003	2.5190	2.5008	2.5732	-0.50	-54
				5.0002	5.0765	5.0007	5.1294	-0.50	-53
			3.0	.00030	.0020	.0008	.0684	-0.50	-66
				2.5002	2.5178	2.5007	2.5845	-0.50	-67
				5.0003	4.9985	5.0008	5.0660	-0.50	-68

*After integrated nuclear exposure of 2.1×10^{11} ergs/gm-(C) and 9.1×10^{16} n/cm^2

**The diodes are HP1002 Silicon Epitaxial Planar

TABLE 11 POST-TEST EVALUATION OF SYSTEM 2 DIODE GATES

System No.	Gate No.	Diode** No.'s	Control Current	Analog Input		Analog Output		Offset (mv)	
				Before	After	Before	After	Before	After*
2	1	CR17-CR20	0.5 ma	.00013	.0014	.00080	-.0188	-0.67	+20.2
				2.5006	2.5007	2.5012	2.4800	-0.60	+20.7
				5.0009	5.0025	5.0016	4.9814	-0.70	+21.1
			1.0	.00097	.0020	.00182	-.0223	-0.85	+21.3
				2.5002	2.5043	2.5010	2.4798	-0.80	+24.5
				5.0009	5.0004	5.0017	4.9757	-0.80	+24.7
			3.0	.00030	.0017	.00125	-.0264	-0.95	+28.1
				2.5009	2.4991	2.5018	2.4710	-0.90	+28.1
				5.0008	4.9990	5.0018	4.9707	-1.00	+28.3
2	2	CR21-CR24	0.5 ma	.00114	.0020	.00107	-.0079	+0.07	+9.9
				2.4990	2.5011	3.4988	2.4915	+0.20	+9.6
				5.0007	5.0134	5.0009	5.0029	-0.10	+10.5
			1.0	.00103	.0017	.00070	-.0102	+0.30	+11.9
				2.4995	2.5021	2.4992	2.4904	+0.30	+11.7
				4.9998	5.0120	4.9995	5.0000	+0.30	+12.0
			3.0	.00125	.0020	.00081	-.0119	+0.44	+13.9
				2.4990	2.4934	2.4986	2.4794	+0.40	+14.0
2	3	CR25-CR28	0.5 ma	.00107	.0015	.00093	.0525	+0.14	-51
				2.4999	2.5085	2.4998	2.5600	+0.10	-52
				4.9998	5.0000	4.99966	5.0520	+0.14	-52
			1.0	.00129	.0020	.00116	.0620	+0.13	-60
				2.4994	2.4975	2.4993	2.5580	+0.10	-61
				5.0001	5.0026	4.9999	5.0628	+0.20	-60
			3.0	.00102	.0017	.00087	.0747	+0.15	-73
				2.4990	2.5034	2.4988	2.5765	+0.20	-73
				5.0009	4.9825	5.0010	5.0560	-0.10	-74
2	4	CR29-CR32	0.5 ma	.00007	.0020	.00098	.0890	-0.91	-87
				2.5006	2.5100	2.5014	2.5965	-0.80	-87
				5.0009	4.9960	5.0018	5.0829	-0.90	-87
			1.0	.00010	.0018	.00070	.1040	-0.60	-102
				2.5002	2.5070	2.5008	2.6092	-0.60	-102
				4.9998	4.9935	5.0005	5.0955	-0.70	-102
			3.0	.00030	.0020	.00060	.1275	-0.30	-126
				2.5007	2.5095	2.5005	2.6350	-0.20	-126
				5.0011	4.9846	5.0014	5.1100	-0.30	-125

*After integrated nuclear exposure of 2.5×10^{11} ergs/gm-(C) and $1.1 \times 10^{17} n/cm^2$

**The diodes are HP1002 Silicon Epitaxial Planar

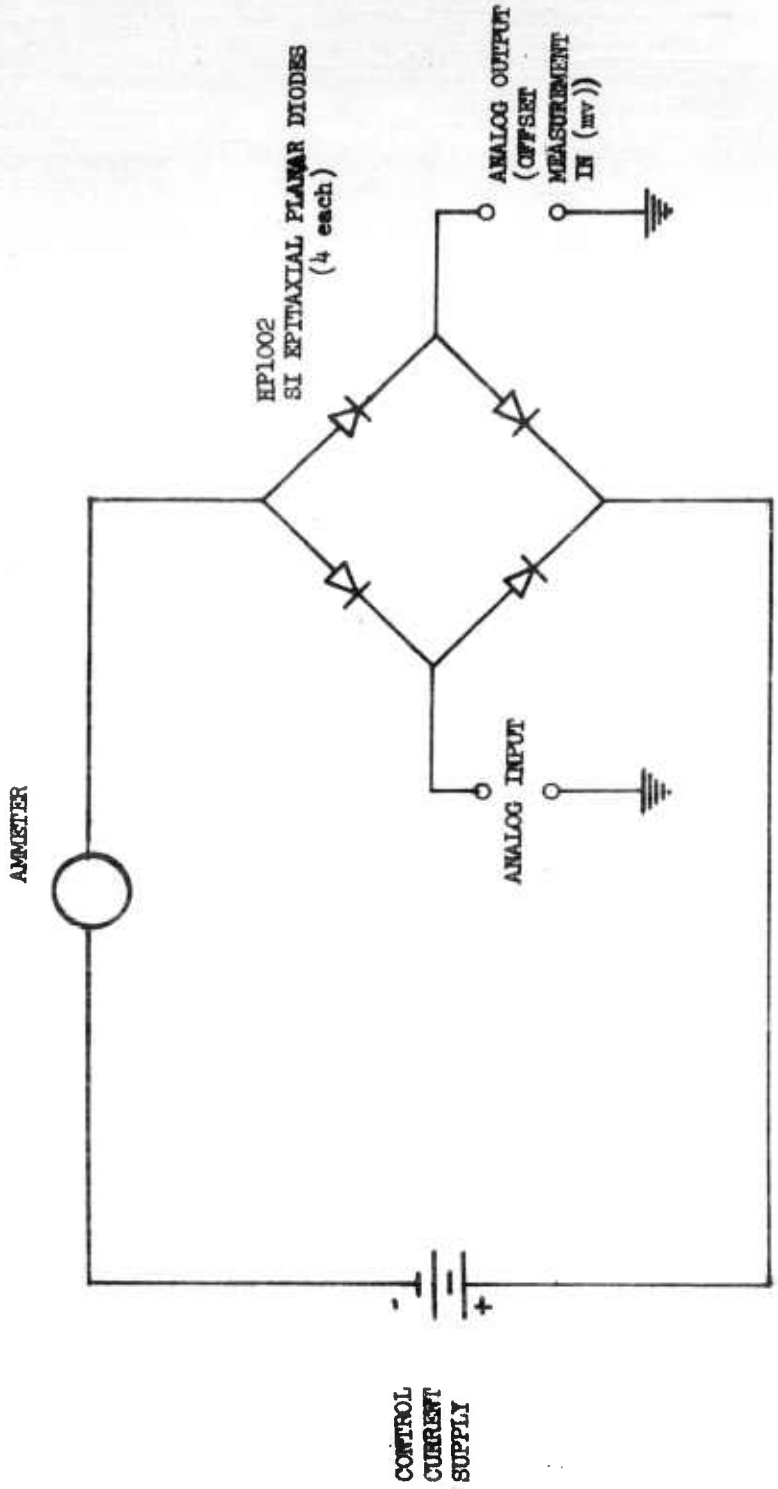

FIGURE 45 POST-TEST DIODE QUAD TEST SCHEMATIC

4.0 INERTIAL REFERENCE SYSTEM

4.1 INTRODUCTION AND TEST ARTICLE DESCRIPTION

The experience gained in radiation effects testing under the LASV-N1 program and the knowledge obtained from static testing of inertial components from past radiation tests put the Autonetics Division of North American Aviation inertial reference system in a position with a two-fold purpose. A large stride was taken in this radiation effects test by testing a two-axis inertial platform and its electronics as shown in Figure 46, while retaining the benefit of testing inertial sensors. The inertial system test procedure was designed to allow test continuation of other components should a failure be encountered in any single component of the system.

Radiation hardened precision electronics circuits were designed and fabricated by Autonetics to fulfill requirements for voltage reference devices, chopper stabilized DC amplifiers, and stable capacitors.

4.1.1 INERTIAL PLATFORM SYSTEM

The two-axis inertial test system consists of three assemblies:

(a) two-axis platform

(b) platform electronics

(c) control console

4.1.1.1 Two-Axis Platform

The platform mechanization was a locally level, north referenced type. A significant savings was accomplished without loss of test data by using only one G9 gyro and one level axis. A two level axis inertial platform obeys the same physical laws and thus one axis provides the same type information. The test system used a two-axis gyro which controlled the platform about one level axis and the vertical or aximuth axis. Two electromagnetic accelerometers were included, one pointing eastwardly and the other pointing north. The east pointing sensor was used to measure platfrom tilt in the level axis. Other platform components tested in the nuclear environment were two synchro receivers, two gimbal torquer motors, two sets of gimbal bearings, and H-film polyimide wire.

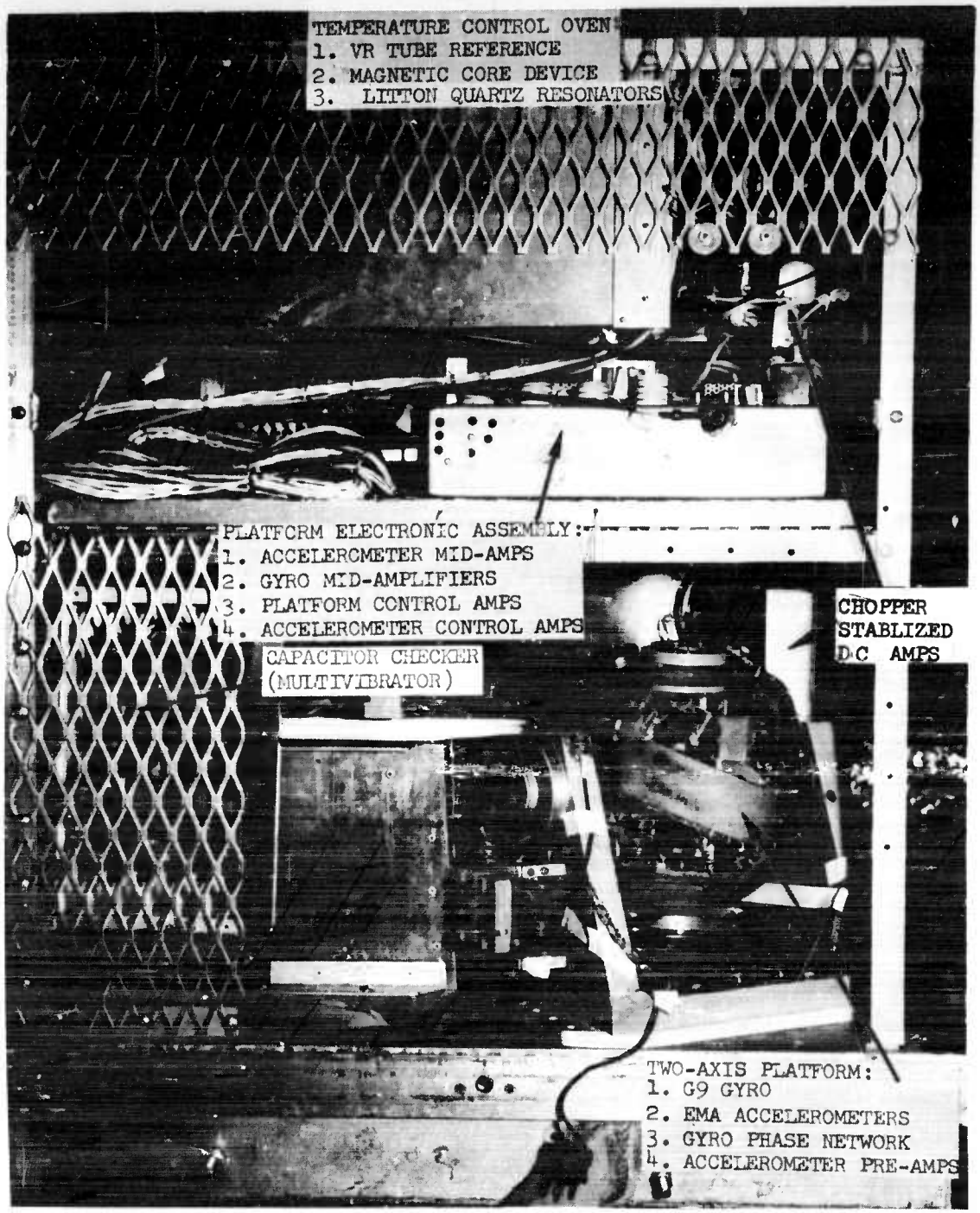

FIGURE 46 INERTIAL REFERENCE SYSTEM AND ASSOCIATED ELECTRONIC CIRCUITS LOCATED ON THE GTR WEST PALLET

4.1.1.2 Platform Electronics

The control electronics for the platform exposed to the nuclear environment included:

(a) Two accelerometer preamplifiers which are capacitance coupled preamplifiers that isolate pickoff transformers from electrical leads, raise the signal level, and reduce the impedance level to improve noise characteristics. Components used were RCA 7895 Nuvistors, wirewound resistors, mylar film dielectric capacitors, and pre-irradiated polyolefin insulated wire.

(b) Four mid-amplifiers which raise the accelerometer preamplifiers and gyro outputs and drive the 150-foot cables to the control room. Each mid-amplifier used four capacitance coupled stages using RCA 7895 Nuvistors with a cathode follower output.

(c) One accelerometer control amplifier which receives the amplified accelerometer signal and provides torqueing current for the accelerometer forcer coils. The amplifier uses 16 RCA Nuvistors (eleven 7895, four 8056, and one 75B6 Nuvistors) in a servo circuit which demodulates the incoming signal, feeds it through a shaping network, modulates and amplifies the network output, then demondulates and drives the accelerometer torquer.

(d) One platform control amplifier that receives the amplified gyro output, shapes its response, and drives the platform gimbal torquer. The amplifier uses thirteen RCA Nuvistors, two GE Z2354 ceramic tubes and eight Z2731 ceramic diodes.

4.1.1.3 Control Console

The control console for the platform subsystem was located in the reactor control room with approximately 150 feet of cable separation from the west irradiation test cell. The console consisted of the following:

(a) Two accelerometer control amplifiers (one redundant)

(b) Two platform control amplifiers (one redundant)

(c) A two-channel analog gyro torque computer

(d) Two resolver transmitters including dials and readout meters

(e) Control electronics for mode switching

(f) Power supplies and signal conditioning devices

Outputs from the control console were measured and recorded throughout the test. Temperature measurements of the irradiated devices were recorded continuously during the test. The most significant test article parameters measured during the irradiation were:

(a) Two accelerometer outputs

(b) Gyro torquer amplifier outputs

(c) Platform gimbal single position

(d) Measurements of amplifier outputs, nulls, power supplies, accelerometer scale factor, and gyro wheel speed.

4.1.2 VOLTAGE REFERENCE GAS TUBE CIRCUITS

Not included in the platform subsystem were several precision electronics test circuits. The voltage reference gas tube devices consisted of three circuits, each with ten GE Z2692 gas discharge tubes in parallel. The purpose of this arrangement was to reduce the effect of random variations in each tube by averaging ten of them to obtain a stable voltage output. Wire-wound resistors were also used in the same circuits. A schematic of the voltage reference circuit is shown in Figure 47.

4.1.3 MAGNETIC CORE VOLTAGE REFERENCE DEVICES

A second voltage reference device was designed as an alternate to the gas tube circuit. Its principle of operation was based on saturation of certain magnetic materials. The results obtained from the LASV-N1 radiation test of supermendur magnetic cores forced a change to aluminum-iron cores for the LASV-N2 irradiation test. The circuits tested used specially wound toroidal core transformers which were driven to saturation on each excursion of their 400-cycle input. The output was rectified by a temperature compensated full wave rectifier located in the control room. If the output from this transformer core hystersis loop remains unchanged, the saturation amplitude, and thus the output amplitude, will be constant. The schematic of the magnetic core voltage reference circuits is shown in Figure 48.

4.1.4 CHOPPER STABILIZED DC AMPLIFIERS

The schematic for this unit is shown in Figure 49. The basic requirements of a DC amplifier to be used in servo applications

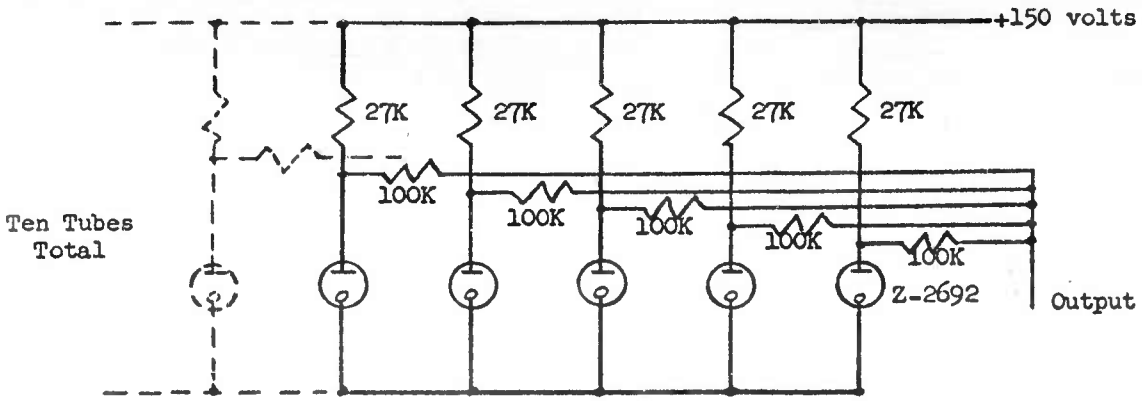

FIGURE 47 SCHEMATIC DIAGRAM OF THE GAS TUBE VOLTAGE REGULATOR

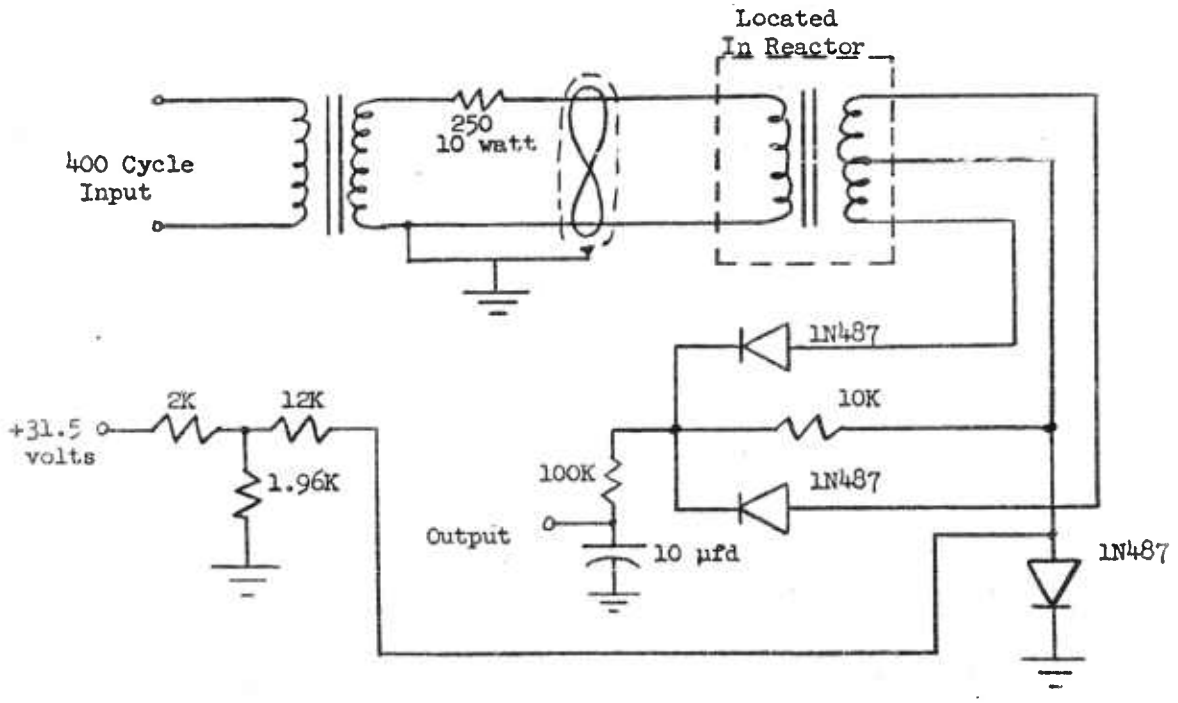

FIGURE 48 SCHEMATIC DIAGRAM OF THE MAGNETIC CORE VOLTAGE REFERENCE

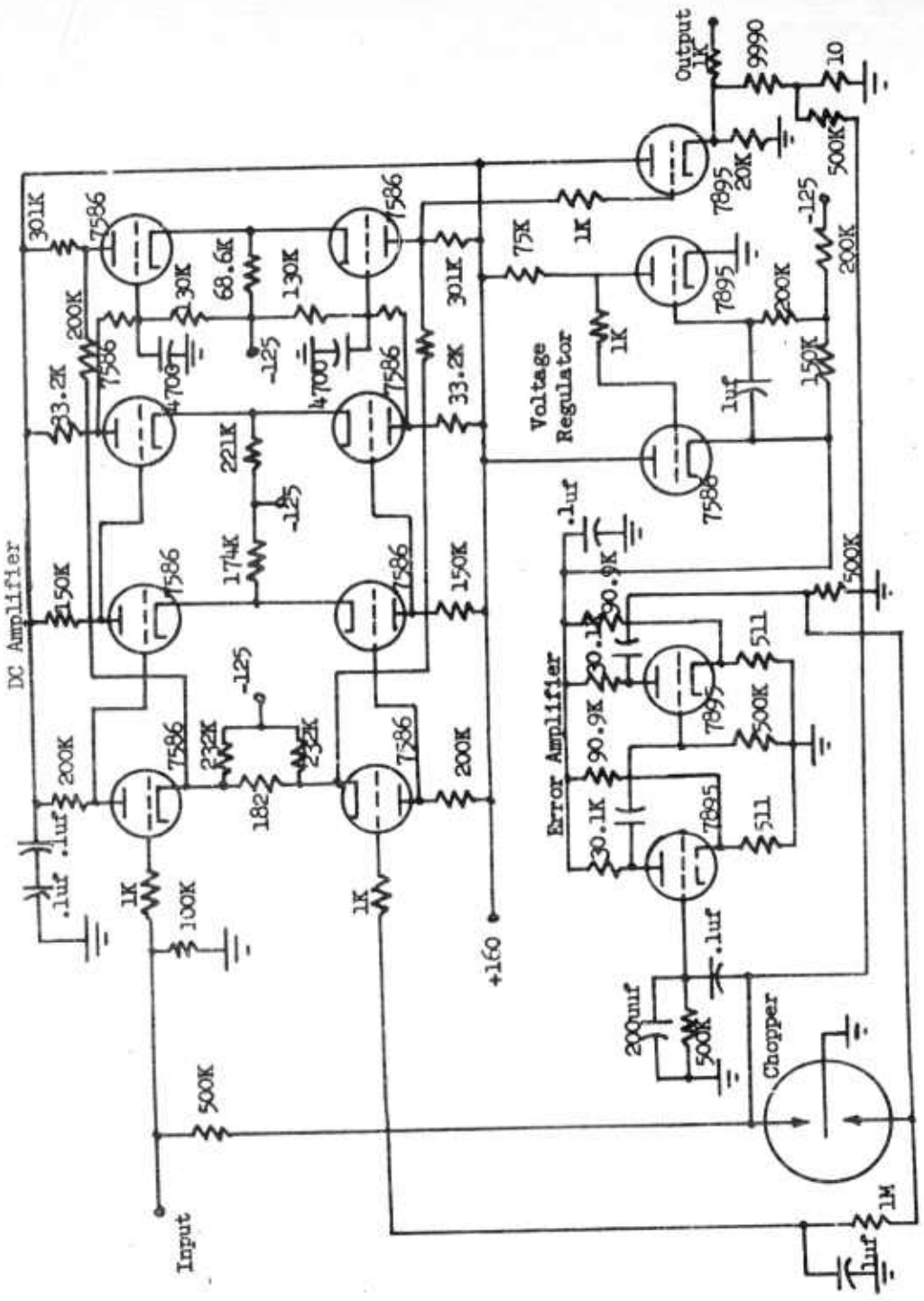

FIGURE 49 SCHEMATIC DIAGRAM OF THE CHOPPER STABILIZED D C AMPLIFIER

are:

(a) High open loop gain

(b) Good gain stability

(c) Good zero stability

Chopper stabilization is the most popular method of controlling drift and stabilizing the amplifier at the lower end of its bandwidth. The circuits tested in this irradiation test used components from the approved parts list and a special radiation-hardened electromechanical 400-cycle chopper.

4.1.5 CAPACITOR CHECKERS

Stability of capacitors in a radiation environment is of primary interest in inertial reference systems applications. An effort was made to monitor stability of three types of capacitors under radiation by using them in free-running multivibrator circuits as shown in Figure 50. The RC time constant determines the output frequency and, provided constant value resistors are used, the output frequency is a function of the capacitance.

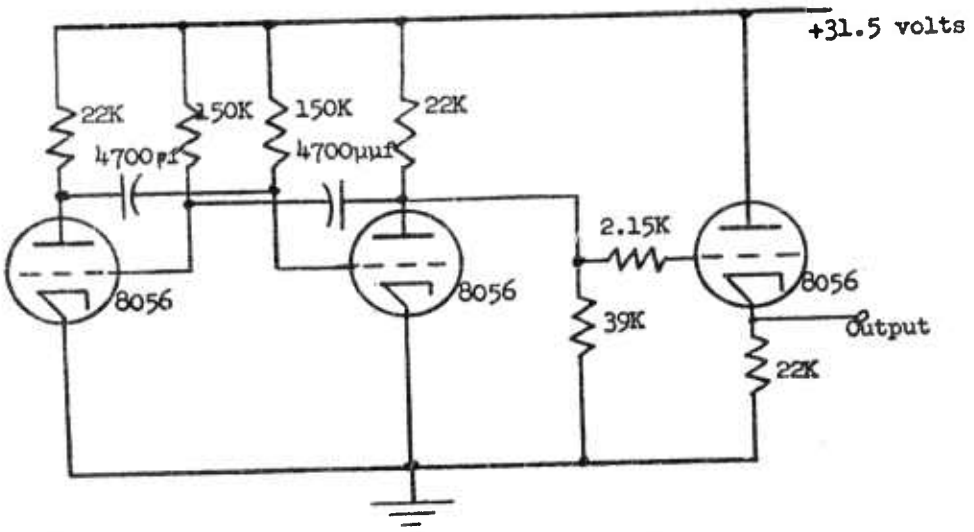

FIGURE 50 SCHEMATIC DIAGRAM OF THE FREE-RUNNING MULTIVIBRATOR CAPACITOR CHECKER

4.1.6 QUARTZ RESONATORS

The only accuracy dependent components of the accelerometer are the quartz resonators. Two of these were enclosed in separate evacuated glass tubes for dynamic evaluation in the nuclear radiation environment. Each resonator was in a bridge-type which oscillated at the frequency of the resonator. The associated electronics were located in the GTR control room with only the frequency determining unit (resonator) subjected to the nuclear radiation. The significant parameter monitored was frequency.

4.2 NUCLEAR ANALYSIS

4.2.1 AUTONETICS INERTIAL REFERENCE SYSTEM

A radiation effects analysis of the materials and parts used in the G9 two-axis gyro, electromagnetic accelerometers, two-axis platform, platform electronic assembly, VR tube voltage reference, magnetic core voltage reference, capacitor checker, and chopper stabilized DC amplifiers is presented in Tables 12 through 19 respectively. Each item was analyzed for radiation tolerance, and when required, replaced with an acceptable alternate.

These test articles were designed to withstand an integrated neutron flux of 5.0×10^{15} n/cm^2 and a gamma dose of 9.0×10^9 ergs/gm-(C). The test articles and materials used in this test have a nuclear threshold function greater than the environment experienced during irradiation testing and operated to radiation levels which exceeded the design goal.

The majority of the materials expected to outgas in the G9 gyro were located in the outer case and were not expected to affect the performance of the gyro. Pre-irradiated (to 1.6×10^{16} n/cm^2) gyro pickoff transformer cores were used in an effort to reduce the change in permeability; however, their degradation was still sufficient to cause unsatisfactory operation of the two-axis platform during the irradiation.

Although some outgassing was expected from several of the electromagnetic accelerometer materials (See Table 13), it was not expected to affect the performance of the accelerometers.

No degradation was anticipated on the two-axis platform test jig and it operated satisfactorily throughout the test. The flexible Dupont polyimide (H-film) wire was as flexible after the irradiation test as before testing.

4.2.2 LITTON QUARTZ CRYSTAL RESONATORS

A nuclear radiation effects analysis of the quartz resonators is presented in Table 20.

TABLE 12

SHEET 1 OF 6

NUCLEAR RADIATION EFFECTS ANALYSIS OF THE GYRO

NUCLEAR DESIGN REQUIREMENT: GAMMAS: 9(9) ERGS/GM-(C)
NEUTRONS: 5(15) N_p/CM^2

MANUFACTURER: AUTONETICS MODEL: G8

CODE NO.	GENERAL DESCRIPTION OF CIRCUIT, PART OR ELEMENT	VALUE	ORIGINAL ELEMENT			LIMITING NUCLEAR EXPOSURE		REMARKS
			PART OR DRAWING NUMBER	MFR	ELEMENT MATERIAL DESCRIPTION	ERGS/GM (C)	N_p/CM^2	
	Resolver							
	Stator Plates		Commercial		4750 steel (50% nickel)		1(18)	
	Winding				"ML" cross lined polymer base enamel MIL-W-583B			Outgassing expected 9.0x10^{-8} ml/gm/rad outgassing
	Retainer		Mylar Sheep	Dupont	Polyethylene Terephthalate	1(10)		4 x 10^{-9} ml/gm/rad outgassing
	Potting Compound		BC-340	J.C.Dolph Co.	Impregnating Varnish	1(10)		Outgassing expected. expect 30% decrease in strength.
	Lamination Insulator		E-304	Armstrong Resin, Inc.	Epoxy Resin	1(10)		
	Lead Wire			Raychem	Irradiated polyethylene	6(10)		
	Case Rotation Motor							
	Housing, End Cap, Covers				303 Stainless steel		1(18)	
	spacers, etc.							
	Gears, Pinions, and shafts				416 stainless steel		1(18)	
					440C stainless steel		1(18)	
	Bearings				440C stainless steel		1(18)	
	Retainers				Impregnating Phenolic	1(11)		
	Lubricant			Dow Corning	polyphenol ether	1(11)		
	Gear Lubricant			Shell	Shell APL	1(11)		
	Magnet Wire				Formvar coated copper	3(10)		Slight outgassing
	Impregnating compound		996	Dow Corning		1(10)		Outgassing expected expected to decrease 30% in strength.

NOTES: (X) INDICATES POWERS OF TEN

TABLE 12

NUCLEAR RADIATION EFFECTS ANALYSIS OF THE GYRO

NUCLEAR DESIGN REQUIREMENT: GAMMAS: 9(9) ERGS/GM-(C)
NEUTRONS: 5(15) N_v/CM^2

MANUFACTURER: AUTONETICS MODEL: G9

CODE NO.	GENERAL DESCRIPTION OF CIRCUIT, PART OR ELEMENT	VALUE	ORIGINAL ELEMENT			LIMITING NUCLEAR EXPOSURE		REMARKS
			PART OR DRAWING NUMBER	MFR	ELEMENT MATERIAL DESCRIPTION	ERGS/GM (C)	N_v/CM^2	
	Lead Wire			Raychem	Irradiated polyethylene	6(10)		Has been exposed to 10^{10} nvt with good results
	Case Rotation Bearing				52100 steel		1(18)	
	Lubricant			Dow Corning	Polyphenol ether	1(11)		
	Limit Stop Bearing				521-- Steel		1(18)	
	Lubricant			Dow Corning	Polyphenol ether	1(11)		
	Fuse Buttons				97% Cu, 3% Ag alloy		1(18)	
					gold plated		1(18)	
	Electrical Feed-Throughs			Tylem Industries Inc.	Inconel X and		1(16)	
	(Inconel X and Ceramic)				ceramic			
	Cement		LCA-4	Bacon Ind.	Epoxy Cement	1(10)		
	Slipring							
	Housing				303 stainless steel		1(18)	
	Bearing				52100 Steel		1(18)	
	Retainer		Synthane		Phenolic	1(11)		
	Lubricant			Dow Corning				
	Wiring			Raychem	Irradiated polyethylene	6(10)		Exposed to 10^{10} nvt with good results.
	Potting compound		1119	Bacon Ind.	Epoxy	1(10)		Outgassing expected decrease in strenght by 30%
	Electromagnetic Actuator							
	Inner Core				Mumetal			
					(M1-Fe per AB0170-C16)		1(18)	Slight decrease in permeability expected

NOTES: (X) INDICATES POWERS OF TEN

TABLE 12

NUCLEAR RADIATION EFFECTS ANALYSIS OF THE GYRO

NUCLEAR DESIGN REQUIREMENT: GAMMAS: 9(9) ERGS/GM-(C)
NEUTRONS: 5(15) N_v/CM^2

MANUFACTURER: AUTONETICS

MODEL: G9

CIRCUIT NO.	GENERAL DESCRIPTION OF CIRCUIT, PART OR ELEMENT	VALUE	ORIGINAL ELEMENT			LIMITING NUCLEAR EXPOSURE		REMARKS
			PART OR DRAWING NUMBER	MFR	ELEMENT MATERIAL DESCRIPTION	ERGS/GM (C)	N_v/CM^2	
	Outer Core		Spec. AB0170-016		Mumetal (Ni-Fe)		1(13)	Slight decrease in permeability expected
	Terminal Board		MIL-P-18177 Type GEE		Epoxy-glass	1(11)		Slight outgassing expected
	Terminal		Spec. QQ-B-626		Brass Rod		1(13)	
	Insulator	7.5	Mylar	Dupont	Polyethylene Terephthalate	1(10)		9×10^{-6} ml/gm/rad outgassing
	Winding (Copper wire)			Hudson WireCo	Copper Wire		1(13)	
	Winding Insulation		Formvar		Vinyl-Acetal	3(10)		Outgassing expected
	Winding			Welber B. Driver Co.	Nickel Wire		1(13)	Outgassing expected
	Potting Compound		1119	Bacon Ind.	Epoxy	1(10)		Outgassing expected decrease in strength by 30%
	Upper External Housing:							
	Plain Housing				Beryllium		1(13)	Slight dimensional change expected
	Shield				Mumetal		1(13)	Slight decrease in permeability
	Retaining Strap		MIL-S-5059		302 Cres		1(13)	
	Upper Internal Housing							
	Plain Housing				Beryllium		1(13)	Slight dimensional change expected
	Check Value Components		Spec. AMS 5667		Ni-Cr Bar		1(13)	
	Gyro Rotor							
	Rotor-less sleeves				Beryllium		1(13)	Slight dimensional change expected
	Motor Sleeve				Copper		1(13)	
	Sleeve Cement		LCA-4	Bacon Ind.	Epoxy Resin	1(10)		
	Torquer Sleeve				Low Metal (95% Cu, 5% Mn)		1(13)	
	Sleeve Cement		LCA-4	Bacon Ind.	Epoxy Resin	1(10)		

NOTES: (X) INDICATES POWERS OF TEN

TABLE 12

NUCLEAR RADIATION EFFECTS ANALYSIS OF THE GYRO

NUCLEAR DESIGN REQUIREMENT: GAMMAS: 9(9) ERGS/GM-(C)
NEUTRONS: 5(15) N_v/CM^2

MANUFACTURER: AUTONETICS

MODEL: G9

CODE NO.	GENERAL DESCRIPTION OF CIRCUIT, PART OR ELEMENT	VALUE	ORIGINAL ELEMENT			LIMITING NUCLEAR EXPOSURE		REMARKS
			PART OR DRAWING NUMBER	MFR	ELEMENT MATERIAL DESCRIPTION	ERGS/GM (C)	N_v/CM^2	
	Spherical Bearing and Shaft				Beryllium		1(19)	Slight dimensional change expected
	Ball Coating				Cr plated		1(13)	
	Shaft Coating		LCA-4	Bacon Ind.	Epoxy Plated	1(10)		
	Lower Internal Housing							
	Plain Housing				Beryllium		1(19)	Slight Dimensional change expected
	Pickoff Ring			American Lava	Al-Si-Fe 1961-4 Ceramic		1(16)	
	Shield				Mumetal		1(13)	Slight dimensional change expected
	Motor							
	Retaining Ring		Spec. ANC 5007		Ni-Cr Bar		1(13)	
	Insulator, Disk, Motor Stator		Type GEE Formica FF91		Epoxy-Glass MIL-P-15037		1(11)	Slight Outgassing expected
	Winding (copper wire)			Hudson Wire Co.	Copper Wire.		1(19)	
	Winding Insulation		Formvar		Vinyl-Acetal	3(10)		9×10^{-9} ml/gm/rad outgassing
	Insulation	3 MIL	Mylar	Dupont	Polyethylene Terephthalate	1(10)		4×10^{-9} ml/gm/rad outgassing
	Stator Plates		Commercial		4750 Steel(50% Ni)		1(19)	
	Potting Compound		1119	Bacon Ind.	Epoxy Resin	1(10)		Outgassing expected decrease in strenght by 30%
	Core			ARMCO	Silicon steel M-15		1(13)	
	Core Cement		LCA-4	Bacon Ind.	Epoxy	1(10)		
	Shaft Nut Insulator				Aluminum Oxide		1(13)	
	Gasket	2MIL	Commercial		Gold		1(19)	
	Lower External Housing							
	Plain Housing				Beryllium		1(19)	Slight dimensional change
	Shield				Mumetal		1(19)	Slight decrease in permeability

NOTES: (X) INDICATES POWERS OF TEN

TABLE 12

NUCLEAR RADIATION EFFECTS ANALYSIS OF THE GYRO

NUCLEAR DESIGN REQUIREMENT: GAMMAS: 9(9) ERGS/GM-(C)
NEUTRONS: 5(15) N$_v$/CM^2

MANUFACTURER: AUTONETICS

MODEL: G9

CODE NO.	GENERAL DESCRIPTION OF CIRCUIT, PART OR ELEMENT	VALUE	ORIGINAL ELEMENT			LIMITING NUCLEAR EXPOSURE		REMARKS
			PART OR DRAWING NUMBER	MFR	ELEMENT MATERIAL DESCRIPTION	ERGS/GM (C)	N$_v$/CM^2	
	Lower Cover				Beryllium		1(18)	Slight dimensional change
	Plain Cover				Mumetal		1(18)	Slight decrease in permeability
	Shield				416 Cres Bar		1(18)	
	Bracket		QQ-S-763, Cond A		Ni-Cr Bar		1(18)	
	Nut and Pin		Spec. AMS 5667					
	Wiring Module							
	Terminal Board			Carborundum Co.	Dow 332 resin and Lithafrax	1(11)		Expected to maintain physical and electrical properties
	Terminal		QQ-B-626, Comp 22		Brass Bar		1(18)	
	Alignment Pin		QQ-S-763 Cond A		303 Cres Steel		1(18)	
	Slipping Nut		MIL-L-7720, Cond A		303 Cres steel		1(18)	
	Electrical Contact Holder		Spec. AMS 5667		Ni-Cr Bar		1(18)	
	Resolver Clamps		QQ-S-763, Cond A		440C Cres steel		1(18)	
	Bearing Retaining Ring		QQ-S-763		303 Cres steel Bar		1(18)	
	Cover				Mumetal		1(18)	Slight Decrease in Permeability
	Retaining Strap		MIL-S-5059		302 Cres Steel		1(18)	
	Pickoff Transformer							
	Core (Irradiated)							Has been exposed once at 10^{16} n/cm^2 (E > 0.3 Mev)
	Core Winding			Allegeheny-Ludlum	Supermalloy		1(16)	Expect less than 1% permeability change
	Core Case				Polystyrene	1(11)		Hermetically sealed. Outgassing of 2.5×10^{-10} ml/gm/rad expected change in polystyrene.
	Core filler				Magnesium oxide		1(16)	

NOTES: (X) INDICATES POWERS OF TEN

TABLE 12

NUCLEAR RADIATION EFFECTS ANALYSIS OF THE GYRO

NUCLEAR DESIGN REQUIREMENT: GAMMAS: 9(9) ERGS/GM-(C)
NEUTRONS: 5(15) N_v/CM^2

MANUFACTURER : AUTONETICS MODEL : G9

CODE NO.	GENERAL DESCRIPTION OF CIRCUIT, PART OR ELEMENT	VALUE	ORIGINAL ELEMENT			LIMITING NUCLEAR EXPOSURE		REMARKS
			PART OR DRAWING NUMBER	MFR	ELEMENT MATERIAL DESCRIPTION	ERGS/GM (C)	N_v/CM^2	
	Winding (copper wire)			Hudson Wire Co.	Copper Wire		1(18)	
	Winding insulation		Formvar		Vinyl-acetal coated copper (MIL-W-583-72)	3(10)		Outgassing of 9×10^{-8} ml/gm/rad
	Winding potting compound		Scotchcast 808A	3M	Epoxy Resin	1(10)		Outgassing expected. Expected decrease in strength by 30%
	Wiring			Raychem Corp	Irradiated Polyethylene	6(10)		Thermorad covered copper wire
	Hydrogen Gas	50 cc at 10 psig			Hydrogen			Hydrogen should be unaffected by radiation
	O-rings				Neoprene	5(90		A repeated seal will get hard but usable
	Nylock Balance Screws				90% platinum and 10% dridium		1(18)	No measureable change in balance expected
	Lock		Nylon		Nylon insert	1(9)		Good locking torque. Use with G6B4 with good result
	Resistor pickoff 443-0147	.125w±1%	AC443-005	I.R.C.	Metal Film		1(16)	
	Motor			Dalohm	wirewound (ceramic bobbin)		1(16)	

NOTES: (X) INDICATES POWERS OF TEN

TABLE 13

NUCLEAR RADIATION EFFECTS ANALYSIS OF THE EMA ACCELEROMETER

NUCLEAR DESIGN REQUIREMENT: GAMMAS: 9(9) ERGS/GM-(C)
NEUTRONS: 5(15) N_r/CM^2

MANUFACTURER: AUTONETICS

CODE NO.	GENERAL DESCRIPTION OF CIRCUIT, PART OR ELEMENT	VALUE	ORIGINAL ELEMENT			LIMITING NUCLEAR EXPOSURE		REMARKS
			PART OR DRAWING NUMBER	MFR	ELEMENT MATERIAL DESCRIPTION	ERGS/GM (C)	N_r/CM^2	
	Proof Mass			Autonetics				
	Stator				Invar		1(16)	
	Stator Standoff				Fiberglass		1(18)	
	Slim				Silver			
	Reed			Corning Glass	Fused silica		1(16)	Chromium and gold plated
	Reed Coating			"	Chromium & Gold		1(18)	
	Servo Coil			Autonetics				
	Coil Form				Aluminum		>1(18)	
	Coil Form Coating				Hard Anodize		1(18)	
	Coil Wire				Copper		>1(18)	
	Coil Wire Coating				Double Formvar	3(10)		Outgassing expected
	Coil Wire Cement		Epon 828	Shell Chemical Co.	Epoxide	5(10)		Outgassing expected
	Base Washer				Copper		>1(18)	
	Solder		Commercial		50% Indium & 50% tin		>1(18)	
	Interior Washer				Brass		>1(18)	
	Solder				60% Tin & 40% Lead		>1(18)	
	Magnet			Autonetics				
	Magnetic Core		Alnico VIII		35% Co, 5% Ni, 4% Cr, 5% Ti, 7% Al, 34% Fe		1(18)	
	Pole Tip				4750 Steel		1(18)	
	Pole Tip Cement		Epon 828	Shell Chemical Co.	Epoxide	5(10)		Outgassing expected
	Magnetic Case		Invar		36% Ni, 63.8% Fe, 0.2% Cr		1(16)	

NOTES: (X) INDICATES POWERS OF TEN

TABLE 13

NUCLEAR RADIATION EFFECTS ANALYSIS OF THE EMA ACCELEROMETER

NUCLEAR DESIGN REQUIREMENT: GAMMAS: 9(9) ERGS/GM (C)

NEUTRONS: 5(15) N_v/CM^2

MANUFACTURER AUTHORIZED

CODE NO.	GENERAL DESCRIPTION OF CIRCUIT, PART OR ELEMENT	VALUE	ORIGINAL ELEMENT			LIMITING NUCLEAR EXPOSURE		REMARKS
			PART OR DRAWING NUMBER	MFR	ELEMENT MATERIAL DESCRIPTION	ERGS/GM (C)	N_v/CM²	
	Electrical Feed-Thru			Stupkoff				
	Outer Jacket				Invar			
	Coating				Gold		1(18)	
	Center Pin				Invar			
	Coating				Gold		1(18)	
	Center Insulator			Corning	7052 Glass		1(18)	
					20% B_2O_3			
	Cement		Epon 828	Shell Chemical Co.	Epoxide	5(10)		Outgassing expected
	Transformer			Autonetics				
	Core Tape			Magnetics Inc	Supermalloy		1(16)	Expected change in permeability
	Core Tape Coating			Magnetics Inc	MgO		1(16)	
	Damping Material			Maguetics Inc	MgO		1(16)	
	Case			G.E.	Lexan			
	Wire				Copper		>1(18)	
	Wire Coating				Formvar	1(10)		9 x 10-9 ml/gm/rad outgassing
	Winding Tape				Mylar Tape			
	Mounting Can			Autonetics	Invar		1(18)	
	Accelerometer Case			"	Aluminum		1(18)	
	Electrical Hookup			Raychem Corp	Irradiated Polyethylene	6(10)		Copper wire
	Electrical Connector			Cannon				
	Insulator				Diallyl Phthalate	5(10)		
	Heater Wire				Tophet C			
	Insulation				Formvar	3(10)		9 x 10-9 ml/gm/rad outgassing
	Sensor Wire Insulation			Belco	Formvar	3(10)		9 x 10-9 ml/gm/rad outgassing

NOTES: (X) INDICATES POWERS OF TEN

TABLE 14

NUCLEAR RADIATION EFFECTS ANALYSIS OF THE TWO - AXIS PLATFORM

NUCLEAR DESIGN REQUIREMENT: GAMMAS : 9(9) ERGS/GM-(C)
NEUTRONS : 5(15) N_r/CM^2

MANUFACTURER: AUTONETICS

CODE NO.	GENERAL DESCRIPTION OF CIRCUIT, PART OR ELEMENT	VALUE	ORIGINAL ELEMENT			LIMITING NUCLEAR EXPOSURE		REMARKS
			PART OR DRAWING NUMBER	MFR	ELEMENT MATERIAL DESCRIPTION	ERGS/GM (C)	N_r/CM^2	
	Gyro Connectors		SRE 29JT, SRE 7JT	Winchester				
	Connector Body				Diallyl Phthalate (glass filled)	5(10)		
	Pins				Beryllium Copper		>1(18)	Gold plated
	Torquer Motor Connectors		SRE 5G SRE 5P	Winchester				
	Connector Body				Diallyl Phthalate (galss filled)	5(10)		
	Pins				Beryllium Copper		>1(18)	Gold plated
	EMA Connectors		DB-255, C33	Cannon				
	Connector Body				Diallyl Phthalate (glass filled)	5(10)		
	Pins				Brass		>1(18)	Gold plated over silver
	EMA Preamplifiers Connectors		SRE 11S-G	Winchester				
	Connector Body				Diallyl Phthalate (glass filled)	5(10)		
	Pins				Beryllium Copper		>1(18)	Gold plated
	Interconnecting Cable Connectors		XAC42PC1A306S	Winchester				
	Connector Body				Diallyl Phthalate (glass filled)	5(10)		
	Pins				Beryllium copper		>1(18)	Gold plated
	Resolvers		27 RD-13	Solvere				
	Lamination		H1MU80		Electrical Steel		1(18)	
	Lamination Cement		Cycleband 55-9	Cycleweld Chemical	Phenolic Thermo-setting Adhesive	1(10)		
	Winding				Copper Wire		>1(18)	Coated with "ML" cross linked polymerbase enamel
	Splice Insulation			Dacron	Mylar	5(10)		
	Lead Wire		Thermorad	Raychem	Irradiated Poly-ethylene	6(10)		
	Potting compound		8C-340	Dolph	Impregnating varnish	1(10)		

NOTES: (X) INDICATES POWERS OF TEN

TABLE 14

NUCLEAR RADIATION EFFECTS ANALYSIS OF THE TWO - AXIS PLATFORM

NUCLEAR DESIGN REQUIREMENT: GAMMAS: 3(9) ERGS/GM (C)
NEUTRONS: 5(15) N_F/CM^2

MANUFACTURER: AUTONETICS

CODE NO.	GENERAL DESCRIPTION OF CIRCUIT, PART OR ELEMENT	VALUE	ORIGINAL ELEMENT			LIMITING NUCLEAR EXPOSURE		REMARKS
			PART OR DRAWING NUMBER	MFR	ELEMENT MATERIAL DESCRIPTION	ERGS/GM (C)	N_F/CM^2	
	Ring		QQ-S-763A, close 6, Type A		416 Stainless Steel		>1(18)	
	Gimbal Bearings		SFR6S-DF-20	Barden				
	Retainers and Shield				Stainless steel		>1(18)	
	Balls and Races				440 Stainless steel		>1(18)	
	Torquer Motor		2813-1000					
	Brush Rigging							
	Brushes		506	Stackpole	Copper		>1(18)	Plated graphite
	Springs				Beryllium Copper		>1(18)	
	Block				Epoxy Glass Laminate	5(10)		Some outgassing expected
	Cement			Foibard	Epoxy	5(10)		
	Field		Alnico V		Magnet		1(18)	Cadmium plated iron
	Armature							
	Laminations				Electrical steel		1(18)	Iron and Cobalt
	Lamination Lacquer		DK-2	H sol	Polymer			polymerization of Etich-lorohydrun with bisphenolA
	Winding				ML Copper wire		1(18)	
	Commutator				Copper		1(18)	
	Sleeving				Fiberglass			
	Encapsulant		Epon 828	Shell Chemical Co.	Epoxide	5(10)		Slight outgassing
	Azimuth Resolver Support		67626-301		2024 Al		>1(18)	
	EMA Housing		67627-301		303 Stainless steel		>1(18)	
	Roll Resolver Support		67623-301		2024 Al			
	Azimuth and Roll Shaft		67629-301		Stainless Steel		>1(18)	
	Hookup wire				Conductor (copper)		>1(18)	
	Insulation			Dupont	Poly Imide (H-Film)	9(9)	2(15)	change expected in elongation and tensile strength

NOTES: (X) INDICATES POWERS OF TEN

TABLE 15

NUCLEAR RADIATION EFFECTS ANALYSIS OF THE PLATFORM ELECTRONICS ASSEMBLY

NUCLEAR DESIGN REQUIREMENT: GAMMAS: 9(9) ERGS/GM—(C)
NEUTRONS: 5(15) N_v/CM^2

MANUFACTURER: AUTONETICS

CODE NO.	GENERAL DESCRIPTION OF CIRCUIT, PART OR ELEMENT	VALUE	ORIGINAL ELEMENT			LIMITING NUCLEAR EXPOSURE		REMARKS
			PART OR DRAWING NUMBER	MFR	ELEMENT MATERIAL DESCRIPTION	ERGS/GM (C)	N_v/CM^2	
	Vacuum Tube		Z2354	G.E.	Ceramic and Metal		1(16)	Platform control power amplifier
	Vacuum Tube		Z2731	G.E.	Ceramic and Metal		1(16)	Platform control power demodulation
	Nuvistor		JAN 7895	RCA	Ceramic and metal		1(16)	High mu triode
	Nuvistor		JAN 7586	RCA	"		1(16)	Medium mu triode
	Nuvistor		JAN 7587	RCA	"		1(16)	Sharp cutoff tetrode
	Nuvistor		JAN 8056	RCA	"		1(16)	low R_p, medium mu triode
	Tube Sockets		5NS-1	Cinch Jones		2(10)		
	Capacitors	.001-1.0ufd	Military grade	G.E.	Mylar film dielectric	5(10)	1(16)	
	Capacitors	1.0-2.0 µfd	Commercial grade	G.E.	"	5(10)	1(16)	
	Capacitors	.01 µfd		Centralab	Ceramic Dielectric		1(16)	
	Capacitors	.01 µfd		Vitramon	Ceramic dielectric		1(16)	
	Resistors	1-175K	Type RH	Dale Mfg.	Wire wound	1(11)	5(16)	
	Resistors	10-500 K	Type S	Corning	Metal film		1(16)	
	Resistors	500	600 Series	Keys	Ceramic & metal film		1(16)	
	Transformer			North American Aviation			1(16)	Some outgassing from formvar & small buildup pres.
	Connectors		Series SRE	Winchester	Diallyl Phthalate	2(10)		Used on preamps.
	Connectros		Series XAC	Winchester	Diallyl Phthalate	2(10)		
	Relays		BA	C.P. Clare		5(10)	3(16)	Dry type, 2 ampere contacts
	Insulating Sleeving			Raychem	Irradiated Polyolefin	6(10)		
	Circuit Boards		GEE		MIL-P-18177	2(10)		Epoxy-glass fiber laminate
	Hook-up Wire			Raychem	Irradiated Polyolefin insulation	6(10)	1(16)	Pure fiberglass insulation spray with silicone for binding
	Chassis				Aluminum		>1(18)	
	Potting compounds		Scotchcast 305A	Minnesota Minning	Epoxy Resin			

NOTES: (X) INDICATES POWERS OF TEN

TABLE 16

NUCLEAR RADIATION EFFECTS ANALYSIS OF THE VR TUBE VOLTAGE REFERENCE

NUCLEAR DESIGN REQUIREMENT: GAMMAS: 9(9) ERGS/GM-(C)
NEUTRONS: 5(15) N_v/CM^2

MANUFACTURER: AUTONETICS

CODE NO.	GENERAL DESCRIPTION OF CIRCUIT, PART OR ELEMENT	VALUE	ORIGINAL ELEMENT			LIMITING NUCLEAR EXPOSURE		REMARKS
			PART OR DRAWING NUMBER	MFR	ELEMENT MATERIAL DESCRIPTION	ERGS/GM (C)	N_v/CM^2	
	Reference Tube		Z 2692	G.E.	Metal & Ceramic		1(18)	
	Resistor	27 K	N205A	Ultronix	Wirewound Alkyd Resin Core	1(11)	5(16)	
	Resistor	100 K	N205A	Ultronix	"	1(11)	5(16)	
	Resistor	16 K	N205A	Ultronix	"	1(11)	5(16)	
	Hook-up Wire			Raychem	Irradiated polyethylene	6(10)		
	Heater				Manganin Wire		1(18)	Slight outgassing expected
	Chassis				Anodized aluminum		>1(18)	
	Connector		XAC14SF24016	Winchester	Diallyl phthalate	2(10)		

NOTES: (X) INDICATES POWERS OF TEN

TABLE 17

NUCLEAR RADIATION EFFECTS ANALYSIS OF THE MAGNETIC CORE VOLTAGE REFERENCE

NUCLEAR DESIGN REQUIREMENT: GAMMAS: 9(9) ERGS/GM-(C)
NEUTRONS: 5(15) N_r/CM^2

MANUFACTURER: AUTONETICS

CODE NO.	GENERAL DESCRIPTION OF CIRCUIT, PART OR ELEMENT	VALUE	ORIGINAL ELEMENT					REMARKS
			PART OR DRAWING NUMBER	MFR	ELEMENT MATERIAL DESCRIPTION	LIMITING NUCLEAR EXPOSURE ERGS/GM (C)	LIMITING NUCLEAR EXPOSURE N_r/CM^2	
	Core		A5662R8S1 & 51002-4K-1	Autonetics	Silicon aluminum		1(16)	Some permeability change expected
	Magnet Wire Insulation				Formvar & Irradiated Polyethylene	3(10)		
	Wire				Copper		>1(18)	

NOTES: (X) INDICATES POWERS OF TEN

TABLE 18

NUCLEAR RADIATION EFFECTS ANALYSIS OF THE FREE-RUNNING MULTIVIBRATOR CAPACITOR CHECKER

NUCLEAR DESIGN REQUIREMENT: GAMMAS: 9(9) ERGS/GM—(C)
NEUTRONS: 5(15) N_p/CM^2

MANUFACTURER: AUTONETICS

CODE NO.	GENERAL DESCRIPTION OF CIRCUIT, PART OR ELEMENT	VALUE	ORIGINAL ELEMENT			LIMITING NUCLEAR EXPOSURE		REMARKS
			PART OR DRAWING NUMBER	MFR	ELEMENT MATERIAL DESCRIPTION	ERGS/GM (C)	N_p/CM^2	
	Thyristor Tube		Type 8056	RCA	Metal & Ceramic		1(18)	
	Tube Sockets		5NS-1	Cinch-Jones		2(10)		Mica filled phenolic insert
	Resistors	22 K	M205A	Ultronix	Wirewound Alkyd Resin Core	1(11)	5(16)	
	Resistors	150 K	"	"	"	1(11)	5(16)	
	Resistors	39 K	"	"	"	1(11)	5(16)	
	Resistors	2.2 K	"	"	"	1(11)	5(16)	
	Capacitors	4700 Pfd, 300V		G.E.	Ceramic		1(18)	
	Capacitors	4700 μfd			Polyetynun			
	Hook-up Wire			Raychem	Irradiated Polyethylene	6(10)		
	Chassis				Aluminum		>1(18)	
	Connector	XAC14SF24016		Winchester	Diallyl phthalate	2(10)		

NOTES: (X) INDICATES POWERS OF TEN

TABLE 19

SHEET 1 OF 2

NUCLEAR RADIATION EFFECTS ANALYSIS OF THE CHOPPER STABLIZED DC AMPLIFIER

NUCLEAR DESIGN REQUIREMENT: GAMMAS: 9(9) ERGS/GM-(C)
NEUTRONS: 5(15) N_v/CM^2

MANUFACTURER: AUTONETICS

CODE NO.	GENERAL DESCRIPTION OF CIRCUIT, PART OR ELEMENT	VALUE	ORIGINAL ELEMENT			LIMITING NUCLEAR EXPOSURE		REMARKS
			PART OR DRAWING NUMBER	MFR	ELEMENT MATERIAL DESCRIPTION	ERGS/GM (C)	N_v/CM^2	
	Nuvistor Tube		7586	RCA	Metal & Ceramic		1(13)	
	Nuvistor Tube		7895	RCA	Metal & Ceramic		1(13)	
	Tube Sockets		5N5-1	Cinch-Jones		2(10)		Mica filled phenolic insert
	Resistor	200K ohms	N205A	Ultronix	Wirewound Alkyd Resin Core	1(11)	5(16)	
	"	150K ohms	"	"	"	1(11)	5(16)	
	"	33.2K ohms	"	"	"	1(11)	5(16)	
	"	30.1K ohms	"	"	"	1(11)	5(16)	
	"	10 ohms	"	"	"	1(11)	5(16)	
	"	9.99K ohms	"	"	"	1(11)	5(16)	
	"	43K ohms	"	"	"	1(11)	5(16)	
	"	130K ohms	"	"	"	1(11)	5(16)	
	"	232K ohms	"	"	"	1(11)	5(16)	
	"	182 ohms	"	"	"	1(11)	5(16)	
	"	174K ohms	"	"	"	1(11)	5(16)	
	"	221K ohms	"	"	"	1(11)	5(16)	
	"	68.6K ohms	"	"	"	1(11)	5(16)	
	"	75K ohms	"	"	"	1(11)	5(16)	
	"	90.9K ohms	"	"	"	1(11)	5(16)	
	"	1000K ohms	"	"	"	1(11)	5(16)	
	Capacitor	0.1ufd,100V		G. E.	Lectrofilm "B" mylar film	5(10)	1(16)	
	Capacitor	1ufd, 100V		G.E.	"	5(10)	1(16)	
	"	4700ufd,30V		G.E.	Ceramic		1(13)	
	Hook-up Wire			Raychem	Irradiated polyethylene	6(10)		
	Chassis				Aluminum		>1(13)	
	Chopper		940	Air Pak			1(16)	
	Internal Parts				Brass, silver, & palladium		1(13)	
	Coil Wire		[illegible]		Magnet Wire		1(13)	

NOTES: (X) INDICATES POWERS OF TEN

TABLE 19

NUCLEAR RADIATION EFFECTS ANALYSIS OF THE CHOPPER STABLIZED DC AMPLIFIER

NUCLEAR DESIGN REQUIREMENT: GAMMAS: 9(9) ERGS/GM-(C)

NEUTRONS: 5(15) N_r/CM^2

MANUFACTURER: AUTONETICS

CODE NO.	GENERAL DESCRIPTION OF CIRCUIT, PART OR ELEMENT	VALUE	ORIGINAL ELEMENT					REMARKS
			PART OR DRAWING NUMBER	MFR	ELEMENT MATERIAL DESCRIPTION	LIMITING NUCLEAR EXPOSURE		
						ERGS/GM (C)	N_r/CM^2	
	Coil Form				Fiberglass		1(16)	
	Coil Lead				Ceramic Insulated wire		1(16)	
	Connector		XAC14SF24016	Winchester	Diallyl Phthalate	2(10)		

NOTES: (X) INDICATES POWERS OF TEN

TABLE 20

NUCLEAR RADIATION EFFECTS ANALYSIS OF THE QUARTZ CRYSTAL RESONATORS

NUCLEAR DESIGN REQUIREMENT: GAMMAS: 9(9) ERGS/GM-(C)
NEUTRONS: 5(15) N_v/CM^2

MANUFACTURER: LITTON INDUSTRIES

CODE NO.	GENERAL DESCRIPTION OF CIRCUIT, PART OR ELEMENT	VALUE	ORIGINAL ELEMENT			LIMITING NUCLEAR EXPOSURE		REMARKS
			PART OR DRAWING NUMBER	MFR	ELEMENT MATERIAL DESCRIPTION	ERGS/GM (C)	N_v/CM^2	
	Case		Commercial		Aluminum 6061-T651-O		>1(18)	
	Flexure Support		Commercial		Aluminum 6061-T651-O		>1(18)	
	Proof Mass		Mallory 1000		Tungsten Alloy		1(18)	
	Resonator (Quartz)		Optical Grade		Aluminum Plated		1(18)	
	Resonator and Button		Code 0080, 200892	Corning	Glass	1(10)		Will darken
	Lead Wire		Gauge 26		Copper		>1(18)	Will get brittle
	Adhesive		K8-4238	Hysol	Conductive Epoxy	1(10)		Will change color
	Adhesive		Epon 828	Shell	Epoxy cement	1(10)		Will change color
	Adhesive		Emerson and Cuming 2216	3M	Epoxy cement	1(10)		Will change color

NOTES: (X) INDICATES POWERS OF TEN

These resonators are off-the-shelf items and the materials used should withstand the design goal of an integrated neutron flux of 5.0×10^{15} n/cm^2 and a gamma dose of 9.0×10^9 ergs/gm-(C).

4.3 TEST PROCEDURES

Several modes of operation were incorporated into the design of the platform subsystem in order that one component failure would not cause loss of data for the remaining systems. Some of these test modes were gyro compassing, leveling, free drift, free inertial, rotor coast down time, accelerometer scale factor and bias, and gimbal freedom. The precision testing involved only one mode of operation for most circuits. This type of data was taken along with temperature information periodically throughout the irradiation.

4.3.1 PLATFORM AND INERTIAL SENSOR TESTING

Performance parameters of the platform subsystem were monitored under several different modes of operation. The modes, their description, and purpose are as follows:

(a) Gimbal Cage Mode - In this mode, the platform was manually controlled by the resolver transmitters located in the control console. The platform was coarse aligned in azimuth and leveled by this means.

(b) Level Mode - In this mode, the gyro was running and an accelerometer was used as a level sensor. The accelerometer output was operated by a servo loop to derive a torquing signal for the gyro which precessed and moved the gimbal toward the level position.

(c) Gyro Compassing Mode - A similarity exists between this mode and the leveling modes, in fact, it operated simultaneously with the leveling mode. The accelerometer output was operated by a separate analog servo whose output drove the platform about the azimuth axis. When the level gyro axis was due east, no component of earth's turning vector was sensed by the gyro, and thus it did not attempt to tip the platform about the level axis. In the resultant stable position, the level gyro axis was due east and the level accelerometer was perpendicular to the gravity vector.

(d) Free Inertial Mode - In this mode, the system was Schuler tuned in the leveling axis and controlled by the azimuth gyro about the vertical axis. Since no motion was physically imposed, the velocity continued at an identically zero indication, and the level and azimuth angles were maintained. When a disturbance was deliberately introduced into the leveling loop, the frequency of oscillation could be determined and tuning parameters verified.

(e) Free Drift Mode - In this mode, the gyro axes were untorqued and allowed to drift at a rate dependent upon their orientation with respect to the earth's turning vector and instrument drifts. This mode was used to determine changes in the drift characteristics of the gyros.

(f) Gimbal Freedom Test - In this test, the gyro wheel was stopped and the platform was in the gimbal cage mode. The gimbals were torqued around to their stops and the angles recorded. This mode was used primarily to check the condition of the synchro receivers.

(g) Accelerometer Scale Factor and Bias Test - The gimbal cage mode was used in this situation to orient the accelerometer so that a $\pm$ g and zero-g reading could be taken and a scale factor and bias be determined.

4.3.2 VOLTAGE REFERENCE GAS TUBES

During the testing of the VR voltage reference circuits, the three output voltages and the common input voltage were recorded, as shown in Figure 47.

4.3.3 MAGNETIC CORE VOLTAGE REFERENCE

Since the magnetic core operation was somewhat dependent upon the input frequency, both the output voltage and the 400 cycle frequency supply were measured.

4.3.4 CHOPPER STABILIZED DC AMPLIFIERS

Several different inputs were made available for the DC amplifier circuits. Over the instrumentation cables the input could be changes to any one of three modes: shorted input, open input, and one-millivolt input. Variables recorded for these circuits were output voltages as a function of the three input modes and the 31 volt supply voltage.

4.3.5 CAPACITOR CHECKERS

The RC time constant in the free-running multivibrator circuits determines the frequency of operation of the circuit. Stable resistors were chosen for this application in order that changes in the capacitance could be determined. Parameters recorded were output frequency of each of the three circuits supply voltage and the tube vias voltage.

4.3.6 QUARTZ RESONATORS

The primary interest in the resonators were changes in resonant frequency of the quartz crystals. To determine drift characteristics, averaged frequency period measurements were recorded.

4.4 TEST RESULTS AND CONCLUSIONS

The precision electronics circuits withstood the 69 hours of irradiation without catastrophic failure. The platform and its electronics operated satisfactorily for fifty-four hours of irradiation, then the reactor scrammed and thereafter the platform failed to stabilize. After subsequent efforts to stabilize the platform had failed, the power to the gyro was turned off after several tests were made on the inertial components. The time of the platform failure corresponds to an integrated neutron exposure of 8.5×10^{15} n/cm^2 and a gamma dose of 1.5×10^{8} ergs/gm-(C). Several gimbal, scale factor, and bias tests were run on the platform and accelerometers at the conclusion of the irradiation. Figure 51 presents the nuclear radiation exposure versus time for all components located in the two-axis platform.

Prior to the occurrence of the scram no degradation was noted in any of the platform stabilized modes. The following reasons may be postulated as possible causes for lack of stabilization after that time:

(a) The G9 gyro pickoff module suffered a catastrophic failure in the fifty-fourth hour of irradiation such that enough quadrature existed to "dump" the platform, or

(b) The pickoff module deteriorated gradually during the test. The case rotation motor failed, stopping the case in an orientation to exhibit the quadrature in the level stabilization loop, or

(c) The case rotation continued throughout the test causing the quadrature in the pickoff to be distributed between the two axis and not remaining on either of them long enough for the platform to become unstable.

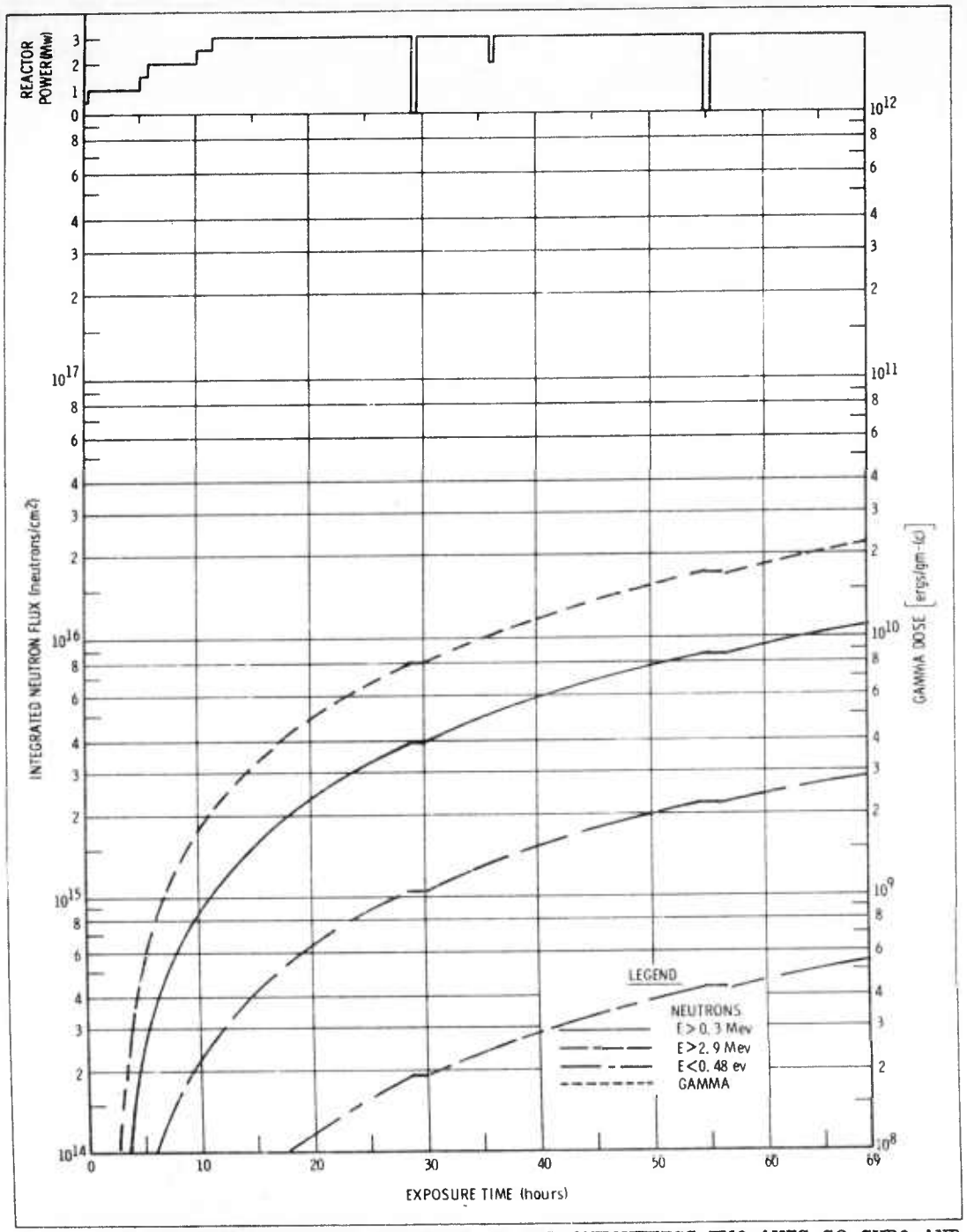

FIGURE 51 NUCLEAR RADIATION EXPOSURE OF THE AUTONETICS TWO-AXIS G9 GYRO AND ELECTROMAGNETIC ACCELEROMETERS

(d) Malfunction in the electronics caused the platform to "dump" after 54 hours of irradiation.

The Dupont H-film polyimide wire used on the platform withstood the irradiation with little evidence of degradation. No cracking or brittleness was noted and flexibility did not seem to be altered by nuclear exposure. Gimbal bearings exhibited easy freedom of movement. Information regarding the performance of the inertial sensors and platform electronics is contained in the following paragraphs. Autonetics has conducted data analysis and post-irradiation testing on these test articles. The results of this effort were not made available in time to be included in this report, but are to be included in Autonetics final report as a supplement to Volume II of this report.

4.4.1 G9 GYRO

The intertial sensor irradiated in this test was returned to Autonetics for post-irradiation performance tests. Table 21 is a listing of gyro performance changes noted in post-irradiation tests before and after the gyro was refilled with non-contaminated gas lubricant. (A detail evaluation of the gyro performance parameters are listed in the Guidance and Mission Control, Volume II, of this final report.) Bias on both axis appeared to be slightly out of tolerance, however, it is an improvement over the G6B4 gyro drift rate of ten degrees per hour obtained as a result of Radiation Effects Test No. 9. Design goal for torquer scale factor stability was one part in ten thousand. At the end of the test a change of sixty-six parts in ten thousand was observed in the "A" axis and nine parts in ten thousand in the "B" axis.

Prior to obtaining these coefficients, the gyro pick-off module and case rotation motor required replacing. Due to deterioration of the pickoff transformers, the pickoff module exhibited quadrature in some orientations of the outer case with respect to the inner case and no quadrature at other positions. The gear case was stuck fast when testing was initiated at the Autonetics facility. It is not known whether case rotation failed during the fifty-fourth hour or if the gears became immovable after the reactor had scrammed. Previous experience indicates that under certain circumstances polyphenol ether becomes highly viscous in the presence of phenolic under radiation. Phenolic bearing retainers were used in the gear case and polyphenol ether was employed as a bearing and gear lubricant. Further testing was conducted to determine causes of failure in both cases. A post-test analysis of the gas bearing lubricant indicates that nitrogen with some carbon dioxide and water vapor contaminated the hydrogen lubricant.

The fast rotor coast down time of the irradiated gyro indicates contamination of the gas lubricant. The dilution of the hydrogen by air has the effect of slowing rotor speed, increasing operating temperature, and changing the viscous shear torque of the

TABLE 21 GYRO PERFORMANCE CHANGES

TEST	POST-IRRADIATION	POST-IRRADIATION REFILLED
G and G^2 Coefficients*		
C (deg/hr/g)	-0.083	+0.191
D (deg/hr/g)	-0.088	+0.013
B (deg/hr/g^2)	+0.034	-0.061
E (deg/hr/g^2)	+0.098	+0.047
Gyro Bias		
A Axis (deg/hr)	-0.009	+0.002
B Axis (deg/hr)	-0.032	-0.021
Torquer Scale Factor		
A Torquer (deg/hr/ma)	+0.65%	+0.41%
B Torquer (deg/hr/ma)	+0.94%	+0.78%
Wheel Coast Time (i/e)		
Average	-37.7%	-5.2%

*Definition of Coefficients:
C - Axial Unbalance
D - Motor Effect
B - G-Product Along Spin and Input Axes
E - G-Product Along Spin and Output Axes

gas lubricant thereby contributing to drift in non-case rotated sensors. None of the internal components showed corrosion or oxidation due to gas contamination.

4.4.2 ELECTROMAGNETIC ACCELEROMETER (EMA)

The nuclear radiation exposure versus time for this accelerometer is given in Figure 51. The post-test performance parameters listed in Table 22 indicates that the EMA accelerometer characteristics changed very little during the irradiation test. Some increase in shock sensitivity, bias drift, and bias shift due to thermal hysteresis can be noted in Instrument No. 3. Scale factor increases were 0.2 and 0.22 percent for Instrument 2 (X EMA) and Instrument 3 (Y EMA), respectively, which is an improvement over the EMA's tested under LASV-N1 program. The instruments evaluated in Radiation Effects Test No. 9 showed a decrease in scale factor of 0.3 percent. Since the scale factor is proportional to the spring mass and inversely proportional to the magnetic flux density in the magnetic circuit, the LASV-N1 accelerometer scale factor change was attributed primarily to mass loss. The EMA's exposed to the irradiation test changed primarily due to loss in magnetic field intensity of the field magnets. Vacuum baking of the forcer coils prior to installation has overcome proof mass loss in the accelerometers. A further improvement in the stability of scale factor could be made through use of different magnetic materials, less susceptible to change under radiation. One such material is Ticonal XX, another which is yet untested is Alnico IX.

Bias shift in the invar stator accelerometers was slightly larger than two mg, as compared with 200 mg in the quartz stator instruments. This small shift by comparison was attributed to corrosion between a silver shim and the stator blocks, and the thickness of the quartz flexure. Stability may be improved by use of the noncorrosive materials, a different shim material, and a thinner quartz flexure with smaller spring constant.

4.4.3 PLATFORM ELECTRONICS

The nuclear radiation exposure values for the platform electronics are given in Table 23. Testing of irradiated platform electronics circuits was not complete by publication data of this report. A more thorough analysis may be found in the subcontractor's final report. The gyro mid-amplifiers previously thought to be a possible cause of failure in the fifty-fourth hour were tested and found to be operating within tolerances. Scheduled for future testing were the platform control amplifier and the accelerometer control amplifier.

TABLE 22 POST-IRRADIATION PERFORMANCE PARAMETERS FOR THE EMA ACCELEROMETERS

	INST #2		INST #3	
TEST	PRE RAD	POST RAD	PRE RAD	POST RAD
Shock Sensitivity (μg)	<20	<10	<20	<40
Bias Temperature Sensitivity (μg/F°)@1g	+10	+10	-1.5	+2.5
Scale Factor Temperature Sensitivity (μg/F°)@1g	-40	-35	-1.3	-6.6
Thermal Hysteresis (Bias) (μg)	<10	--	<20	+50
Bias Stability at 1g				
Drift (μg)	(6 hrs) <10	--	(4 hrs) 20	--
RMS (μg)	~10	--		--
Drift (μg)	(11 hrs) 10	(13 hrs)<10	(16 hrs) <10	(12 hrs) ~40
RMS (μg)	20	~10	~10	~10
Scale Factor (ma/g)	3.6021	3.6094	3.1564	3.1633
Bias (mg)	+11.62	+11.70	+1.43	+3.87

TABLE 23

NUCLEAR RADIATION EXPOSURE VALUES FOR THE PLATFORM ELECTRONICS

Test Article	Integrated Neutrons (n/cm^2)			Gammas ergs/gm-(C)
	nE < 0.48ev	nE > 2.9Mev	nE > 0.3Mev	
Acc. Mid-Amplifier No. 1 and 2	4.2(14)	6.6(15)	2.7(16)	3.5(11)
Gyro Mid-Amplifier No. 1 and 2	3.4(14)	3.1(15)	1.3(16)	9.6(10)
Platform Control Amplifier	3.4(14)	2.2(15)	8.9(16)	3.9(10)
Acc. Control Amplifier	3.9(14)	2.5(15)	1.0(16)	8.4(10)

Numbers in parentheses indicate powers of 10, e.g. 4.2×10^{14}.

4.4.4 VOLTAGE REFERENCE TUBE CIRCUITS

The nuclear radiation exposure for these circuits versus time is shown in Figure 52. The design goal for a radiation-hardened voltage reference device is a stability within one part in ten thousand. The least measured variation attained during the test was slightly greater than nine parts in ten thousand. A graphical representation of their performance is shown in Figure 53. It is believed, however, that the actual performance of the voltage reference tube devices was somewhat better than the measured data indicates. A closer observation shows a high degree of correlation between all four circuits and the input. A question arises as to whether the output of the voltage reference tubes varied as a function of the input voltage or that both input and output were subject to the same perturbation. Figure 54 shows regulated DC voltages measurements. The individual curves are point averages of the different types of circuits. From Figure 54, curve 1 is a plot of point by point average of three magnetic core circuits; curve 2 is a point by point average of four voltage reference tube circuits; curve 3 is the average of three multivibrator circuit bias voltages. All of these types of circuits are fed by different power supplies. The high degree of correlation between these independent outputs indicates that there was a common perturbation injected either at the digital voltmeter or in the signal switching mechanism.

To obtain better information concerning random variation from this correlated perturbation, Figure 55 was constructed. This is a plot of individual voltage reference tubes circuit point by point deviation from the point by point average of all four circuits. (Note: the design goal is one part in ten thousand variation.) The maximum variation noted in this figure is about 1.25 parts in ten thousand. This type of approach is not completely valid because it removes correlation due to input variations. However, it is reasonable to claim that the voltage reference tube circuit operated within two parts per ten thousand.

4.4.5 MAGNETIC CORE VOLTAGE REFERENCE CIRCUITS

The nuclear radiation exposure for these circuits versus time is shown in Figure 52. Figure 56 indicates the behavior of the four magnetic cores under irradiation. Three of the cores were located in the irradiation test cell, and the fourth core remained in the control room as a control sample. Variation in the control sample is somewhat larger than that of the other three. This is attributed to the stray magnetic fields in the control room. Overall variation of the three cores in the test cell amounted to two parts in a thousand, far below the design goal but almost an order of magnitude better than the core samples exhibited during past irradiation tests. Most of this variation is

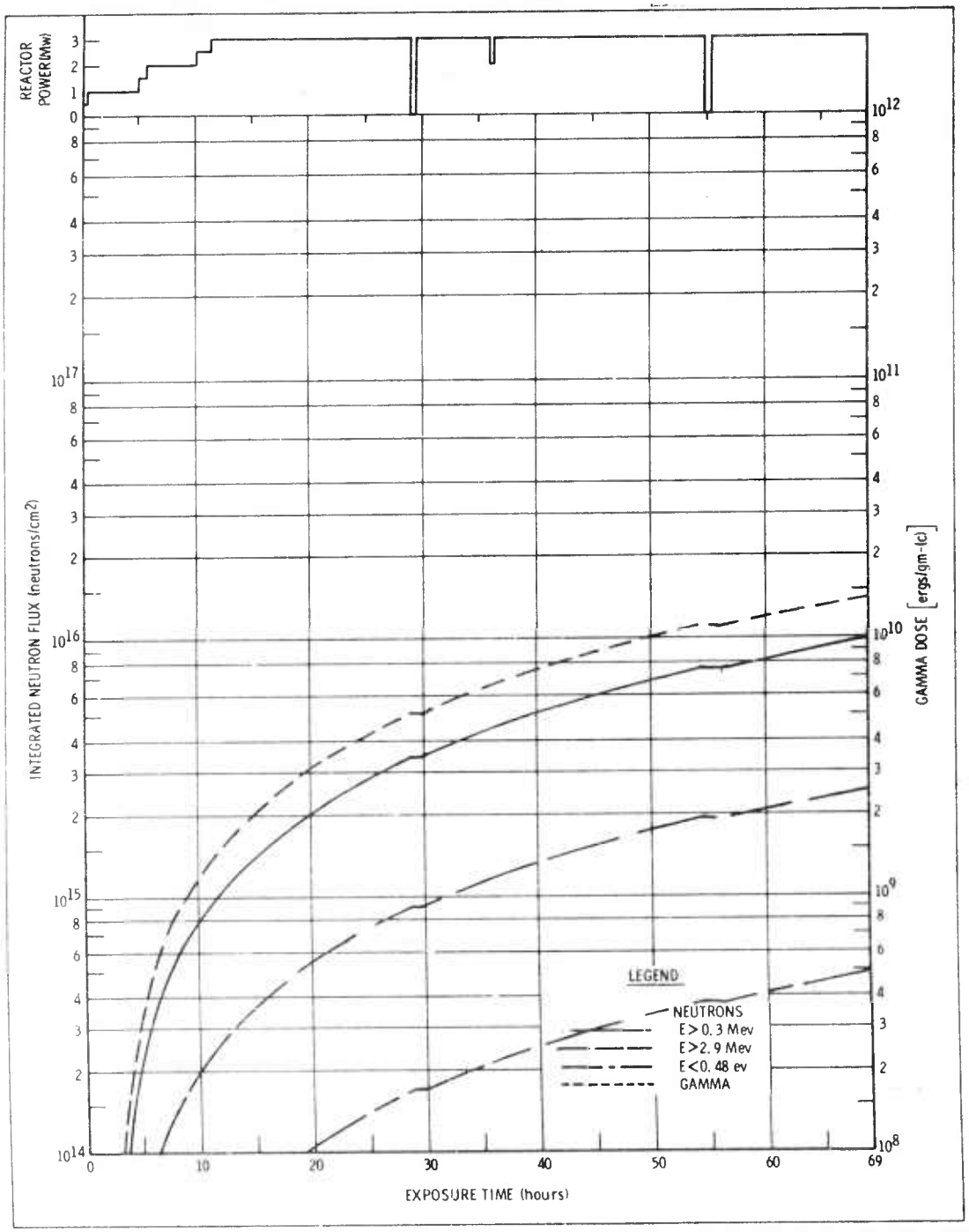

FIGURE 52 NUCLEAR RADIATION EXPOSURE FOR THE RESONATORS, VR TUBE VOLTAGE REFERENCE, AND THE MAGNETIC CORE VOLTAGE REFERENCE CIRCUITS

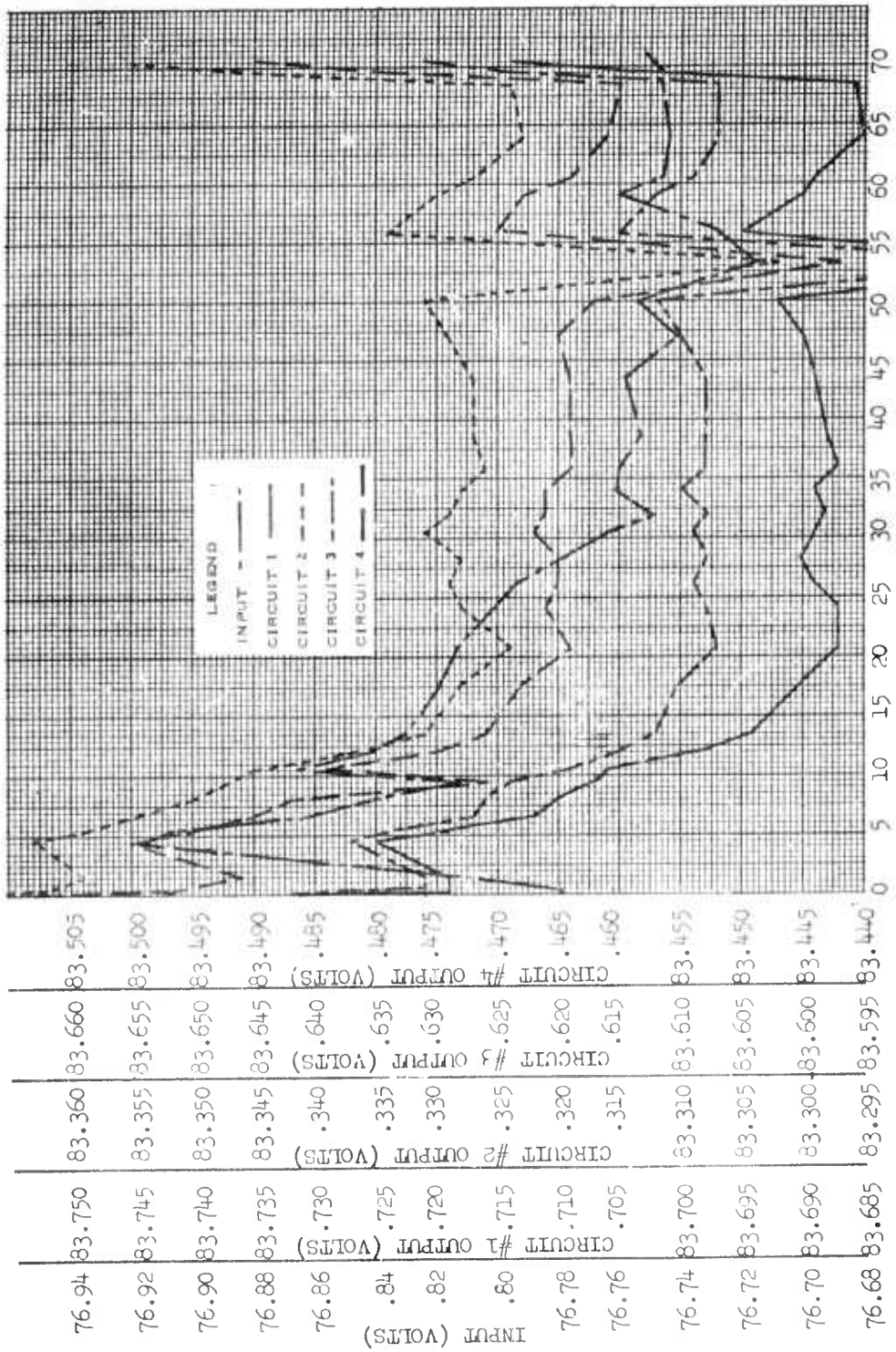

FIGURE 53 VOLTAGE REFERENCE TUBE CIRCUIT OUTPUT VERSUS REACTOR TIME

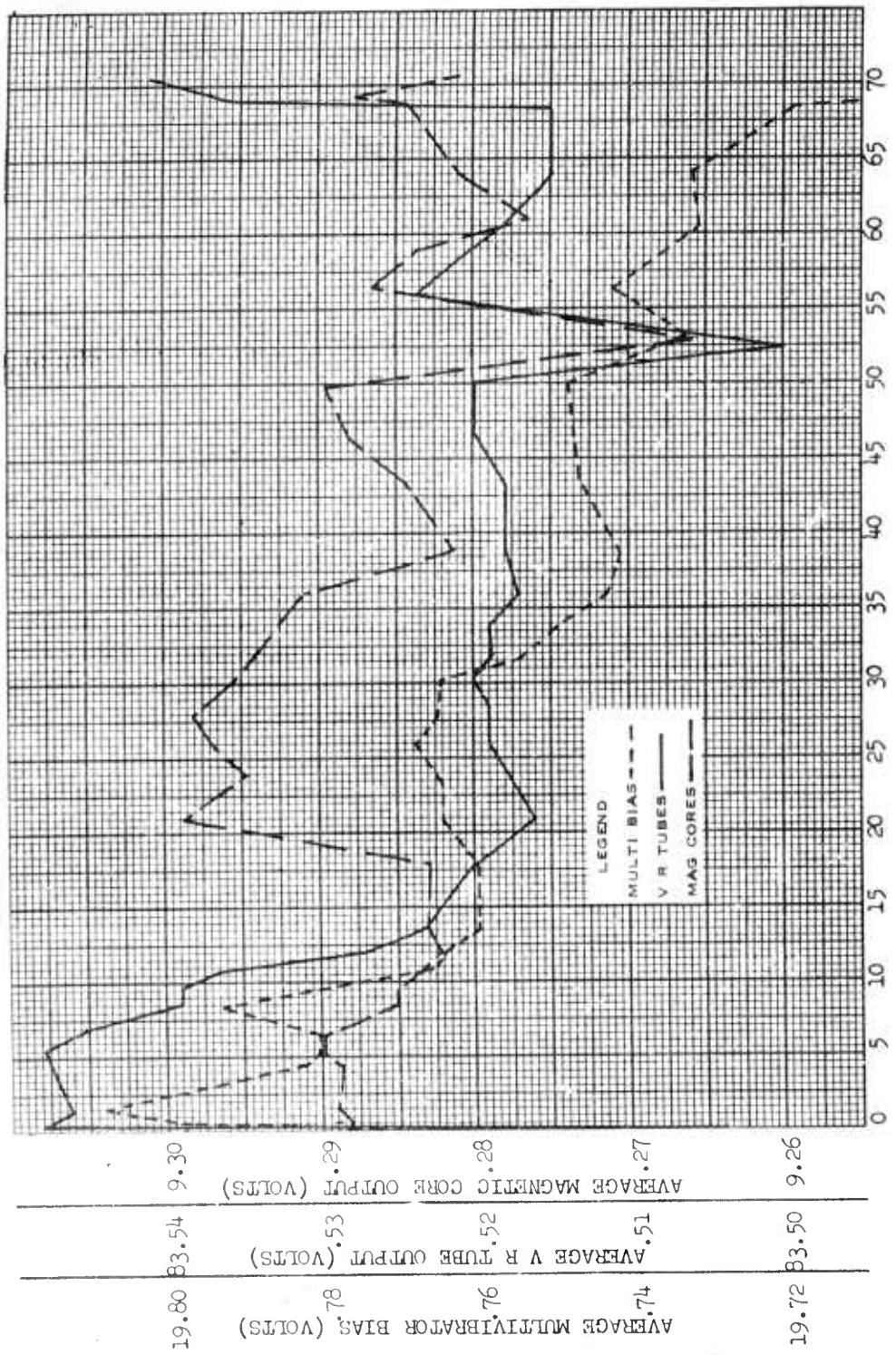

FIGURE 54 POINT BY POINT AVERAGED DC MEASUREMENTS

FIGURE 55 VR TUBE CIRCUITS DEVIATION FROM POINT BY POINT AVERAGE

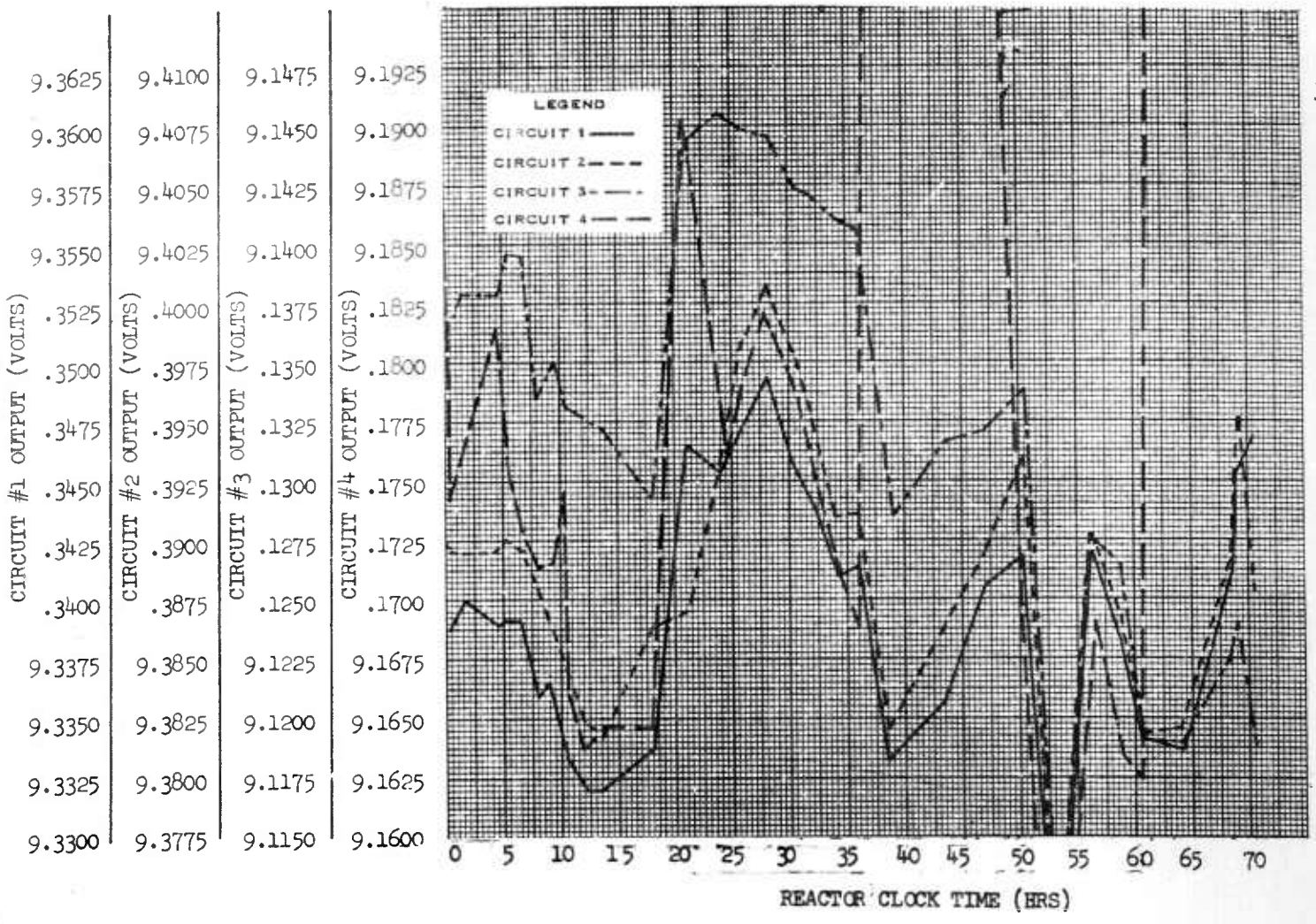

FIGURE 56 MAGNETIC CORE VOLTAGE REFERENCE OUTPUT VERSUS REACTOR TIME

attributed to stray magnetic fields in the irradiation test cell area. Although there is some degree of correlation between these DC measurements and the other DC parameters measured, the largest excursion cannot be correlated with a common variation. In future tests the magnetic cores should be enclosed in mumetal shields to retard output variations due to stray or changing magnetic fields.

4.4.6 CHOPPER STABILIZED DC AMPLIFIERS

The nuclear radiation exposure values for the chopper stabilized DC amplifiers are given in Table 24. The DC amplifiers were designed for a 60-db gain, but this value and the bias level dropped off with irradiation time until the reactor was shut down as shown in Figures 57, 58, 59, and 60. After manual scramming of the reactor, the values were restored to near their original conditions. Overall operation of the DC amplifiers was not satisfactory and a new design or new chopper should be considered.

TABLE 24

NUCLEAR RADIATION EXPOSURE VALUES FOR THE CHOPPER STABILIZED DC AMPLIFIERS

Test Article	Integrated Neutrons - n/cm^2			Gammas ergs/gm-(C)
	nE< 0.48ev	nE > 2.9Mev	nE > 0.3Mev	
No. 1	3.0 (14)	5.9 (15)	2.4 (16)	1.8 (11)
No. 2	3.8 (14)	4.0 (15)	1.7 (16)	1.0 (11)
No. 3	2.5 (14)	4.6 (15)	1.9 (16)	1.7 (11)
No. 4	2.8 (14)	3.1 (15)	1.3 (16)	1.0 (11)

Numbers in parentheses indicate powers of 10, e.g. 3.0×10^{14}.

Temperature was not considered to be a drift contributing factor in the operation of the resonator. Quartz "GT" cut crystals have a negligible temperature coefficient over a wide range of temperatures. To avoid temperature excursions the resonators were enclosed in evacuated glass tubes and placed in a temperature controlled atmosphere of $94^{o}(\pm 1)$F.

4.4.7 CAPACITOR CHECKERS

The required stability of the capacitors was 0.01%. Each multivibrator was made utilizing one of the three types of

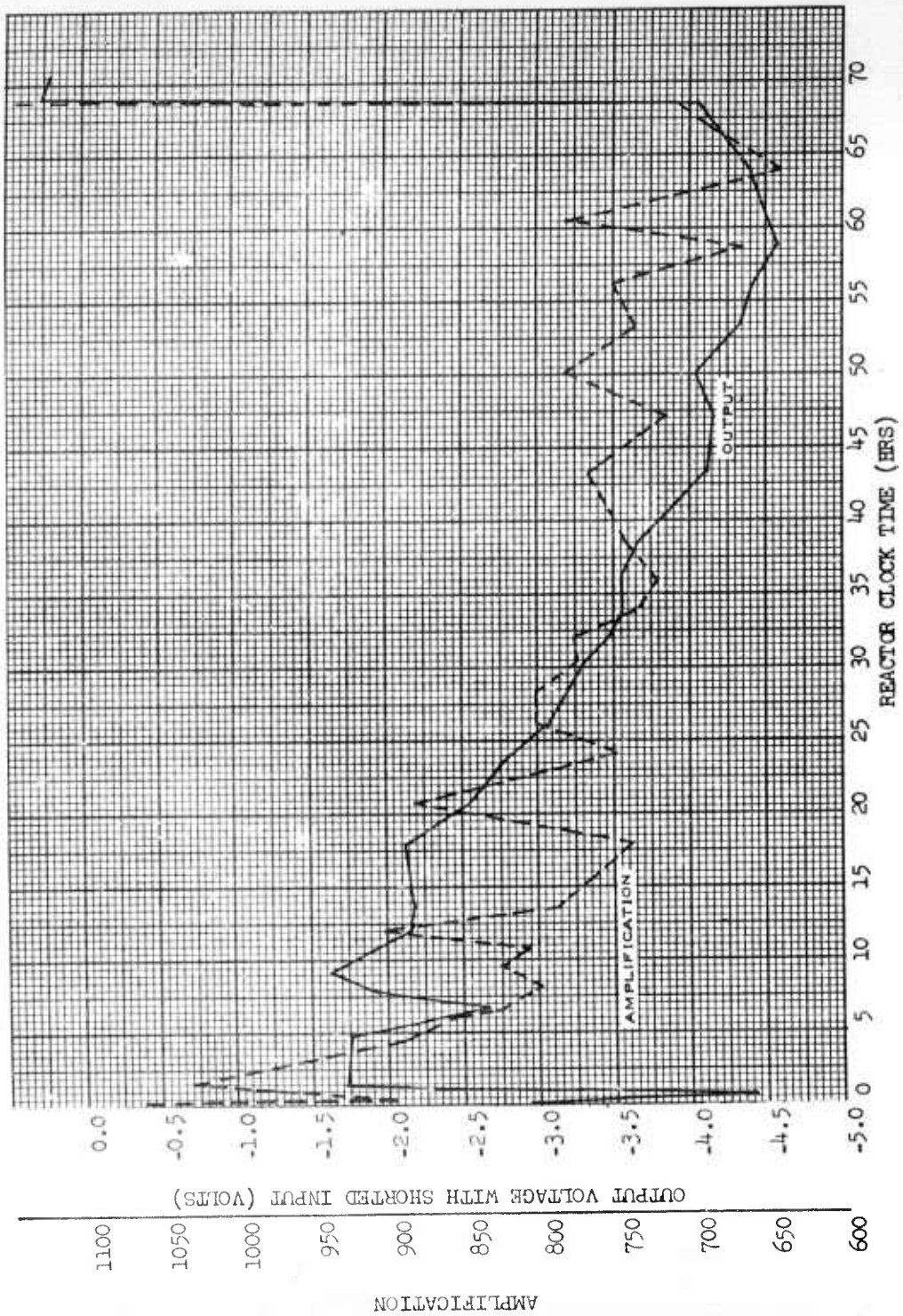

FIGURE 57 AMPLIFICATION AND OUTPUT VERSUS REACTOR TIME FOR DC AMPLIFIER NO. 1

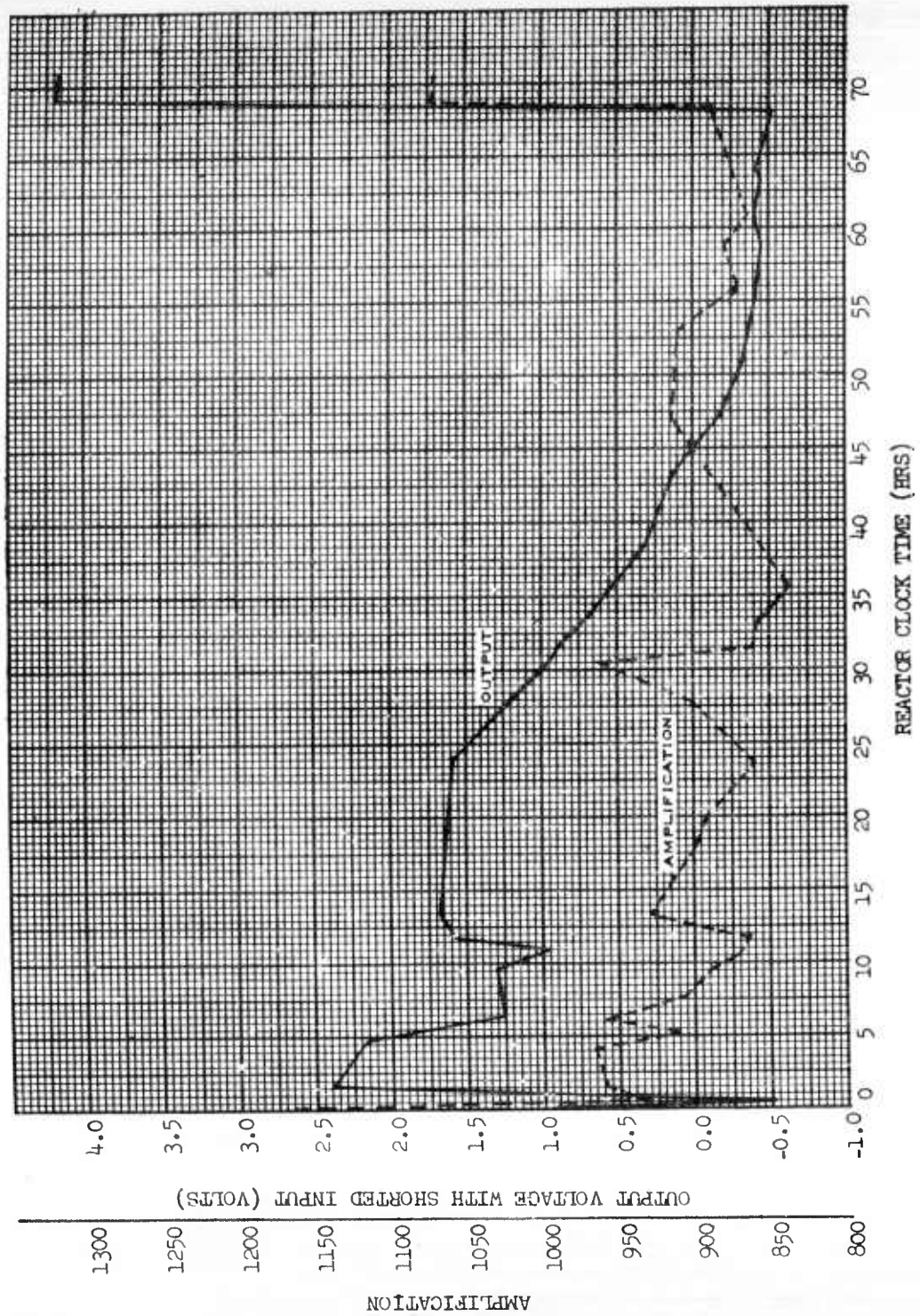

FIGURE 58 AMPLIFICATION AND OUTPUT VERSUS REACTOR TIME FOR DC AMPLIFIER NO. 2

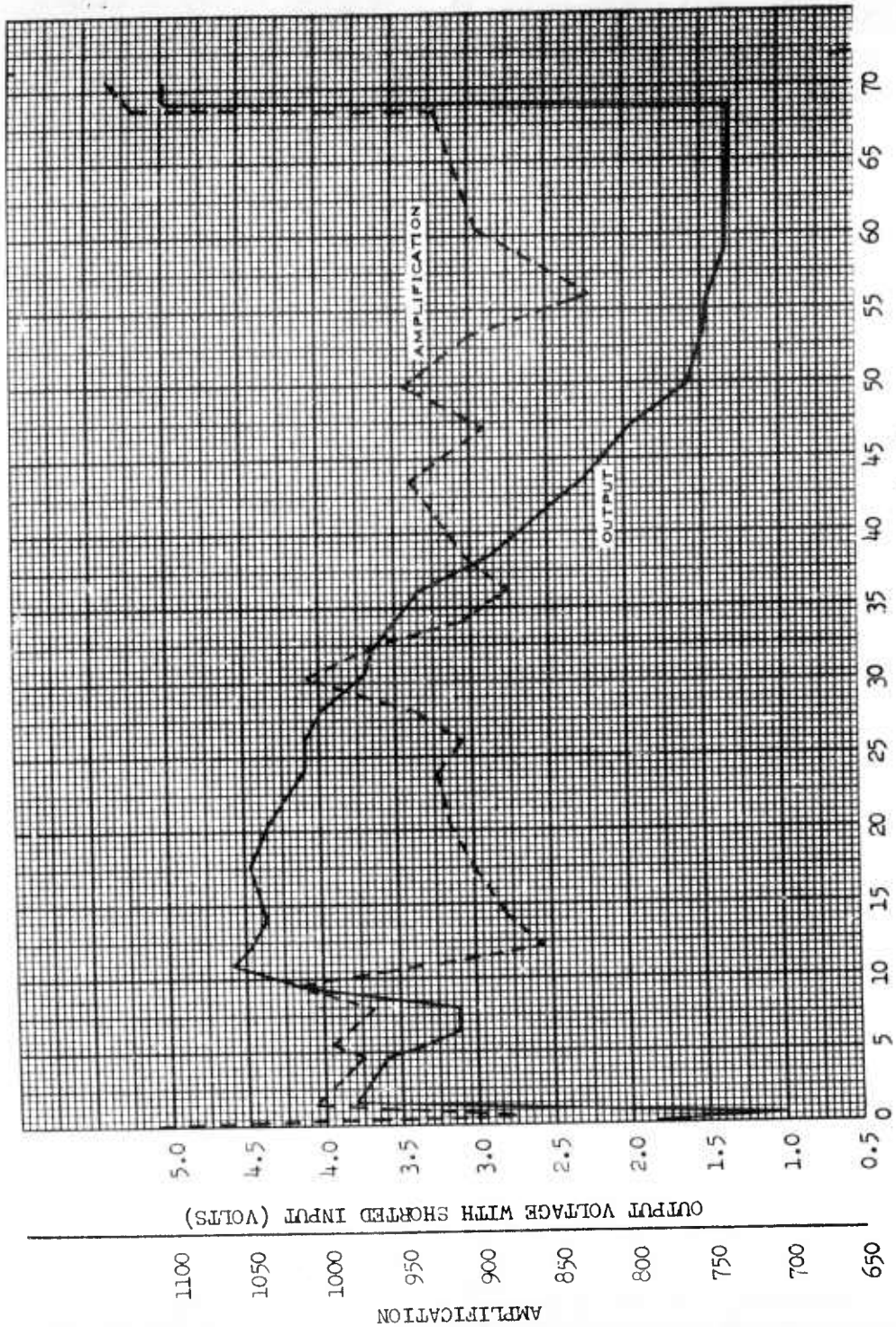

FIGURE 59 AMPLIFICATION AND OUTPUT VERSUS REACTOR TIME FOR DC AMPLIFIER NO. 3

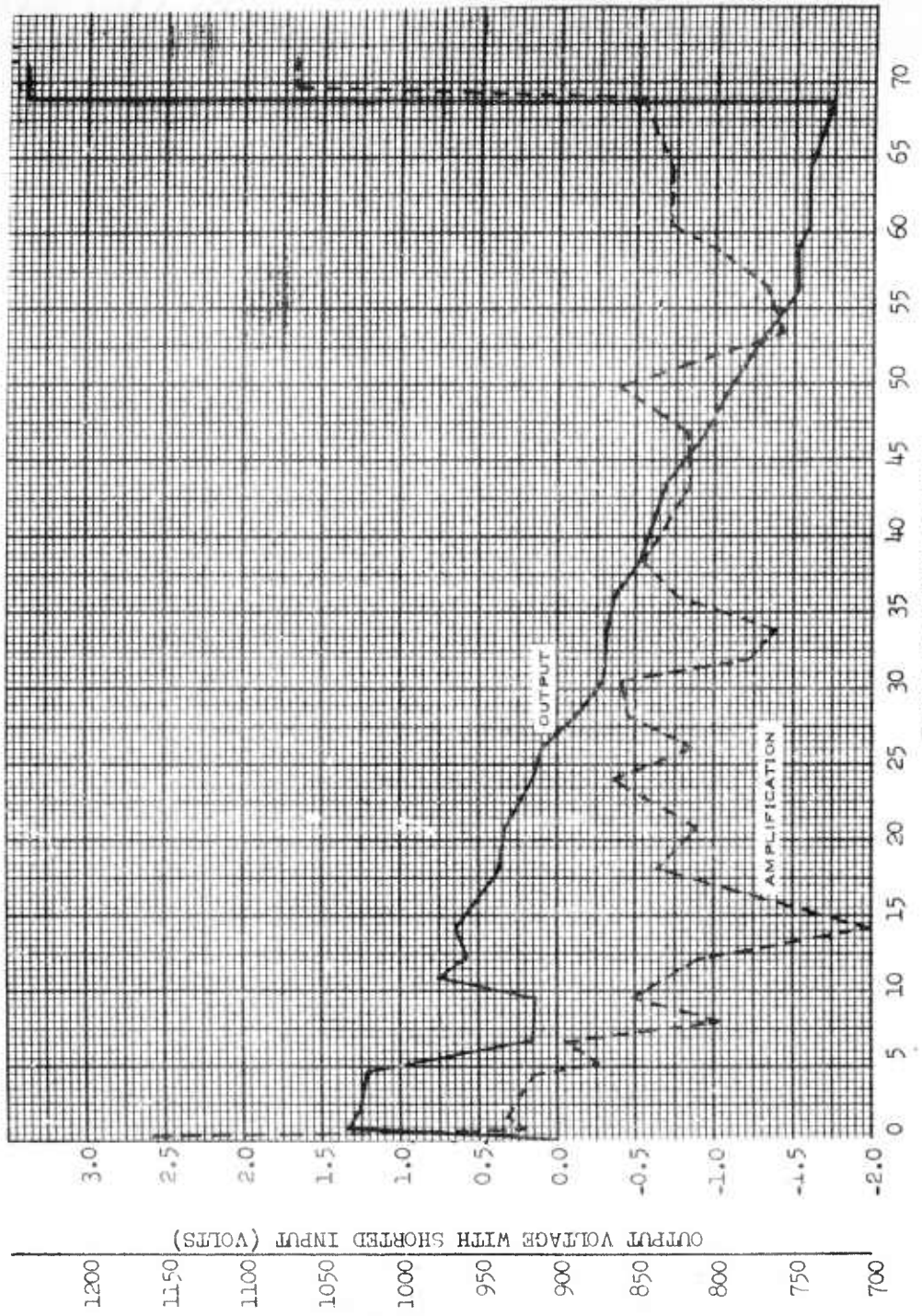

FIGURE 60 AMPLIFICATION AND OUTPUT VERSUS REACTOR TIME FOR DC AMPLIFIER NO. 4

capacitors listed below. All were 4700 picofarad ±5% values.

Type	Mfr.	Part No.	Circuit No.
Ceramic	Vitramon	VY32C472K	1
Mylar	G.E.(Lectrofilm B)	CPM472APK	2
Polystyrene	Hopkins	1P1472	3

The maximum gamma rate was 2.8×10^8 ergs/gm-(C)-hr with a total exposure of 1.6×10^{10} ergs/gm-(C). The maximum neutron flux ($E > 0.3$ Mev) was 4.8×10^{10} n/cm^2-sec., with an integrated exposure of 1.0×10^{16} n/cm^2.

Figures 61, 62 and 63 show that circuit No. 3 (polystyrene capacitors) showed a stability of approximately 0.2% and circuits No. 1 and No. 2 a lesser degree of stability. None of the capacitors are suitable to be used in an area requiring the needed stability.

4.4.8 QUARTZ RESONATORS

The nuclear radiation exposures curves versus time for the resonators are given in Figure 52. Prior to irradiation, the Litton quartz resonators were operated intermittently in an effort to obtain pre-irradiation drift data and aging characteristics. At that time the resonators exhibited poor repeatability so that no long term drift pattern could be determined. During the thirty-hour pre-irradiation test, one resonator drifted forty-four parts per million per day while the other drift was negligible. Had these resonators been installed in an inertial accelerometer, the instrument would show a null drift of 44×10^{-4}g/day.

No failure of the resonators were experienced during this irradiation test, however, some parasitic oscillations were noted on the waveform of the previously drifting resonator. Drift rates increased substantially under irradiation testing to the extent that the resonator which exhibited no net drift before then showed a twenty-two part per million per day drift while the other increased from 44 to 117 ppm/day as shown in Figure 64.

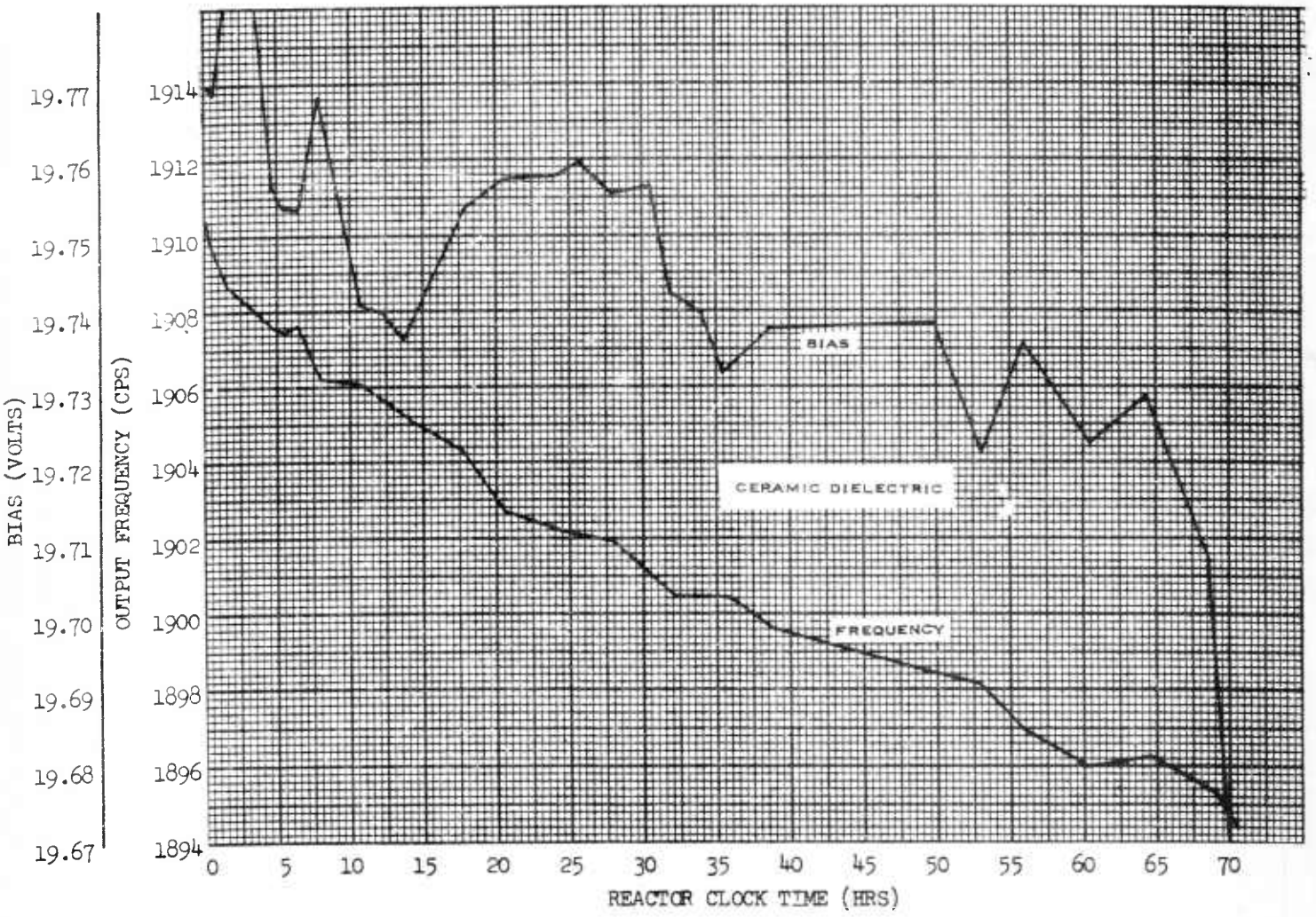

FIGURE 61 FREQUENCY AND BIAS VERSUS REACTOR TIME FOR MULTIVIBRATOR CIRCUIT NO. 1

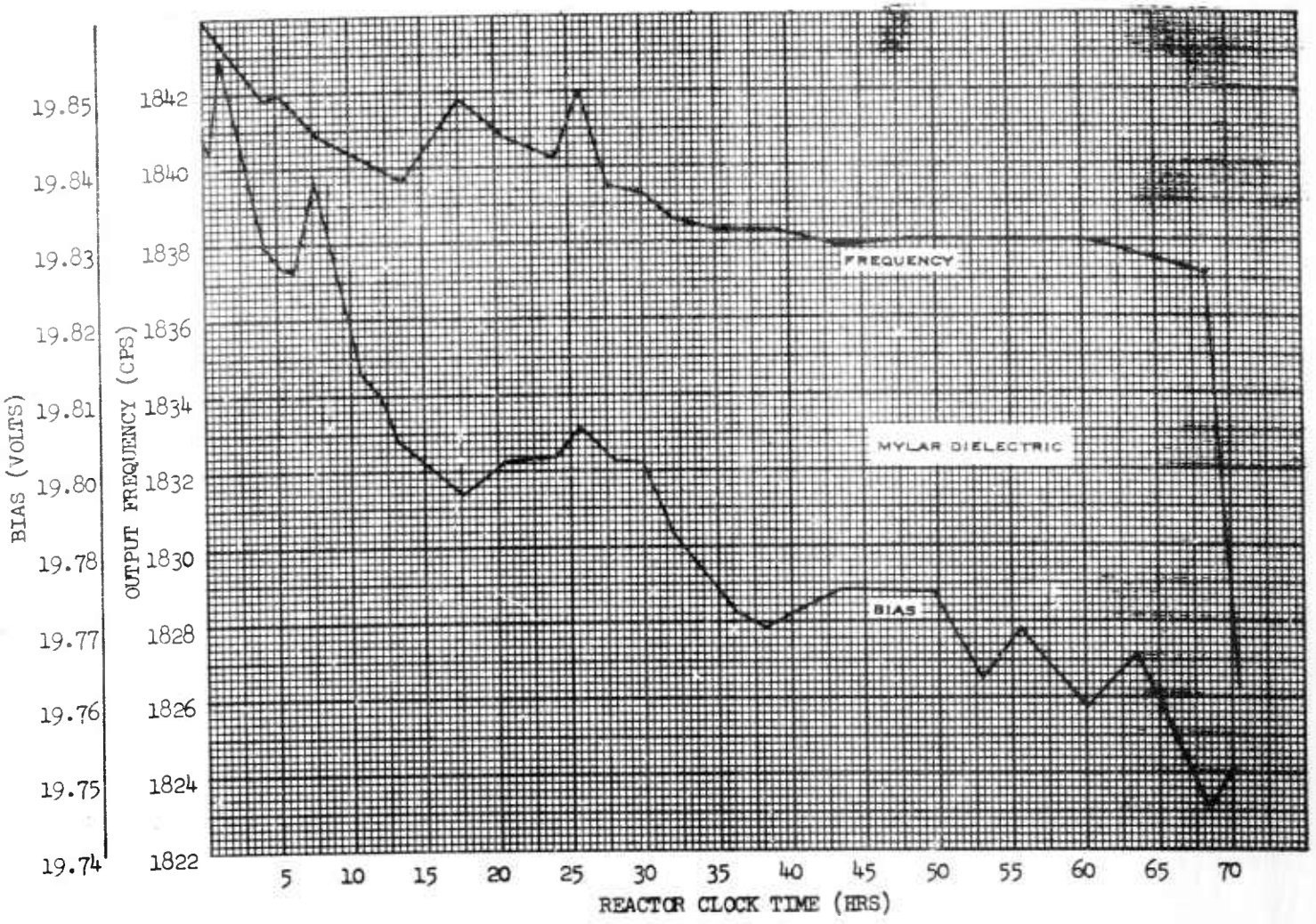

FIGURE 62 FREQUENCY AND BIAS VERSUS REACTOR TIME FOR MULTIVIBRATOR CIRCUIT NO. 2

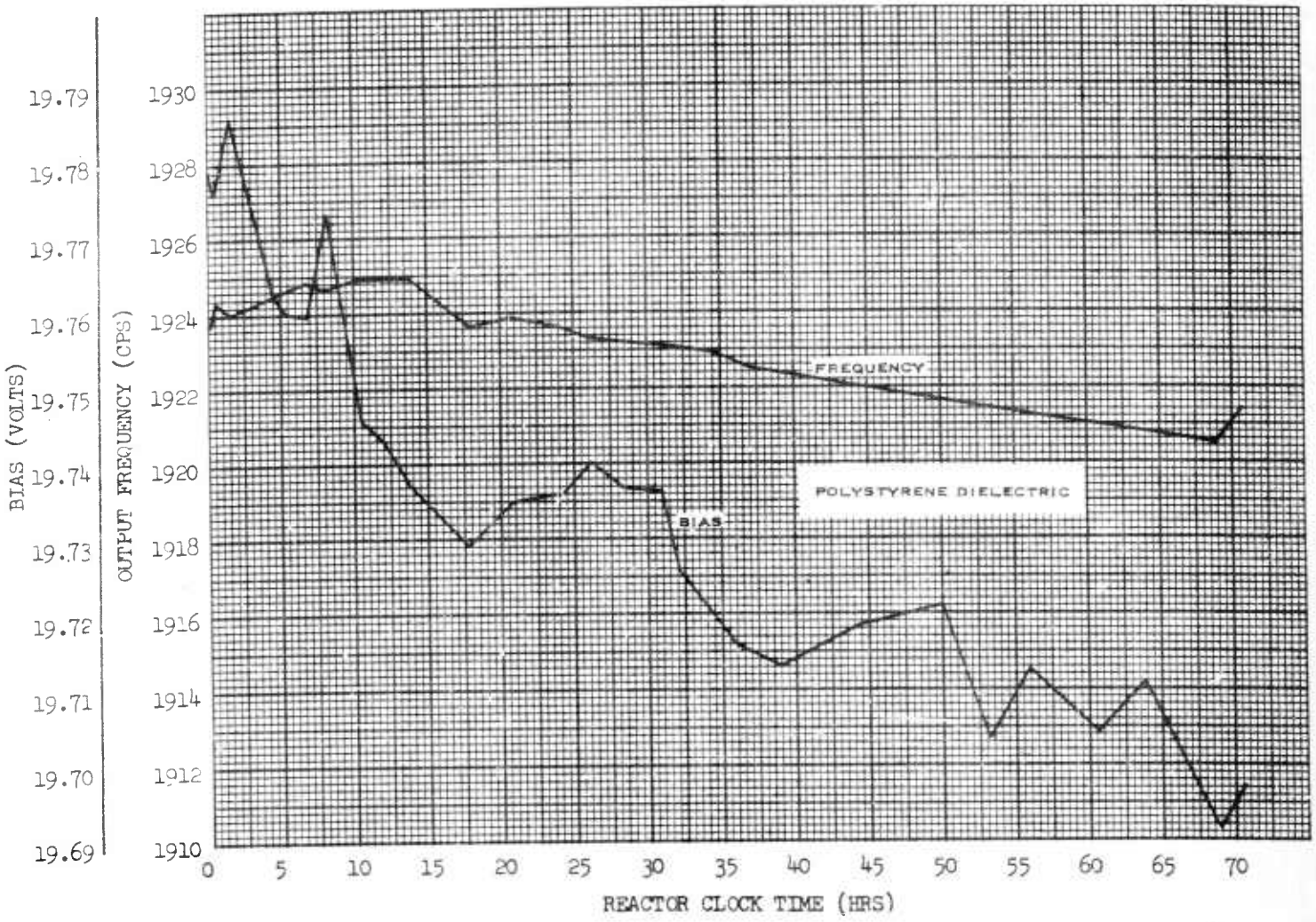

FIGURE 63 FREQUENCY AND BIAS VERSUS REACTOR TIME FOR MULTIVIBRATOR CIRCUIT NO. 3

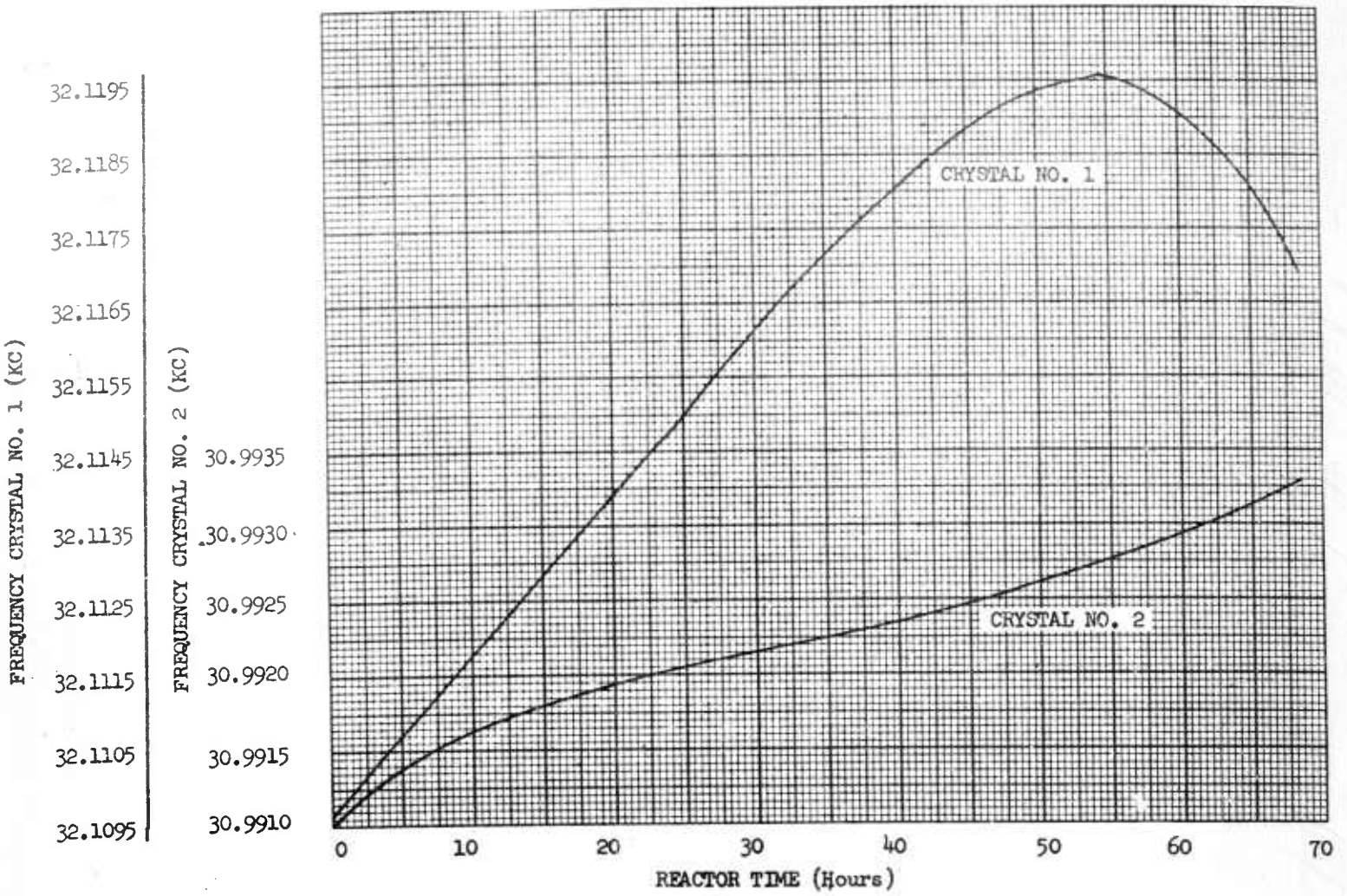

FIGURE 64 FREQUENCY OF QUARTZ RESONATORS VERSUS REACTOR TIME

5.0 CONTROL SYSTEMS

5.1 TEST ARTICLE DESCRIPTION

The flight control test articles consisted of two Humphrey model RG47-0101-1 rate gyros, one Humphrey model IG03-0101-1 rate integrating gyro, and two electromechanical filters from a pitch-control breadboard designed and fabricated by LTV. The rate gyros were selected for testing because of their suitability for attitude stabilization throughout the design flight. The rate integrating gyro was considered the most suitable type for pitch-attitude control during boost. The filters, shown in Figure 65, were closed loop position servos designed for forward-loop compensation in the pitch control channel of the missile autopilot. Figure 66 is the circuit diagram for the electronic amplifiers used in the electromechanical filters.

5.2 NUCLEAR ANALYSIS

Nuclear hardening specifications established by LTV resulted in the gyros being fabricated from the most radiation resistant materials available. Similarly, materials going into the pitch axis breadboard were reviewed and selected according to their radiation resistance potential. Tables 25 and 26 list the radiation susceptible materials and their limiting nuclear exposures that went into the gyros and pitch breadboard.

5.3 TEST SETUP AND PROCEDURE

5.3.1 GYROS

For the irradiation test the gyros were mounted on a remotely controlled two-axis, radiation hardened, flight-motion-simulation table as shown in Figure 67. The table displacement range about each of the two-axis was +10 degrees. Measurement capabilities for both types of gyros included output null and sensitivity, frequency response, and threshold. The gyros were cooled by a controlled flow of gaseous nitrogen through the area in which the gyros were mounted.

During the irradiation test, measurements and data were recorded for both static and dynamic conditions. The rate integrating gyro was subjected also to a closed loop test as illustrated in the block diagram of Figure 68.

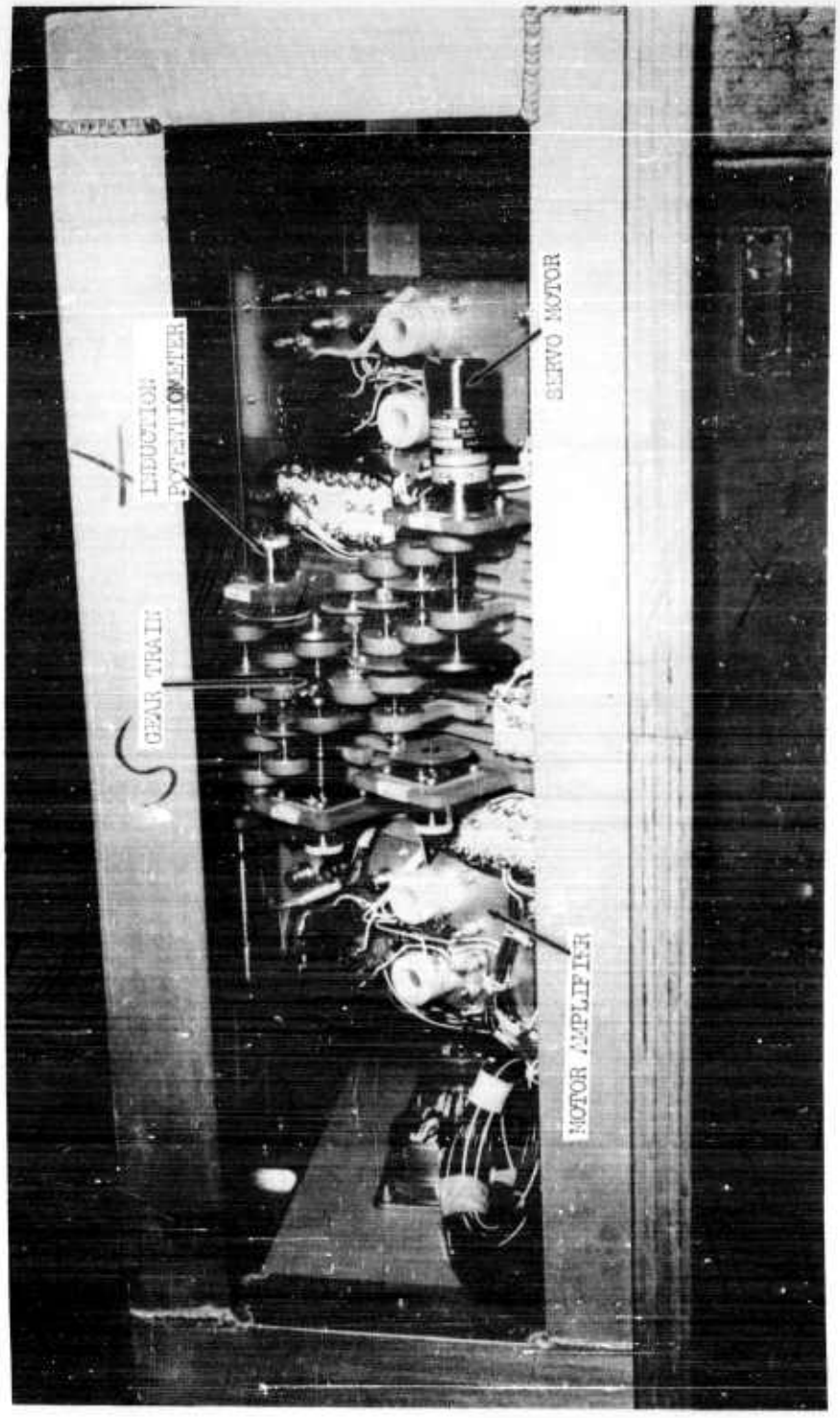

FIGURE 65 ELECTROMECHANICAL FILTER

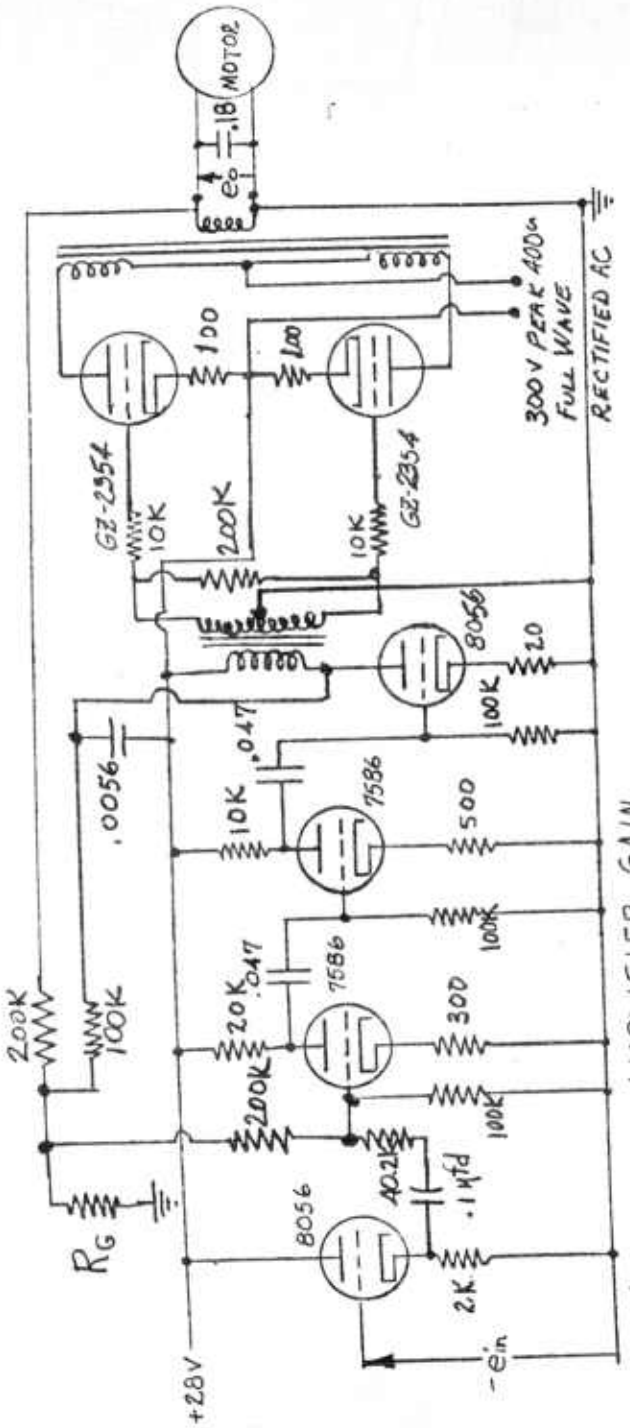

FIGURE 66 SCHEMATIC DIAGRAM OF AMPLIFIER CIRCUIT FOR THE ELECTROMECHANICAL FILTERS

TABLE 25

NUCLEAR RADIATION EFFECTS ANALYSIS OF THE RATE AND RATE-INTEGRATING GYROS

NUCLEAR DESIGN REQUIREMENT: GAMMAS: 9(9) ERGS/GM-(C)
NEUTRONS: 5(15) N_F/CM^2

MANUFACTURER: HUMPHREY, INC. MODEL: 1G03-0101-1 AND RG47-0101-1

CODE NO.	GENERAL DESCRIPTION OF CIRCUIT, PART OR ELEMENT	VALUE	ORIGINAL ELEMENT			LIMITING NUCLEAR EXPOSURE		REMARKS
			PART OR DRAWING NUMBER	MFR	ELEMENT MATERIAL DESCRIPTION	ERGS/GM (C)	N_F/CM^2	
	Magnet Wire			Anaconda	Formvar	3(10)		
	Hookup Wire			Raychem	Irradiated polyolefin	5(10)		
	Damper Piston				Carbon			
	Pivot Bearings			Turtle	Synthetic ruby,		1(18)	
				Mount Ord. Plant	Synthetic sapphire		1(18)	
	Insulation, Winding and Laminations			Emerson & Cummings	Stycast Epoxy	1.5(10)		
	Lamination Cement			Shell Chem.	Epoxy Cement	1.5(10)		
	Coil Spool				Melomine Impreg. Fiberglass	2(11)		
	Insulation Tape			Scotch	Fiberglass	2(11)		
	Solder Joint Insl			Raychem	Irrad. Polyolefin	5(10)		
	Damper Seal Insl			G.E.	Glyntal, Black	1(10)		
	Insl Motor				Diall Phthalate	2(10)		
	Screw Thread Locking			American Sealants, Inc	Polyester Resin	1(11)		
	Encapsulation, Spin Motor		#77	Corvel	Epoxy Resin	2(10)		
	Connector Pin Insl		#9010	Corning	Glass	1(12)		
	Bearing Lubrication		#796	Bray	----	1(10)		
	Bearing Lubrication			Monsanto	Polyphenyl ether	1(10)		
	Impregnation, Winding			Hi-Temp Epoxy	Varnish	5(9)		
	Impregnation, Winding				Mylar	2(10)		

NOTES: (X) INDICATES POWERS OF TEN

TABLE 26

SHEET 1 OF 2

NUCLEAR RADIATION EFFECTS ANALYSIS OF THE PITCH AXIS BREADBOARD

NUCLEAR DESIGN REQUIREMENT: GAMMAS:9(9) ERGS/GM—(C)
NEUTRONS:5(15) N_F/CM^2

MANUFACTURER: LING—TEMCO—VOUGHT, INC.

CODE NO.	GENERAL DESCRIPTION OF CIRCUIT, PART OR ELEMENT	VALUE	ORIGINAL ELEMENT					REMARKS
			PART OR DRAWING NUMBER	MFR	ELEMENT MATERIAL DESCRIPTION	LIMITING NUCLEAR EXPOSURE		
						ERGS/GM (C)	N_F/CM^2	
	Transformer:							
	Winding Wire				Formvar	3(10)		
	Coil Form				Fiberglass	2(11)		
	Coil Impregnation				Epon 815	1(10)		
	Tape				Fiberglass	2(11)		
	Tape				Mylar	1(11)		
	Induction Potentiometer,			Daystrom				
	Synchro Transmitter, and							
	Synchro Transformer:							
	Magnet Wire				ML Polymer	1(11)		
	Encapsulation		997	DowCorning	Silicone Varnish			
	Lamination Bond		Epon 815	Shell	Epoxy Resin	2(10)		
	Slot Insulation				Mylar			
	Lubrication Oil		No. 358	Cal Research	------	1(10)		
	Lubrication Grease		No. 159	"	------	1(10)		
	Electronic Components:							
	Lead Insulation				Mylar	1(11)		
	" "			Raychem	Irradiated Polyethylene	5(10)		
	Triodes		Z-2358	G. E.	Ceramic		1(16)	
	Nuvistors		7586	RCA	Ceramic		1(16)	
	Nuvistors		8056	RCA	Ceramic		1(16)	
	Nuvistors		7895	RCA	Ceramic		1(16)	
	Nuvistor Sockets		5NS-1		Bakelite		1(16)	
	Capacitors			G. E.	Mylar	2(10)		

NOTES: (X) INDICATES POWERS OF TEN

TABLE 26

NUCLEAR RADIATION EFFECTS ANALYSIS OF THE PITCH AXIS BREADBOARD

NUCLEAR DESIGN REQUIREMENT: GAMMAS 9(9) ERGS/GM-(C)

NEUTRONS 5(15) N_F/CM^2

MANUFACTURER: LING-TEMCO-VOUGHT, INC.

CODE NO.	GENERAL DESCRIPTION OF CIRCUIT, PART OR ELEMENT	VALUE	ORIGINAL ELEMENT					REMARKS
			PART OR DRAWING NUMBER	MFR	ELEMENT MATERIAL DESCRIPTION	LIMITING NUCLEAR EXPOSURE		
						ERGS/GM (C)	N_F/CM^2	
	Resistors			Corning	Metal Oxide	1(10)		
	Terminal Lugs				on Pyrex			
					Ceramic on		1(18)	
	Terminal Board				Aluminum			
					Fiberglass	1(12)		

NOTES: (X) INDICATES POWERS OF TEN

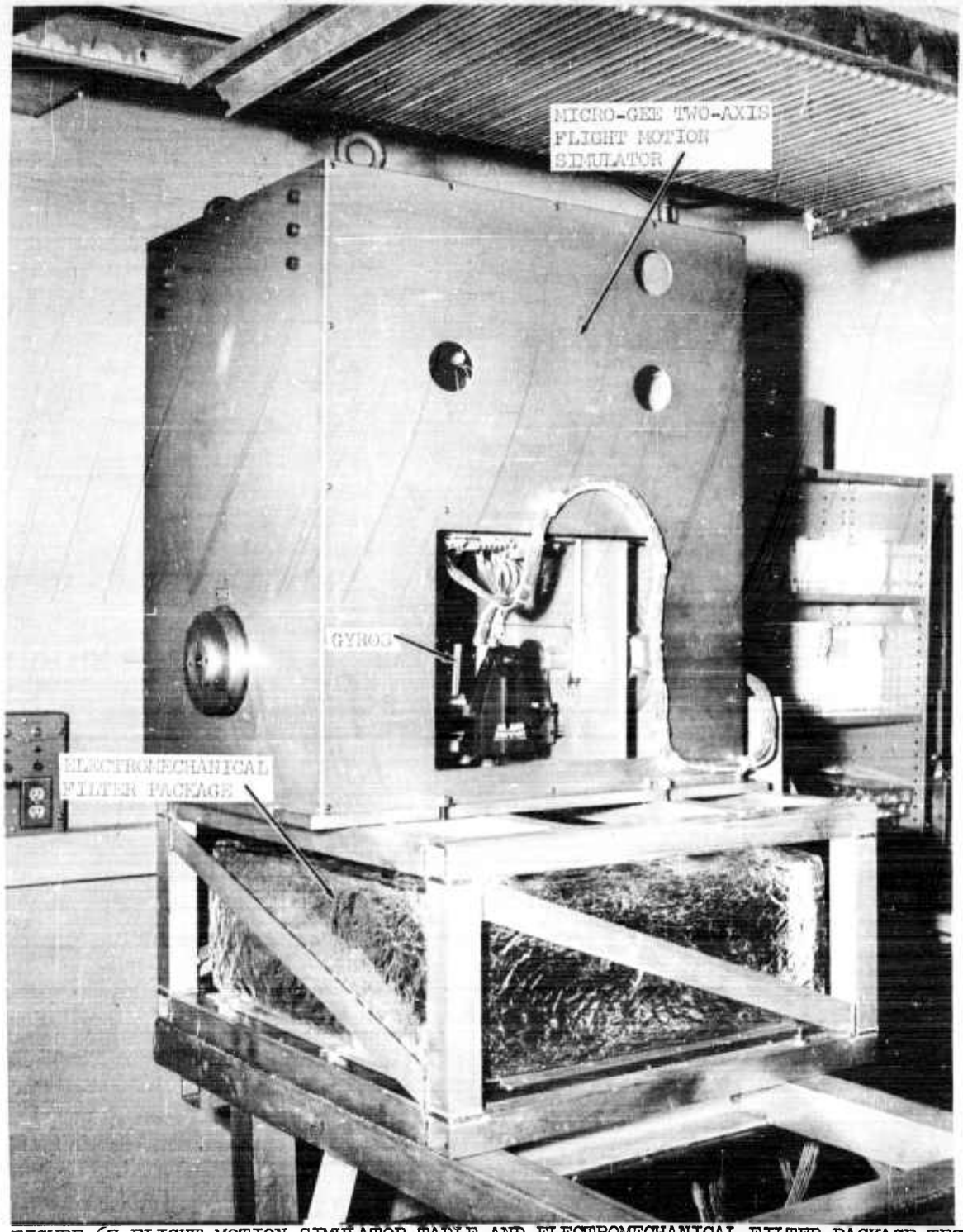

FIGURE 67 FLIGHT MOTION SIMULATOR TABLE AND ELECTROMECHANICAL FILTER PACKAGE TEST SETUP

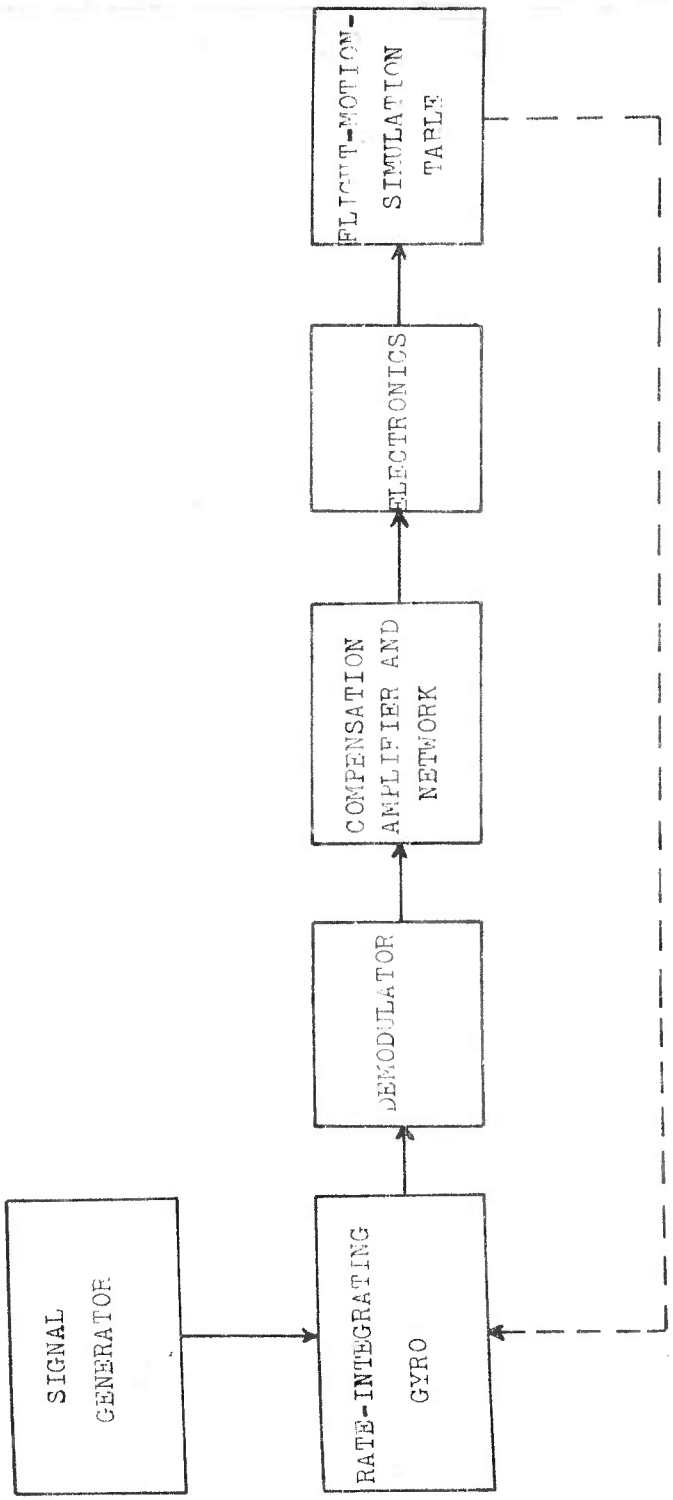

FIGURE 68 BLOCK DIAGRAM OF CLOSED-LOOP TEST ON RATE-INTEGRATING GYRO

5.3.2 ELECTROMECHANICAL FILTERS

The electromechanical filter package was mounted in a temperature controlled box below the two-axis rate table as is shown in Figure 67. The filters were instrumented to allow monitoring of the frequency response, threshold response, transient response, amplifier gains, and cathode voltages during the irradiation test.

5.4 TEST ENVIRONMENT

5.4.1 TEMPERATURES

The gyro temperatures were maintained around 170°F throughout the test by varying the flow of gaseous nitrogen. The electromechanical filter temperatures were held to around 140°F through control of the irradiation facility air circulation system.

5.4.2 NUCLEAR RADIATION

The gyros sustained average nuclear exposures of 3.6×10^{16} n/cm^2 and 1.9×10^{11} ergs/gm-(C) gamma during the irradiation. Figure 69 gives the time integrated buildup of radiation dose for the gyros.

The electromechanical filters sustained nuclear exposures of 2.4×10^{16} n/cm^2 and 6.9×10^{10} ergs/gm-(C) gamma. Figure 70 shows the time integrated nuclear exposure curve for the filters.

5.5 TEST RESULTS AND CONCLUSIONS

5.5.1 GYROS

The voltage gradient of the rate-integrating gyro dropped about 12 percent during the test period. The self-test torquer of one of the rate gyros ceased operating early in the test, a failure unlikely to have resulted from irradiation. The other rate gyro became inoperable briefly toward the end of the test. Figure 71 shows the variation in rate gyro output null voltage during the test. Inasmuch as the test duration exceeded the design life of the gyros, only the erratic and excessive output null voltage increase occurring during the design life is of significance when considering radiation damage. Frequency responses taken during and after irradiation showed little change in the gyro dynamics. Figure 72 shows a sample recording of the closed-loop operation of the rate-integrating gyro, demonstrating its

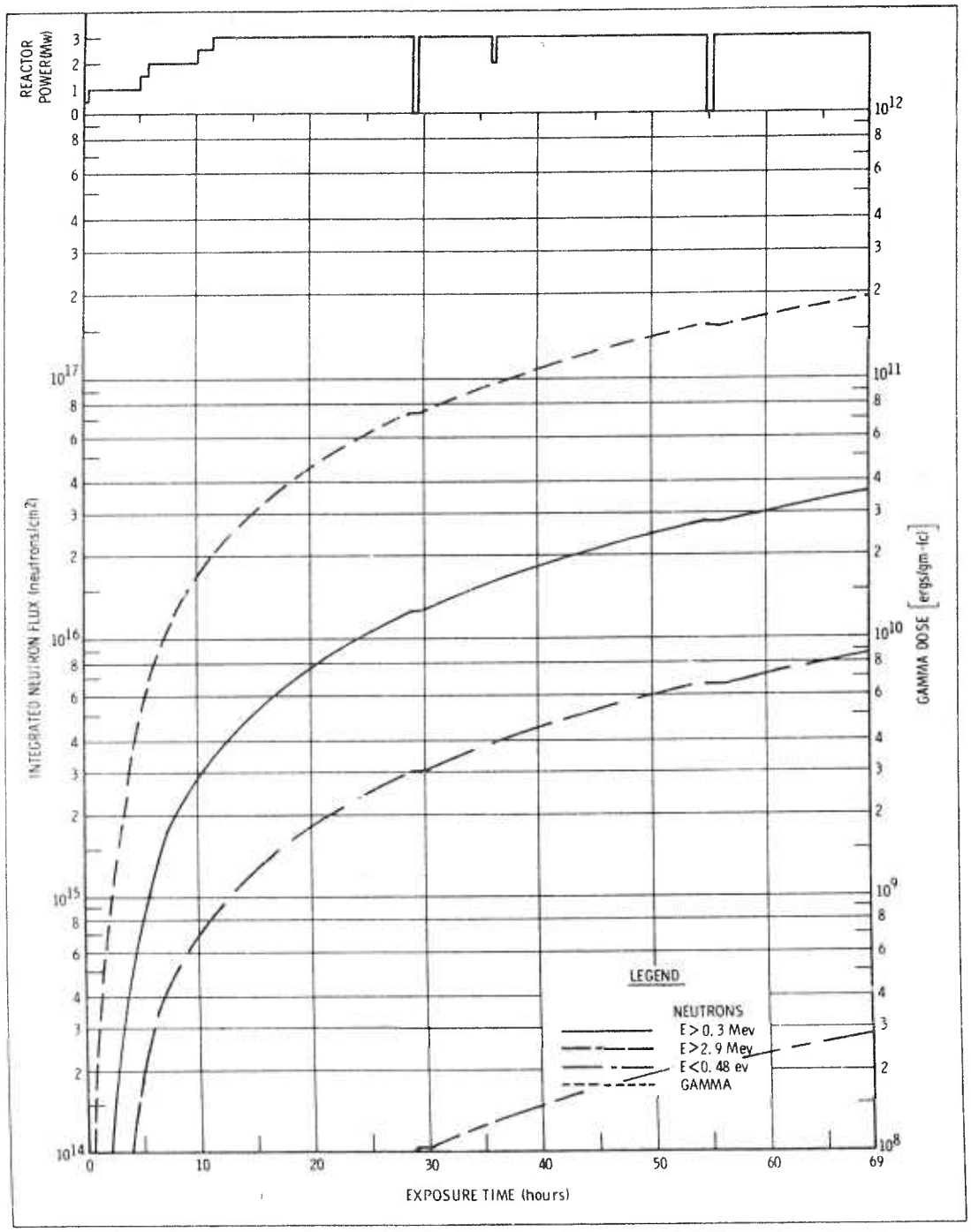

FIGURE 69 NUCLEAR RADIATION EXPOSURE OF THE HUMPHREY RATE GYROS

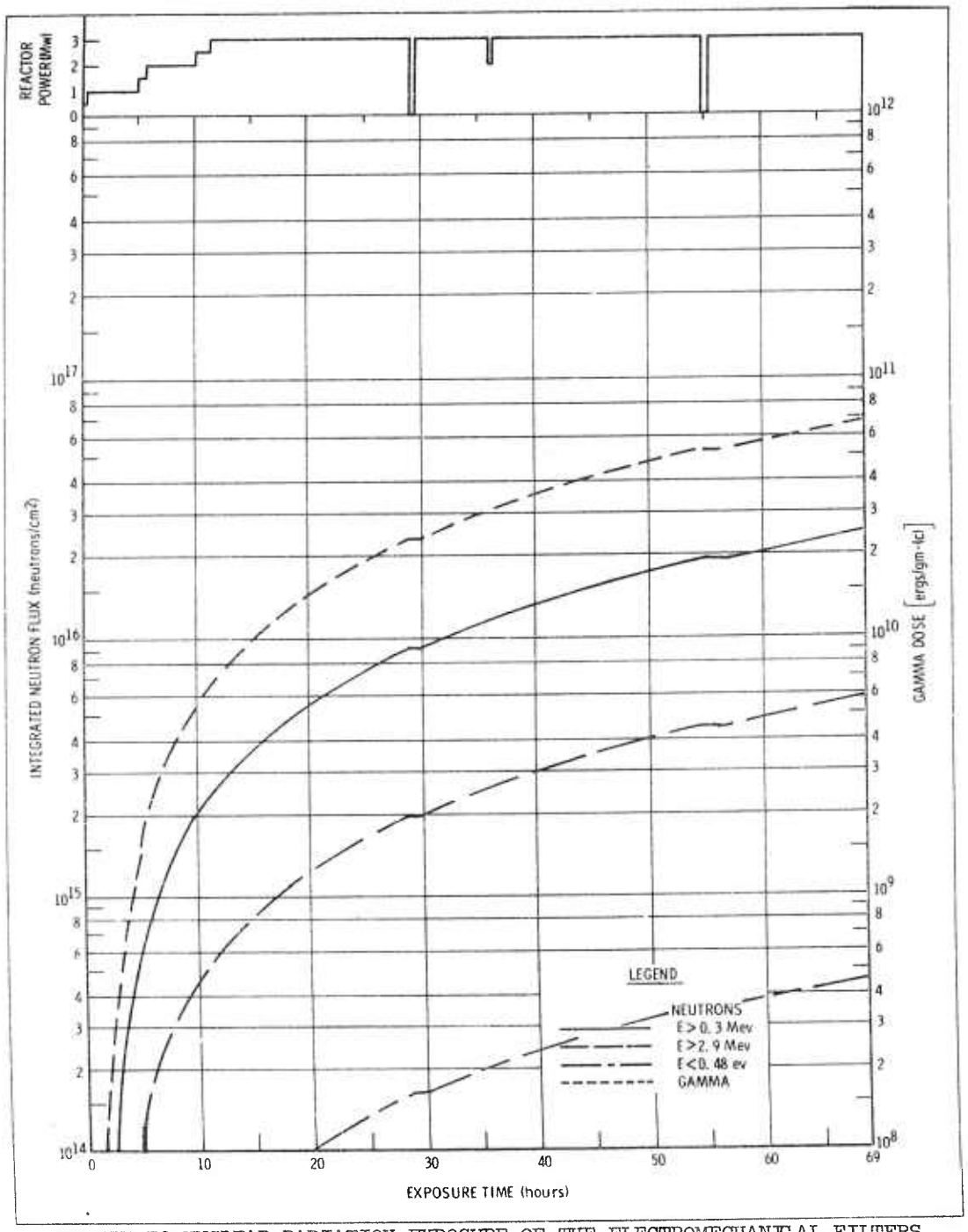

FIGURE 70 NUCLEAR RADIATION EXPOSURE OF THE ELECTROMECHANICAL FILTERS

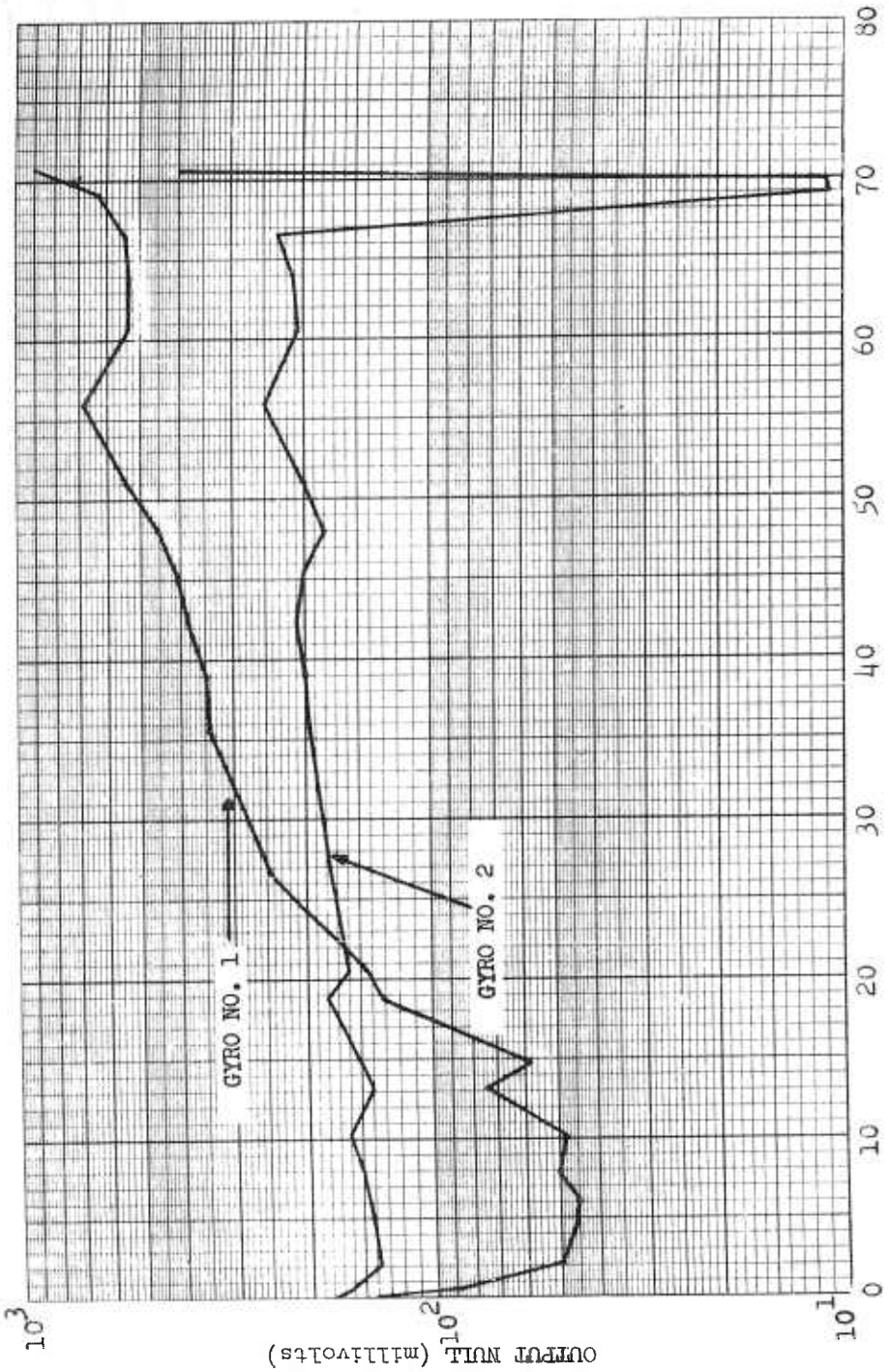

FIGURE 71 VARIATION IN RATE GYRO OUTPUT NULL VOLTAGE

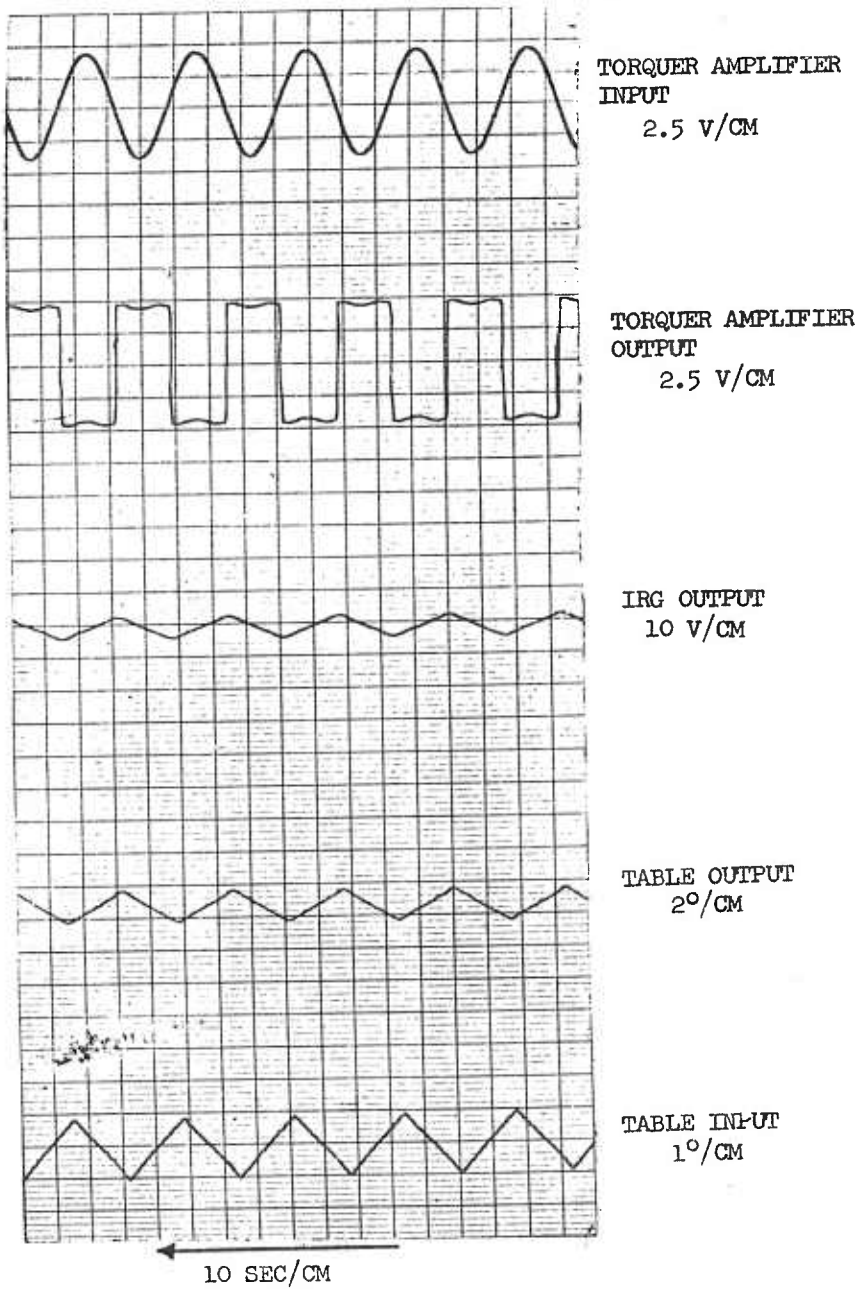

FIGURE 72 TYPICAL DATA SAMPLE OF RATE-INTEGRATING GYRO CLOSED-LOOP OPERATION

ability to integrate the sum of electrical and mechanical input signals. It is concluded that the rate-integrating gyro can be considered capable of withstanding the design nuclear environment of 5×10^{15} n/cm^2 and 9×10^9 ergs/gm-(C). In view of the unsatisfactory output nulls of one of the rate gyros, however, further developmental work on the rate gyro is considered necessary for achievement of a consistently reliable design.

5.5.2 ELECTROMECHANICAL FILTERS

Frequency response data taken before and after irradiation indicated inconsequential changes in the filter characteristics, as shown in Figures 73 and 74. The low-level threshold of the breadboard did not change detectably during the test, indicating that friction levels in the mechanical parts had not changed significantly.

A 10 percent loss in amplifier gain was attributed to a filament overvoltage and not to radiation damage. No other significant performance changes were detected. It is concluded that the filter components are capable of meeting functional requirements after withstanding the design nuclear environment of 5×10^{15} n/cm^2 and 9×10^9 ergs/gm-(C).

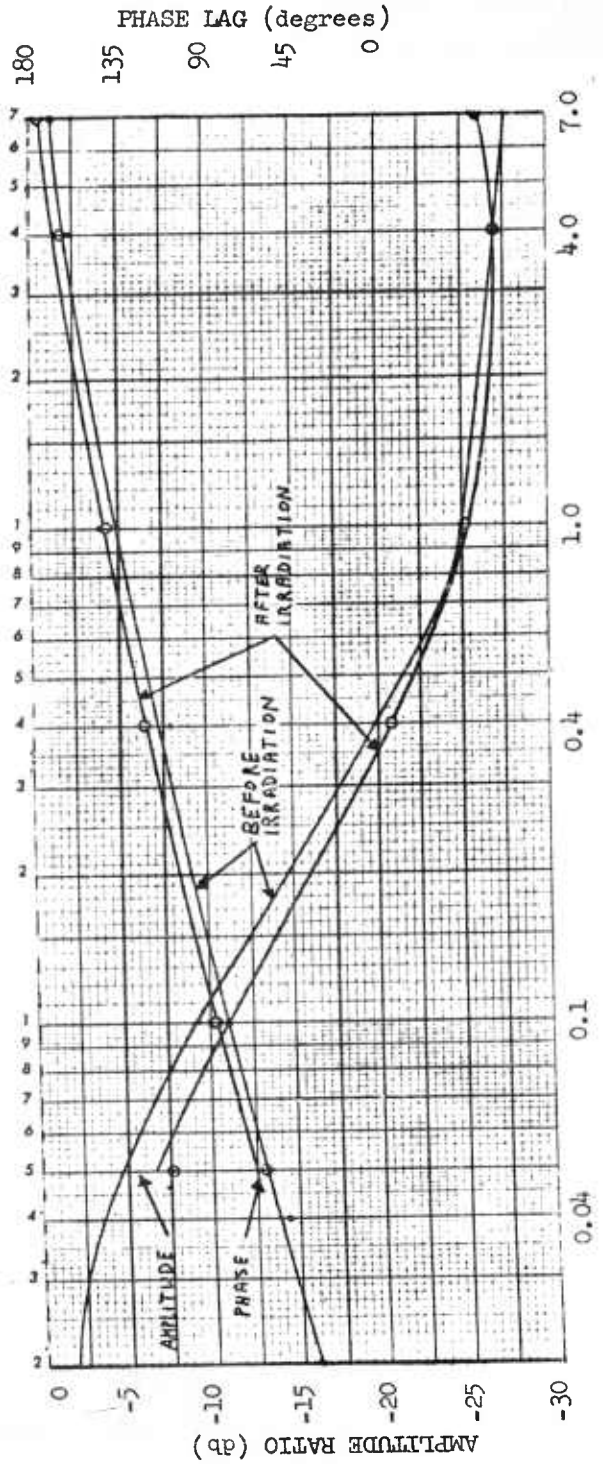

FIGURE 73 FREQUENCY RESPONSE OF ELECTROMECHANICAL FILTER NO. 1

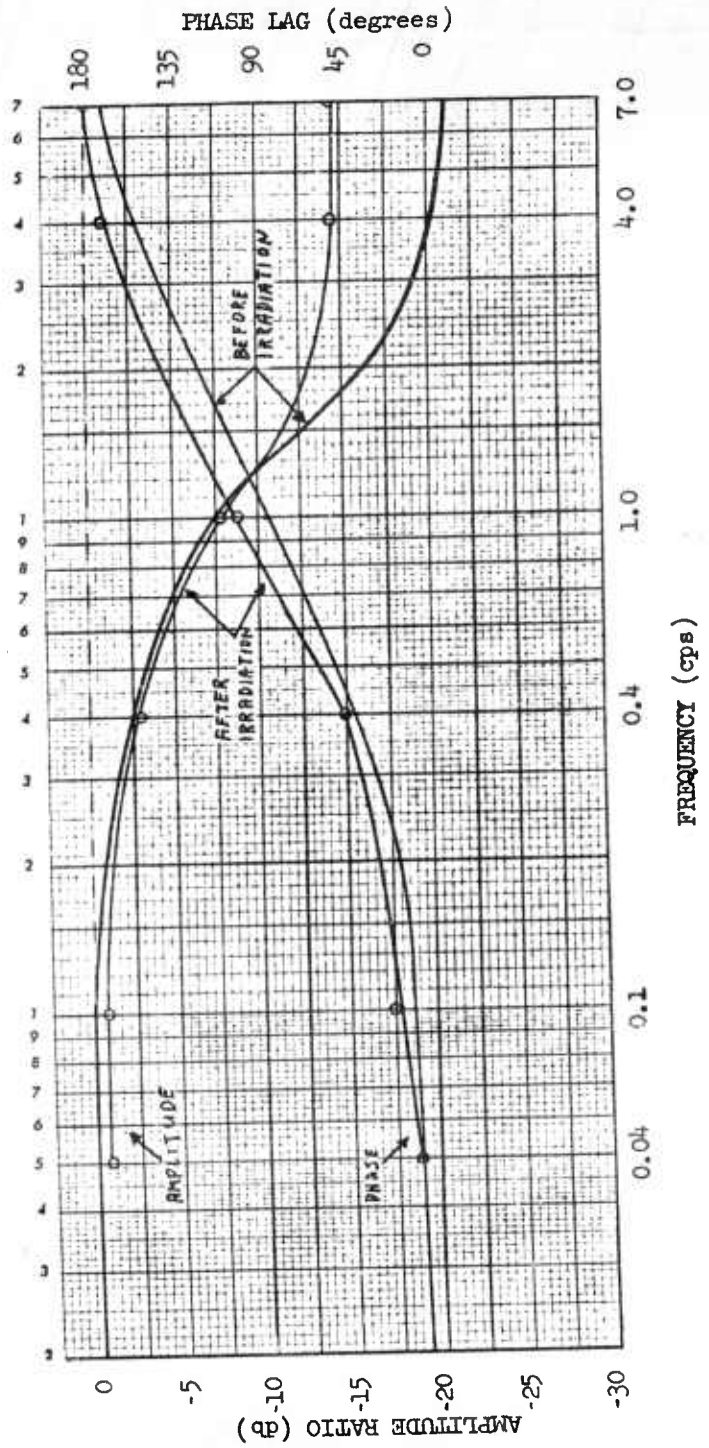

FIGURE 74 FREQUENCY RESPONSE OF ELECTROMECHANICAL FILTER NO. 2

6.0 THIN-FIIM FIELD-EFFECT TRANSISTOR

6.1 INTRODUCTION AND TEST ARTICLE DESCRIPTION

A thin-film field-effect transistor developed by Melpar Inc., was dynamically tested in Radiation Effects Test No. 18. This device is still in the development stage, however, since it is a majority carrier semiconductor device it should have higher nuclear radiation tolerance than typical minority carrier semiconductors devices.

There is a need for an active semiconductor component which will function in a severe nuclear radiation environment. As well as being a semiconductor component, the thin-film transistor is also microelectronic in size and can be either used in minature or microelectronic circuits.

This thin-film field-effect transistor was deposited on a glass insulating substrate by evaporation techniques. Figure 75 is a schematic representation of the internal configuration of the device. In general, the devices consists of two electrodes, designated the source and drain which connect a conducting channel of semiconductor material, and a gate electrode which is insulated from the channel material but is so positioned as to modulate the channel current. The thin-film field-effect transistor possesses voltage-current characteristics similar to those of a vacuum tube pentode.

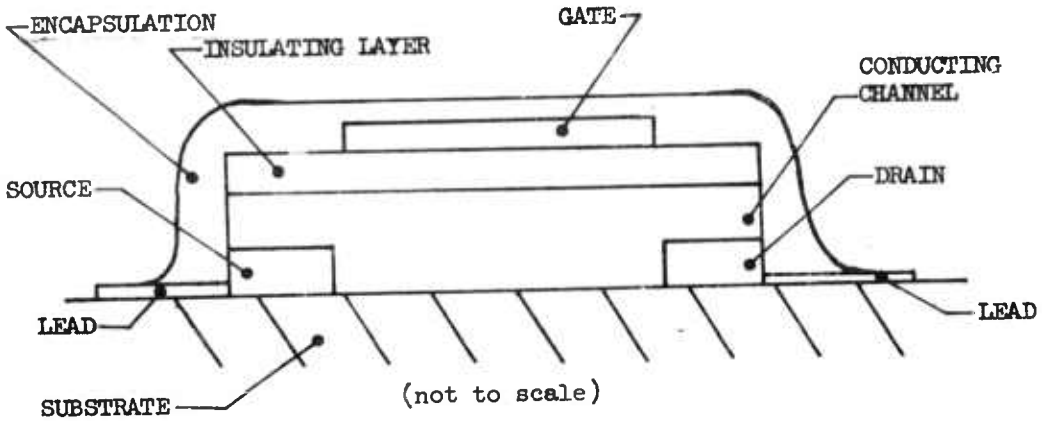

FIGURE 75 INTERNAL CONFIGURATION OF THIN-FIIM FIELD-EFFECT TRANSISTOR

6.2 NUCLEAR RADIATION EFFECTS ANALYSIS

The following materials make up the field-effect transistor as presented in Figure 75:

(a) Insulating substrate - Corning Microsheet No. 0211 glass

(b) Source and drain electrodes - 2,000-angstroms thick chromium (nichrome)

(c) Conducting semiconductor channel - 6,000-angstrom thick polycrystalline cadmium selenide

(d) Insulating layer between the gate and conducting channel - 1,200-angstrom thick silicon monoxide

(e) Gate electrode - 500-angstrom thick aluminum

(f) Leads - vacuum deposited gold film and silver epoxy paint

(g) Solder - Cerroseal No. 35, low temperature fluxless type

(h) Mounting board - G-10 fiber glass epoxy

(i) Encapsulating material - 5,000 - angstrom thick silicon monoxide

A similar type of thin-film field-effect transistor was statically evaluated in Radiation Effects Test No. 9 in October 1963. The results of the evaluation indicated that the voltage current characteristics actually improved after a nuclear radiation exposure of 5×10^{16} n/cm^2 and 9×10^{10} ergs/gm-(C).

A significant degree of nuclear radiation tolerance for the Melpar thin-film field-effect transistor was predicted based upon:

(a) Majority carrier operation which is not as sensitive to nuclear radiation as minority carrier lifetime

(b) The fact that the conducting channel is a polycrystalline material (cadmium selenide) which is already disordered to begin with, therefore, further disordering by neclear radiation is not very effective in changing its bulk properties

(c) Previous static irradiation of a similar device demonstrated an improvement in voltage-current characteristics as a result of the nuclear radiation exposure

6.3 TEST PROCEDURE

A schematic diagram of the instrumentation employed to dynamically evaluate the Melpar thin-film field-effect transistor is presented in Figure 76. The parameters measured during the irradiation were:

(a) Drain current with constant drain and gate voltages and

(b) Y_{F_S}, the static value of the forward transadmittance.

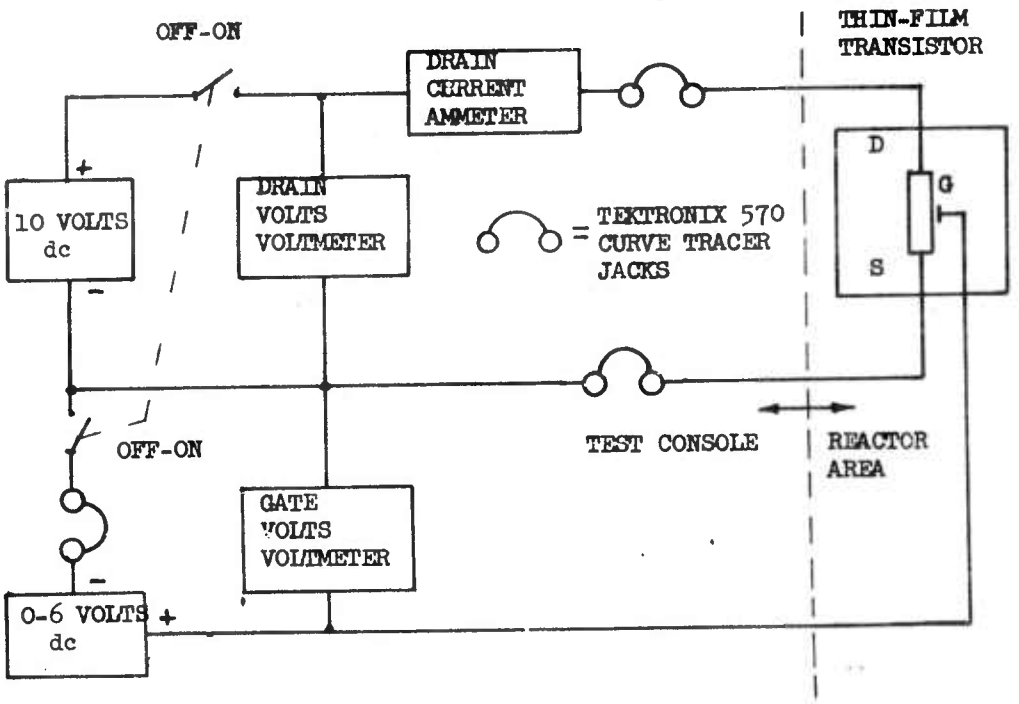

FIGURE 76 TEST CIRCUIT SCHEMATIC FOR THIN-FILM FIELD-EFFECT TRANSISTOR

For the drain current measurement a 10-volt DC drain to source bias and also a 5-volt DC source to gate bias was applied. It was necessary to bias the gate positive with respect to the source since the channel material operates in the enhancement mode and would not conduct otherwise.

The forward transadmittance, Y_{F_S}, is defined as the ratio of the change in drain current to the change in gate voltage. For this test the drain voltage was held at 10-volts dc. The gate bias was set at 5-volts dc and the value of the drain current recorded. The gate voltage was then reduced to 4-volts dc and the drain current was again recorded. The temperature of the device was measured by a thermocouple located on the device fixture adjacent to it.

6.4 TEST RESULTS AND CONCLUSIONS

The thin-film field-effect transistor operated satisfactorily with no signs of degradation for 19.6 hours which corresponded to a nuclear radiation exposure of 9×10^{15} n/cm^2 and 1.2×10^{10} ergs/gm-(C). At that time there occurred an indicated step increase in forward transadmittance of about 27 percent. This was related to a simultaneous step decrease in the drain current of about 25 percent. It was later learned that these events were immediately preceded by an increase in the temperature of the transistor from 80°F to 100°F due to an increase in the environmental chamber inlet air. At 20.0 hours test time the drain current dropped drastically from 3 milliamps to 0.2 milliamps. The temperature of the transistor was 107° F at that time. At 20.1 hours test time the environmental chamber air temperature was decreased such that the transistor temperature dropped to 90° F and the drain current began to gradually increase and after 21.9 hours test time it had reached 1.8 milliamps. An attempt was made to measure the forward transadmittance but the gate had lost all control over the current, hence the transadmittance was zero.

After 40.5 hours of irradiation the forward transadmittance was still zero and the drain current was 2.0 milliamps. It was decided to discontinue taking data since the transistor had failed after 21.9 hours irradiation and had not shown any tendency to recover since that time.

Failure of the thin-film field-effect transistor after a nuclear radiation exposure of 9×10^{15} n/cm^2 and 1.2×10^{10} ergs/gm-(C) was attributed to:

(a) Temperature breakdown of the transistor and

(b) Neutron degradation of the silicon monoxide insulating layer between the gate and the conducting channel.

7.0 STATIC SAMPLES

7.1 AUTONETICS STATIC SAMPLES

Several static components and materials for the two-axis gyro, electromagnetic accelerometers, and two-axis platform electronic systems were exposed during Radiation Effects Tests Nos. 10 and 18, and they are discussed separately herein.

These samples were submitted to LTV Vought Aeronautics by Autonetics, a Division of North American Aviation, Inc., for irradiation testing. They were tested at Autonetics before shipment, exposed to radiation, and returned to Autonetics for post analysis. They were non-operating during radiation exposure and were not instrumented.

7.1.1 STATIC SAMPLES FROM RADIATION EFFECTS TEST NO. 10

The static samples for the G9 gyro, electromagnetic accelerometer, and platform electronics were exposed in Radiation Effects Test No. 10. The post-irradiation evaluations of the gyro components and materials have been completed, and a list of comments on the test results follow:

(a) Sample of Raychem "Thermorad" insulated wire - the insulation was stiffer than before radiation, but this should not affect the operation of the gyro.

(b) Gyro Pickoff Resolver - No degradation noted except that a small amount of Teflon insulation remaining on the pigtails deteriorated completely. This was anticipated and a material substitution (Thermorad) was already planned.

(c) Radiated Polyethylene Shrink-Fit Tubing - The tubing was stiffer than before radiation, but this will not affect the gyro.

(d) Gyro Pickoff Transformer - Three of seven of these transformers were previously irradiated and this test was intended to evaluate the results of a second exposure. The changes were relatively minor and will not affect the gyro performance.

(e) Ferrite Cores - These cores were evaluated for possible pickoff transformer use. No significant degradation was noted.

(f) Neoprene O-ring - The O-ring was harder than before irradiation but no other degradation was noted. This O-ring is a temporary seal for use during gyro assembly and test and cannot affect the gyro other than through outgassing. Based on the appearance and a comparison of pre- and post-irradiation weights, this O-ring will not outgas enough to affect the gyro.

Post-irradiation evaluations of the electromagnetic accelerometer components and materials as listed below have not been completed.

(a) Accelerometer pickoff transformers

(b) EMA forcer coil - LASV-N1 type

(c) EMA forcer coil - similar to (b) except Epon 828 was used as a coil cement

(d) Ceramic (Duroc) insulated magnetic wire

(e) Three samples of Bacon LCA-4 epoxy

(f) Three samples of Epon 828

(g) Three samples of Bacon 1119 epoxy

(h) Sodium silicate

All of the EMA samples but the pickoff transformers were sealed in evacuated pyrex tubes so gas evaluation could be determined. The gases generated by the radiation were subjected to gas chromatography for analysis. The gas chromatographic identifications by the various gases were made by comparing the retention times of known gaseous standards with the retention times obtained from the gas analysis of irradiated samples.

Four Clare relays (two BA1B201K00 and two BA1C300K00) used in the platform electronics system were exposed in Radiation Effects Test No. 10. Comparison of these relays with new relays of the same type have revealed no degradation of contact resistance, pull-in voltage, or drop-out voltage.

A list of the static samples for the gyro, electromagnetic accelerometer, and platform electronic system and their time integrated exposures during Radiation Effects Test No. 10 are listed in Table 27.

TABLE 27 STATIC SAMPLES FROM RADIATION EFFECTS TEST NO. 10

ITEMS	Thermal Neutron (E<0.48 ev) N/cm^2	Fast Neutrons (E>0.3 Mev) N/cm^2	Gamma Ergs/gm-C
Raychem Insulated Wire	2.7(14)*	2.9(16)	4.5(10)
Gyro Pickoff Resolver	4.7(14)	5.0(16)	1.2(10)
Radiated Polyethylene Shrink-fit Tubing	2.7(14)	2.9(16)	4.5(10)
Gyro Pickoff Transformer	2.7(14)	2.9(16)	4.5(10)
Ferrite Cores	2.7(14)	2.9(16)	4.5(10)
Neoprene O-ring	2.7(14)	2.9(16)	4.5(10)
EMA Pickoff Transformer	2.7(14)	2.9(16)	4.5(10)
EMA Forcer Coil - New	3.4(14)	4.3(16)	7.7(10)
Ceramic (Duroc) Insulated Magnetic Wire	5.4(14)	3.6(16)	8.2(10)
Bacon LCA-4	5.1(14)	3.8(16)	8.1(10)
Bacon LCA-4	2.9(14)	2.3(16)	4.0(10)
Bacon LCA-4	4.5(14)	13.(16)	3.5(10)
Epon 828	6.1(14)	3.2(16)	6.2(10)
Epon 828	4.0(14)	2.1(16)	3.2(10)
Epon 828	4.5(14)	9.8(15)	1.7(10)
Bacon 1119	3.8(14)	5.3(16)	8.5(10)
Bacon 1119	4.0(14)	1.9(16)	2.2(10)
Bacon 1119	4.0(14)	9.7(15)	2.2(10)
Sodium Silicate	4.9(14)	4.0(16)	8.0(10)
Clare Relays	4.4(14)	2.6(16)	4.7(10)
EMA Forcer Coil (LASV-N1 type)	5.4(14)	3.9(16)	7.2(10)
Radiated Polyethylene Insulated Wire	2.7(14)	2.9(16)	4.5(10)
FEP and H-Film Insulated Wire	2.9(14)	2.3(16)	4.0(10)

* 2.7(14) denotes 2.7×10^{14}

7.1.2 STATIC SAMPLES FROM RADIATION EFFECTS TEST NO. 18

Twenty-two static wire samples were sealed in evacuated (air and vacuum) pyrex tubes, irradiated, and returned to Autonetics for post-irradiation analysis. The gases generated by the irradiation will be subjected to gas chromatography for analysis. A list of the twenty-two static wire samples and their time integrated exposure during Radiation Effects Test No. 18 are listed in Table 28.

Post-irradiation analyses of these static samples are not available at this time, but will be included in the Autonetics final report as an Addendum to Volume 11 of this report.

7.2 CERAMIC STATIC SAMPLES

7.2.1 INTRODUCTION

Two types of ceramic dielectric materials were obtained from Corning Glass Works, Corning, New York, for radiation effects study. The main purpose of the test was to determine the effects of radiation on the dielectric constant and loss tangent of these samples. One sample was PYROCERAM (Registered tradename) brand glass-ceramic, Code 9606, and the other was fused silica, Code 7941. Four samples were irradiated, two for each type of material, and two samples of each material were used as control samples.

7.2.2 NUCLEAR ANALYSIS

The samples to be irradiated were placed in aluminum cans, one sample per can, and placed in the west pallet. The dielectric samples received a gamma dose of 1.5×10^{11} ergs/gm-(C) and an integrated neutron flux of 9.2×10^{16} neutrons/cm^2.

7.2.3 TEST PROCEDURE

There are several methods available to determine the dielectric constant and loss tangent of dielectric materials. After some study it was determined to utilize the method described in the paragraphs that follow.

The sample materials were obtained in 12-inch square sample sheets. The first step was to cut the samples to the correct size. The measurements were to be made at 13.5 kmc, or Ku-band, so this determined two of the dimensions. Using this procedure also required a third dimension of the sample, called the optimum sample length (le). This was determined by the following equations.

TABLE 28 STATIC WIRE SAMPLES FROM RADIATION EFFECTS TEST NO.18

ITEMS	Thermal Neutrons ($E < 0.48$ ev) n/cm^2	Fast Neutrons ($E > 0.3$ Mev) n/cm^2	Gamma Ergs/gm-C
WTE 1932A-TFE (Vacuum)	C.R.<1	2.9(16)*	3.8(10)
PVC B4B 1932U (Vacuum)	C.R.<1	2.9(16)	3.9(10)
WTE 1932A-SB (Vacuum)	C.R.<1	3.0(16)	5.0(10)
SR8-M (Vacuum)	C.R.<1	3.1(16)	6.0(10)
RTM 1927A (Vacuum)	C.R.<1	3.3(16)	8.2(10)
H Film-ML-ADH Auto (Vacuum)	3.5(14)	3.4(16)	1.1(11)
1938 H Film (Vacuum)	3.5(14)	3.4(16)	1.4(11)
SR8 Surok (Vacuum)	3.5(14)	3.5(16)	2.1(11)
SR-34 1932 (Vacuum)	3.6(14)	3.3(16)	2.9(11)
IMP Kynar (Vacuum)	3.8(14)	3.1(16)	3.7(11)
FEP LTM 1932A-SK (Vacuum)	3.8(14)	3.1(16)	3.7(11)
1938 H Film (Air)	4.3(14)	2.8(16)	2.3(11)
WTE 1932A - SB (Air)	4.7(14)	2.6(16)	8.5(10)
RTM 1927A (Air)	4.7(14)	2.6(16)	8.5(10)
H Film-ML-ADH Auto (Air)	3.0(14)	1.6(16)	2.8(10)
SR8-M (Air)	3.0(14)	1.6(16)	2.8(10)
WTE 1932A - TFE (Air)	C.R.<1	1.6(16)	4.0(10)
SR8 Surok (Air)	C.R.<1	1.6(16)	5.2(10)
FEP LTM 1932A-SK (Air)	C.R.<1	1.6(16)	5.2(10)
SR-34 1932 (Air)	4.2(14)	1.6(16)	4.2(10)
PVC B4B 1932U (Air)	4.2(14)	1.5(16)	3.1(10)
IMP Kynar (Air)	4.2(14)	1.5(16)	3.1(10)

* 2.9(16) denotes 2.9×10^{16}
C. R. Cadmium Ratio

$$\lambda_{g\epsilon} = \frac{\lambda}{\sqrt{\epsilon' - (\lambda/2a)^2}} \qquad (1)$$

$\lambda_{g\epsilon}$ = guide wavelength in the dielectric

λ = wavelength in free space

ϵ' = approximate dielectric constant of the sample

a = broad dimension of the guide

$$\ell_\epsilon = (2C+1)\lambda_{g\epsilon}/8 \qquad \text{when } C = 0, 1, 2, 3, \ldots \qquad (2)$$

Using Equations (1) and (2) and the approximate dielectric constant of the samples (9606-5.5 and 7941-3.3), two samples of each type of material were fabricated. Due to an error the 9606 samples were cut to the wrong optimum length. To correct for this and at the same time maintain the correct sample length, the frequency was adjusted to compensate for the error. Table 29 shows the sample length and the frequency at which the measurements were made.

TABLE 29

SAMPLE LENGTH AND FREQUENCY

	FREQUENCY	SAMPLE 1 Length	SAMPLE 2 Length
7941	13.5 kmc	.196"	.326"
9606	12.93 kmc	.154"	--
9606	12.82 kmc	--	.362"

Figure 77 shows the test setup used.

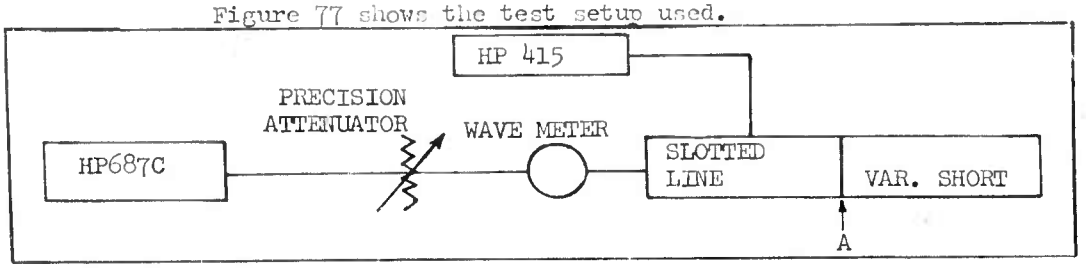

FIGURE 77 TEST SETUP FOR CERAMIC SAMPLES MEASUREMENTS

The HP687C was turned on and allowed to warm up so that no frequency drift would occur during the data runs. The generator was then set on the desired frequency by the use of the wavemeter. It was necessary to take two sets of measurements for each dielectric sample; one with the variable short circuit touching the sample, short circuit condition (S_1), and the other with the variable short a certain distance away from the sample, open circuit condition (S_2). The following equations were used to determine S_1 and S_2:

$$S_1 = M\lambda_g/2 \qquad \text{where } M = 0, 1, 2, 3, \ldots \qquad (3)$$

$$S_2 = (2N+1)\lambda_g/4 \qquad \text{where } N = 0, 1, 2, 3, \ldots \qquad (4)$$

λ_g = guide wavelength in air

Both M and N were arbitrarily chosen to equal zero, therefore $S_1 = 0$ and $S_2 = \lambda_g/4$. These values for S_1 and S_2 were used for all dielectric samples. A typical data run was as follows:

(a) Set the generator to the desired frequency. Determine λ_g by measuring the distance between alternate voltage minimums.

(b) Place the sample into the waveguide (Refer to Figure 77, point A).

(c) Set the variable short circuit so that it is touching the face of the dielectric sample ($S_1 = 0$, short circuit condition).

(d) Adjust the slotted line carriage to a voltage minimum. Record D_1 (distance between the face of the sample nearest the generator and the slotted line probe).

(e) Measure the VSWR. Use the precision attenuator to determine VSWR. Measure the db difference between the voltage minimum and a voltage maximum. Record the db reading as db_1.

(f) Set the variable short circuit as $S_2 = \lambda_g/4$ (distance between the face of the sample nearest the short circuit and the face of the variable short), open circuit condition .

(g) Repeat step (d), but record this distance as D_2.

(h) Repeat step (e), but record this db reading as db_2.

This completes the necessary measurements. The above data is then applied to the following equations which determine the dielectric constant and loss tangent of the dielectric sample:

$$\text{Log VSWR} = \frac{db_k}{20} \; ; \; \text{VSWR} = \Gamma_k \; ; \; k = 1,2 \tag{5}$$

$$K = \frac{2\pi}{\lambda_g} \tag{6}$$

$$|\Gamma_{in}|_k = \frac{\Gamma_k - 1}{\Gamma_k + 1} \; ; \; k = 1,2 \tag{7}$$

$$Y_{ik} = \frac{1 + |\Gamma_{in}|_k e^{j2kD_k}}{1 - |\Gamma_{in}|_k e^{j2kD_k}} \; ; \; k = 1,2 \tag{8}$$

$$\text{Solve } Y_\epsilon = Y_{i_1}, Y_{i_2} \tag{9}$$

$$Y_\epsilon = g_\epsilon - B_\epsilon \tag{10}$$

$$\epsilon' = \frac{g_\epsilon + \left(\frac{\lambda_g}{2a}\right)^2}{1 + \left(\frac{\lambda_g}{2a}\right)^2} \; ; \quad \epsilon' = \text{dielectric constant}, \; a = \text{width of wavelength} \tag{11}$$

$$\epsilon'' = -\frac{B_\epsilon}{1 + \left(\frac{\lambda_g}{2a}\right)^2} \tag{12}$$

$$\text{Tan } \delta = \frac{\epsilon''}{\epsilon'} \quad ; \text{ loss tangent} \tag{13}$$

Formulas 5 through 13 are then used to determine the dielectric constant (11) and loss tangent (13) of each sample.

7.2.4 TEST RESULTS AND CONCLUSIONS

Four data runs were made for each sample, except the 7941-.196 irradiated sample. The average for the four runs was then taken. Table 30 lists the dielectric constant ϵ' and loss tangent ($\tan \delta$) for each sample length (le) for both the control sample and irradiated samples.

TABLE 30

DIELECTRIC CONSTANT AND LOSS TANGENT
FOR THE CERAMIC SAMPLES

Code	ℓ_ϵ		ϵ'	tan δ
9606	.362	Control	5.73	404 X 10^{-4}
		Test	5.79	305 X 10^{-4}
9606	.154	Control	5.79	544 X 10^{-4}
		Test	5.77	279 X 10^{-4}
7941	.326	Control	3.31	192 X 10^{-4}
		Test	3.11	100 X 10^{-4}
7941	.196	Control	3.32	94 X 10^{-4}
		Test	3.20	202 X 10^{-4}

Table 31 lists the dielectric constant and loss tangent obtained by taking the average of the values listed in Table 30 above for the 9606-.362 and 9606-.154 control sample and then repeating for the 9606 test samples. This was also done for the 7941 material.

TABLE 31

AVERAGE DIELECTRIC CONSTANT AND
LOSS TANGENT FOR THE CERAMIC SAMPLES

		ϵ'	Tan δ
9606	Control	5.76	474 X 10^{-4}
	Test	5.78	291 X 10^{-4}
7941	Control	3.32	143 X 10^{-4}
	Test	3.15	151 X 10^{-4}

A few points should be brought out at this time concerning the data. During the process of cutting and/or handling of the 7941 control samples, small chips occurred. The 7941-.196 control sample had a fairly large chip while the 7941-.326 control sample had a small chip in one corner. Both irradiated samples and all of the 9606 samples were in excellent condition. The fact that the 7941 control samples were not perfect has a direct bearing on the results of the measurements. Also, during the data runs on the 7941-.196 test sample the material fractured when it was removed from the guide. Unfortunately, this happened on the first data run; therefore only one data run was obtained on this sample.

Referring to Table 30 we see the measured dielectric constant and loss tangent for each sample. As can be seen, the 9606-.362 test sample shows essentially no change in dielectric constant. The loss tangent value has changed slightly. The 9606-.154 test sample shows essentially no change in dielectric constant, however more change is noted in the loss tangent. The 7941-.326 sample shows a slight change in both dielectric constant and loss tangent. The same is true of the 7941-.196 sample.

The following conclusions were drawn concerning the dielectric samples. Although the data for the 7941 samples indicate a change in dielectric constant of the irradiated samples, this change is not believed to be caused by radiation, but is believed to be due to the control sample imperfections which affected the dielectric constant measurements. The 9606 samples which were in good condition exhibited essentially no change in dielectric constant.

There was, however, a change in the loss tangent of both dielectric materials and a definite increase in the VSWR measurements of the irradiated samples. This would bear out the conclusion that a decrease in the loss tangent of both materials did occur.

It is concluded therefore that no change in dielectric constant occurred, or that the change was so small that it was not within the measuring accuracy of the system. Also, it was concluded that a slight decrease in the loss tangent did occur as shown in Tables 30 and 31.

It is recommended that additional samples of these two dielectric materials be prepared for future testing and that the number of irradiated samples be increased considerably so that enough data can be obtained to substantiate the findings. It is also recommended that a method be devised whereby more precise measurements can be used to obtain the desired data.

7.3 ELECTRONIC COMPONENT TEST

7.3.1 INTRODUCTION

Ten JFD trimmer capacitors, two JFD Uniceram capacitors, four Babcock magnetic latching relays, six Dickson 1N3826 zener diodes, six Dickson 1N2995 zener diodes and seventeen Dickson 1N823 temperature compensated zener diodes were tested under static electrical conditions in a nuclear radiation environment in order to determine the feasibility of their use in a neutron-gamma environment. Electrical characteristics of each of these components were recorded before and after exposure to the nuclear radiation environment. The only components which underwent significant change were the zener diodes.

7.3.2 DICKSON ZENER DIODE TEST

Only one of the 1N823 zeners of the nine which were irradiated to 6.5×10^{16} n/cm^2 and 2.0×10^{11} ergs/gm-(C) could be evaluated after the test, all others were essentially open circuited. One of the 1N823 zener diodes of the five which were irradiated to 2.5×10^{16} n/cm^2 and 4.6×10^{10} ergs/gm-(C) and one of the three which were irradiated to 1.6×10^{16} n/cm^2 and 4.6×10^{10} ergs/gm-(C) also appeared to be open circuited. Photographs were taken of all diode characteristics before and after irradiation. Typical changes can be seen in Figures 78 through 84. As can be noted from Figures 78, 79, 82, and 83 the use of the 1N823 and 1N3826 diodes are marginal at 1.6×10^{16}n/cm^2 and 4.6×10^{10} ergs/gm-(C) and would be unacceptable for most applications after an exposure of 6.5×10^{16} n/cm^2 and 2×10^{11} ergs/gm-(C). Figures 80 and 81 show the 1N2995A to be completely unacceptable at the exposure of 1.6×10^{16} n/cm^2 and 4.6×10^{10} ergs/gm-(C). The typical forward characteristic change for the 1N2995A and 1N3826 zener diodes is presented in Figure 84.

7.3.3 JFD CAPACITORS

Ten JFD trimmer capacitors and two JFD Uniceram fixed capacitors were tested in static electrical conditions. The Uniceram units showed no change in capacitance or dissipation factor (within .5%) after an integrated nuclear exposure of 6.5×10^{16} n/cm^2 and 2.0×10^{11} ergs/gm-(C). Ten trimmer capacitors which were built by JFD for test in the nuclear environment were monitored before and after exposure. A problem arose in measuring the capacitance accurately due to its low value (30 pf). After considering bridge error (.5%) and error induced by different lead configuration (1.5%), it was concluded that the measurements taken were accurate to 2%. Table 32 presents the test results for the JFD trimmer capacitors. It should be noted that no significant change occurred except for the units receiving integrated exposure of 6.5×10^{16} n/cm^2 and 2.0×10^{11} ergs/gm-(C).

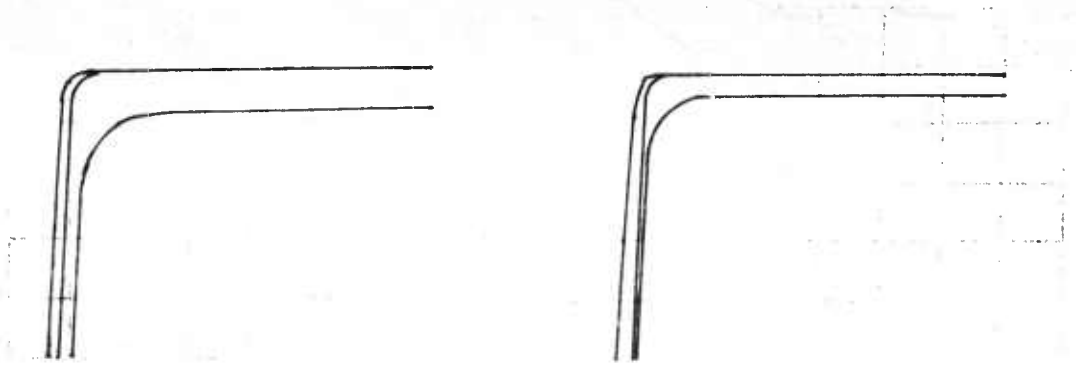

PRE-TEST CONTROL POST-TEST CONTROL

VOLTAGE SCALE 1 V/div
CURRENT SCALE 15.8 ma/div
1.58 ma/div
.158 ma/div

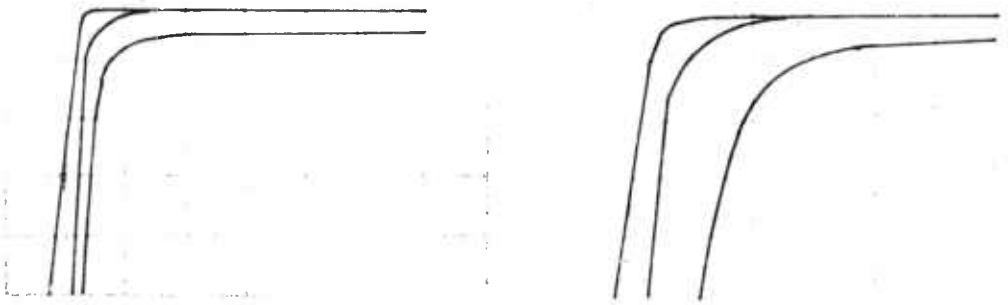

PRE-TEST AFTER 1.6×10^{16} n/cm^2 and 4.6×10^{10} ergs/gm-(C)

FIGURE 78 PRE- AND POST-TEST REVERSE CHARACTERISTICS OF THE 1N823 ZENER DIODE

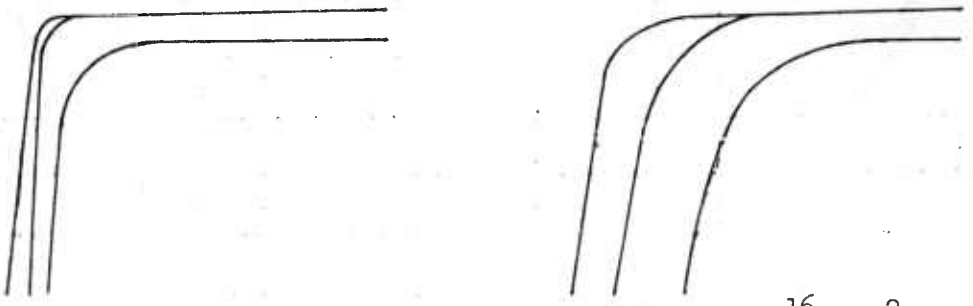

PRE-TEST

AFTER 2.5×10^{16} n/cm^2 and 4.6×10^{10} ergs/gm-(C)

VOLTAGE SCALE 1 V/div
CURRENT SCALE 15.8 ma/div
1.58 ma/div
.158 ma/div

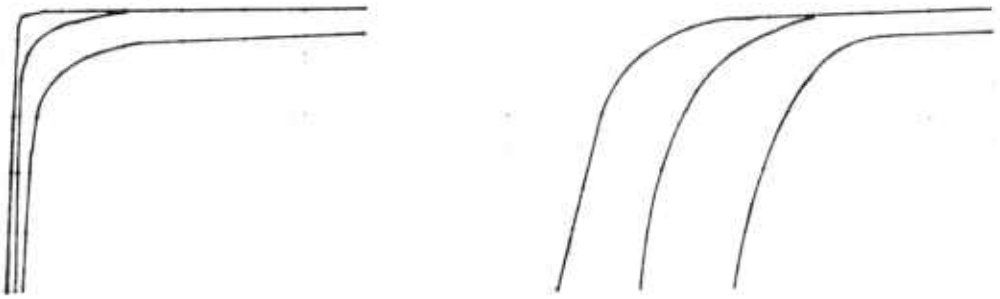

PRE-TEST

AFTER 6.5×10^{16} n/cm^2 and 2.0×10^{11} ergs/gm-(C)

FIGURE 79 PRE- AND POST-TEST REVERSE CHARACTERISTICS OF THE 1N823 ZENER DIODE

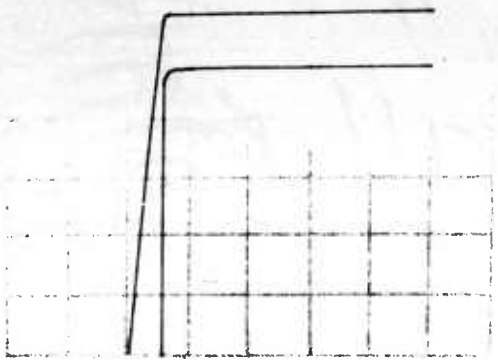

PRE-TEST CONTROL

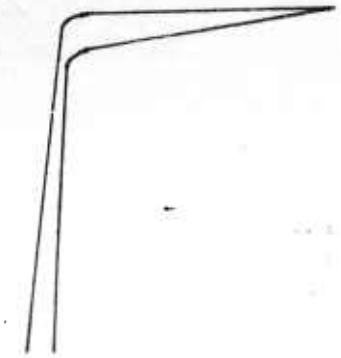

POST-TEST CONTROL

VOLTAGE SCALE 10 V/div
CURRENT SCALE 10^{-5} a/div
5×10^{-5}a/div

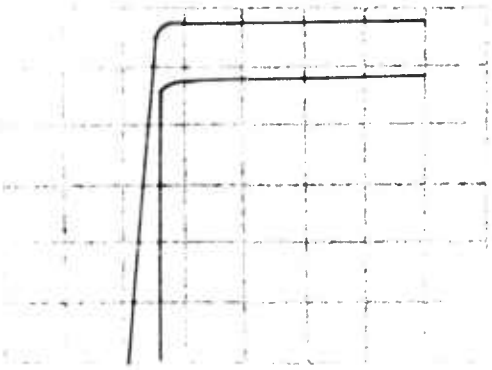

PRE-TEST

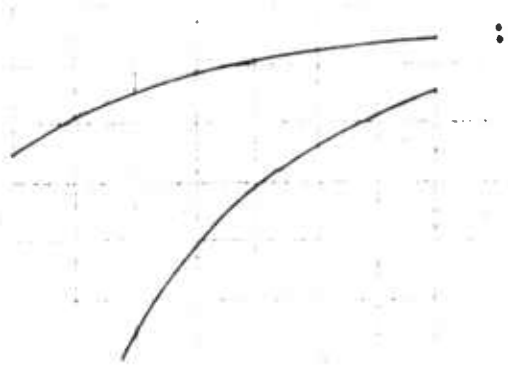

AFTER 1.6×10^{16} n/cm^2 and
4.6×10^{10} ergs/gm-(C)

FIGURE 80 PRE- AND POST-TEST REVERSE CHARACTERISTICS OF THE 1N2995A ZENER DIODE

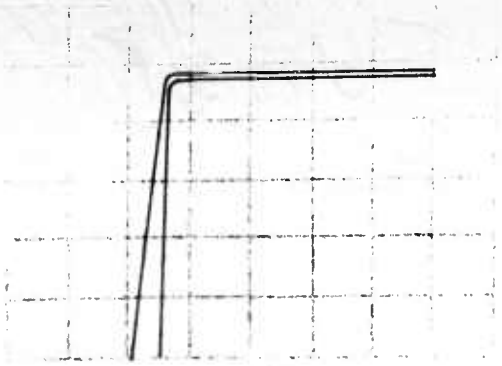

PRE-TEST

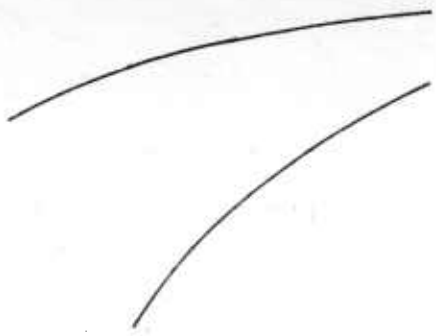

AFTER 2.5 x 10^{16} n/cm^2 and
4.6 x 10^{10} ergs/gm-(C)

VOLTAGE SCALE 10 V/div
CURRENT SCALE 10^{-5} a/div
5×10^{-5} a/div

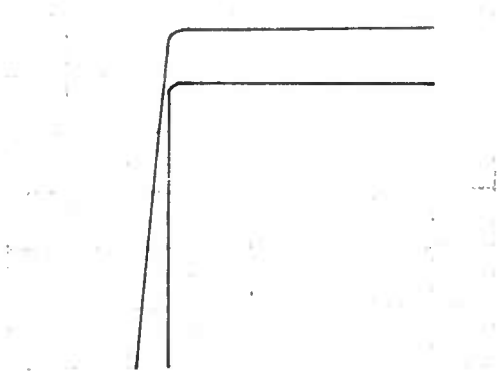

PRE-TEST

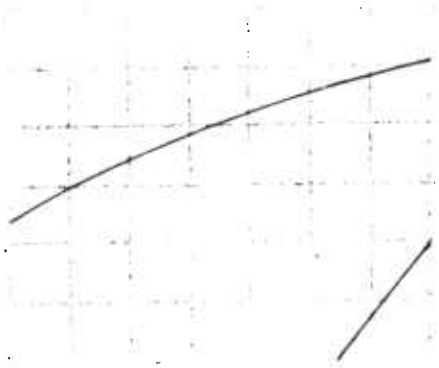

AFTER 6.5 x 10^{16} n/cm^2 and
2.0 x 10^{11} ergs/gm-(C)

FIGURE 81 PRE- AND POST-TEST REVERSE CHARACTERISTICS OF THE 1N2995A ZENER DIODE

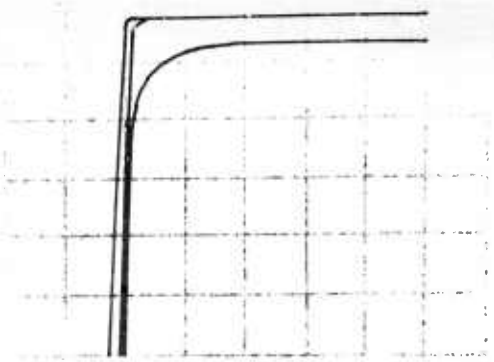

PRE-TEST CONTROL

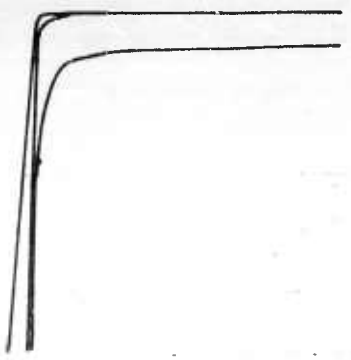

POST-TEST CONTROL

VOLTAGE SCALE 1 V/div
CURRENT SCALE 15.8 ma/div
1.58 ma/div
.158 ma/div

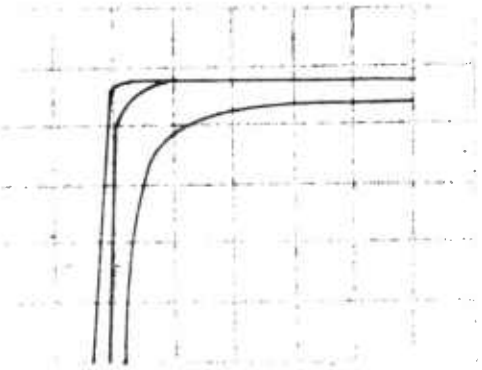

PRE-TEST

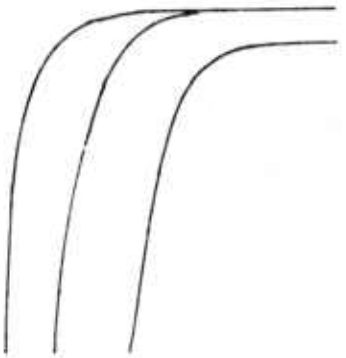

AFTER 1.6×10^{16} n/cm^2 and 4.6×10^{10} ergs/gm-(C)

FIGURE 82 PRE- AND POST-TEST REVERSE CHARACTERISTICS OF THE 1N3826 ZENER DIODE

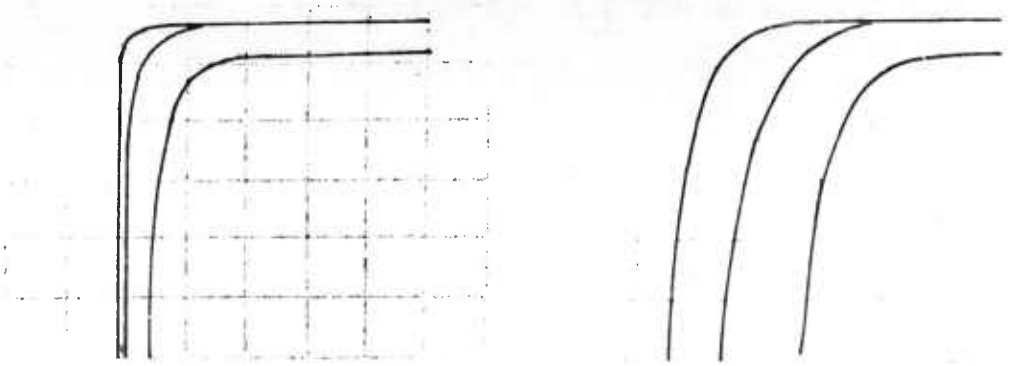

PRE-TEST

AFTER 2.5 x 10^{16} n/cm^2 and
4.6 x 10^{10} ergs/gm-(C)

VOLTAGE SCALE 1 V/div
CURRENT SCALE 15.8 ma/div
1.58 ma/div
.158 ma/div

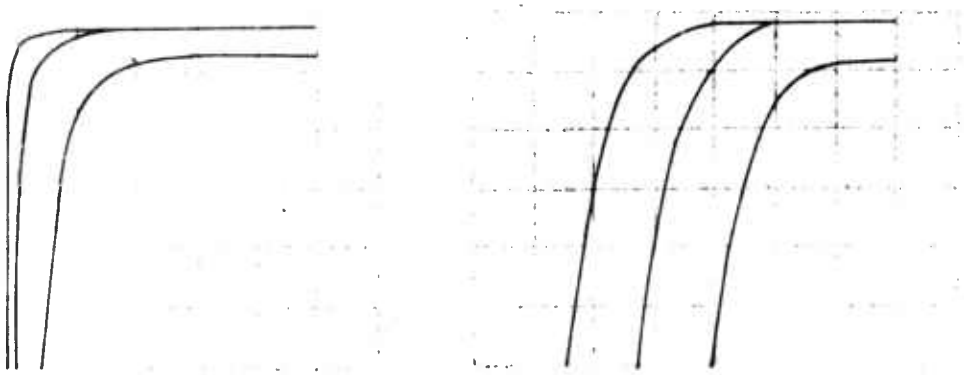

PRE-TEST

AFTER 6.5 x 10^{16} n/cm^2 and
2.0 x 10^{11} ergs/gm-(C)

FIGURE 83 PRE- AND POST-TEST REVERSE CHARACTERISTICS OF THE 1N3826 ZENER DIODE

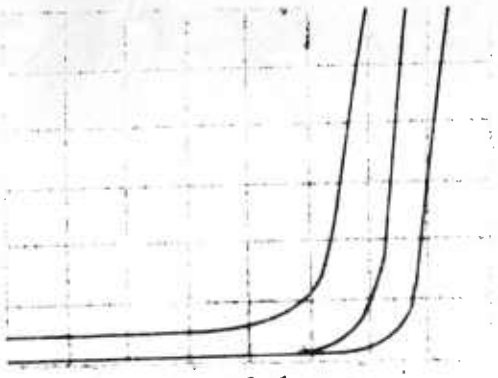

PRE-TEST 1N3826 FORWARD CHARACTERISTICS

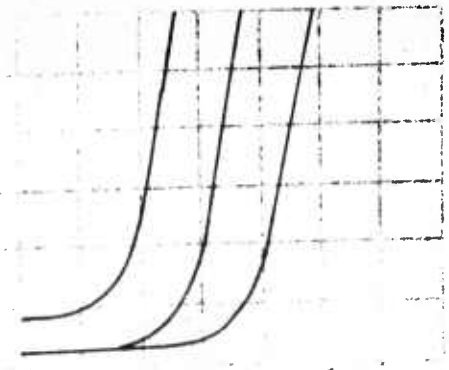

1N3826 AFTER 2.5×10^{16} n/cm^2 and 4.6×10^{10} ergs/gm-(C)

VOLTAGE SCALE 100 V/div
CURRENT SCALE 15.8 ma/div
1.58 ma/div
.158 ma/div

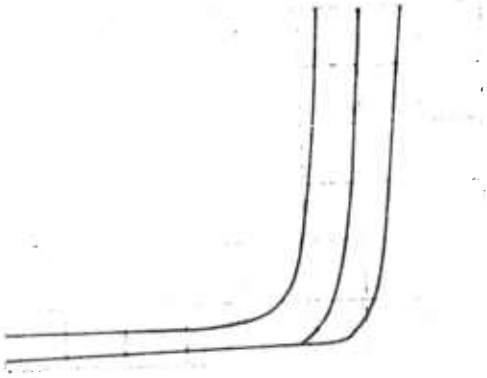

PRE-TEST 1N2995A FORWARD CHARACTERISTICS

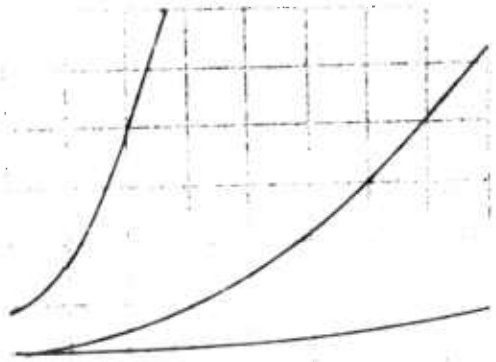

1N2995A AFTER 1.6×10^{16} n/cm^2 and 4.6×10^{10} ergs/gm-(C)

FIGURE 84 TYPICAL PRE- AND POST-TEST CHARACTERISTICS OF THE 1N2995A AND 1N3826 ZENER DIODES

TABLE 32 CAPACITANCE AND DISSIPATION FACTOR FOR JFD VARIABLE TRIMMER CAPACITORS

Nuclear Exposure	Pre-Test* Cap. pf	Post-Test* Cap. pf	% Ch.	Pre-test D.F.	Post-Test D.F.	% Ch.
$1.6 \times 10^{16} n/cm^2$ 4.6×10^{10} ergs/gm-(C)	31.0 30.9 30.95	31.5 31.6 31.9	+ 2 + 2 + 3	.011 .010 .012	.052 .058 .070	+372 +480 +483
$2.5 \times 10^{16} n/cm^2$ 4.6×10^{10} ergs/gm-(C)	31.0 30.7 30.9	31.1 30.95 31.0	+.3 +.5 +.3	.011 .010 .011	.019 .0145 .019	+73 +45 +73
$6.5 \times 10^{16} n/cm^2$ 2.0×10^{11} ergs/gm-(C)	31.5 31.0 30.95 30.9	33.6 32.4 32.3 33.5	+ 7 + 8 + 7 + 8	.014 .010 .0115 .0115	.102 .067 .099 .085	+629 +570 +761 +639
Control	30.85 31.0	30.75 30.9	+.3 +.3	.0105 .011	.0105 .014	0 +27

* Bridge readings accurate within 2%

7.3.4 BABCOCK MAGNETIC LATCHING RELAYS

Four Babcock BR9-DX-G8-V5-S20 magnetic latching relays were irradiated in a static condition in order to determine the feasibility of their use in the nuclear environment. These units are constructed with diallyl SS5 glass-filled bobbin, 3M Scotchweld #583, G.E. 201 urethane tape, and irradiated polyethylene. The contacts were heavy gold plate. It was estimated that no change could be detected in the performance of these units until an integrated exposure greater than 4×10^{10} ergs/gm-(C) had been reached. Up to this exposure no significant changes should occur in any of the organic insulating materials which are used in these units. Pull-in voltage and current was measured for each relay before and after irradiation as well as contact resistance for all four contacts of each relay. As can be noted in Table 33 no change which could be attributed to nuclear radiation was detected for any unit even after an integrated exposure of 6.5×10^{16} n/cm^2 and 2.0×10^{11} ergs/gm-(C). The pin layout for this relay is as shown:

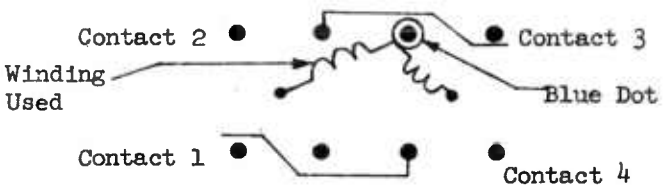

The pull-in voltage for contacts 1 and 3 was measured after which the polarity of the voltage was reversed and pull-in for contacts 2 and 4 was measured. After reduction of the data it was concluded that these units may be used in nuclear radiation environments up to 6.5×10^{16} n/cm^2 and 2.0×10^{11} ergs/gm-(C).

TABLE 33 RELAY CHARACTERISTICS BEFORE AND AFTER IRRADIATION

Part No.	Radiation Exposure		Pre-test Pull-in (volts)		Post-test Pull-in (volts)		Pre-test Pull-in Current (ma)		Post-test Pull-in Current (ma)	
	n/cm^2	ergs/gm-(C)	Contacts 1 and 3	Contacts 2 and 4	Contacts 1 and 3	Contacts 2 and 4	Contacts 1 and 3	Contacts 2 and 4	Contacts 1 and 3	Contacts 2 and 4
1	2.5×10^{16}	4.6×10^{10}	52.5	46.5	51.5	51.5	5	4.4	4.9	5.0
2	1.6×10^{16}	4.6×10^{10}	50	54	54	54	4.6	5.0	5.4	5.3
3	6.5×10^{16}	2.0×10^{11}	51	44.5	44	48	4.75	4.1	4.5	4.8
4	6.5×10^{16}	2.0×10^{11}	55	52.5	52.5	46	5.3	5.0	5.2	4.6

Part No.	Radiation Exposure		Contact Resistance (OHMS)							
	n/cm^2	ergs/gm-(C)	Pre-test #1	Post-test #1	Pretest #2	Post-test #2	Pretest #3	Post-test #3	Pretest #4	Post-test #4
1	2.5×10^{16}	4.6×10^{10}	.084	.012	.032	.016	.042	.003	.046	.029
2	1.6×10^{16}	4.6×10^{10}	.042	.013	.070	.023	.042	.024	.038	.044
3	6.5×10^{16}	2.0×10^{11}	.063	.027	.037	.010	.046	.023	.023	.006
4	6.5×10^{16}	2.0×10^{11}	.017	.020	.034	.003	.030	.021	.001	.002

8.0 INSTRUMENTATION

Briefly the instrumentation for this test consisted of the equipment required to supply raw and regulated power and input signals to the test articles and to monitor the output signals from the test articles.

The instrumentation in the reactor (GTR) control room consisted of 26 consoles 6 feet by 24 inches by 22 inches and is shown in Figures 85, 86, and 87. These included highly regulated DC power supplies, primary regulated AC filament power supplies, function generators, precision pulse generators, test article control panels, counters, strip chart recorders, digital volt meters, temperature recorders, and various other test equipment along with the Data Management System (DMS). The DMS consisted of the main frame (SDS 920 computer), two tape decks, two interface consoles and two typewriters.

The AC filament voltages were monitored at the load end of the 150-feet power cables. The primaries of all filament circuits were fused and switched and continuously variable through 100% of their range. The AC and DC supply voltages were routed from the power supply consoles Figure 86 to an adjacent console patching system to facilitate initial wiring assignments and any subsequent wiring changes. Precision DC power supply voltages were fused and switched individually. Critical input voltage levels were measured at the load end to the nearest millivolt and printed out with an index of circuit designation and test time. Test article temperatures were monitored at 72 locations with $1^{\circ}F$ resolutions and recorded at one minute intervals throughout the entire test.

The Molecular Research multiplexer was monitored during the irradiation by the SDS 920 of the DMS (Figure 85). Gate linearity measurements were made with source impedances of 10 ohms and 10K ohms. For the gate linearity, the computer digital-to-analog converter provided precise voltage increments (0 to 5 volts) in one-volt step to the multiplexer input. After a period of two seconds, the computer analog-to-digital converter samples the multiplexer channel and stored the output voltage value. This process was repeated for all four channels of both multiplexer units. Waveforms were periodically recorded on a Tektronix 545 oscilloscope.

The Litton V-scan A-to-D shaft position encoder was monitored during the irradiation by the SDS 920 of the DMS. The output signals were monitored on two sets of twelve and one common lead. Each binary count from the encoder was compared with a known count in the computer. Any missing bits were then retained as errors. The encoder was cycled once and the errors recorded. Then it was reversed for one cycle and the process repeated. Provisions were made in the control room for visually monitoring the brush activity on a cathode ray oscilloscope.

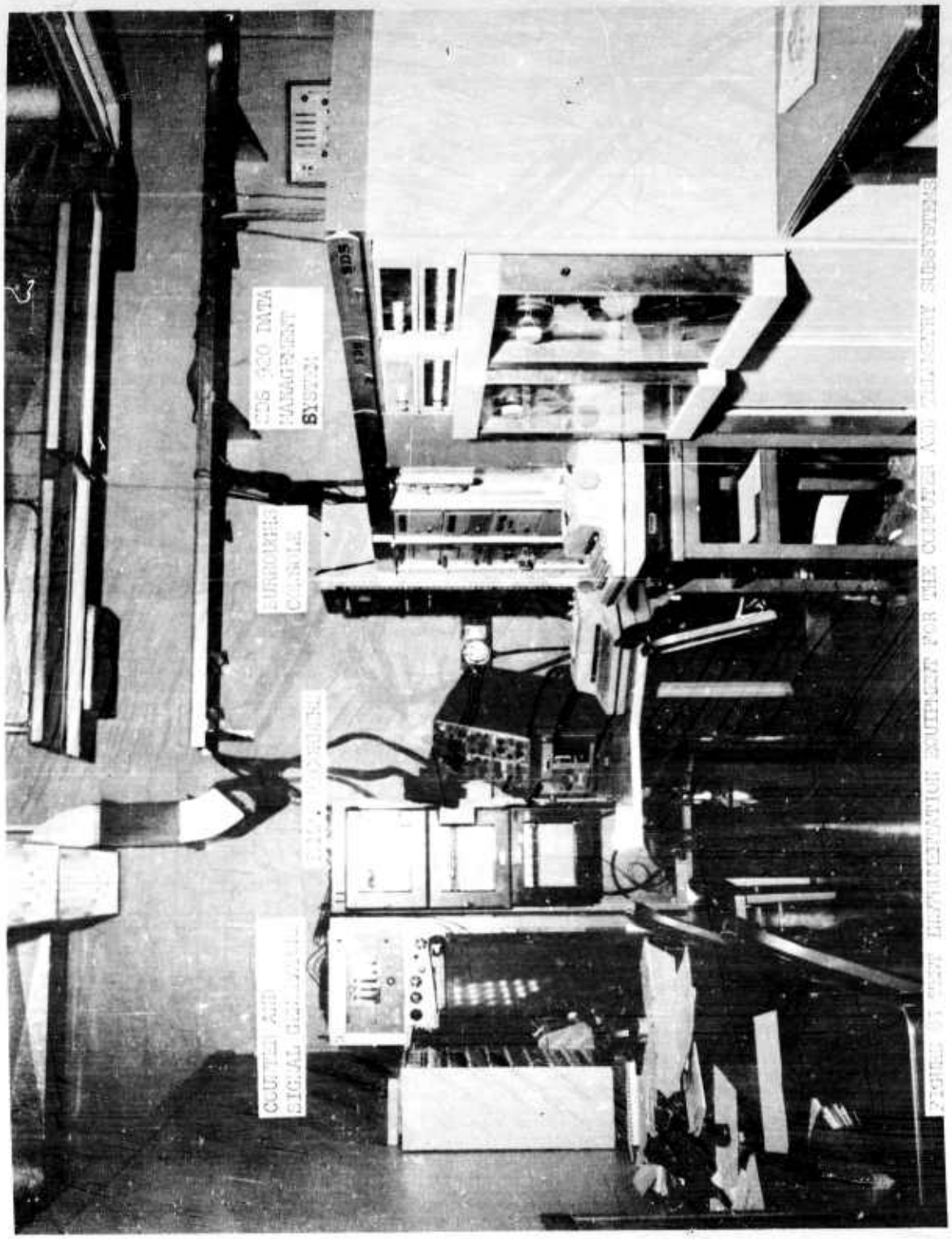

FIGURE 11 TEST INSTRUMENTATION EQUIPMENT FOR THE COMPUTER AND TELEMETRY SUBSYSTEMS

FIGURE 86 POWER DISTRIBUTION CONSOLES

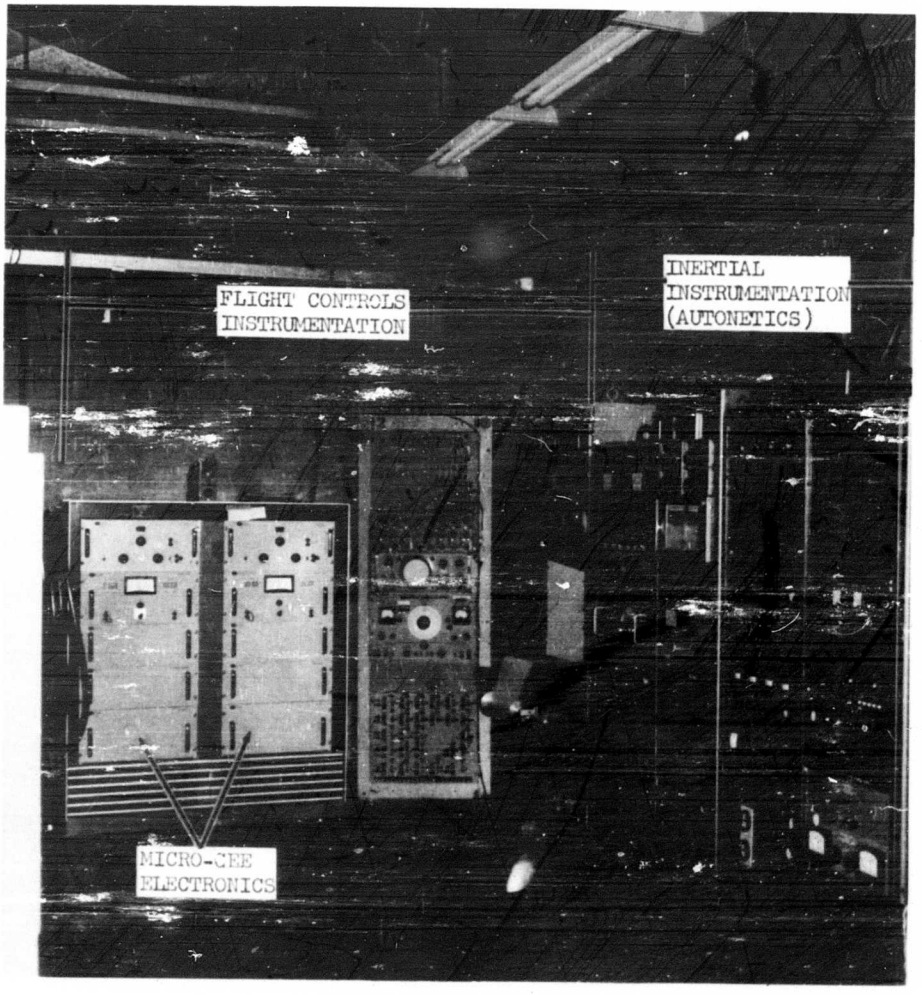

FIGURE 87 CONTROLS AND INERTIAL SUBSYSTEM INSTRUMENTATION CONSOLES

The Autonetics inertial test articles were controlled and monitored using the instrumentation consoles shown in Figure 87. A 5-kc pickoff signal and a 20-kc accelerometer pickoff signal were provided by an Autonetics console. The analog accelerometer output was measured and recorded with a resolution of 0.1 of a millivolt. The gyro wheel speed was measured from the modulation of the pickoff signal. Recordings were made by a Westronics millivolt chart recorder of the azimuth position errors on two channels and azimuth and level amplifier outputs on two other channels. A cathode-ray oscilloscope was used to monitor amplifier phase shift, accelerometer output waveforms, and azimuth and level amplifier outputs. Four console panel meters were used to continuously monitor X and Y accelerometer amplifier output, azimuth gimbal torquer current, and level gimbal torquer current. The noise attenuation between test pallets and control instrumentation was gained through widespread use of shielding and low pass filters.

The flight control equipment instrumentation consoles are shown in Figure 87. The majority of the signals from the controls test articles were recorded by an eight channel Offner strip chart recorder. A central control panel switched the thirty input signals to the chart recorder, indicated the channels being monitored and also provided a visual indication of the gyro spin motor currents and motor speeds. Test points on the control panel provided access to the measurement of such parameters as power voltage, cathode voltage, amplifier gain and saturation, breadboard transient and frequency response, gyro static characteristics, rate gyro torquer response gyro sensitivities and frequency responses.

The Burroughs radiation-hardened, general purpose, airborne computer test vehicle was designed to be dynamically tested in any of three modes; the SDS 920 DMS mode, the card reader mode, and the manual mode. Normal operation was in the SDS 920 mode in which a diagnostic program, previously recorded on magnetic tape, examined the operation of all elements of the computer. The results obtained from the SDS 920 diagnostic routine were recorded on magnetic tape. When errors occurred, the associated instructions were repeated two additional times in the same run to determine whether the errors were of a permanent or transient nature. All errors were recorded on magnetic tape and also printed out for visual analysis. The diagnostic program was conducted in such a manner so that the computer vehicle was subject to two basic tests:

(a) The data processing capability of the unit at periodic intervals

(b) Operating limits definition as a function of several current and voltage parameters.

9.0 DOSIMETRY FOR RADIATION EFFECTS TEST NO. 18

9.1 INTRODUCTION

The basis for analyzing and reporting the effects of nuclear radiation on the functional and physical characteristics of test articles is the amount of radiation to which these articles have been exposed. The leakage radiation from the Air Force Ground Test Reactor at the Nuclear Aerospace Research Facility at General Dynamics/Fort Worth consists primarily of neutrons and gamma rays of various energies. The amount of neutron radiation is expressed in terms of the time integrated flux, i.e., the total number of neutrons per square centimeter of energy greater than 0.3 Mev. For gamma rays the exposure dose is expressed as ergs per gram referenced to carbon, abbreviated ergs/gm-(C). The integrated neutron fluxes were measured with phosphorous and "sulfoxy" sulfur detectors, and the gamma dose was measured with nitrous-oxide dosimeters. All dosimetry materials and readout services were furnished by the Nuclear Aerospace Research Facility.

The Ground Test Reactor (GTR) operation log, Figure 38, presents the reactor power level and accumulated energy as a function of real time.

9.2 PROCEDURE

The foils and nitrous-oxide dosimeters were grouped in packets consisting of:

(a) One bare phosphorous detector

(b) One cadmium-covered phosphorous detector

(c) One sulfoxy-sulfur detector

(d) One nitrous-oxide dosimeter

These packets were attached directly to or as close as possible to the individual test articles to provide measurements of the radiation field to which each article was exposed.

Bare and cadmium covered phosphorous detectors were used to measure the thermal neutron flux ($E<0.48$ ev). Sulfur detectors were used to measure the "fast" neutron flux ($E>2.9$ Mev). The total neutron flux ($E>0.3$ Mev) is obtained from the sulfur data by the relationship $\phi(0.3\ \text{Mev}) = 4.09\ \phi\ (2.9\ \text{Mev})$ which has been previously determined from the GTR spectrum. Details of these neutron detectors are given in Tables 34 and 35.

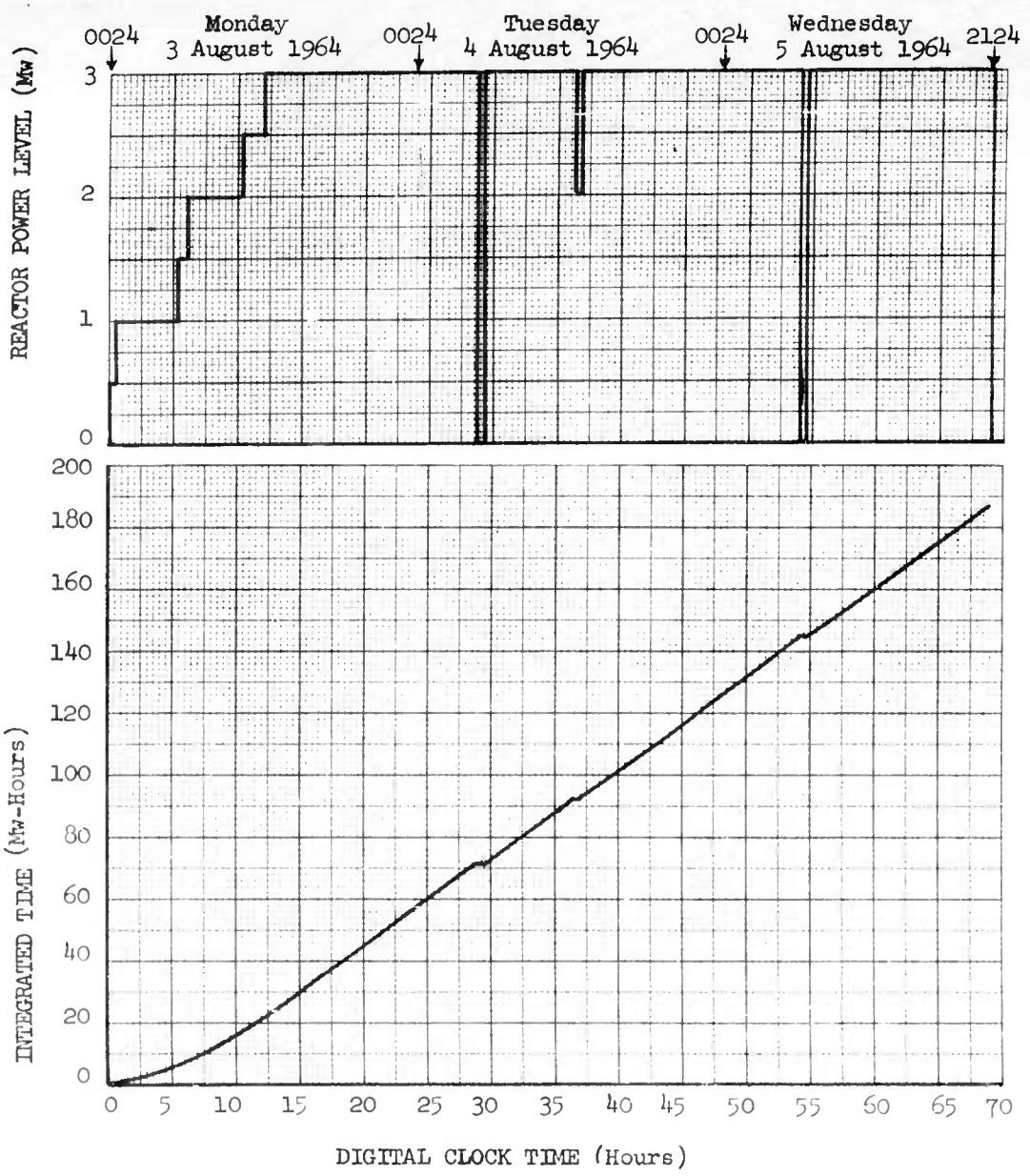

FIGURE 88 SUMMARY OF GROUND TEST REACTOR LOG FOR RADIATION EFFECTS TEST NO. 18

TABLE 34

NUCLEAR CHARACTERISTICS OF THE NEUTRON DETECTORS

Detector	Reaction	Half Life (Days)	Effective Energy Threshold	Activation Cross Section (mb)
Phosphorous	P^{31} (n, γ)P^{32}	14.3	E < 0.48 ev	190 ± 10%
Sulfur	S^{32} (n,p)P^{32}	14.3	E > 2.9 Mev	300 ± 10%

TABLE 35

PHYSICAL CHARACTERISTICS OF THE NEUTRON DETECTORS

Detector	Area (cm^2)	Thickness (mils)	Isotopic Weight (gm)	Comments
Phosphorous	1.00	125	30.975	
Sulfur	2.85	250	0.0853 ± 1%	High temperature dosimeter, epoxy resin 12.9% sulfur by weight.

The total gamma dose at each packet position was determined from nitrous-oxide dosimeters. The operating principle is based on gas phase decomposition in which nitrogen, oxygen, and nitrogen-dioxide are formed from nitrous-oxide by radiation induced reactions.

The nitrous-oxide dosimeters measures the gamma dose fields in the range 1.0×10^{7} to 5.0×10^{11} ergs/gm-(C). The nitrous-oxide is encapsulated in quartz ampules 4.75 inches long and 0.845 inch diameter. Quartz is used as the container because of its low activation cross section and short half life for induced radioactivity.

Sixty-four dosimeter packets were distributed throughout the three irradiation test pallets in a manner which would yield the most realistic value for measuring the radiation field of the test articles. Whenever possible, packets were placed on all sides of the test articles. Thus, the flux perturbation and attenuation factors through and around the test articles was partially accounted for by averaging the measurements obtained from nearby dosimeters.

Values obtained for the integrated neutron fluxes and gamma exposure dose for each test article (dynamic and static) are given in Table 36.

The neutron and gamma spectrum for the Ground Test Reactor is graphically presented in Figures 89, 90, and 91 as a function of distance from the reactor closet with four inches of water separating the reactor and north closet. Figures 92 and 93 present the average neutron flux and gamma dose values on the reactor centerline with distance from the reactor closet. Ratio of the values on the reactor centerline to the values in the corner of each test pallet will vary by a factor of two to ten depending on distance from the reactor closet.

Results from a dosimetry mapping of all three irradiation test pallets indicate that the fast neutron spectrum is slightly harder than the nominal spectrum for the east and west pallet. Further, the spectrum becomes somewhat softer with distance from the closet (Figure 92), which is more apparent for the north data than for the east and west data. It is expected that greater thicknesses of water tend to increase spectral hardness while scattering, with a corresponding build-up of lower energy fluxes at the expense of fast flux, is more readily observed at greater distances from the closet and tends to soften the fast neutron spectrum. The latter is also apparent for the increase of thermal ($E < 0.48$ ev) flux with distance from the reactor closet.

9.3 ACCURACY OF MEASUREMENTS

In all cases the detectors were counted at least five times with at least 10,000 counts accumulated during each counting interval to ensure a small statistical error in the average count rate. The overall accuracy of the foil technique is estimated to be $\pm$ 10 percent.

In general, most of the uncertainty in the information obtained by the neutron detectors was due to the uncertainty of the counter efficiency which is estimated to be $\pm$ 10 percent.

The nitrous-oxide dosimeters were read by means of standard vacuum technique procedures set up in the General Dynamics/ Fort Worth Nuclear Chemistry Laboratory. The accuracy of this method is estimated to be $\pm$ 10 percent.

TABLE 36 (SHEET 1) NUCLEAR RADIATION EXPOSURE OF EACH TEST ARTICLE

Test Articles	Subcontractor	Integrated Neutrons n/cm²			Gammas
		E<0.48 ev	E>2.9 Mev	E>0.3 Mev	Ergs/gm-(C)
Dynamic					
Voltage Reference Tube and Magnetic Core Device	Autonetics	4.8(14)*	2.4(15)	9.9(15)	1.1(10)
Sola Transformer	Autonetics	5.2(14)	3.6(15)	1.5(16)	5.3(10)
Multivibrator	Autonetics	5.2(14)	2.6(15)	1.0(16)	1.6(10)
Chopper Stabilized DC Amp No. 1	Autonetics	3.0(14)	5.9(15)	2.4(16)	1.8(11)
Chopper Stabilized DC Amp No. 2	Autonetics	3.8(14)	4.0(15)	1.7(16)	1.0(11)
Chopper Stabilized DC Amp No. 3	Autonetics	2.5(14)	4.6(15)	1.9(16)	1.7(11)
Chopper Stabilized DC Amp No. 4	Autonetics	2.8(14)	3.1(15)	1.3(16)	1.0(11)
Two-Axis Platform (G9 Gyro and EMA's)	Autonetics	2.8(14)	3.1(15)	1.3(16)	1.0(11)
Accelerometer Mid-Amplifier No. 1	Autonetics	5.3(14)	2.6(15)	1.1(16)	2.1(10)
Accelerometer Mid-Amplifier No. 2	Autonetics	4.2(14)	6.6(15)	2.7(16)	3.5(11)
Gyro Mid-Amplifier No. 1	Autonetics	3.4(14)	3.1(15)	1.3(16)	9.6(10)
Gyro Mid-Amplifier No. 2	Autonetics	3.4(14)	3.1(15)	1.3(16)	9.6(10)
Platform Control Amplifier	Autonetics	3.4(14)	2.2(15)	8.9(15)	3.9(10)
Accelerometer Control Amplifier	Autonetics	3.9(14)	2.5(15)	1.0(16)	8.4(10)
Three - Phase Transformer	Autonetics	3.0(14)	3.6(15)	1.5(16)	1.1(11)
Resonators	Litton	4.8(14)	2.4(15)	9.8(15)	1.4(10)
Rate Gyro No. 1	Humphreys	2.7(14)	8.5(15)	3.5(16)	1.9(11)
Rate Gyro No. 2	Humphreys	2.8(14)	8.1(15)	3.3(16)	1.5(11)
Integrating Gyro	Humphreys	2.8(14)	8.7(15)	3.5(16)	2.4(11)
Electro-Mechanical Filter System	LTV	5.0(14)-4.1(14)	5.7(15)-5.9(15)	2.3(16)-2.4(16)	8.8(10)-4.9(10)
Magnetic Core Controlled Multiplexer No. 1	Molecular Research	7.2(14)	2.2(16)	9.1(16)	2.1(11)
Magnetic Core Controlled Multiplexer No. 2	Molecular Research	7.2(14)	2.8(16)	1.1(17)	2.5(11)
Computer	Burroughs	2.4(14)-6.6(14)	1.6(16)-4.3(15)	6.3(16)-1.8(16)	2.9(11)-5.4(10)
Encoder	Litton	3.5(14)	2.0(16)	8.3(16)	2.9(11)
Thin-Film FET (Irradiated)	Melpar	8.3(15)	2.2(16)	9.1(16)	2.0(11)
Thin-Film FET (Non-Irradiated)	Melpar	7.4(14)	3.1(16)	1.2(17)	1.9(11)

TABLE 36 (SHEET 2) NUCLEAR RADIATION EXPOSURE OF EACH TEST ARTICLE

Test Articles	Subcontractor	Integrated Neutrons n/cm²			Gammas
		E<0.48 ev	E>2.9 Mev	E>0.3 Mev	Ergs/gm-(C)
Static					
Pyrex Tube No. 1	Autonetics	C.R.<1	7.0(15)	2.9(16)	3.8(10)
Pyrex Tube No. 2	Autonetics	C.R.<1	7.2(15)	2.9(16)	3.9(10)
Pyrex Tube No. 3	Autonetics	C.R.<1	7.4(15)	3.0(16)	5.0(10)
Pyrex Tube No. 4	Autonetics	C.R.<1	7.7(15)	3.1(16)	6.0(10)
Pyrex Tube No. 5	Autonetics	C.R.<1	8.2(15)	3.3(16)	8.2(10)
Pyrex Tube No. 6	Autonetics	3.5(14)	8.3(15)	3.4(16)	1.1(11)
Pyrex Tube No. 7	Autonetics	3.5(14)	8.4(15)	3.4(16)	1.4(11)
Pyrex Tube No. 8	Autonetics	3.5(14)	8.5(15)	3.5(16)	2.1(11)
Pyrex Tube No. 9	Autonetics	3.6(14)	8.1(15)	3.3(16)	2.9(11)
Pyrex Tube No. 10	Autonetics	3.8(14)	7.6(15)	3.1(16)	3.7(11)
Pyrex Tube No. 11	Autonetics	3.8(14)	7.6(15)	3.1(16)	3.7(11)
Pyrex Tube No. 14	Autonetics	4.3(14)	6.9(15)	2.8(16)	2.3(11)
Pyrex Tube No. 15	Autonetics	4.7(14)	6.3(15)	2.6(16)	8.5(10)
Pyrex Tube No. 16	Autonetics	4.7(14)	6.3(15)	2.6(16)	8.5(10)
Pyrex Tube No. 17	Autonetics	3.0(14)	3.9(15)	1.6(16)	2.8(10)
Pyrex Tube No. 18	Autonetics	3.0(14)	3.9(15)	1.6(16)	2.8(10)
Pyrex Tube No. 19	Autonetics	C.R.<1	3.8(15)	1.6(16)	4.0(10)
Pyrex Tube No. 20	Autonetics	C.R.<1	4.0(15)	1.6(16)	5.2(10)
Pyrex Tube No. 21	Autonetics	C.R.<1	4.0(15)	1.6(16)	5.2(10)
Pyrex Tube No. 22	Autonetics	4.2(14)	3.8(15)	1.6(16)	4.2(10)
Pyrex Tube No. 23	Autonetics	4.2(14)	3.6(15)	1.5(16)	3.1(10)
Pyrex Tube No. 24	Autonetics	4.2(14)	3.6(15)	1.5(16)	3.1(10)
Circuit Boards	Burroughs	7.2(14)	3.0(15)	1.2(16)	4.7(10)
Tube No. 1	Chathan/Tung-Sol	5.7(14)	2.1(15)	8.5(15)	9.4(10)
Tube No. 2	Chathan/Tung-Sol	8.2(14)	2.3(16)	9.4(16)	2.9(11)
Tube No. 3	Chathan/Tung-Sol	7.0(14)	2.2(16)	9.2(16)	3.7(11)
Dielectric Materials (Can A)	LTV	C.R.<1	2.9(16)	1.2(17)	8.2(10)
Capsule Materials (Can B)	LTV	5.7(14)	2.0(15)	8.2(15)	1.9(10)
Dielectric Materials (Can C)	LTV	5.9(14)	4.8(15)	2.0(16)	5.4(10)
Capsule Materials (Can D)	LTV	7.5(14)	4.3(14)	1.8(15)	9.0(9)

TABLE 36 (SHEET 3) NUCLEAR RADIATION EXPOSURE OF EACH TEST ARTICLE

Test Articles	Subcontractor	Integrated Neutrons n/cm^2			Gammas
		E<0.48 ev	E>2.9 Mev	E>0.3 Mev	Ergs/gm-(C)
Capsule Materials (Can E)	LTV	5.7(14)	1.8(15)	7.4(15)	3.5(10)
Assorted Elect. Comp. No. 1	LTV	4.4(14)	1.6(16)	6.5(16)	2.0(11)
Assorted Elect. Comp. No. 2	LTV	5.9(14)	4.0(15)	1.6(16)	4.6(11)
Assorted Elect. Comp. No. 3	LTV	2.5(14)	6.2(15)	2.5(16)	4.6(11)
Diodes	LTV	2.9(14)	2.8(16)	1.1(17)	6.6(11)

C.R. - Cadmium Ratio
*(x) Denotes powers of 10

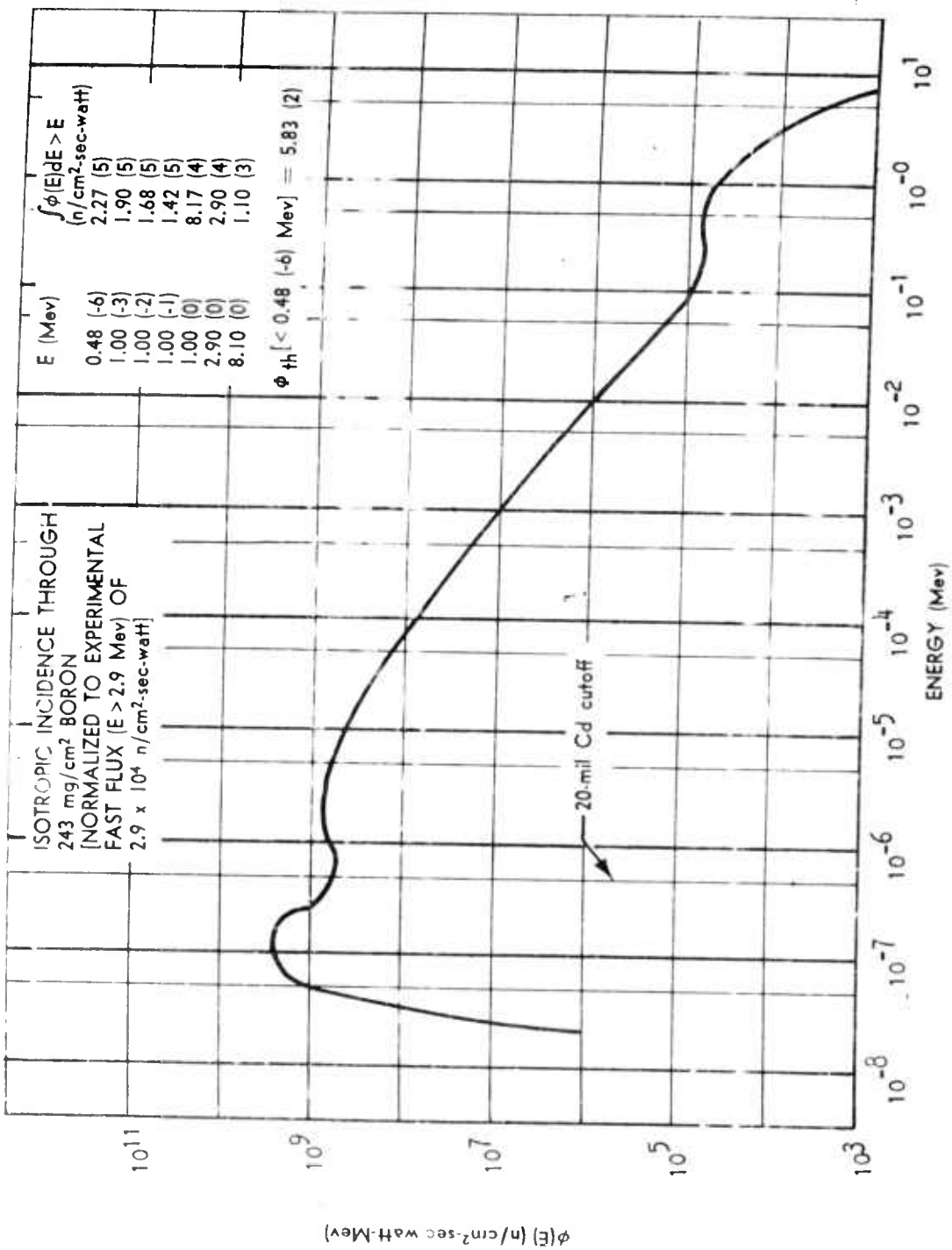

FIGURE 89 GROUND TEST REACTOR NEUTRON SPECTRUM

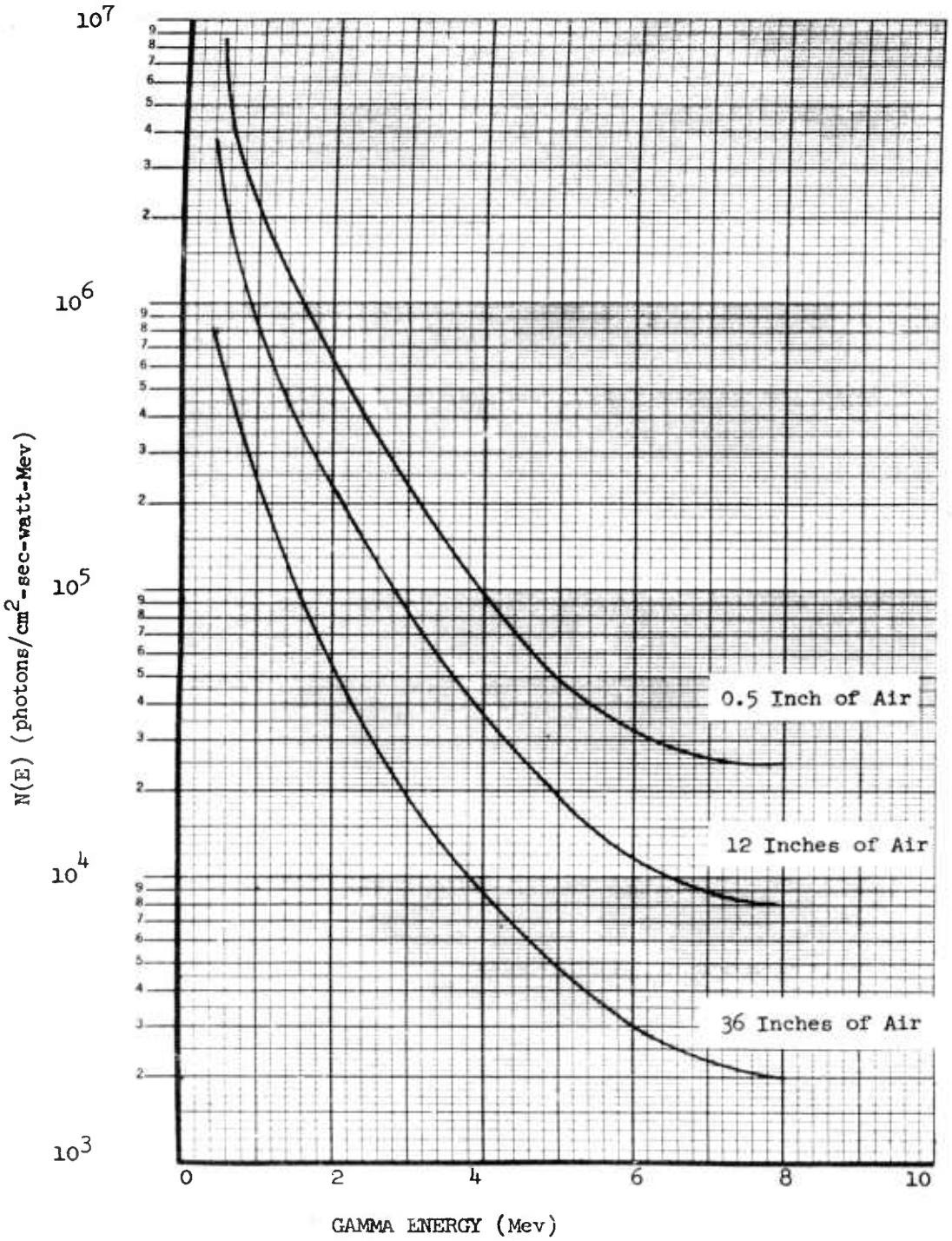

FIGURE 90 NORTH PALLET CENTERLINE GAMMA SPECTRA IN AIR

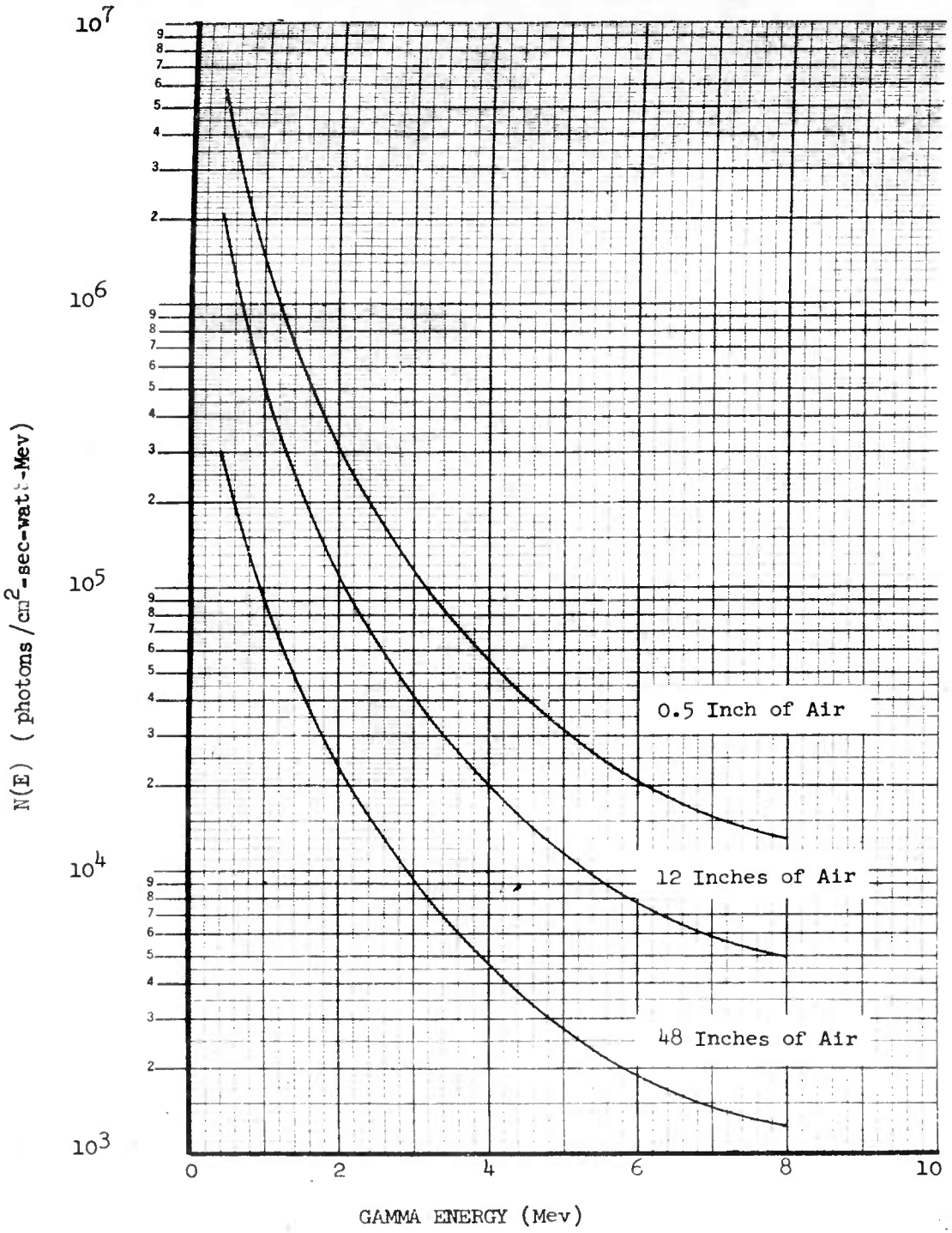

FIGURE 91 EAST AND WEST PALLET CENTERLINE GAMMA SPECTRA IN AIR

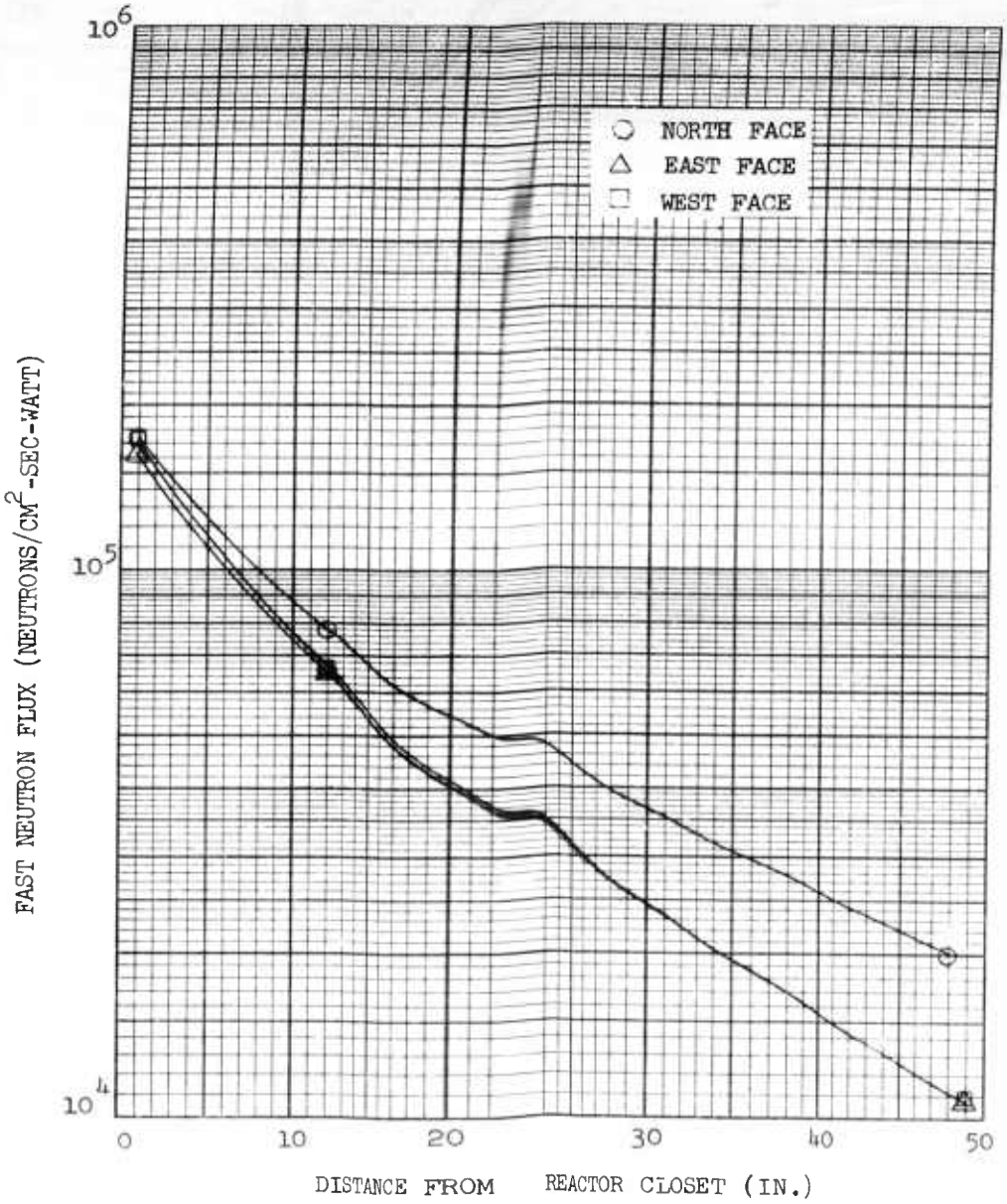

FIGURE 92 AVERAGE NEUTRON FLUXES ON REACTOR CENTERLINE (E>0.3 Mev)

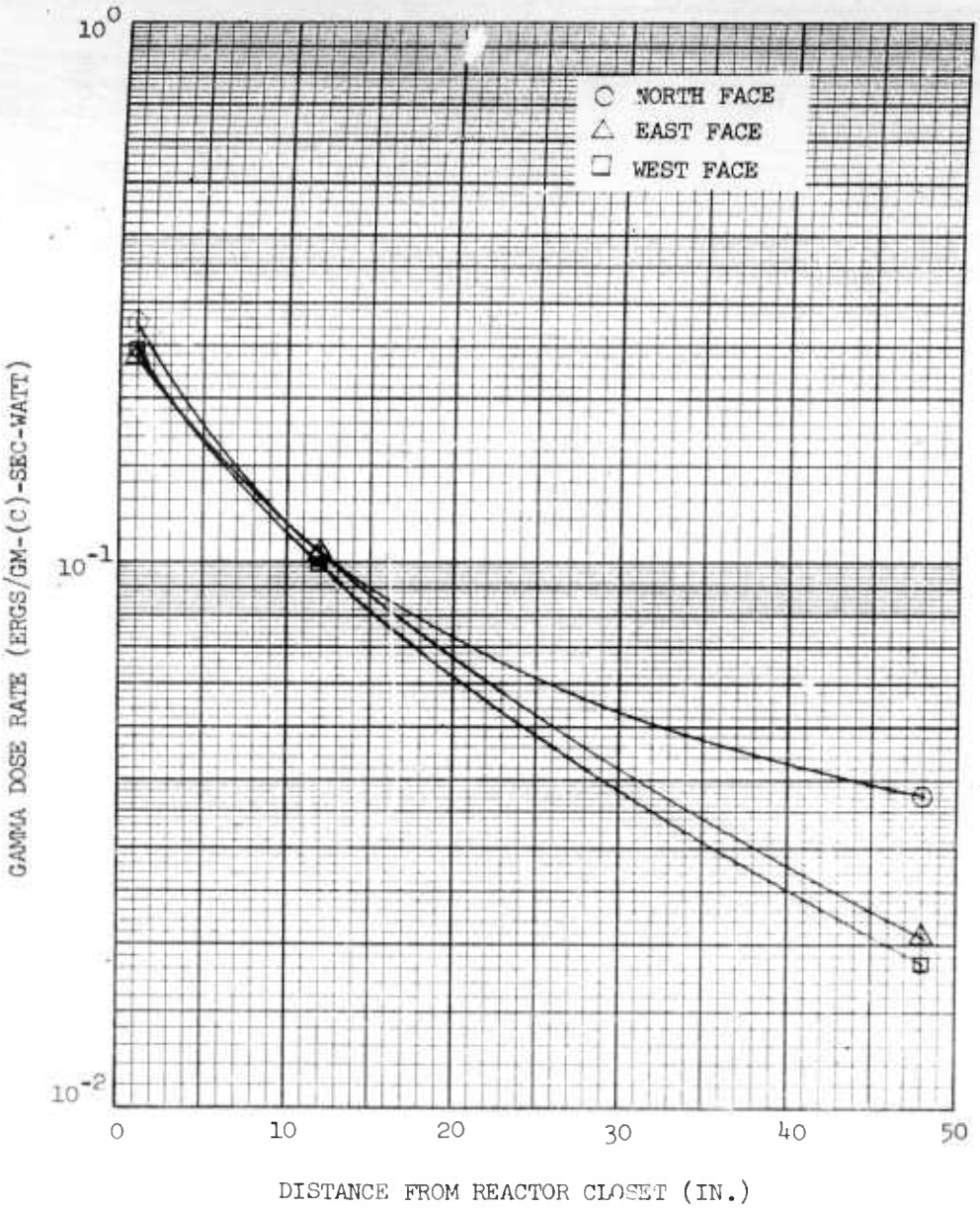

FIGURE 93 AVERAGE GAMMA DOSE RATE VALUES ON REACTOR CENTERLINE

LIST OF REFERENCES

Reference

1 "V-Brush Scanning Encoders," T. T. Ota, Technical Memorandum 3241-65-84, Autonetics, A Division of North American Aviation, Inc., 28 April 1960.

2 "LASV-N2 Computer Implementation Techniques," G. E. Lund, V. Z. Smith and J. T. Lynch, Mid-Term Report to Ling-Temco-Vought, Inc. by Burroughs Laboratories, 23 July 1964.

3 "LASV-N2 Computer Implementation Techniques," G. E. Lund, V. Z. Smith and J. T. Lynch, Final Report to Ling-Temco-Vought, Inc. by Burroughs Laboratories on P.O. No. P-060369, 25 September 1964.